PNL--4847

DE84 010574

CESIUM CHLORIDE COMPATIBILITY TESTING PROGRAM ANNUAL REPORT - FISCAL YEAR 1983

G. H. Bryan

March 1984

DISCLAIMER

This report was prepared as an account of work sponsored by an agency of the United States Government. Neither the United States Government nor any agency thereof, nor any of their employees, makes any warranty, express or implied, or assumes any legal liability or responsibility for the accuracy, completeness, or usefulness of any information, apparatus, product, or process disclosed, or represents that its use would not infringe privately owned rights. Reference herein to any specific commercial product, process, or service by trade name, trademark, manufacturer, or otherwise does not necessarily constitute or imply its endorsement, recommendation, or favoring by the United States Government or any agency thereof. The views and opinions of authors expressed herein do not necessarily state or reflect those of the United States Government or any agency thereof.

Prepared for the U.S. Department of Energy
under Contract DE-AC06-76RLO 1830

Pacific Northwest Laboratory
Richland, Washington 99352

DISTRIBUTION OF THIS DOCUMENT IS UNLIMITED

ABSTRACT

A program was started in FY 1982 to evaluate the compatibility of WESF-produced CsCl with 316L stainless steel under the thermal conditions that would be encountered in a geologic repository. The program is funded through the long-term High-Level Defense Waste Program of the Department of Energy. The major part of the program involves compatibility testing of six standard WESF CsCl capsules at a maximum CsCl/metal interface temperature of 450°C. The capsules are allowed to self heat to the test temperature in insulated containers and then held at temperature for 2200 to 32,000 h. After thermal aging, the capsules are destructively examined to determine the extent of the metal attack by the CsCl. This report describes the test procedure and summarizes the results obtained during the second year of the program.

Metallographic examination was completed of the two zero-time capsules. The photomicrographs obtained of the metal samples indicate the maximum metal attack resulting from the capsule-filling operation was about 25 μm (0.001 in.).

Metallographic examination of the WESF CsCl capsules held at temperature for 2208 and 4392 h was completed. Both capsules exhibited substantial attack by the CsCl. Maximum attack observed in the 2208-hour capsule was estimated to be about 60 μm (0.0024 in.), while maximum attack in the 4392-h capsule was estimated at 110 μm (0.0043 in.). The data indicate the corrosion rate is linear with time for the first 4392 h.

Thermal aging of the 8394-h capsule was completed, and metallographic examination of the capsule is underway. Thermal aging of the three remaining test capsules is continuing.

When the 4392-h capsule was opened for metallographic examination, it was found that the outer surface of the inner capsule was discolored and pitted at several locations. Metallographic examination of the affected areas showed pits up to 300-μm (0.012-in.) deep in some areas. The maximum depth observed corresponded to about 9% of the initial capsule wall thickness. No similar pitting conditions observed on the outer surface of the 2208-h inner capsule; but was observed, although apparently to a lesser degree, on the outer surface of the 8784-h inner capsule.

ACKNOWLEDGMENTS

The author would like to thank H. T. Fullam for his assistance and guidance in the preparation of this document. Without his knowledge and willingness to help, completion would have been extremely difficult within the imposed time restraints.

CONTENTS

1.0 INTRODUCTION 1.1

2.0 OBJECTIVES 2.1

3.0 TESTING CRITERIA 3.1

4.0 RADIOACTIVE COMPATIBILITY TESTS 4.1

4.1 TESTING PROCEDURE 4.1

4.2 CAPSULE FABRICATION 4.1

4.3 ZERO-TIME CAPSULES 4.2

4.4 CAPSULE AGING 4.5

4.5 CAPSULE SECTIONING AND EXAMINATION 4.9

4.6 METAL CONTROL SPECIMENS 4.11

5.0 TEST RESULTS 5.1

5.1 ZERO-TIME CAPSULES 5.2

5.2 THERMAL AGING TESTS 5.5

5.3 METAL CONTROL SPECIMENS 5.17

5.4 EXTERNAL CAPSULE CORROSION 5.17

6.0 REFERENCES 6.1

FIGURES

1 Locations Where the Wall Thickness of the Inner WESF Capsule were Measured 4.3

2 Sketch of a WESF Capsule in its Insulated Container 4.6

3 Insulated Containers in a Holding Rack in the Hot Cell 4.7

4 Locations Where the Capsule Surface Temperatures are Measured 4.8

5 Sectioning of the Zero-Time Inner Capsules 4.10

6 Mounting of the Metal Samples Showing the Problem of Sample Alignment 5.2

7 Photomicrographs from Samples of Zero-Time Capsule 19459 ..... 5.3

8 Photomicrographs from Samples of Zero-Time Capsule 19073F 5.4

9 Average Temperature Profiles for the WESF Capsule held at Temperature for 2208 Hours 5.6

10 Average Temperature Profiles for the WESF Capsule held at Temperature for 4392 Hours 5.7

11 Average Temperature Profiles for the WESF Capsule Held at Temperature for 8784 Hours 5.8

12 Temperature Fluctuations Observed with the Capsule Held at Temperature for 2208 Hours 5.9

13 Temperature Fluctuations Observed with the Capsule Held at Temperature for 4392 Hours 5.10

14 Temperature Fluctuations Observed with the Capsule Held at Temperature for 8784 Hours 5.11

15 Photomicrographs of Samples Taken from the Capsule that was Thermally Aged for 2208 Hours - Showing the Metal/CsCl Interface 5.12

16 Photomicrographs of Samples Taken from the Capsule that was Thermally Aged for 4392 Hours - Showing the Metal/CsCl Interface 5.13

17 Maximum Metal Attack as a Function of Exposure Time - As Determined from Photomicrographs of Samples Taken from the Test Capsules 5.15

18 Metal Control Samples, 400°C 5.19

19 Metal Control Samples, 450°C 5.20

20 Metal Control Samples, 500°C 5.21

Figures (cont'd)

21 Areas on the Outer Surface of the Inner Capsule (from the 4392 Hour Capsule) that were Sampled for Metallographic Examination 5.22

22 Additional Areas on the Outer Surface of the Inner Capsule that were Sampled for Metallographic Examination 5.23

23 Photomicrographs of Area A, Outer Surface of Inner Capsule 5.24

24 Photomicrographs of Area B, Outer Surface of Inner Capsule 5.25

25 Photomicrographs of Area C, Outer Surface of Inner Capsule 5.26

26 Photomicrographs of Area D, Outer Surface of Inner Capsule 5.27

27 Photomicrographs of Area E, Outer Surface of Inner Capsule 5.28

28 Photomicrographs of Area F-1, Outer Surface of Inner Capsule 5.29

29 Photomicrographs of Area F-2, Outer Surface of Inner Capsule 5.30

30 Photomicrographs of Area F-3, Outer Surface of Inner Capsule 5.31

31 Photomicrographs of Area G, Outer Surface of Inner Capsule 5.32

TABLES

1 Wall Thickness Data for Three of the 316L Stainless Steel Inner Capsules Used in Fabricating the Test Capsules 4.4

2 Pertinent Data on the Six WESF CsCl Capsules Used in the Thermal Aging Tests 4.5

3 Estimates of Metal Attack in the Zero-Time Capsules 5.5

4 Estimated Metal Attack in the Thermally Aged WESF CsCl Capsules 5.14

5 Wall Thickness Data for the WESF CsCl Test Capsules 5.16

1.0 INTRODUCTION

At Hanford, fission product cesium, containing 20-40% ^{137}Cs, is recovered from the high-level waste (HLW) and converted to cesium chloride (CsCl). The CsCl is doubly encapsulated in small high-integrity 316L stainless steel (SS) capsules. The CsCl capsules are then stored in water basins on the Hanford Reservation.

The CsCl is loaded into the inner 316L SS capsules by melt casting. Each capsule, which has an ID of two inches and an inner length of about 19 in., contains up to three kg of CsCl. The capsules contain up to about 70,000 Ci of ^{137}Cs, depending on the age and purity of the fission product CsCl.

Recovery of the Cs from the HLW and its subsequent purification take place in B-Plant. Conversion of the purified Cs to CsCl, encapsulation of the CsCl, and storage of the CsCl capsules take place in the Waste Encapsulation and Storage Facility (WESF). Both facilities are currently operated for the Department of Energy (DOE) by Rockwell Hanford Operations (Rockwell).

The Department of Energy is currently considering the geologic disposal of the CsCl capsules produced and stored at WESF. In order to evaluate the hazards associated with the geologic disposal of the WESF CsCl capsules, reliable estimates are required of long-term attack of the capsule material by the CsCl under repository conditions. Currently, available data on the compatibility of WESF-produced CsCl with 316L SS are not adequate for making the required estimates. The Cesium Chloride Compatibility Testing Program was started at the Pacific Northwest Laboratory in FY 1982 to obtain the needed compatibility data. The program will take ~5 years to complete. The work is funded by the long-term High-Level Defense Waste Program of the DOE. This report summarizes the program activities for Fiscal Year 1983.

2.0 OBJECTIVES

The primary objective of the Cesium Chloride Compatibility Testing Program is to evaluate the compatibility of WESF-produced CsCl with the 316L SS capsule material under the conditions that would be encountered in a geologic repository. Sufficient short-term compatibility data are to be obtained with the WESF-produced CsCl to permit useful estimates of long-term attack of the 316L SS by the CsCl under repository conditions.

Secondary objectives of the program are to:

- determine the effects of impurities in the WESF-produced CsCl on the attack of the SS and identify the reaction mechanisms involved
- determine the effects of the impurities in the WESF-produced CsCl on the melting point and solid-solid phase transition of CsCl.

3.0 TESTING CRITERIA

A number of variables can affect the compatibility of the WESF-produced CsCl with 316L SS in a geologic repository. The more important variables include:

- the reaction temperature (316L SS/CsCl interface temperature)
- impurities in the WESF-produced CsCl
- changes in the microstructure of the 316L stainless steel due to thermal aging reactions (i.e., precipitation of carbide phases, etc.)
- degree of contact between the 316L SS and the CsCl.

Program scope does not include a detailed testing program to evaluate all of the variables which affect 316L SS/WESF CsCl compatibility, especially with regard to impurity effects. The limited testing program now underway was designed on the following bases:

- the 316L SS/WESF CsCl interface temperatures in the geologic repository will not exceed 450°C
- the WESF CsCl capsules will be placed in the repository in a vertical orientation
- the radioactive compatibility tests are to be carried out with standard production WESF CsCl capsules without regard to possible variations in the composition of the CsCl between capsules.

The last limitation can have a significant effect on the overall validity of the radioactive compatibility data obtained, since theoretical considerations indicate that certain impurities in the CsCl could have a significant effect on the metal attack. The data obtained in the radioactive tests now underway will provide a measure of the metal attack for a given set of WESF capsules, but will not provide a complete picture of how the attack may vary with changes in the CsCl composition.

The CsCl compatibility testing program is divided into five tasks:

1. Radioactive compatibility data lasting up to 32,000 h using standard WESF CsCl capsules aged at elevated temperatures.
2. Heat transfer studies to define the relationship between the surface temperature of the inner and outer capsules of the WESF CsCl capsule.
3. Chemical analysis of the CsCl from a batch of WESF-produced CsCl (the CsCl product from WESF is not analyzed, although the Cs feed solution to WESF is analyzed).
4. A thermodynamic analysis of the WESF CsCl/316L SS system.
5. Physical property measurements on CsCl-impurity mixtures.

The major emphasis throughout the duration of the program is on the first task. Tasks 2-5 were completed during FY 1982 (Fullam 1982b).

4.0 RADIOACTIVE COMPATIBILITY TESTS

The radioactive compatibility tests are designed to provide the short-term data needed to estimate long-term attack of 316L SS by WESF-produced CsCl at a maximum metal/CsCl interface temperature of 450°C. The data obtained from the tests should meet this requirement, within the limitations described in the previous section.

4.1 TESTING PROCEDURE

In the radioactive compatibility tests, six standard WESF CsCl capsules are placed vertically in individual insulated containers and allowed to self heat to a maximum metal/CsCl interface temperature of 450°C. The capsules are maintained at temperature for times of 2000, 4000, 8000, 16,000, 24,000, or 32,000 h. When thermal aging of a capsule is completed, it is removed from the insulated container, cooled, and shipped to the Oak Ridge National Laboratory (ORNL) for sectioning and examination. At ORNL, small samples are taken from the inner capsule at various locations and subjected to metallographic examination to determine the extent of metal attack by the CsCl. Some of the samples will also be subjected to electron microprobe analysis in an attempt to identify the reaction mechanisms involved in the metal attack.

In addition to the aging tests, two WESF inner capsules were sectioned and examined immediately after filling with CsCl. This provides a measure of the metal attack that occurs during the loading operation when the CsCl is molten. These two "zero time" capsules will serve as the controls for determining the metal attack resulting from the thermal aging tests.

Because of their high ^{137}Cs content, all work with the WESF CsCl capsules, including sectioning and examination of test samples, is carried out in heavily shielded facilities (hot cells).

4.2 CAPSULE FABRICATION

The CsCl capsules used in the radioactive compatibility tests are typical WESF-production capsules prepared in the normal manner and meeting all Rockwell and DOE QC and QA requirements. All capsule components were fabricated in the usual manner with one exception. In order to accurately determine

metal attack by the CsCl, it is necessary to know the initial wall thickness of the inner capsules at the points were the samples are taken for metallographic examination. Therefore, the wall thickness of each of the eight inner capsules used in the tests was measured at the 18 locations shown in Figure 1 before the capsule was filled with CsCl. An ultrasonic procedure was used to determine the wall thickness.

Table 1 shows wall thickness data for three of the inner capsules, which is typical of all eight capsules. The data show that the wall thickness is fairly uniform over the length of a capsule along any given surface element, with thickness variations rarely exceeding 0.003 in. The data also show, however, that the tubing used in fabricating the inner capsules is not concentric, and substantial differences in wall thickness (up to 0.015 in.) were observed at diametrically opposite locations on the capsule. Because of these variations, the initial wall thickness of the inner test capsule is only known, with any degree of certainty, at those locations where the wall thickness measurements were made. The measurement locations are clearly shown on the test capsules by means of location numbers and location lines etched on the surface of the capsule (see Figure 1).

Loading of the molten CsCl into the inner capsules at WESF is a batch operation. Sufficient CsCl is melted in each batch to fill seven capsules. Each of the test capsules, including the two zero-time capsules, was loaded from a different batch of CsCl. Therefore, the chemical composition and cesium isotopic composition of the CsCl in the different test capsules can vary significantly. Table 2 gives the pertinent data on the six capsules used in the thermal aging tests. From the data, one can calculate an approximate ^{137}Cs isotopic concentration for each capsule, but the amount and types of impurities present in each capsule are unknown.

4.3 ZERO-TIME CAPSULES

The two "zero-time" inner capsules were filled with CsCl in the normal manner. After removal from the loading apparatus, the CsCl was removed from the two capsules by water leaching. Each empty capsule was rinsed, thoroughly dried, and then sealed by welding the end cap in place. The sealed inner capsules were decontaminated, leak-checked, and sealed in outer capsules in

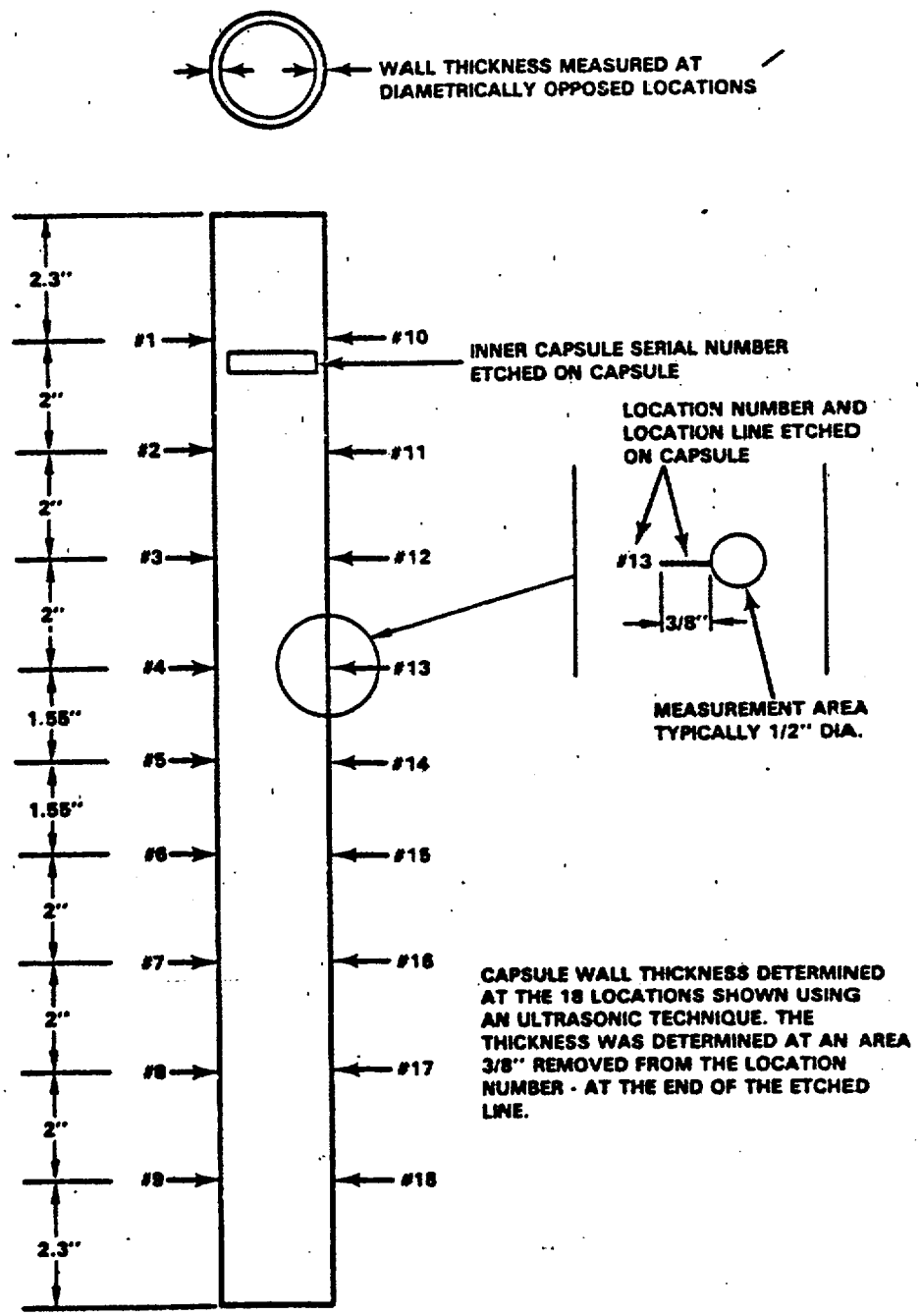

FIGURE 1. Locations Where the Wall Thickness of the Inner WESF Capsules were Measured

TABLE 1. Wall Thickness Data for Three of the 316L Stainless Steel Inner Capsules Used in Fabricating the Test Capsules

Inner Capsule No.	Location No.[a]	Wall Thickness, in.	Location No.[a]	Wall Thickness, in.
19073-A	1	0.1342	10	0.1401
	2	0.1332	11	0.1387
	3	0.1341	12	0.1393
	4	0.1326	13	0.1392
	5	0.1345	14	0.1382
	6	0.1341	15	0.1387
	7	0.1345	16	0.1383
	8	0.1341	17	0.1364
	9	0.1341	18	0.1365
19073-C	1	0.1346	10	0.1431
(8800 h)	2	0.1320	11	0.1425
	3	0.1330	12	0.1417
	4	0.1342	13	0.1431
	5	0.1315	14	0.1414
	6	0.1310	15	0.1419
	7	0.1315	16	0.1399
	8	0.1319	17	0.1411
	9	0.1307	18	0.1422
19073-G	1	0.1455	10	0.1317
(2200 h)	2	0.1441	11	0.1306
	3	0.1458	12	0.1318
	4	0.1455	13	0.1326
	5	0.1444	14	0.1306
	6	0.1456	15	0.1303
	7	0.1435	16	0.1315
	8	0.1454	17	0.1321
	9	0.1445	18	0.1302

(a) See Figure 1 for the meaning of the location numbers.

TABLE 2. Pertinent Data on the Six WESF CsCl Capsules Used in the Thermal Aging Tests[a]

Outer Capsule No.	Inner Capsule No.	CsCl, kg	^{137}Cs, Curies	Watts, t
C-1266 (2200 h)	19073-G	2.388	45,870	220
C-1272	19073-B	2.701	56,930	273
C-1351	19073-E	2.597	52,520	252
C-1365 (4400 h)	19073-D	2.472	44,740	214
C-1451 (8800 h)	19073-C	2.756	54,380	261
C-1486	19073-H	2.716	51,140	245

(a) As of 4-5-82.

the normal manner. The two capsules were then shipped to ORNL for sectioning and metallographic examination. The procedure used in sectioning the capsules is described in Section 4.5.

4.4 CAPSULE AGING

The six WESF CsCl capsules to be thermally aged were placed in insulated containers and allowed to self heat to a maximum metal/CsCl interface temperature of 450°C. Figure 2 shows a sketch of a test capsule in its insulated container. Figure 3 shows a photograph of the insulated containers, containing the CsCl capsules, in a holding rack in the hot cell.

The insulated container consists of a metal canister lined with block insulation on the bottom and pipe insulation on the sides. Loose blanket insulation is placed on top of the capsule in the canister. A SS thermowell, running the length of the WESF capsule, is fastened to each capsule using SS hose clamps. The photograph in Figure 3 shows one of the WESF capsules with the thermowell attached.

Six calibrated movable chromel-alumel thermocouples, each having a different immersion depth, are used to measure the surface temperature of each WESF capsule. Figure 4 shows the locations at which the capsule surface temperature is measured. By rotating the six thermocouples between the thermowells on the six capsules, temperature profiles of each capsule are obtained on a periodic basis. As will be shown later, substantial temperature gradients

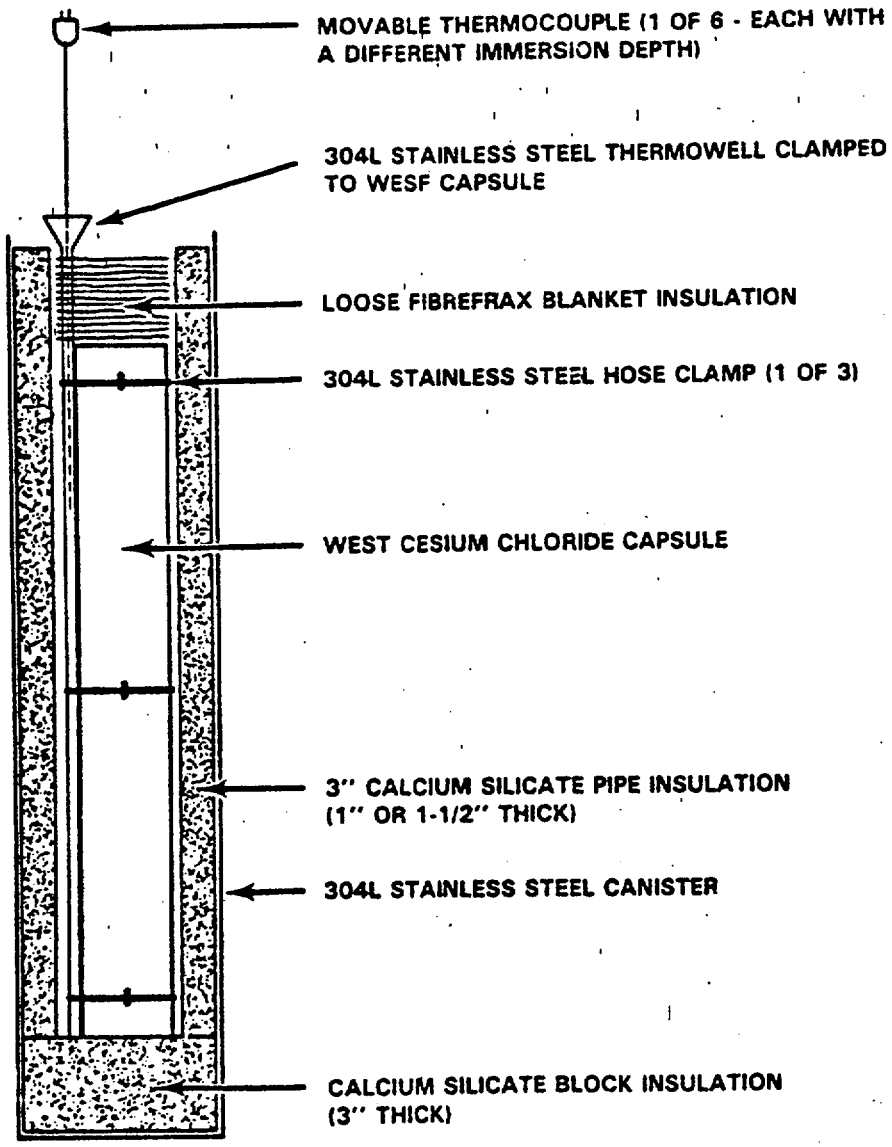

FIGURE 2. Sketch of a WESF Capsule in its Insulated Container

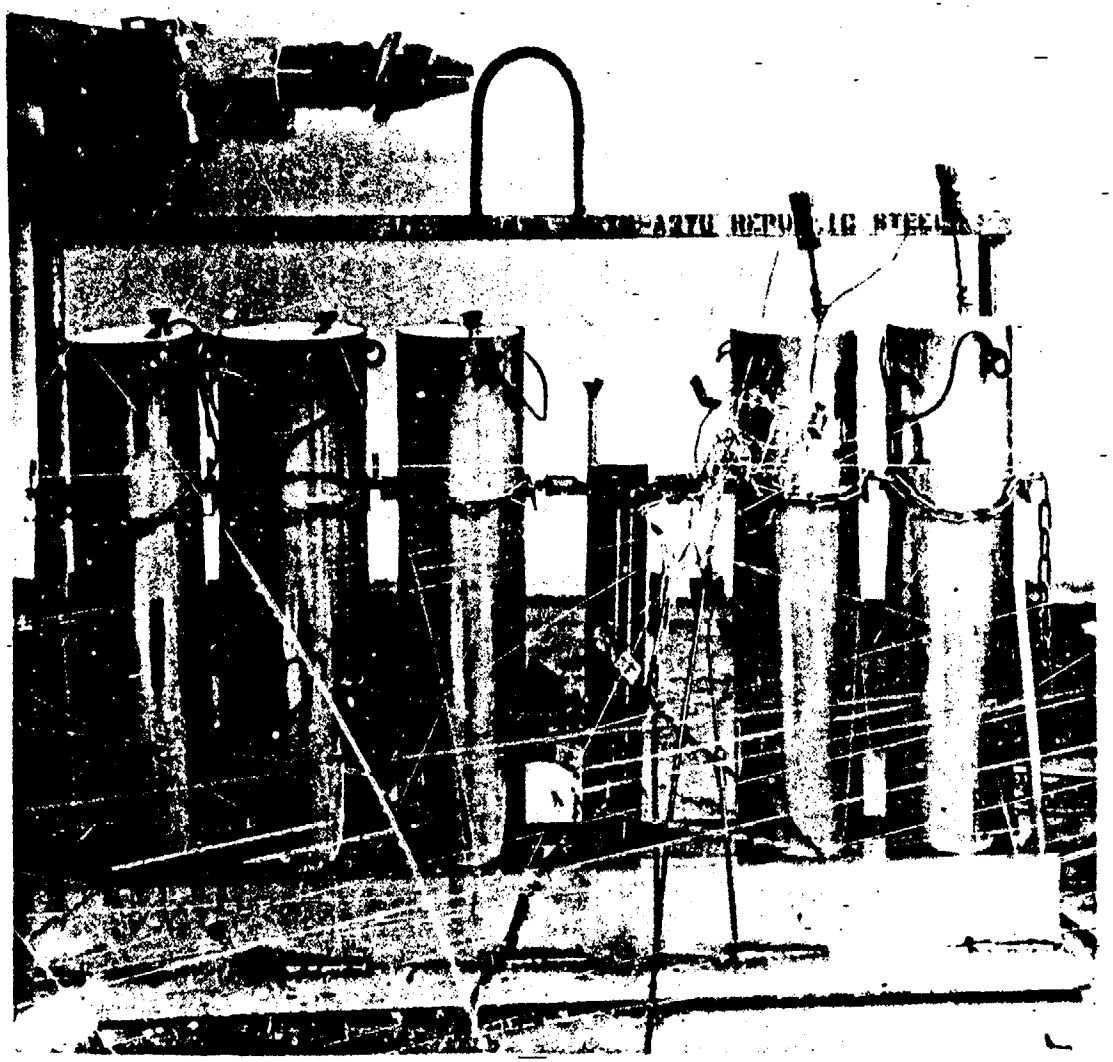

FIGURE 3. The Insulated Containers in a Holding Rack in the Hot Cell

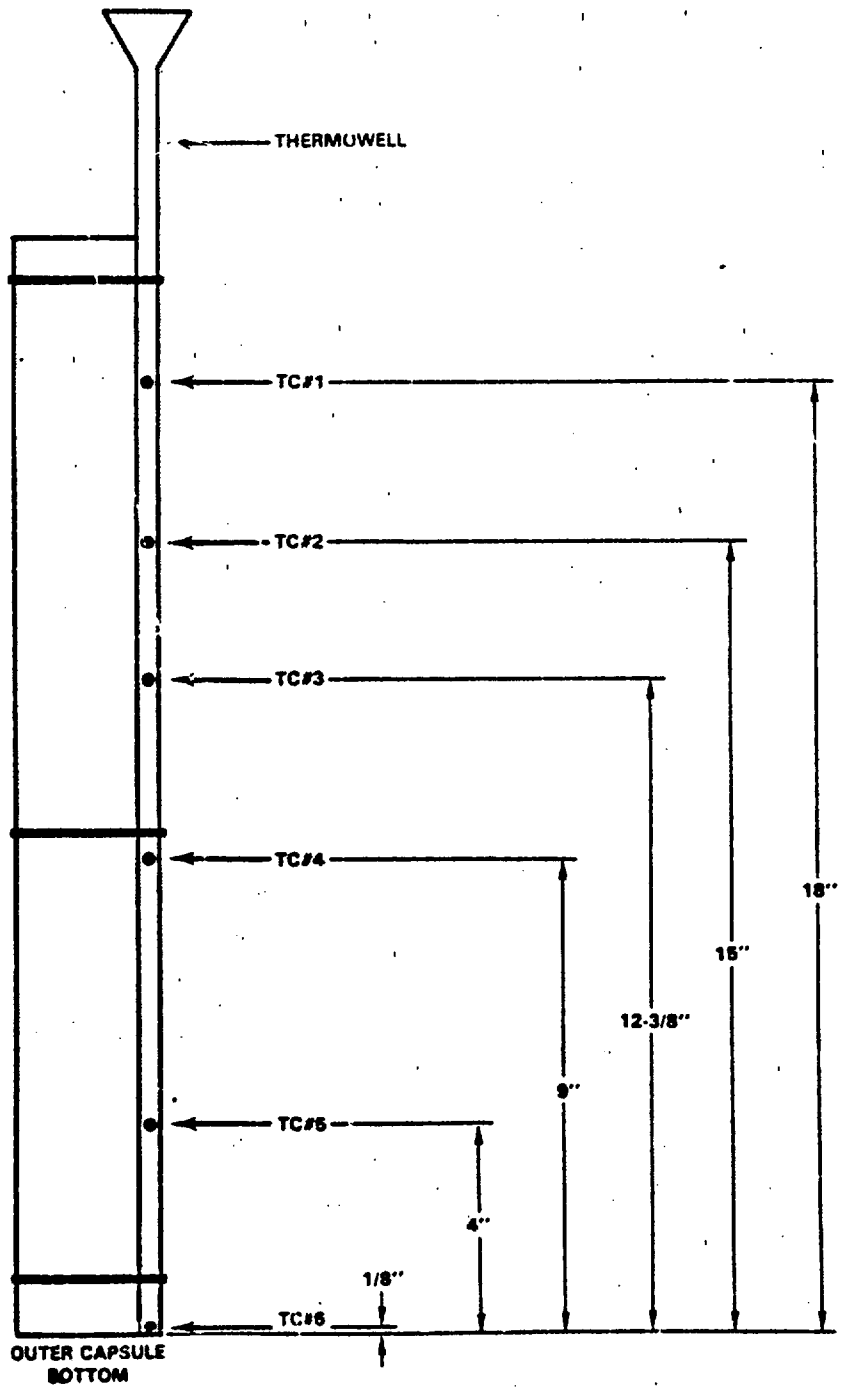

FIGURE 4. Locations where the Capsule Surface Temperatures are Measured

exist between the middle and ends of each capsule. The temperature readings are normally taken on a weekly basis.

The temperature readings obtained provide a measure of the surface temperature of the outer capsule. It was impossible to measure directly the inner capsule/CsCl interface temperature. Therefore, the inner capsule/CsCl interface temperature must be calculated from the outer capsule surface temperature. In order to determine the relationship between the outer capsule surface temperature and the inner capsule/CsCl interface temperature, extensive heat transfer studies were carried out with an electrically heated dummy WESF capsule. Data from the heat transfer studies were also used to design the insulated containers to assure the test capsules reached the required aging temperature.

4.5 CAPSULE SECTIONING AND EXAMINATION

The test capsules are shipped to ORNL for sectioning and examination. In the case of the thermally-aged capsules, the capsules are shipped to ORNL without removing the contained CsCl. At ORNL, the outer capsules are opened and the inner capsules removed. The two zero-time inner capsules were sectioned as shown in Figure 5. Four ring sections were cut from each inner capsule, as shown, and then a small sample was cut from each ring for subsequent examination. Each sample contained an area where the capsule wall thickness had been measured. Each sample was mounted lengthwise, ground to the midpoint, polished, and photomicrographs of the reaction zone obtained. After etching, additional micrographs of the sample were obtained.

The thermally-aged inner capsules were sectioned in slightly different locations than the zero-time capsules. This is necessary because of the temperature gradients that exist over the length of the test capsules during aging. The maximum interface temperature does not correspond to any of the four locations where test samples were taken from the zero-time capsules. Sectioning of the aged capsules was adjusted so that a sample is obtained at the surface element passing through the measurement areas and the point of maximum temperature. This occurs at a point about nine inches up from the bottom of the outer capsule, or between measurement points 5 and 6 on the inner capsule. Since the initial wall thickness along a surface element of a

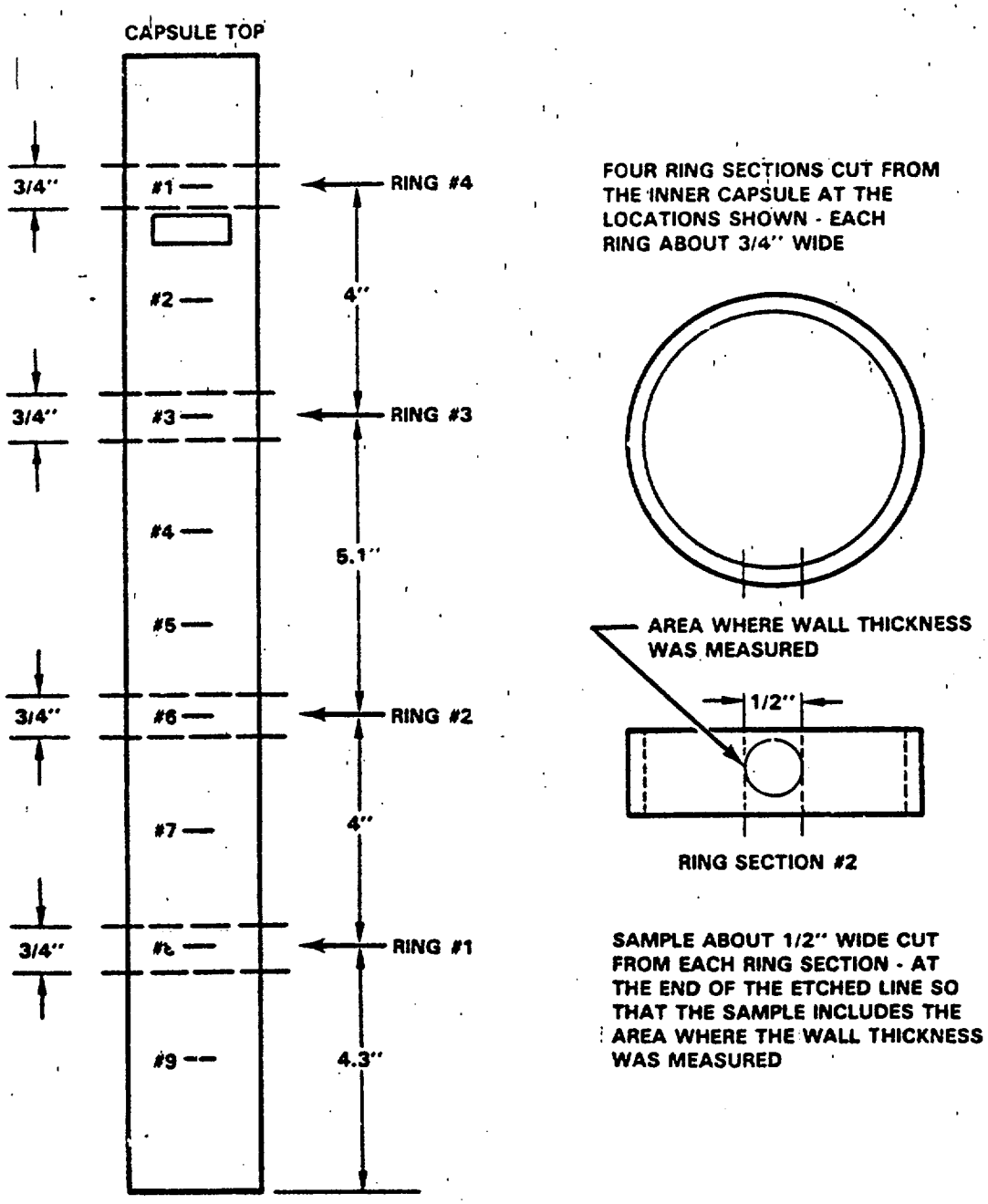

FIGURE 5. Sectioning of the Zero-Time Inner Capsules

5.0 TEST RESULTS

Thermal aging of the three-month (2208-h) capsule was completed in FY 1982. Thermal aging of the six-month (4392-h) and one-year (8784-h) capsules was completed during FY 1983. Destructive examination of the zero time, three month and six month capsules was also completed during the year. Destructive examination of the one year capsule was to be completed in FY 1983, but not in time to include the test results in this report.

In examining the test capsules to determine the extent of metal attack by the WESF CsCl, it was impossible to obtain a precise measure of the corrosion. Although the wall thickness of the inner capsule was accurately measured at 18 locations before testing, it was not possible to obtain similar measurements after testing. Adhesion of CsCl to the capsule surface makes it difficult to measure the wall thickness accurately using a micrometer or similar instrument. The CsCl could not be leached from the metal surface without destroying any reaction layer present. Determining the wall thickness of mounted specimens was equally difficult because of alignment problems. For example, when the metal sample is mounted in plastic in the hot cell for metallographic examination, the sample alignment could be as much as 15° to 20° from a vertical plane (see Figure 6). For a capsule having an initial wall thickness of 0.140 in. at a given location, this error in mounting alignment could result in an error of up to about 0.010 in. in the measured wall thickness. This error would tend to reduce the estimate of metal corrosion since it exaggerates the residual wall thickness of the test samples.

The metal corrosion can be estimated from photomicrographs of the test specimens, assuming the specimens have not suffered extensive uniform corrosion of the surface. Metal attack determined from the photomicrographs represent the minimum attack at a given location, since it is impossible to tell the initial location of the metal surface from the micrographs if there has been significant uniform corrosion. Efforts are still underway to accurately determine the residual wall thickness of the various test specimens. The corrosion data presented in subsequent sections were estimated from photomicrographs. Therefore, the data given represent a minimum measure of the attack; the actual attack could be significantly greater than the values shown. Hopefully, the discrepancies can be resolved when better measurements on the residual sample wall thickness are obtained.

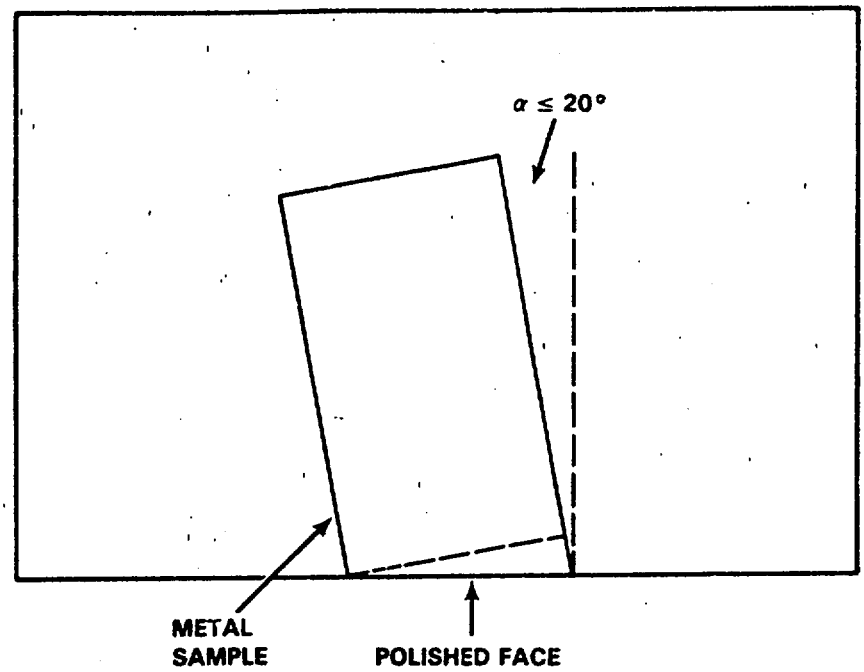

FIGURE 6. Mounting of the Metal Samples Showing the Problem of Sample Alignment

Thermal aging of the three remaining WESF CsCl capsules is continuing. The next capsule will be taken off test in April 1984 after two years at temperature.

5.1 ZERO-TIME CAPSULES

Samples taken from the two zero-time capsules were subjected to metallographic examination. Table 3 provides estimates of the metal attack observed as determined from the photomicrographs obtained of each sample (within the limits described in the previous section). The photomicrographs of the various samples are shown in Figures 7 and 8. Etching of the samples was accomplished using an HNO_3-HCl mixture.

Ring 4 Location 1

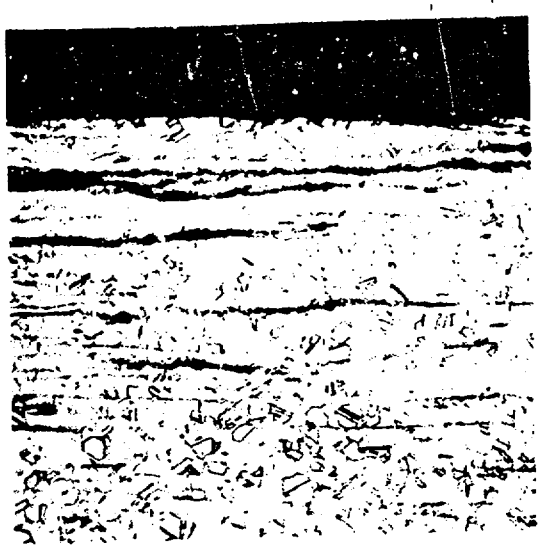

Ring 3 Location 3

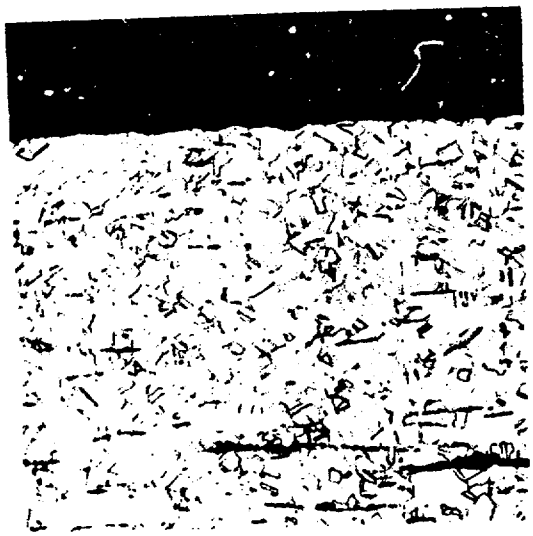

Ring 2 Location 6

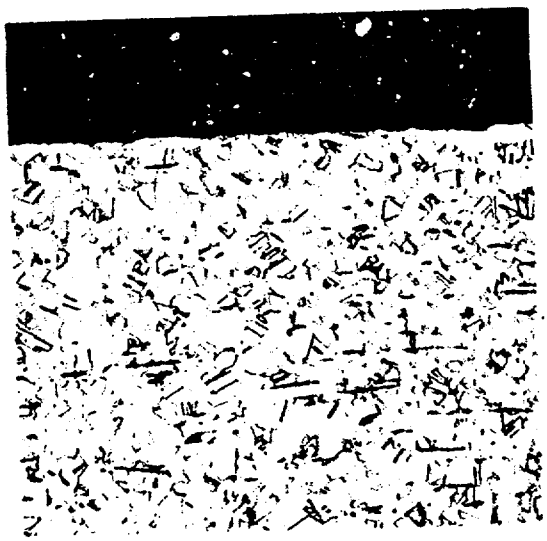

Ring 1 Location 8

200 µm

100X

FIGURE 7. Photomicrographs from Samples of Zero Time Capsule 19459

Ring 4 Location 1

Ring 3 Location 3

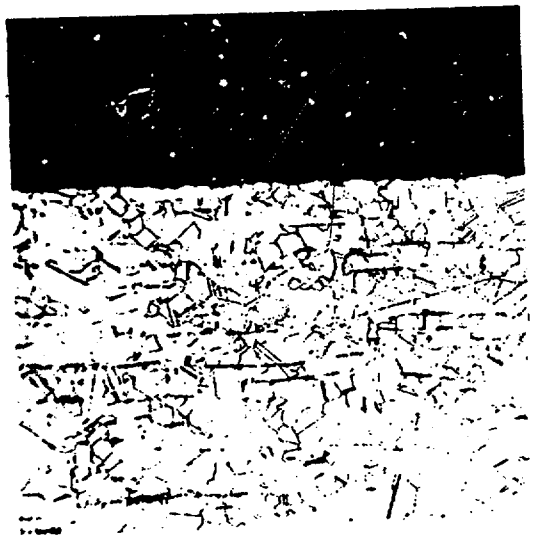

Ring 2 Location 6

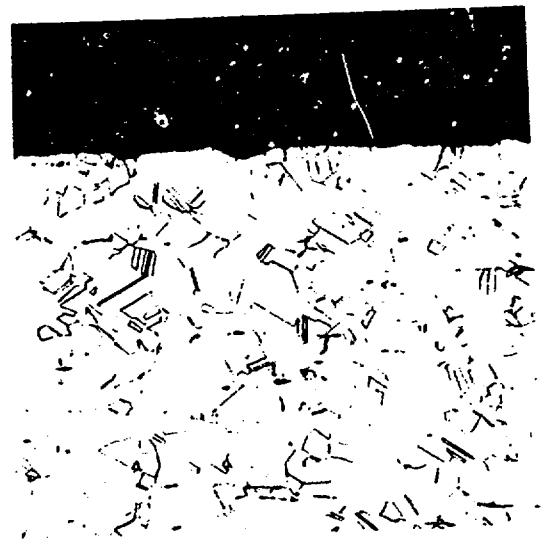

Ring 1 Location 8

200 μm

100X

FIGURE 8. Photomicrographs from Samples of Zero Time Capsule 19073-F

The photomicrographs indicate that filling the capsules with molten CsCl produces relatively little attack of the 316L SS (<0.001 in.). The attack seems to be somewhat greater in the upper part of the capsules. The attack appears to involve general surface dissolution with some limited grain boundary attack at some locations.

TABLE 3. Estimates of Metal Attack in the Zero-Time Capsules

Capsule No.	Depth of Attack,[a] μm (mils)			
	Ring No. 1[b]	Ring No. 2	Ring No. 3	Ring No. 4
19459	10 (0.4)	8 (0.3)	25 (1.0)	25 (1.0)
19073F	18 (0.7)	18 (0.7)	25 (1.0)	18 (0.7)

(a) Minimum attack estimated from photomicrographs - see discussion in text on page 5.1.
(b) See Figure 4 for ring locations on capsule.

5.2 THERMAL AGING TESTS

Figures 9, 10, and 11 show the average surface temperature profiles for the WESF CsCl capsules aged for 2208, 4392, and 8784 h, respectively. The average maximum metal/CsCl interface temperature was 455°C for the 2208-h capsule, 449°C for the 4392-h capsule, and 460°C for the 8784-h capsule. The maximum interface temperature occurred about nine inches up from the bottom of the outer capsule in each case.

Figures 12, 13, and 14 show the inner capsule surface temperature at various locations as a function of time for each of the three aged capsules. All three capsules exhibit substantial fluctuations in temperature as a function of time at each location.

Metal samples from the three aged capsules were subjected to metallographic examination. Estimates of metal attack in the 2208- and 4392-h capsules, based on the photomicrographs obtained, are presented in Table 4. The limitations on the accuracy of the corrosion estimates discussed in the previous sections also apply to the results for the two thermally-aged capsules completed in time to include the results with this report. Photomicrographs of the samples from the 2208- and 4392-h capsules are shown in Figures 15 and 16.

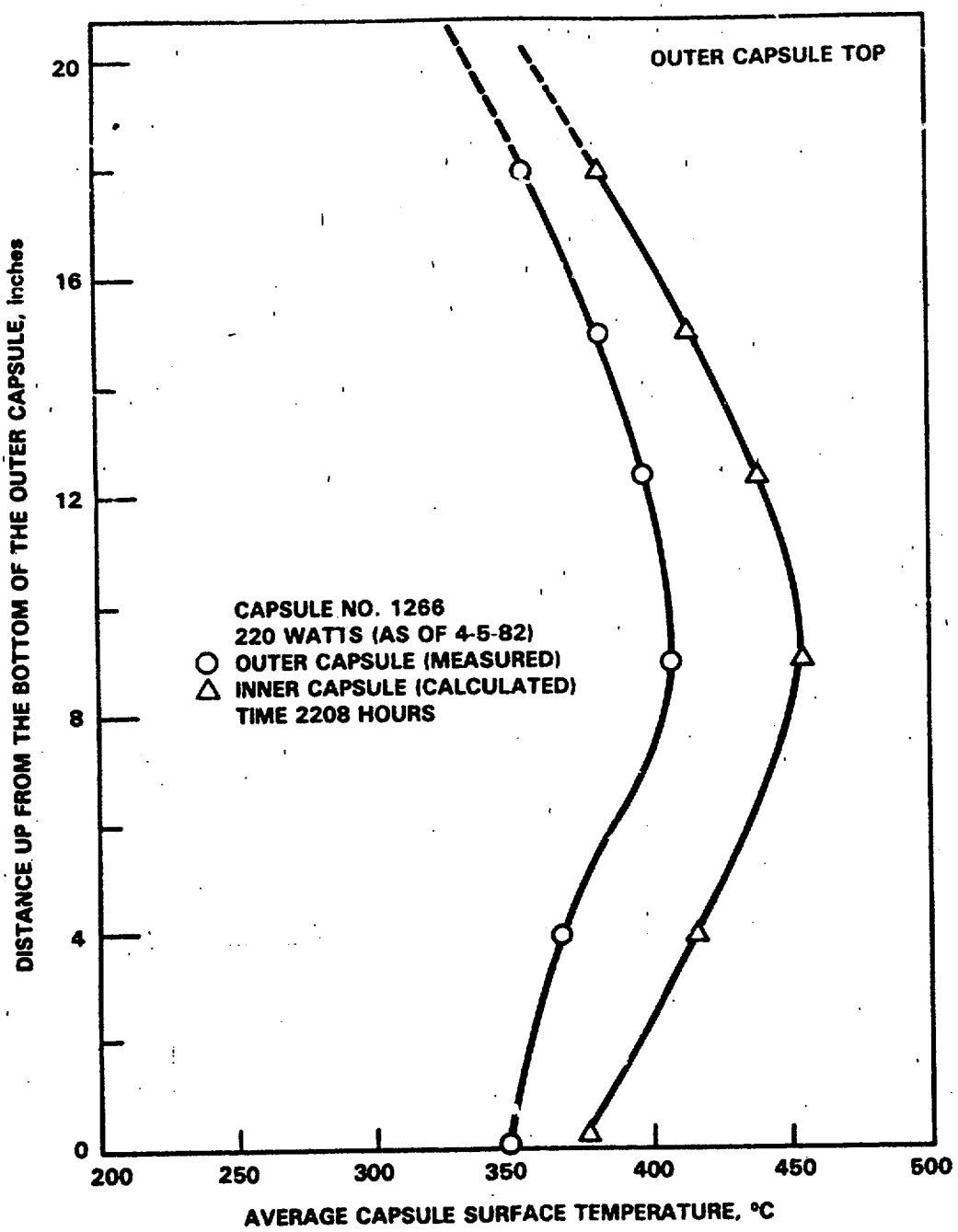

FIGURE 9. Average Temperature Profiles for the WESF Capsule Held at Temperature for 2208 Hours

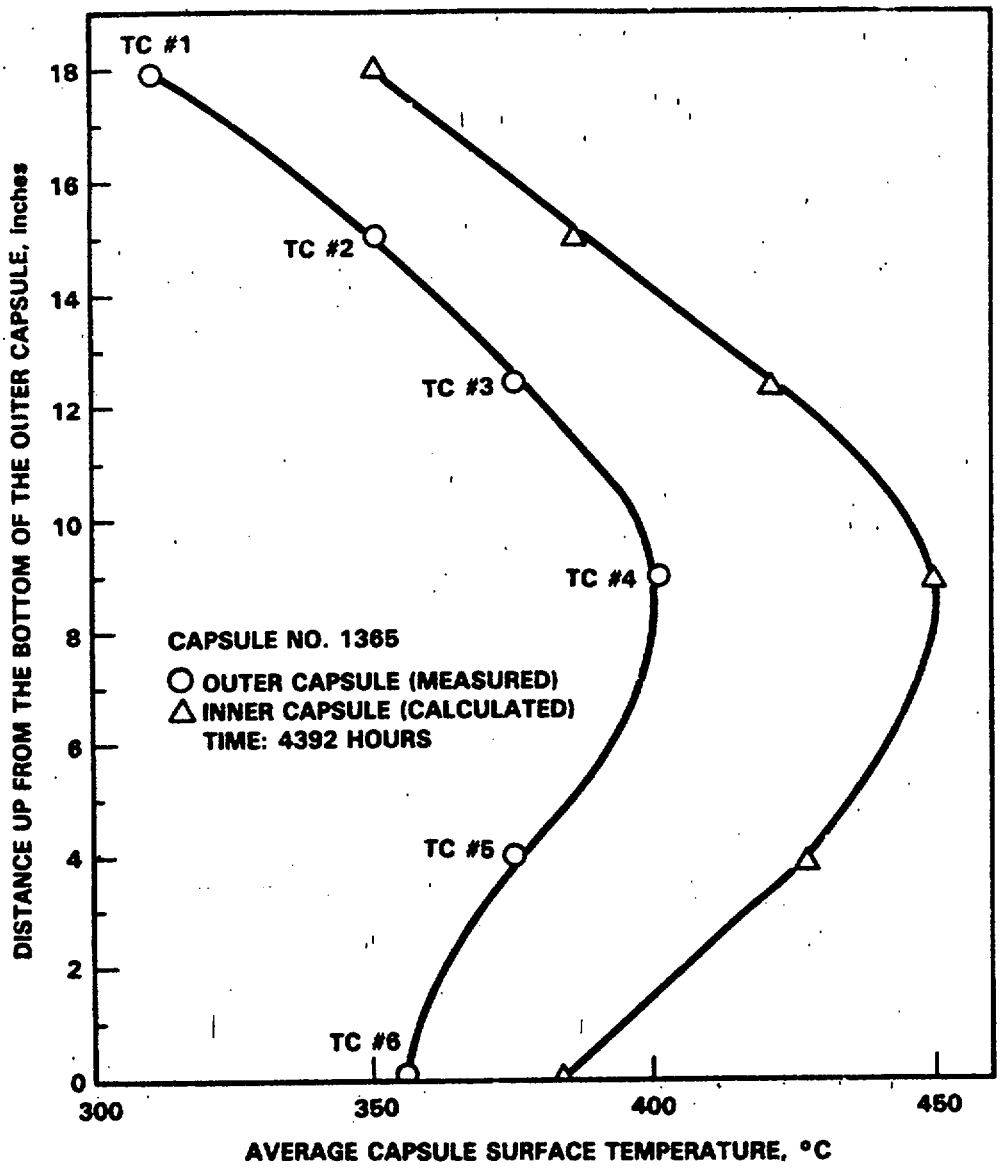

FIGURE 10. Average Temperature Profiles for the WESF Capsule Held at Temperature for 4392 Hours

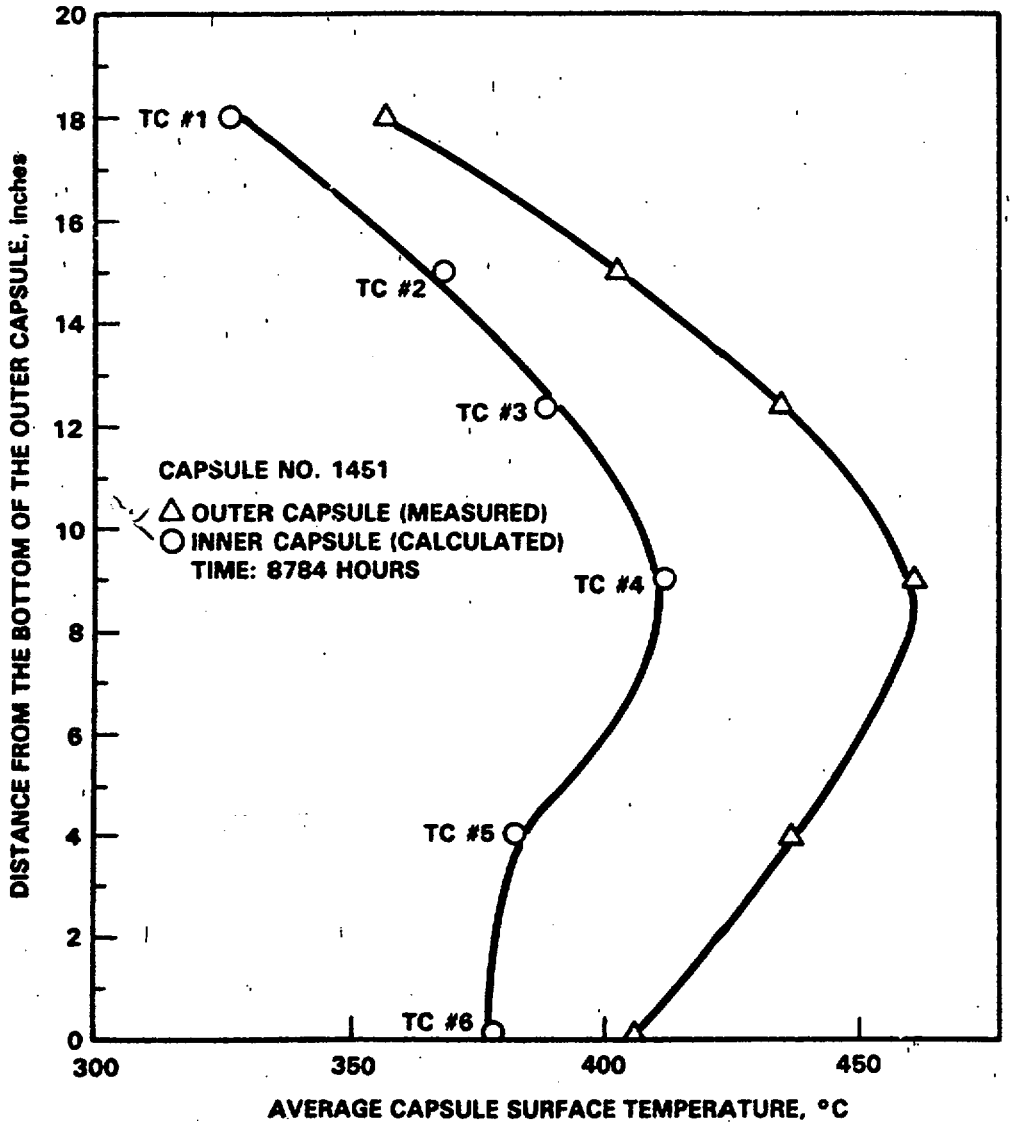

FIGURE 11. Average Temperature Profiles for the WESF Capsule Held at Temperature for 8784 Hours

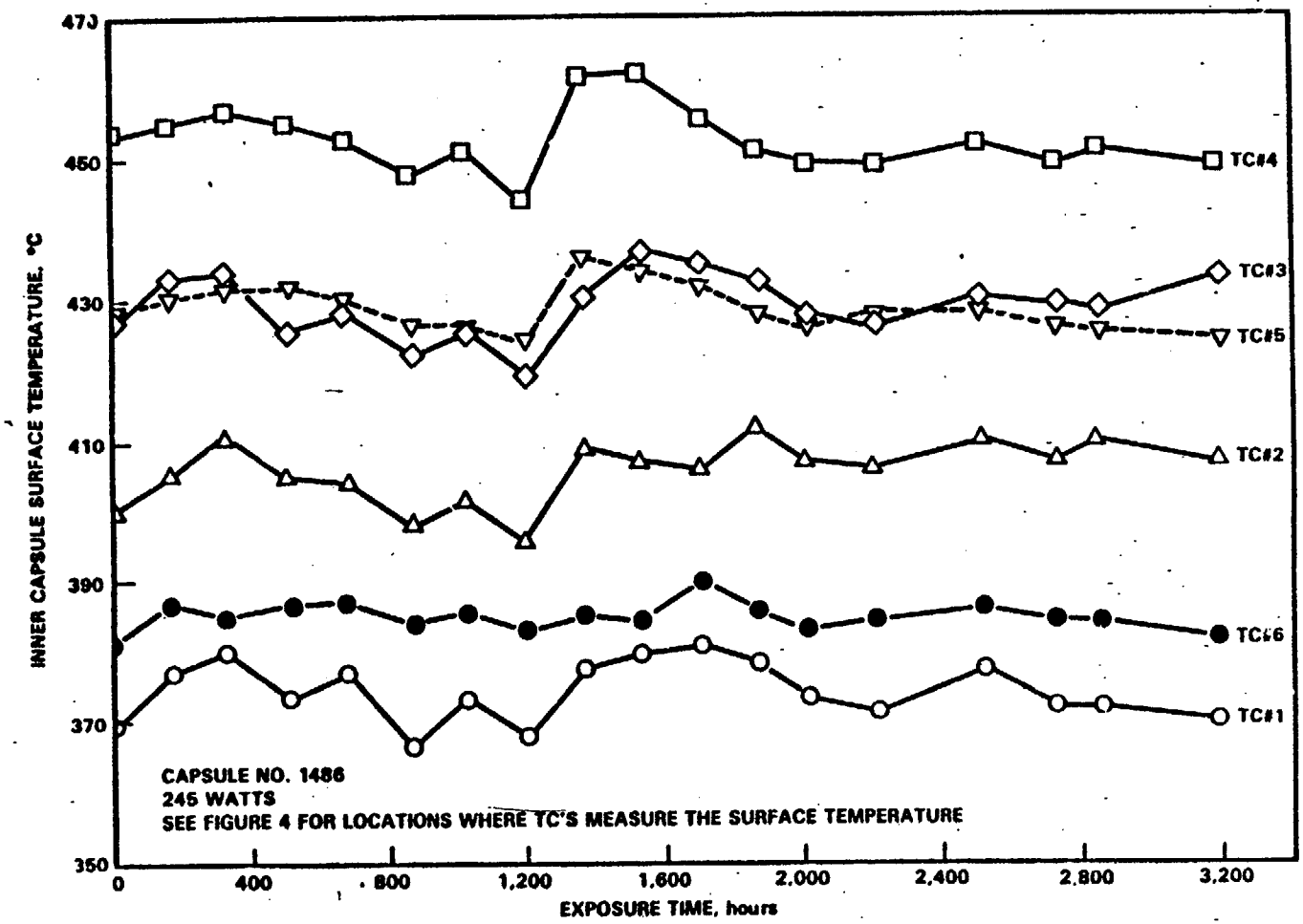

FIGURE 12. Temperature Fluctuations Observed with the Capsule Held at Temperature for 2208 Hours

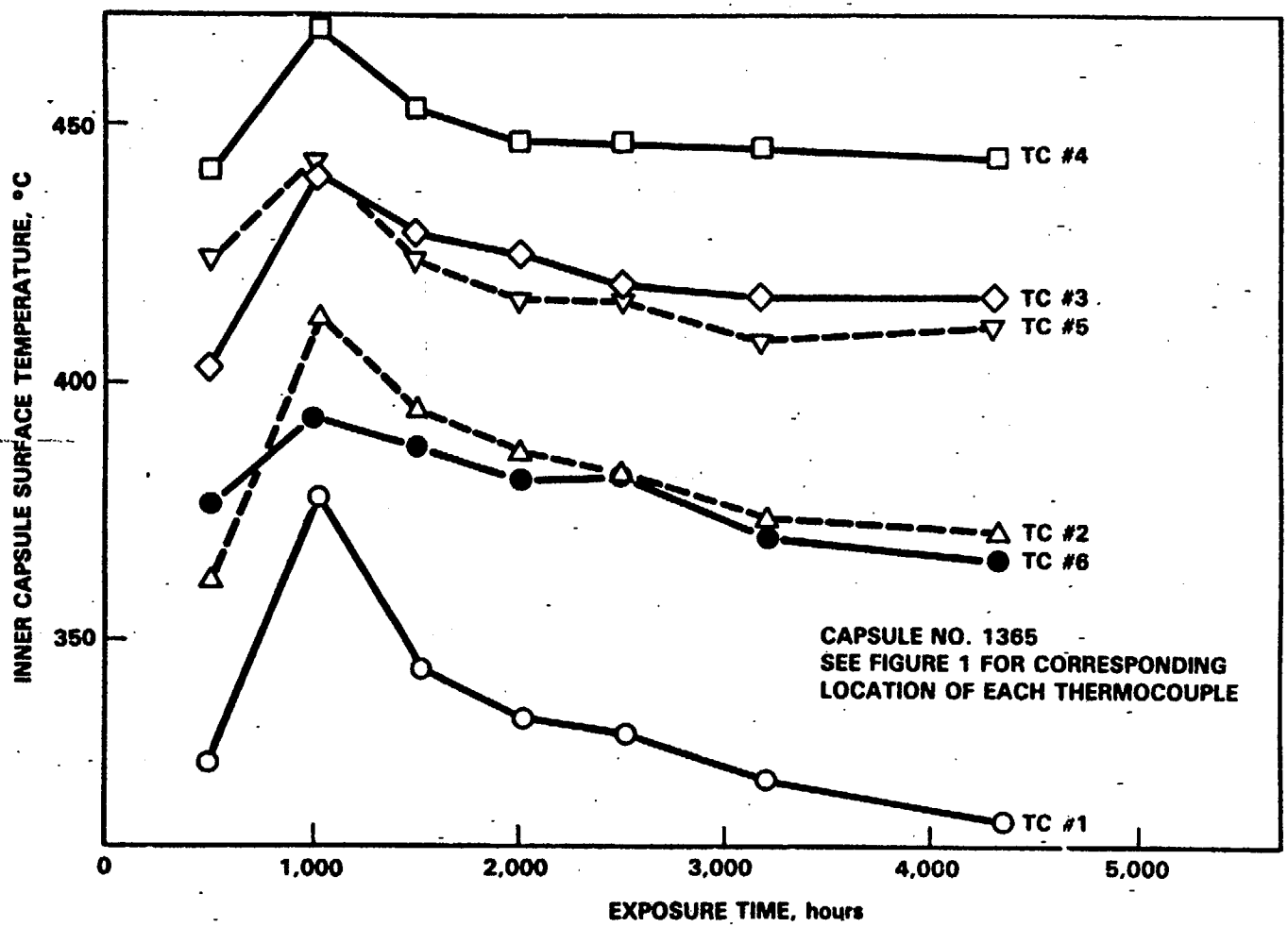

FIGURE 13. Temperature Fluctuations Observed with the Capsule Held at Temperature for 4392 Hours

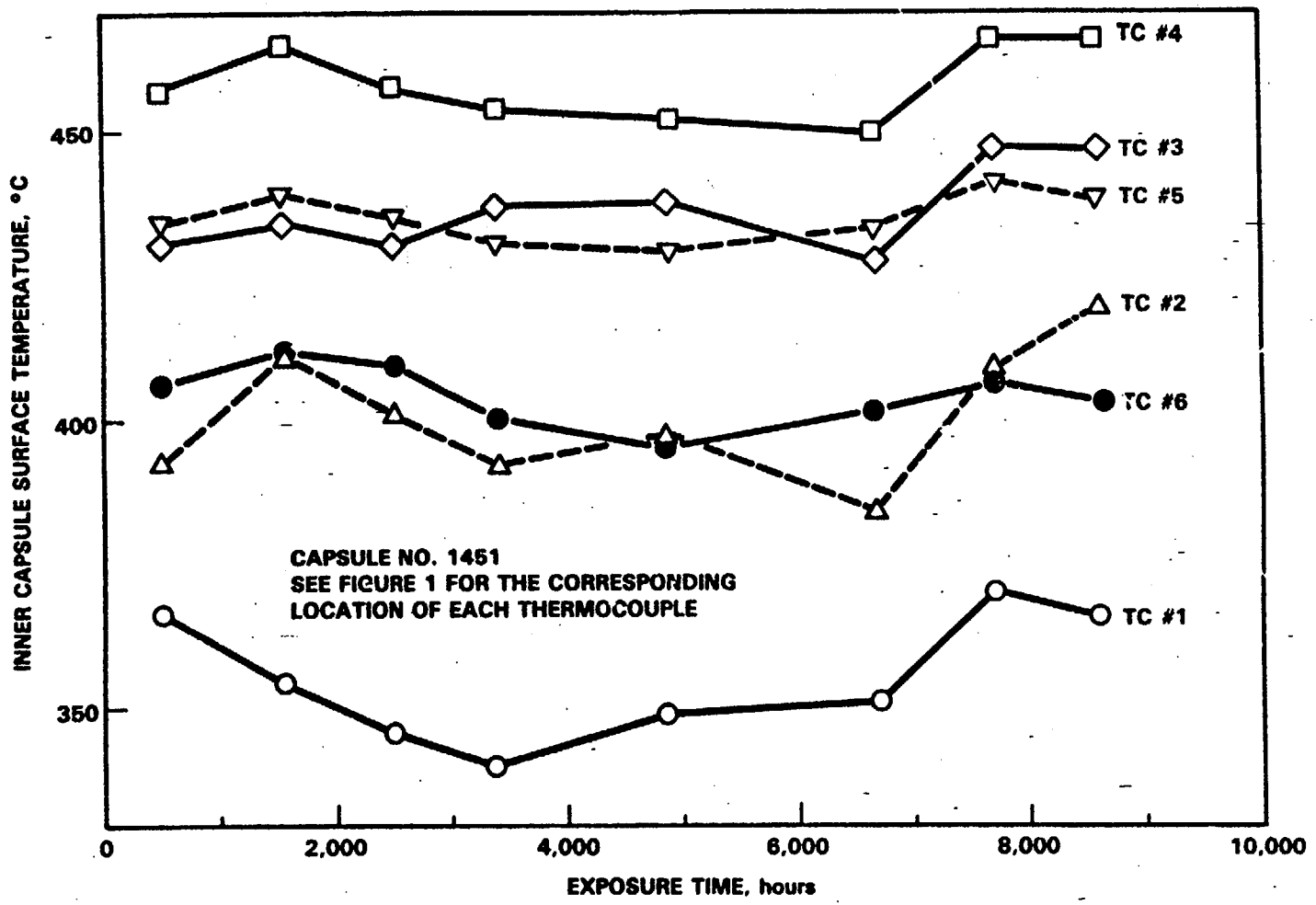

FIGURE 14. Temperature Fluctuations Observed with the Capsule Helo at Temperature for 8784 Hours

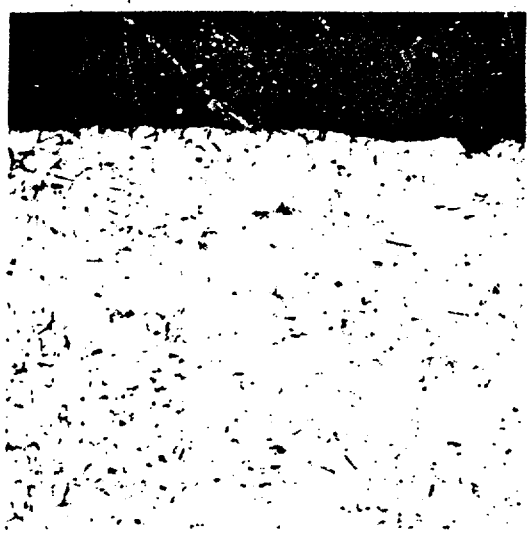

Ring 4 Location 1

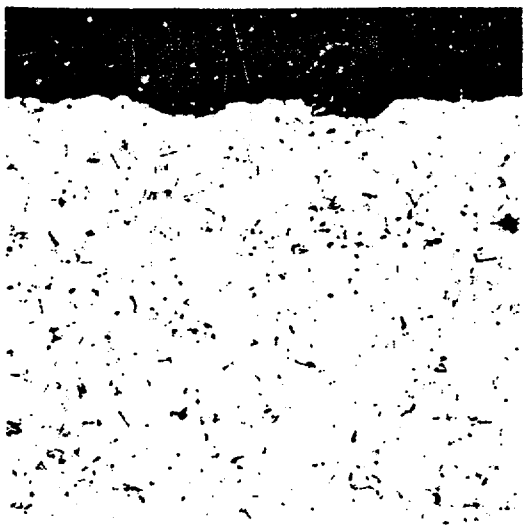

Ring 3 Location 3

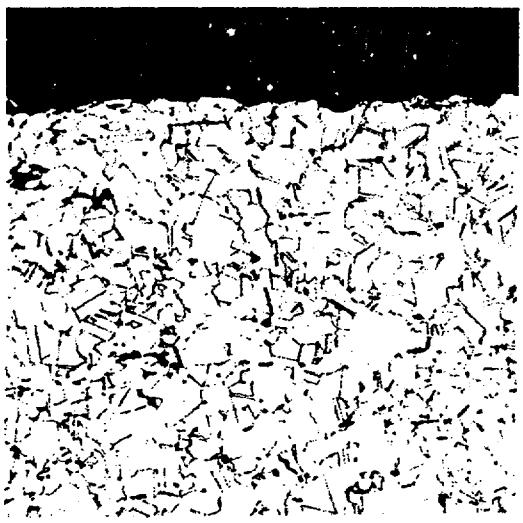

Ring 2 Location 5

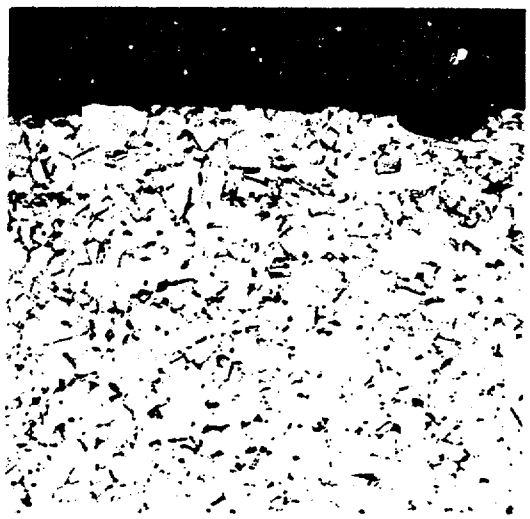

Ring 1 Location 8

200 μm

100X

FIGURE 15. Photomicrographs of Samples Taken from the Capsule that was Thermally Aged for 2288 Hours - Showing the Metal/CsCl Interface

Ring 4 Location 1

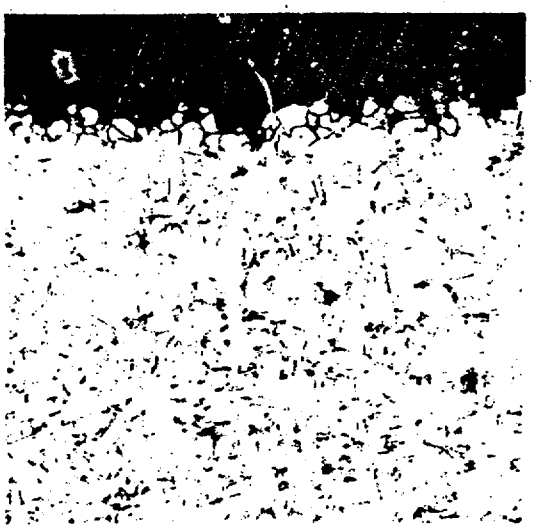

Ring 3 Location 3

Ring 2 Location 5

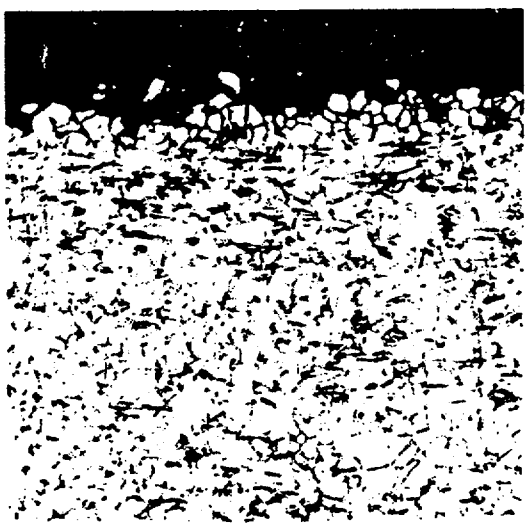

Ring 1 Location 8

200 µm

100X

FIGURE 16. Photomicrographs of Samples Taken from the Capsule that was Thermally aged for 4392 Hours - Showing the Metal/CsCl Interface

Selected samples from the three thermally-aged samples are being subjected to electron microprobe analyses. The work will be completed next fiscal year. The results obtained will be used to help interpret the corrosion data and to try to identify corrosion mechanisms.

The results presented in Table 4 indicate that the maximum metal attack occurs near the bottom of each capsule and not at the point of maximum temperature. Metal attack was much greater in the 4392-h capsule than in the 2208-h capsule. In addition, two of the samples from the 4392-h capsule exhibited extensive intergranular attack that was not observed with the 2208-h capsule. Metal attack in the 2208-h capsule appeared to involve general surface dissolution with some pitting.

Metal attack in the thermally-aged capsules was much greater than that observed in the initial compatibility studies for the WESF program.[2] In the original studies, the maximum corrosion observed when 316L SS was exposed to radioactive CsCl at 400°C for up to 8760 h was 0.001 in. (25 μm). This compared with a maximum attack of about 0.004 in. (110 μm) after 4392 h in the current study. The increased attack observed in the current study is probably due to an increase in impurity levels in the CsCl. Additional work will be required, however, to confirm this assumption.

If one plots the maximum attack observed in the test capsules as a function of exposure time, the corrosion rate appears to be linear with time (see Figure 17). Additional test points are needed, however, to determine the form of the corrosion rate equation. If the results from the remaining capsules under test show that the corrosion rate continues to exhibit a linear relationship with time, it raises serious questions as to the long-term containment of WESF CsCl at the elevated temperatures tested.

TABLE 4. Estimated Metal Attack[a] in the Thermally-Aged WESF CsCl Capsules

Exposure, hours	Ring No. 1[b]		Ring No. 2		Ring No. 3		Ring No. 4	
	Average Temp, °C	Attack μm, mils	Average Temp, °C	Attack μm, mils	Average Temp, °C	Attack μm, mils	Average Temp, °C	Attack μm, mils
2208	415	60(2.4)	455	30(1.2)	420	30(1.2)	354	35(1.4)
4392	430	110(4.3)	449	80(3.2)	400	85(3.4)	350	50(2.0)
8784	432	(c)	460	(c)	415	(c)	356	(c)

(a) Minimum attack estimated from photomicrographs--see discussion in text on p. 30.
(b) See text and Figure 5 for ring locations in capsules.
(c) Results will be presented at a later date.

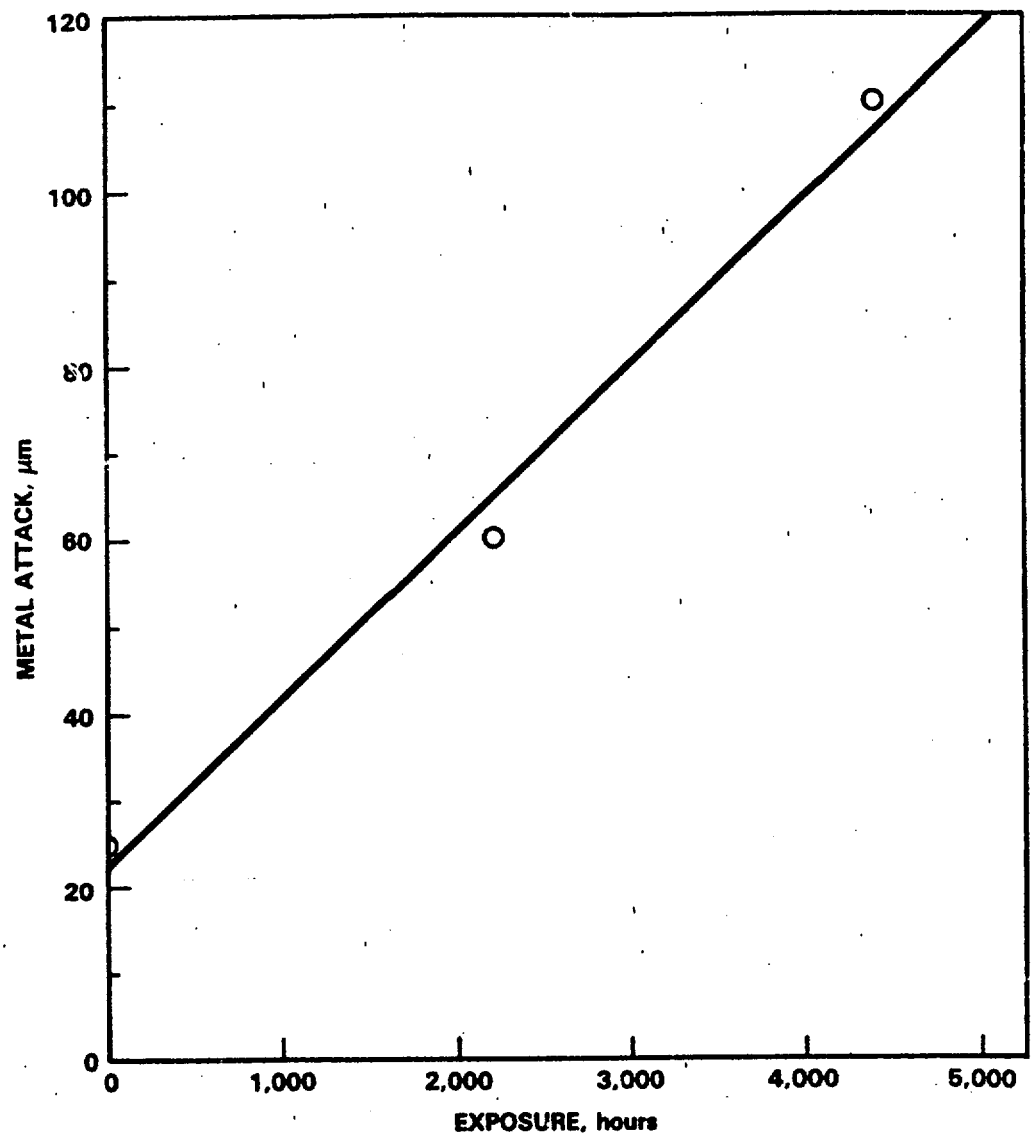

FIGURE 17. Maximum Metal Attack as a Function of Exposure Time - As Determined from Photomicrographs of Samples Taken from the Test Capsules

As discussed earlier, the corrosion data presented in Tables 3 and 4 were estimated from sample photomicrographs. These estimates represent the minimum level of attack that has occurred in each capsule. The attack could be significantly greater than the values given in Tables 3 and 4 if the samples have suffered any degree of general surface dissolution which would not be evident from the micrographs. Some initial attempts were made to determine the residual wall thickness of the mounted samples from which the photomicrographs were obtained. Table 5 lists the initial and residual wall thickness for each of the test specimens examined from one of the two zero-time capsules and the two thermally-aged capsules. In almost every case, the measured residual wall thickness of a sample was equal to or greater than the initial wall thickness. These discrepancies reflect the problems involved in accurately determining the residual wall thickness of a given mounted sample. The results do indicate, however, that the maximum metal corrosion in the test capsule cannot exceed the values given in the test capsule cannot exceed the values given in Tables 3 and 4 by more than about 0.010 in. (254 μm). Additional work is underway at ORNL to obtain more accurate measurements of the residual wall thicknesses of the test samples. This, in turn, will permit more reliable estimates of the metal attack.

TABLE 5. Wall Thickness Data for the WESF CsCl Test Capsules

Capsule No.	Exposure, h	Location Ring No.	Wall Thickness, in. (μm) Initial	Wall Thickness, in. (μm) Residual[a]	Wall Thickness Difference, in. (μm)
19073F	Zero	1	0.139(3530)	0.144(3660)	+0.005(+130)
		2	0.137(3480)	0.140(3560)	+0.003(+80)
		3	0.139(3530)	0.149(3780)	+0.010(+250)
		4	0.139(3530)	0.138(3510)	-0.001(-25)
19073G	2208	1	0.145(3680)	0.150(3810)	+0.005(+130)
		2	0.144(3660)	0.152(3860)	+0.008(+200)
		3	0.146(3710)	0.153(3890)	+0.007(+180)
		4	0.146(3710)	0.146(2710)	0(0)
19073D	4392	1	0.138(3510)	0.140(3560)	+0.002(+50)
		2	0.137(3480)	0.138(3510)	+0.001(+25)
		3	0.138(3510)	0.138(3510)	0(0)
		4	0.139(3530)	0.148(3760)	+0.009(+230)

(a) Residual wall thickness determined from mounted samples.
(b) Difference = residual wall thickness - initial wall thickness

5.3 METAL CONTROL SPECIMENS

The 316L SS control samples held at 400°C, 450°C, or 500°C for 2200, 4400, and 8800 h were subjected to metallographic examination. The photomicrographs obtained are shown in Figures 18 through 20. Examination of the photomicrographs indicate that aging of the alloy at 400°C and 450°C for up to 800 h has little effect on the microstructure of the 316L SS. This agrees with the results obtained with the thermally-aged WESF CsCl capsules. Aging of the alloy at 500°C for up to one year produced some grain boundary precipitation. There may also be some increase in the Figure 18 intragranular precipitates in the samples aged at 450°C and 500°C. The formation of grain boundary precipitates could infuence attack of the metal by the CsCl if the interface temperature exceeds 450°C for any extended period of time.

5.4 EXTERNAL CAPSULE CORROSION

When the 4392-h capsule was opened for metallographic examination, it was found that the outer surface of the inner capsule was discolored and possibly pitted in several locations. Similar damage was not observed with the two zero-time and 2208-h capsules. Additional work was authorized at ORNL to examine the affected areas to determine the extent of the possible damage and identify the probably cause(s). A total of seven areas on the outer surface were examined; these areas are shown in Figures 21 and 22.

Photomicrographs of the affected areas are shown in Figures 23 through 31. The micrographs indicate extensive pitting has occurred at most of the affected areas. The micrographs also indicate the formation of a second phase in most of the affected areas. The maximum attack observed was about 300 μm or 0.012 in. (see Figure 26). This corresponds to about 9% of the initial capsule wall thickness.

Without additional data, it is impossible to determine the composition(s) of the second phases that formed in the affected zones. It is possible that they could be an oxide phase(s) or a modification of the basic 316L SS microstructure. Electron microprobe and/or SEM analysis of the affected areas will be carried out in FY 1984 to help identify the second phases and probable cause(s) of the attack.

At the present time, it is impossible to identify the cause of the attack. Current speculation is that the attack results from arcing, which occurs during the electropolishing operation. The electropolishing step is used to decontaminate the outer surface of the inner capsule after the capsule is filled with CsCl and welded closed, but before it is inserted in the outer capsule. Experimental tests are planned for a separate program to determine if the electropolishing operation is responsible for the attack observed.

When the 8784-h capsule was opened at ORNL, it was found that the outer surface of the inner capsule was also discolored and/or possibly pitted at several locations. The affected areas did not appear to be as extensive as with the 4392-h capsule. Samples from the affected areas may be subjected to metallographic examination after further evaluation.

2200 hr (500X)

4400 hr (500X)

8800 hr (500X)

Figure 18. Metal Control Sample, 400°C.

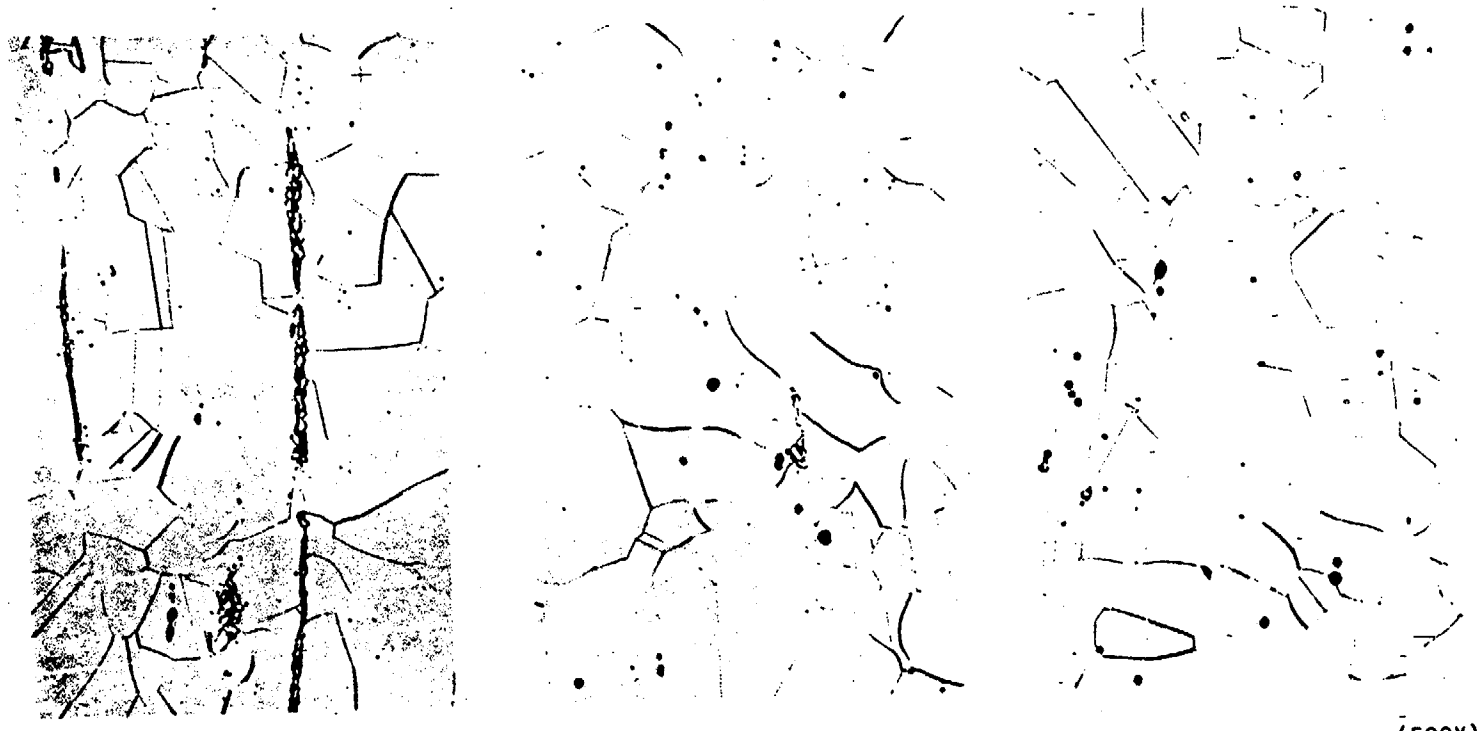

2200 hr (500X) 4400 hr (500X) 8800 hr (500X)

Figure 19. Metal Control Sample, 450°C

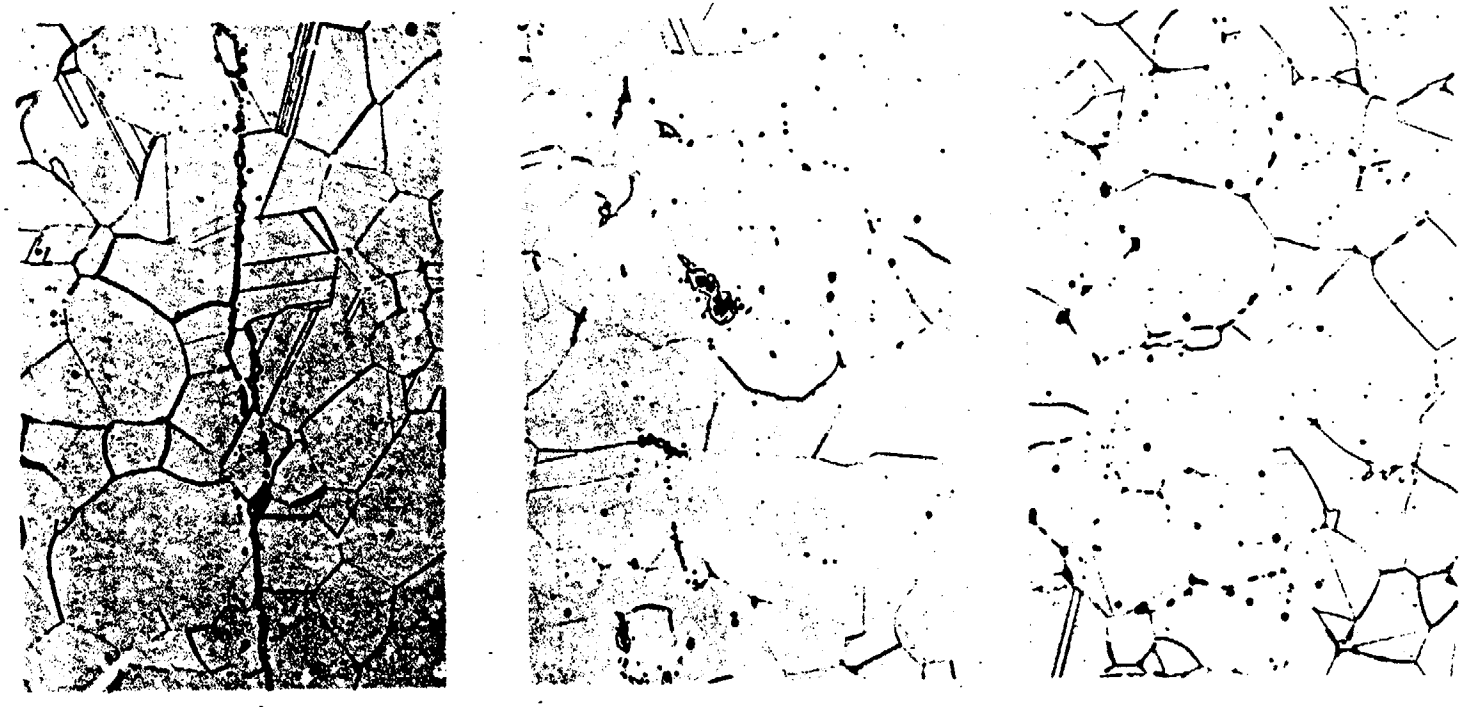

2200 hr (500X) 4400 hr (500X) 8800 hr (500X)

Figure 20. Metal Control Sample, 500°C.

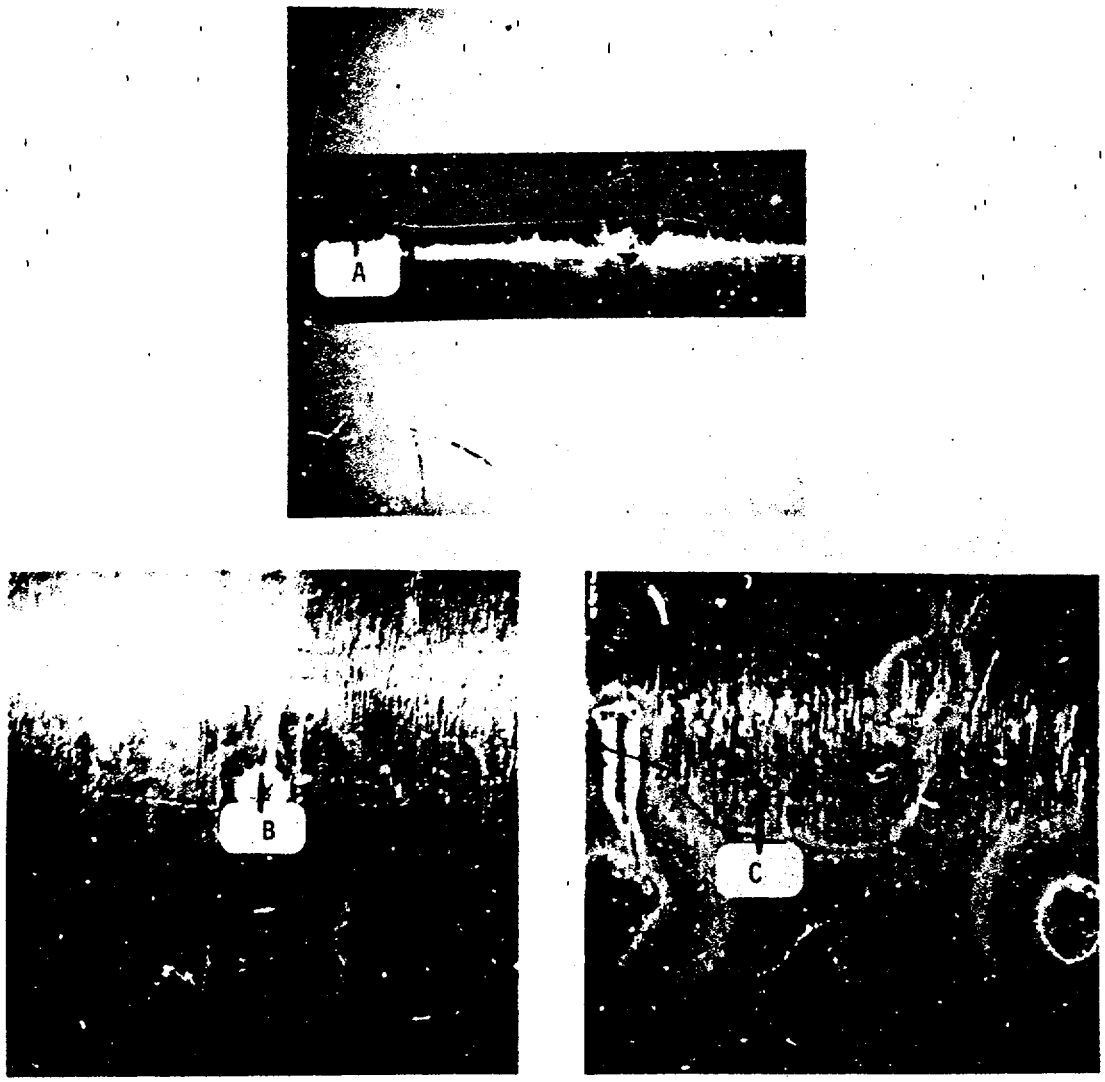

FIGURE 21. Areas on the Outer Surface of the Inner Capsule (from the 4392 Hour Capsule) that were Sampled for Metallographic Examination

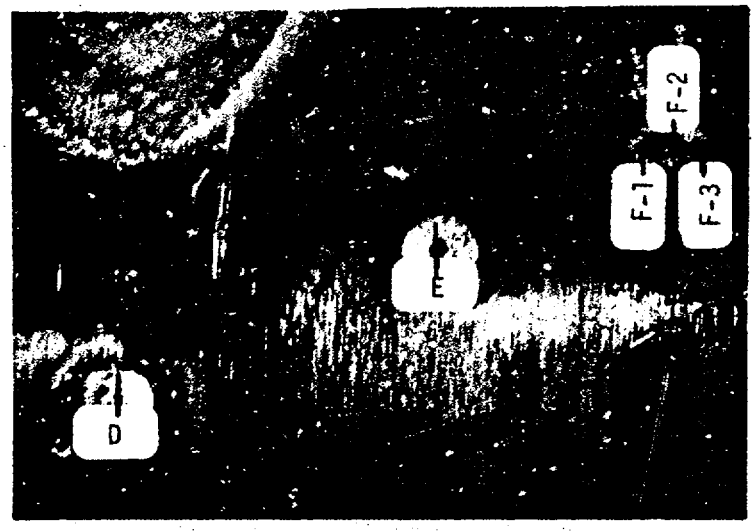

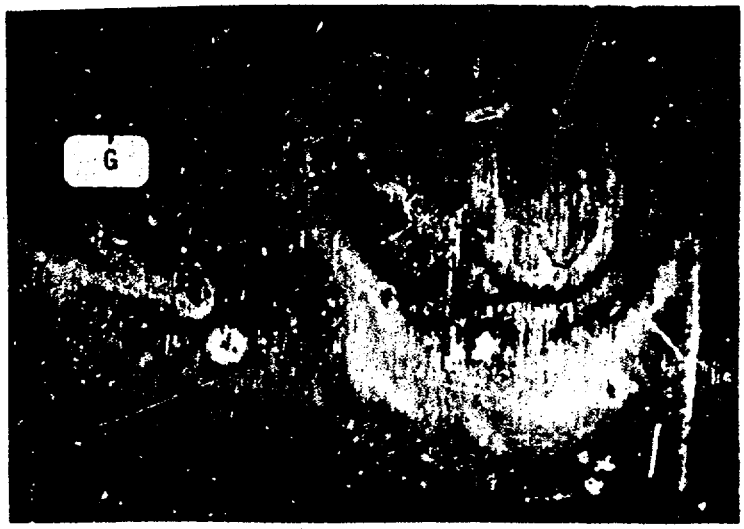

FIGURE 22. Additional Areas on the Outer Surface of the Inner Capsule that were Sampled for Metallographic Examination

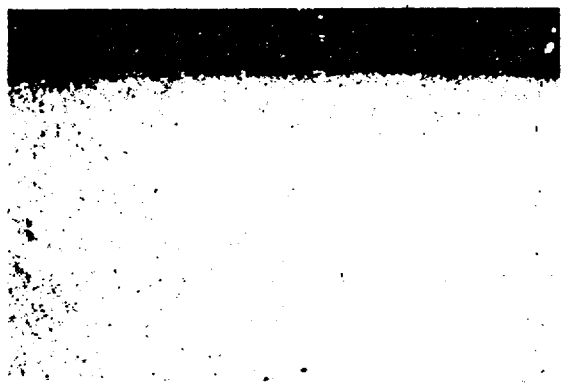

50X

100X

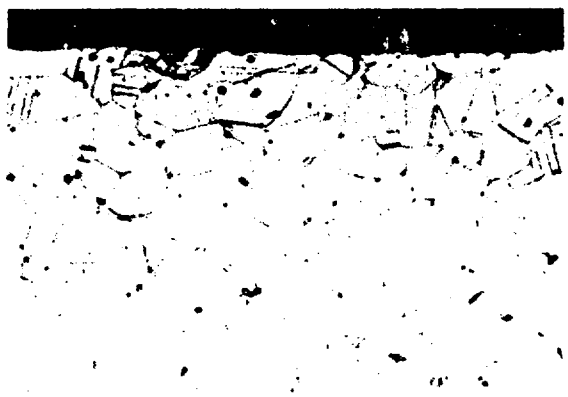

500X

Figure 23. Photomicrographs of Area A, Outer Surface of Inner Capsule.

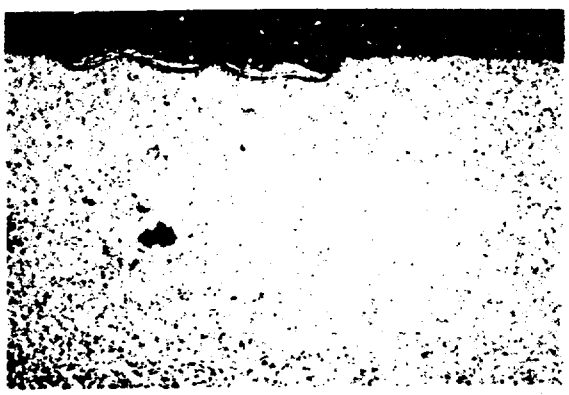

50X

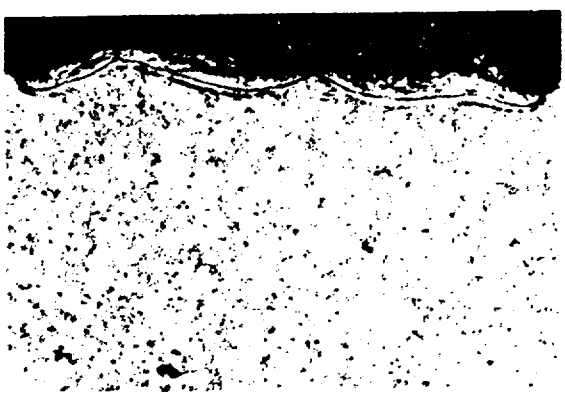

100X

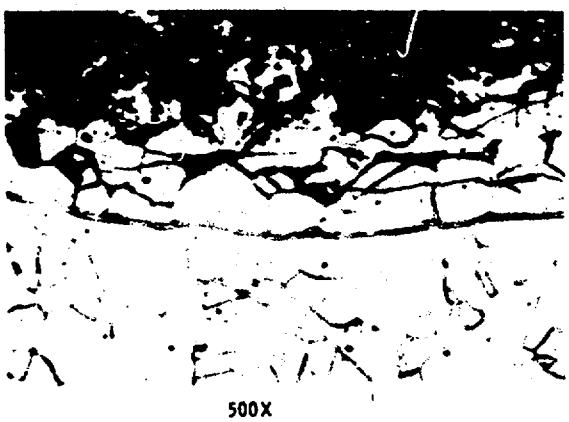

500X

8306099-18

Figure 24. Photomicrographs of Area B, Outer Surface of Inner Capsule.

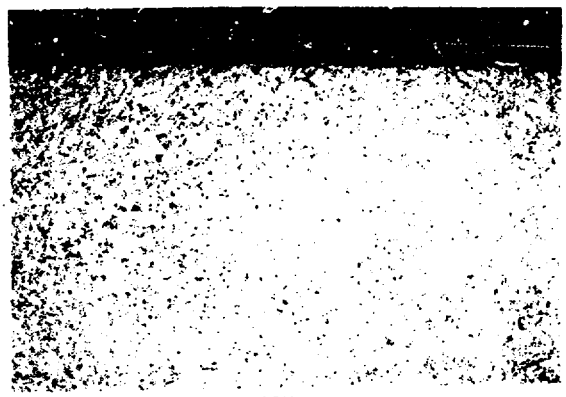

50X

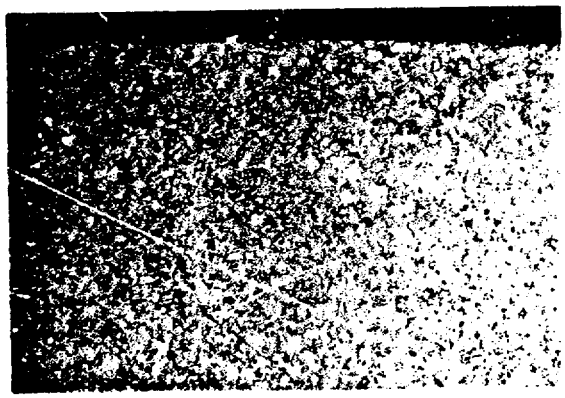

100X

500X

8306099-19

Figure 25. Photomicrographs of Area C, Outer Surface of Inner Capsule.

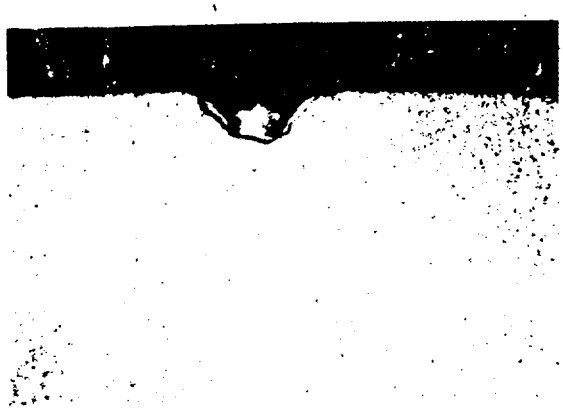

50X

100X

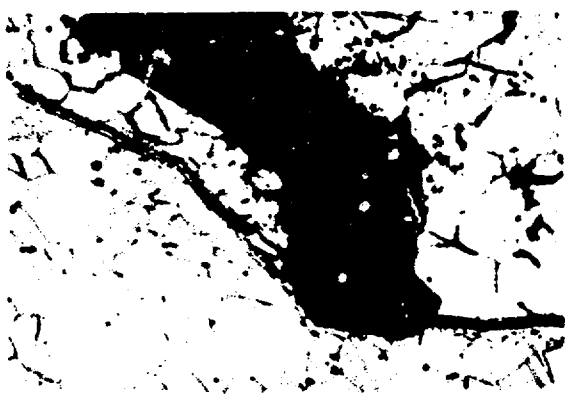

500X

8306099-20

Figure 26. Photomicrographs of Area D, Outer Surface of Inner Capsule.

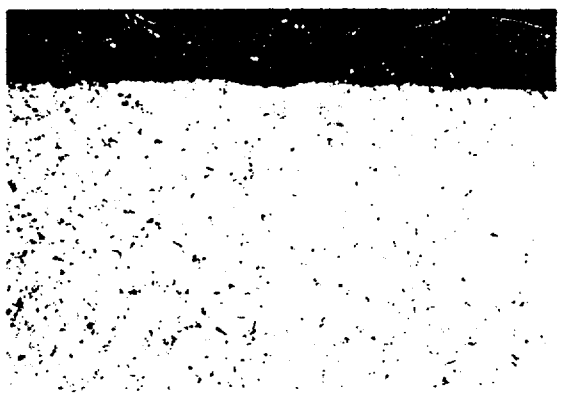

50X

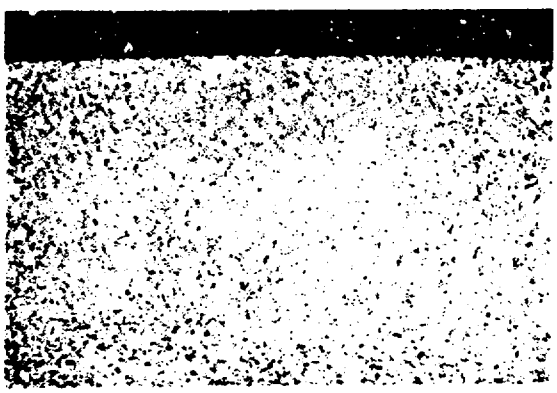

100X

500X

8306099-21

Figure 27. Photomicrographs of Area E, Outer Surface of Inner Capsule.

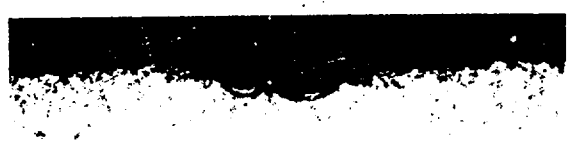

50x

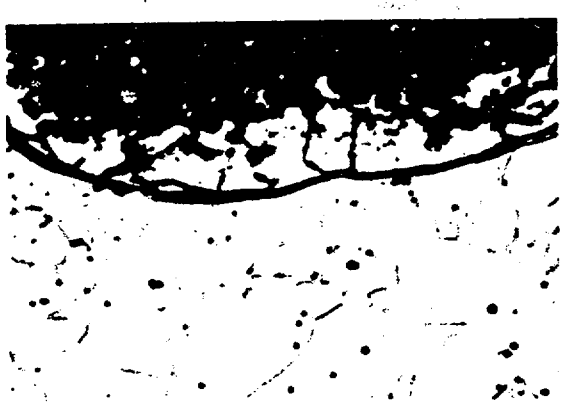

500x

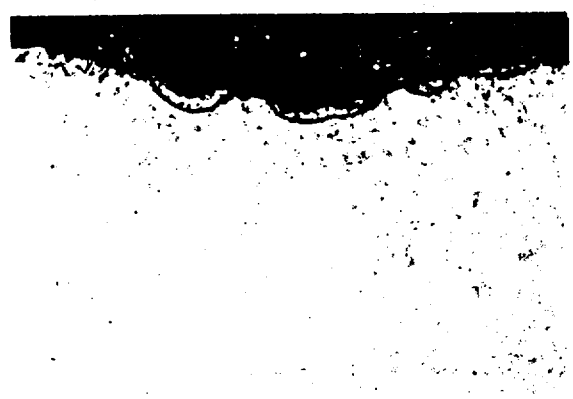

100x

8306099-22

Figure 28. Photomicrographs of Area F-1, Outer Surface of Inner Capsule.

50X

100X

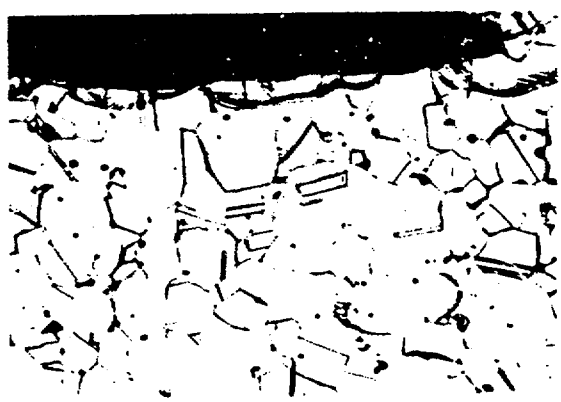

500X

8306099-23

Figure 29. Photomi rographs of Area F-2, Outer Surface of Inner Capsule.

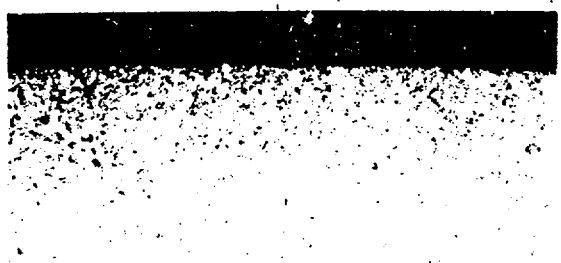

50X

100X

500X

8306099-24

Figure 30. Photomicrographs of Area F-3, Outer Surface of Inner Capsule.

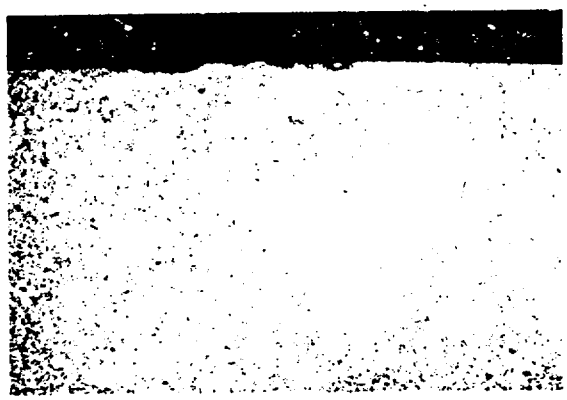

50X

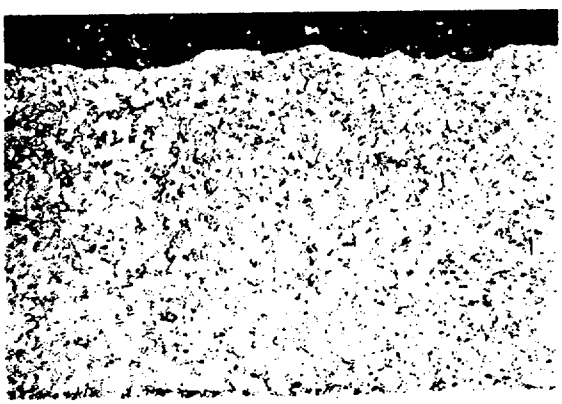

100X

500X

8306099-25

Figure 31. Photomicrographs of Area G, Outer Surface of Inner Capsule.

capsule does not vary by more than 0.001-0.003 inches, the initial wall thickness at the point where the sample is taken will be known with sufficient accuracy. The other three samples were taken at the same locations as those from the zero-time capsules.

4.6 METAL CONTROL SPECIMENS

When 316L SS is held in contact with WESF-produced CsCl at temperatures up to 450°C for extended periods of time, it is possible that chemical attack by the CsCl could produce changes in the microstructure of the metal. The thermal aging of the 316L SS may also produce changes in its microstructure. To help differentiate between microstructural changes produced by thermal aging and those resulting from chemical attack, control samples of 316L SS are being aged in argon at 400°C, 450°C, and 500°C for varying times up to 32,000 h. The aged samples are subjected to metallographic examination. The photomicrographs obtained will show what microstructural changes result from the thermal aging.

The control samples were cut from a rejected WESF SS inner capsule. Each sample was sealed in an argon-filled quartz envelope. The samples are heated in muffle furnaces whose temperatures are maintained within ±2°C of the control temperatures using solid state proportioning controllers. The samples are maintained at temperature for 2000, 4000, 8000, 16,000, 24,000, or 32,000 h (the same times as the radioactive test capsules).

6.0 REFERENCES

1. Fullam, H. T. 1982. Compatibility of Cesium Chloride and Strontium Fluoride with Containment Materials. BNWL-1673, Pacific Northwest Laboratory, Richland, Washington.

2. Fullam, H. T. 1982. Cesium Chloride Compatibility Testing Program Annual Report - Fiscal Year 1982. PNL-4556, Pacific Northwest Laboratory, Richland, Washington.

DISTRIBUTION

No. of Copies

OFFSITE

27 DOE Technical Information Center

2 Nuclear Regulatory Commission
7915 Eastern Avenue
Silver Springs, MD 20910
ATTN: R. E. Cunningham
J. Roberts

R. D. Smith
Division of Waste Management
Nuclear Regulatory Commission
Washington, DC 20555

Materials Section Leader
High-Level Waste Licensing Branch
Nuclear Regulatory Commission
Washington, DC 20555

W. F. Holcomb
Environmental Protection Agency
Office of Radiation Programs
Washington, DC 20460

2 DOE Terminal Waste Disposal and Remedial Action
GTN
Washington, DC 20545
ATTN: F. E. Coffman, NE-20
D. J. McGoff, NE-23

4 DOE Office of Defense Waste and Byproducts Management
GTN
Washington, DC 20545
ATTN: J. E. Dieckhoner
J. J. Jicha
G. K. Oertel
W. C. Remini

No. of Copies

J. W. Bennett
Geologic Repository Division
DOE Nuclear Waste Policy Act Project Office
S-10, Forrestal
Washington, DC 20585

3 Geologic Repository Division
DOE Nuclear Waste Policy Act Project Office
GTN
Washington, DC 20545
ATTN: C. R. Cooley, S-10/NE-22
C. H. George, S-10/NE-22
R. Stein

J. O. Neff
DOE National Waste Program Office
505 King Avenue
Columbus, OH 43201

3 Oak Ridge National Laboratory
P.O. Box Y
Oak Ridge, TN 37830
ATTN: L. J. Mezga
T. H. Row
R. S. Crouse

DOE Savannah River Operations Office
P.O. Box A
Aiken, SC 29801
ATTN: T. B. Hindman

5 W. McMullen
DOE Albuquerque Operations Office
P.O. Box 5400
Albuquerque, NM 87185

No. of Copies

3 Argonne National Laboratory
9700 South Cass Avenue
Argonne, IL 60439
ATTN: J. H. Kittel
M. J. Steindler
L. E. Trevorrow

Battelle Memorial Institute
Office of Nuclear Waste Isolation
505 King Avenue
Columbus, OH 43201
ATTN: N. E. Carter

Beverly Rawles
Battelle Memorial Institute
505 King Avenue
Columbus, OH 43201

K. V. Gilbert
Rockwell International
Rocky Flats Plant
P.O. Box 464
Golden, CO 80401

2 E. I. du Pont de Nemours Company
Savannah River Laboratory
Aiken, SC 29808
ATTN: J. L. Crandall
W. McDonnell

R. Williams
Electric Power Research Institute
3412 Hillview Avenue
P.O. Box 10412
Palo Alto, CA 94304

R. K. Brown
Westinghouse Electric Corporation
Advanced Energy Systems Div.
WIPP Library
P.O. Box 40039
Alburquerque, NM 87196

J. L. Knabenschuh
Nuclear Fuels Services, Inc.
P.O. Box 191
West Valley, NY 14171

No. of Copies

Bechtel National, Inc.
Box 3965
San Francisco, CA 94119
ATTN: J. L. Jardine

J. L. Larocca, Chairman
Energy Research and Development Authority
Empire State Plaza
Albany, NY 12223

R. G. Post
College of Engineering
University of Arizona
Tucson, AZ 85721

S. Ahlstrom
CH2M Hill
6121 Indian School Road
Albuquerque, NM 87110

ONSITE

6 DOE Richland Operations Office

O. J. Elgert
R. D. Izatt
N. Karagianes
H. E. Ransom
J. J. Schreiber
J. W. White

9 Rockwell Hanford Operations

K. A. Gasper
M. W. Gibson
H. E. McGuire
J. W. Patterson
I. E. Reep
J. H. Roecker
P. F. Shaw
D. D. Wodrich
File Copy

UNC United Nuclear Industries

T. E. Dabrowski

Westinghouse Hanford Company

A. G. Blasewitz

No. of Copies	
43	Pacific Northwest Laboratory

W. F. Bonner
G. H. Bryan (10)
L. L. Burger/R. D. Scheele/
L. A. Bray
T. D. Chikalla
R. L. Dillon
J. R. Divine
J. H. Jarrett
D. E. Knowlton
J. M. Latkovich
R. C. Liikala
R. P. Marshall/W. R. Wiley/
D. B. Cearlock
J. L. McElroy
J. E. Mendel/M. D. Merz

No. of Copies

J. E. Minor
K. S. Murthy/R. F. McCallum
I. C. Nelson/J. G. Stephan
A. M. Platt
E. J. Wheelwright
G. L. Tingey
R. P. Turcotte/G. L. McVay
H. H. Van Tuyl
R. E. Westerman
L. D. Williams
Technical Information (5)
Publishing Coordination (2)

END

DATE FILMED

06/04/84

NTIS does not permit return of items for credit or refund. A replacement will be provided if an error is made in filling your order, if the item was received in damaged condition, or if the item is defective.

Reproduced by NTIS
National Technical Information Service
U.S. Department of Commerce
Springfield, VA 22161

This report was printed specifically for your order from our collection of more than 2 million technical reports.

For economy and efficiency, NTIS does not maintain stock of its vast collection of technical reports. Rather, most documents are printed for each order. Your copy is the best possible reproduction available from our master archive. If you have any questions concerning this document or any order you placed with NTIS, please call our Customer Services Department at (703)487-4660.

Always think of NTIS when you want:
- Access to the technical, scientific, and engineering results generated by the ongoing multibillion dollar R&D program of the U.S. Government.
- R&D results from Japan, West Germany, Great Britain, and some 20 other countries, most of it reported in English.

NTIS also operates two centers that can provide you with valuable information:
- The Federal Computer Products Center - offers software and datafiles produced by Federal agencies.
- The Center for the Utilization of Federal Technology - gives you access to the best of Federal technologies and laboratory resources.

For more information about NTIS, send for our FREE *NTIS Products and Services Catalog* which describes how you can access this U.S. and foreign Government technology. Call (703)487-4650 or send this sheet to NTIS, U.S. Department of Commerce, Springfield, VA 22161. Ask for catalog, PR-827.

Name _____
Address _____
_____
_____
Telephone _____

- Your Source to U.S. and Foreign Government Research and Technology.

BNWL-1673
UC-70
Waste Disposal
and Processing

COMPATIBILITY OF CESIUM CHLORIDE AND STRONTIUM FLUORIDE WITH CONTAINMENT MATERIALS

by

Harold T. Fullam
Chemical Technology Department

October, 1972

BATTELLE
PACIFIC NORTHWEST LABORATORIES
RICHLAND, WASHINGTON 99352

COMPATIBILITY OF CESIUM CHLORIDE AND STRONTIUM FLUORIDE WITH CONTAINMENT MATERIALS

ABSTRACT

In the Hanford Waste Management Program Sr and Cs will be recovered from the high-level Purex Acid Waste. Each element will be purified, converted to the appropriate chemical form, and doubly encapsulated for subsequent underwater storage. Strontium fluoride and cesium chloride were the chemical compounds selected for storage.

An extensive compatibility program was carried out to select the best encapsulating materials. The tests were run using both radioactive and inert compounds. The radioactive tests were carried out at 400°C for periods up to one year. The nonradioactive tests were carried out at 400°C and 800°C with SrF_2 and 400°C and 600°C with CsCl. The nonradioactive tests lasted up to three years.

Analysis of the test capsules showed 316L stainless steel is the best material for containing CsCl. Haynes 25 is the best material for containing the SrF_2, but Hastelloy C is almost as good. Estimates of long-term attack, based on the short-term data, show that both compounds can be adequately contained for the required storage period ($\sim$ 600 years) using 316L stainless steel for CsCl and Haynes 25 or Hastelloy C for SrF_2.

TABLE OF CONTENTS

	Page
ABSTRACT	ii
LIST OF FIGURES	v
LIST OF TABLES	ix
INTRODUCTION	1
SUMMARY	1
PROGRAM OBJECTIVES	3
ANTICIPATED WASTE STORAGE CONDITIONS	5
WASTE COMPOSITIONS	8
WASTE STORAGE CONDITIONS	10
EXPERIMENTAL PROGRAM	11
EXPERIMENTAL TEST PARAMETERS	14
Cesium Chloride Testing	14
Strontium Fluoride Testing	17
Cesium Diuranate Testing	21
Strontium Pyrophosphate Testing	23
PREPARATION OF TEST CAPSULES	23
Compound Preparation	25
Can Fabrication	33
Can Loading	34
Can Welding	36
Capsule Testing	38
CAPSULE ANALYSIS AND EVALUATION	38
RADIOLYSIS EXPERIMENTS	40
EXPERIMENTAL RESULTS AND INTERPRETATION	40
CESIUM CHLORIDE COMPATIBILITY	42
STRONTIUM FLUORIDE COMPATIBILITY	46
CESIUM DIURANATE COMPATIBILITY	57
STRONTIUM PYROPHOSPHATE COMPATIBILITY	60
RADIOLYSIS OF PACKAGED WASTES	62

Page

ESTIMATES OF LONG-TERM ATTACK 64
CONCLUSIONS 72
ACKNOWLEDGEMENTS 73
REFERENCES 74
APPENDIX 75
A. FIGURES 75
B. WESF FLOWSHEETS 146
C. CHEMICAL ANALYSIS AND MECHANICAL TESTS OF TEST METALS . 149

LIST OF FIGURES

Figure No.	Title	Page
1	Compatibility Test Capsules	76
2	Metal Cans Used in Fabricating Test Capsules	77
3	Equipment for Loading Test Capsules	78
4	Cesium Chloride Capsule in Various Stages of Fabrication	79
5	Capsule Used in Scouting Studies	80
6	Welding Radioactive Capsules in Shielded Cell	81
7	Sectioning of Individual Test Capsules	82
8	Sectioning of Radioactive Test Capsules	83
9	Reference Metal Samples	84
10	Samples of 316L SS Tested with Radioactive CsCl at 400°C	85
11	Samples of 316L SS Tested with Radioactive CsCl-20 mole % $BaCl_2$ at 400°C	86
12	Sections of 316L SS Capsules After Contact with Radioactive CsCl at 400°C	87
13	Test Specimens - 316L SS/Nonradioactive CsCl - 11 mole % $BaCl_2$ at 400°C	88
14	Test Specimens - 316L SS/Nonradioactive CsCl - 20 mole % $BaCl_2$ at 400°C	89
15	Test Specimens - 316L SS/Nonradioactive CsCl - 20 mole % $BaCl_2$ at 600°C	90
16	Samples of Hastelloy C Tested with Radioactive CsCl at 400°C	91
17	Samples of Hastelloy C Tested with Radioactive CsCl - 20 mole % $BaCl_2$ at 400°C	92
18	Test Specimens - Hastelloy C/Nonradioactive CsCl - 11 mole % $BaCl_2$ at 400°C	93
19	Test Specimens - Hastelloy C/Nonradioactive CsCl - 20 mole % $BaCl_2$ at 400°C	94
20	Test Specimens - Hastelloy C/Nonradioactive CsCl - 20 mole % $BaCl_2$ at 600°C	95
21	Test Specimens - Hastelloy C-276/Nonradioactive CsCl - 11 mole % $BaCl_2$ at 400°C	96
22	Welded 316L SS Samples Tested with Nonradioactive CsCl at 400°C for 4380 Hours	97

Figure No.	Title	Page
23	Welded Hastelloy C Samples Tested with Nonradioactive CsCl at 400°C for 4380 Hours	98
24	Crevice Corrosion in Nonradioactive CsCl Capsules	99
25	Samples of Haynes 25 Tested with Radioactive SrF_2 at 400°C	100
26	Samples of Haynes 25 Tested with Radioactive SrF_2 - 13 mole % ZrF_4 - 13 mole % Zr at 400°C	101
27	Test Specimens - Haynes 25/Nonradioactive SrF_2 at 400°C	102
28	Test Specimens - Haynes 25/Nonradioactive SrF_2 - 6 mole % ZrF_4 - 6 mole % Zr at 400°C	103
29	Test Specimens - Haynes 25/Nonradioactive SrF_2 - 13 mole % ZrF_4 - 13 mole % Zr at 400°C	104
30	Test Specimens - Haynes 25/Nonradioactive SrF_2 - 6 mole % ZrF_4 - 6 mole % Zr at 800°C	105
31	Test Specimens - Haynes 25/Nonradioactive SrF_2 - 13 mole % ZrF_4 - 13 mole % Zr at 800°C	106
32	Samples of Hastelloy C Tested with Radioactive SrF_2 at 400°C	107
33	Samples of Hastelloy C Tested with Radioactive SrF_2 - 13 mole % ZrF_4 - 13 mole % Zr at 400°C	108
34	Test Specimens - Hastelloy C/Nonradioactive SrF_2 at 400°C	109
35	Test Specimens - Hastelloy C/Nonradioactive SrF_2 - 6 mole % ZrF_4 - 6 mole % Zr at 400°C	110
36	Test Specimens - Hastelloy C/Nonradioactive SrF_2 - 13 mole % ZrF_4 - 13 mole % Zr at 400°C	111
37	Test Specimens - Hastelloy C/Nonradioactive SrF_2 at 800°C	112
38	Test Specimens - Hastelloy C/Nonradioactive SrF_2 - 6 mole % ZrF_4 - 6 mole % Zr at 800°C	113
39	Test Specimens - Hastelloy C/Nonradioactive SrF_2 - 13 mole % ZrF_4 - 13 mole % Zr at 800°C	114
40	Samples of Hastelloy X Tested with Radioactive SrF_2 at 400°C	115
41	Samples of Hastelloy X Tested with Radioactive SrF_2 - 13 mole % ZrF_4 - 13 mole % Zr at 400°C	116

Figure No.	Title	Page
42	Test Specimens - Hastelloy X/Nonradioactive SrF_2 at 400°C	117
43	Test Specimens - Hastelloy X/Nonradioactive SrF_2 - 6 mole % ZrF_4 - 6 mole % Zr at 400°C	118
44	Test Specimens - Hastelloy X/Nonradioactive SrF_2 - 13 mole % ZrF_4 - 13 mole % Zr at 400°C	119
45	Test Specimens - Hastelloy X/Nonradioactive SrF_2 at 800°C	120
46	Test Specimens - Hastelloy X/Nonradioactive SrF_2 - 6 mole % ZrF_4 - 6 mole % Zr at 800°C	121
47	Test Specimens - Hastelloy X/Nonradioactive SrF_2 - 13 mole % ZrF_4 - 13 mole % Zr at 800°C	122
48	Samples of 316L SS Tested with Radioactive SrF_2 at 400°C	123
49	Samples of 316L SS Tested with Radioactive SrF_2 - 13 mole % ZrF_4 - 13 mole % Zr at 400°C	124
50	Test Specimens - 316L SS/Nonradioactive SrF_2 at 400°C	125
51	Test Specimens - 316L SS/Nonradioactive SrF_2 - 6 mole % ZrF_4 - 6 mole % Zr at 400°C	126
52	Test Specimens - 316L SS/Nonradioactive SrF_2 - 13 mole % ZrF_4 - 13 mole % Zr at 400°C	127
53	Test Specimens - 316L SS/Nonradioactive SrF_2 at 800°C	128
54	Test Specimens - 316L SS/Nonradioactive SrF_2 - 6 mole % ZrF_4 - 6 mole % Zr at 800°C	129
55	Test Specimens - 316L SS/Nonradioactive SrF_2 - 13 mole % ZrF_4 - 13 mole % Zr at 800°C	130
56	Test Specimens from Scouting Tests with Nonradioactive SrF_2 at 800°C	131
57	Test Specimens from Scouting Tests with SrF_2 - 6 mole % ZrF_4 - 6 mole % Zr at 800°C	132
58	Metal Specimens from 400°C Tests with $Cs_2U_2O_7$	133
59	Metal Specimens from 400°C Tests with $Cs_2U_2O_7$ - 11 mole % BaU_2O_7	134
60	Sectioned $Sr_2P_2O_7$ Capsules - Tested at 1000°C for 3 Months	135
61	Metal Samples from 3-Month - 1000°C Tests with $Sr_2P_2O_7$	136

Figure No.	Title	Page
62	Metal Specimens from 3-Month - 1000°C Tests with $Sr_2P_2O_7$ - 13 mole % ZrP_2O_7 - 13 mole % Zr	137
63	Metal Specimens from 3-Month - 400°C Tests with $Sr_2P_2O_7$	138
64	Metal Specimens from 3-Month - 400°C Tests with $Sr_2P_2O_7$ - 13 mole % ZrP_2O_7 - 13 mole % Zr	139
65	Estimated Long-Term Attack of 316L Stainless Steel by CsCl	140
66	Estimated Long-Term Attack of Hastelloy C by CsCl . . .	141
67	Estimated Long-Term Attack of Haynes 25 by SrF_2	142
68	Estimated Long-Term Attack of 316L Stainless Steel by SrF_2	143
69	Estimated Long-Term Attack of Hastelloy C by SrF_2 . . .	144
70	Estimated Long-Term Attack of Hastelloy X by SrF_2 . . .	145

LIST OF TABLES

Table No.	Title	Page
I	Experimental Conditions for CsCl Compatibility Tests	15
II	Experimental Conditions for SrF_2 Compatibility Tests	18
III	Experimental Conditions for SrF_2 Scouting Studies	19
IV	Experimental Conditions for Scouting Studies with Cesium Diuranate	22
V	Experimental Conditions for Scouting Studies with Strontium Pyrophosphate	24
VI	Nonradioactive Cesium Feed and Product Compositions	26
VII	Radioactive Cesium Feed and Product Compositions	28
VIII	Nonradioactive Strontium Feed and Product Compositions	29
IX	Radioactive Strontium Feed and Product Compositions	31
X	Cesium Chloride Compatibility Data	43
XI	Compatibility of Welded Metals with Cesium Chloride	47
XII	Radioactive Strontium Fluoride Compatibility Data	48
XIII	Nonradioactive Strontium Fluoride Compatibility Data	49
XIV	SrF_2 - Hastelloy C-276 Compatibility Data	53
XV	Compatibility of Welded Metals with Strontium Fluoride at 400°C	56
XVI	Compatibility Data from SrF_2 Scouting Studies	58
XVII	Metal Attack by SrF_2 after 24 Hours at 1100°C	59
XVIII	Cesium Diuranate Compatibility Data	61
XIX	Strontium Pyrophosphate Compatibility Data	63
XX	Estimated Attack of Metals at 400°C by Radioactive Strontium Fluoride	71

COMPATIBILITY OF CESIUM CHLORIDE AND STRONTIUM FLUORIDE WITH CONTAINMENT MATERIALS

Harold T. Fullam

INTRODUCTION

Current radioactive waste management planning at Hanford calls for the separation of the strontium and cesium from the high level waste stream and subsequent purification, conversion to the appropriate chemical form, encapsulation and storage of each of these elements separately in small double-walled high integrity containers. Strontium fluoride and cesium chloride were the chemical compounds selected for storage. The waste containers will be stored initially under water in closely monitored concrete basins on the Hanford site.

This report describes studies carried out to determine the interaction of the strontium fluoride and cesium chloride with potential materials of construction for the storage containers.

The Atlantic Richfield Hanford Company (ARHCO) has the responsibility for operating the Waste Encapsulation and Storage Facilities (WESF) for the USAEC, and the work described here was done under ARHCO sponsorship.

SUMMARY

A study has been carried out to determine the compatibility of cesium chloride and strontium fluoride with candidate containment

materials. The two compounds were prepared using flowsheets which were presumed would be used in the WESF.

Both radioactive and nonradioactive compounds were used in the tests. The radioactive compounds were prepared using feed solutions obtained from ARHCO. To simulate the buildup of barium in the waste due to decay of the ^{137}Cs, barium chloride was added to both the radioactive and nonradioactive wastes in predetermined amounts. Zirconium tetrafluoride and zirconium metal powder were added to the strontium fluoride to simulate the buildup of zirconium due to the decay of ^{90}Sr. The metals tested with cesium chloride were 316L stainless steel and Hastelloy C. Haynes 25, Hastelloy C, Hastelloy X and 316L stainless steel were the metals evaluated with strontium fluoride.

The compatibility test capsules were prepared using procedures approximating those to be used in the WESF. Capsules containing radioactive CsCl or SrF_2 were tested at 400°C for periods up to one year long. Capsules containing inert CsCl were tested at 400°C or 600°C for periods up to three years; those containing inert SrF_2 were held at 400°C or 800°C for periods up to three years.

After testing, the radioactive test capsules were sectioned and the extent of waste-metal interaction was determined by metallographic examination. Waste-metal interactions in the nonradioactive capsules were determined by metallographic examination and electron microprobe analysis.

The tests with CsCl show 316L stainless steel is the best material for containing the CsCl waste. Extrapolation of the short-term data

indicates the attack of the 316L stainless steel by the CsCl waste at 400°C over a 600-year period should not exceed 0.025 in.

Haynes 25 is the preferred material for containing the SrF_2 waste. An estimate of long-term attack, based on the short-term compatibility data, shows that the attack of Haynes 25 should not exceed 0.073 in. after 600 years at 400°C. Hastelloy C (or Hastelloy C-276) can also be used to contain the SrF_2 waste for the required storage period but would show a slightly greater attack (~0.105 in.).

PROGRAM OBJECTIVES

Several factors can influence the selection of the materials used to contain the cesium chloride and strontium fluoride wastes. Material availability, ease of fabrication, welding and cost all must be considered. In the waste encapsulation program, however, the overriding criterion for material selection is safety. Assurance must be provided that the radioactive compounds will be adequately contained during storage. This means that interaction between the radioactive compound and its container material must be sufficiently low that the container maintains its integrity for the required storage period. Only if two or more materials meet the safety criterion can other factors influence the selection of the container material.

The basic objective of the cesium-strontium compatibility testing program was to develop sufficient compatibility data to permit selection of container materials which satisfy the safety requirement. To provide absolute assurance that the container materials selected meet the safety

criterion would require testing the candidate container materials with the radioactive compounds under the exact conditions encountered in the encapsulation plant and storage facilities. This is clearly impossible because the anticipated storage periods will be several hundred years long. It was necessary, therefore, to carry out the compatibility tests under a predetermined set of conditions, approximating those to be encountered in the storage facility, and limit the test duration to reasonable time periods. Plant design and startup deadlines limited the time available for testing to approximately three years. From the short-term test data, extrapolations can be made to estimate the effect of long-term storage on container compatibility.

When the radioactive cesium and strontium wastes are encapsulated, container weight is not a critical factor. Therefore, container thickness can be increased to provide a margin of safety which would offset the uncertainties introduced by extrapolating the time dependent compatibility data. Double encapsulation will be used to provide an additional safety factor. A total wall thickness of at least 0.20 inch was anticipated for the double containment.

Most of the data previously reported on the compatibility of radioactive materials with encapsulating materials has been directed toward the development of reactor fuel elements and heat sources. In such applications it is usually necessary to keep the container wall as thin as possible. As a result the container-compound interaction that can be tolerated is usually very low; initial container corrosion rates of 0.1 mil per year or less can be critical. In the waste encapsulation

program, where a thin container wall is not critical, higher initial container corrosion rates are undesirable but can be tolerated. This is true even considering the long storage periods involved. In the current study, therefore, only a relatively rapid initial attack of a candidate container material will eliminate the material from consideration for use in the encapsulation plant.

ANTICIPATED WASTE STORAGE CONDITIONS

For a given container material the extent of interaction that occurs between the radioactive waste and its container will depend on a number of variables. These factors can be broken down into two general groups. The first and most important group includes those variables which are defined by the entire Waste Encapsulation concept and which are all interrelated. These variables include:

1. waste composition
2. waste-container interface temperature
3. required storage time.

Initial waste compositions will be determined by the flowsheets used to recover the cesium and strontium from the Purex waste and prepare the compounds. The initial waste-container interface temperature will be determined by container design, heat output per container (which is dependent on waste composition and extent of loading) and external conditions. The storage period required will depend on the radioactive cesium or strontium content per container. The waste encapsulation concept calls for storage of the packaged waste for periods in excess

of 600 years. During this time period the radioactive cesium and strontium will have decayed more than twenty half lives, the heat output of the packages will have decreased to essentially zero, and the decay products will have built up sufficiently to constitute a substantial fraction of the waste. For compatibility considerations, it is necessary to know how the changes in waste composition and interface temperature will affect the rate of attack of the container material. Since it is impossible to run compatibility tests at all potential waste compositions and interface temperatures it is necessary to select certain representative conditions and run the tests under those conditions.

The second group of factors which can affect waste-container interaction are those related to the encapsulation process. These parameters are essentially independent of other factors, and depend primarily on the procedures used to prepare the waste containers. They include:

1. uniformity of container composition,
2. effect of fabrication techniques on internal container surfaces,
3. effect of welding,
4. the degree of surface contact between the waste and its container,
5. internal container atmosphere.

By standardizing the encapsulation process(es) and setting stringent container material specifications the effects of these variables on waste-container interaction can be minimized and controlled.

One other factor may have an influence on waste-container interaction. The high radiation field present in the waste container may

result in radiolysis of the waste compound or impurities present. The product(s) of radiolysis may in turn influence the attack of the container material.

In defining a set of experimental conditions for measuring the compatibility of the radioactive waste with container materials, all of the factors discussed above must be considered. The conditions selected for testing should duplicate as closely as possible the conditions which will be encountered by the waste and its container in the encapsulation plant and storage facilities.

When this study was started neither the WESF flowsheets nor waste storage conditions could be completely defined. It was necessary, therefore, to make certain assumptions as to waste compositions, container designs, encapsulating procedures and storage conditions. These assumptions were based on estimates, by ARHCO and Pacific Northwest Laboratory (PNL) personnel, of what the encapsulation processes would consist of and how the containers would be stored. The experimental conditions used in the compatibility tests were based on these assumptions, and are described in the following sections. In some instances, subsequent development work has shown the original assumptions were only partially correct. The possible effects of these differences on material compatibility are discussed in subsequent sections of the report.

Compatibility testing with highly radioactive materials such as ^{90}Sr and ^{137}Cs is costly; therefore many of the tests were performed using simulated waste compositions prepared from nonradioactive strontium and cesium. However, enough tests were run with the radioactive wastes

to allow a comparison of the results obtained with the radioactive and nonradioactive waste compositions.

WASTE COMPOSITIONS

The initial compositions of the packaged wastes will be determined by the flowsheets used to recover the Cs and Sr from the bulk waste and to prepare the compounds. The compositions will change with time as the radioisotopes decay.

Cesium is currently recovered from the Purex acid waste by phosphotungstic acid precipitation and partially purified by ion exchange using an organic cation exchanger. The cesium solution from the ion exchange column contains cesium, sodium and potassium in the approximate molar ratio of 0.3:2.0:1.0. Additional purification is required before the cesium is converted to the chloride for packaging.

The flowsheet which will be used to purify the cesium solution and to prepare and package the chloride is described in the Appendix. Cation exchange, using a synthetic zeolite, will be used to obtain the necessary purification. (The cesium purification will take place in the Waste Fractionization Plant. Preparation and packaging of the CsCl will occur in the WESF.) For the compatibility studies it was assumed that the purity of the CsCl prepared by this procedure will be approximately 99 wt% with sodium and potassium being the only impurities present in greater than trace levels.

The cesium to be encapsulated will contain approximately 40% ^{137}Cs and a much smaller amount of ^{134}Cs ($\sim$0.02%). The cesium will

also contain about 12% ^{135}Cs, but the ^{135}Cs (half life = 3×10^6 years) will not contribute a significant amount to the heat output or radiation level. The ^{137}Cs has a relatively short half life (~30 years), and as it decays the composition of the waste will change according to the reaction

$$^{137}Cs_{55} \rightarrow {}^{137}Ba_{56} + \beta^- + Q$$

In carrying out the compatibility test it is desirable to allow for this changing composition. This was done by preparing waste compositions containing known amounts of barium. There is a problem in characterizing the decay product in terms of normal oxidation states and known chemical compounds. When a $^{137}CsCl$ molecule undergoes decay one atom of barium and one atom of chlorine result.

$$^{137}CsCl \rightarrow {}^{137}Ba[Cl] + \beta^- + Q.$$

Since barium monochloride is not known to exist, the decay product cannot be defined by standard chemical terminology. It can be assumed that the product is a mixture of barium chloride ($BaCl_2$) and barium metal; but there is no experimental evidence to support such an assumption. In this study, $BaCl_2$ was used to simulate the decay of the ^{137}Cs.

When the compatibility program was started it was assumed that strontium would be recovered from the Purex plant waste by solvent extraction. The strontium nitrate solution from the solvent extraction cycle would, in turn, serve as the feed to the WESF. The anticipated flowsheet for preparing the SrF_2 in the WESF is described in the Appendix. It was assumed that the flowsheet as described would yield a fluoride product

of at least 95 wt% purity with sodium and calcium being the principal cation impurities.

Strontium recovered from the Purex plant waste contains about 50-52% ^{90}Sr. The half life of ^{90}Sr is approximately 29 years, and the stable decay product is ^{90}Zr.

$$^{90}Sr_{38} \rightarrow [^{90}Y_{39}] \rightarrow {}^{90}Zr_{40} + 2\beta^- + Q$$

The equilibrium ^{90}Y intermediate concentration is low ($< 10^{-5}$ g atom/g atom ^{90}Sr).

Defining the chemical product of the decay reaction for $^{90}SrF_2$ presents the same problems as $^{137}CsCl$. Decay of a molecule of $^{90}SrF_2$ yields one atom of zirconium and two atoms of fluorine.

$$^{90}SrF_2 \rightarrow \left\{^{90}Y[F_2]\right\} \rightarrow {}^{90}Zr[F_2] + 2\beta^- + Q$$

Zirconium does form some divalent compounds, but there is no experimental evidence that zirconium difluoride is the decay product. Zirconium difluoride has been described in the literature[1] but is an unstable compound and difficult to prepare. In attempting to simulate waste compositions corresponding to various levels of ^{90}Sr decay it was assumed that ZrF_4 and zirconium metal were the decay products. The waste compositions were prepared by blending SrF_2, ZrF_4 powder, and zirconium metal powder.

WASTE STORAGE CONDITIONS

The storage time required for a waste container will depend on the initial content of ^{137}Cs or ^{90}Sr in the container which will, in turn,

depend on container design, waste composition and bulk loading. Based on current container design considerations and National Academy of Science Committee on Radioactive Waste Management recommendations the storage period will be at least 600 years. Initial storage of the waste containers will be underwater.

When the waste containers are stored underwater the waste-container interface temperature will be maintained at a relatively low value. If the containers are removed from water storage (or if the cooling water is lost) the interface temperature will be higher. The temperature which the interface reaches will depend on the container design, heat output of the container, and external storage conditions. Since the heat output of the container decreases with time as the radioisotope decays, the interface temperature will also decrease with time. For the compatibility tests it was assumed that the containers would be stored outside of the water environment for most of the storage period. Container design was such that the waste-container interface temperature would not exceed 400°C when the container was removed from water storage. All compatibility testing with ^{90}Sr and ^{137}Cs was, therefore, carried out at a temperature of 400°C.

EXPERIMENTAL PROGRAM

It is clearly impossible to carry out the compatibility tests for the several hundred year storage period required of the waste containers. It is necessary, therefore, to carry out short duration tests and extrapolate the corrosion data obtained to estimate the effects of long-term

storage. Design and startup requirements for the WESF limited the times available for compatibility testing with nonradioactive compounds to a maximum of three years. The tests with the radioactive compounds were limited to one year.

Extrapolation of the short-term compatibility data to long storage periods presents the possibility for substantial errors in the predicted corrosion rates. However, a margin of safety is introduced by carrying out the radioactive and nonradioactive short-term tests at 400°C. By extrapolating data obtained at 400°C the predicted corrosion rates should represent the maximum attack possible because the container-waste interface temperature will be much less than 400°C during most of the storage period. In addition, some short-term tests were carried out with nonradioactive compounds at temperatures substantially above 400°C. These tests also lasted up to three years. A test temperature of 600°C was used with CsCl, and 800°C with SrF_2. Extrapolation of the high temperature data to long storage times provided an additional margin of safety in predicting long-term container corrosion rates.

Based on a number of factors, cesium chloride and strontium fluoride were selected as the optimum compounds for packaging.[2] Cesium diuranate ($Cs_2U_2O_7$) and strontium pyrophosphate ($Sr_2P_2O_7$) were selected as back-up components for encapsulation in case subsequent development results made it necessary to reject either or both of the primary candidates.

A limited amount of work reported by ORNL[3] has shown that 316L stainless steel is satisfactory for containing cesium chloride at relatively low temperatures. Hastelloy C also appeared to be a possible

candidate for CsCl encapsulation. Some compatibility data on strontium fluoride have been reported by the Martin Co.[4,5] Hastelloy C, Hastelloy X, and Haynes 25 appear to be the best of the materials tested. There are no reports in the literature of any work on the compatibility of either cesium diuranate or strontium pyrophosphate with containment materials.

As indicated, the compatibility data available on cesium chloride and strontium fluoride are limited; and the data which are available are not completely applicable to the conditions which will be encountered in the WESF. For this reason, it was decided that additional detailed studies on the compatibility of CsCl and SrF_2 with containment materials were necessary; and at least scouting studies were needed on the compatibility of the back-up compounds.

The experimental program followed in evaluating the compatibility of cesium and strontium wastes with containment materials can be divided into four phases:

1. selection of appropriate testing parameters,
2. fabrication of compatibility test capsules,
3. testing under controlled conditions,
4. analysis of test capsules to determine the extent of waste-container interaction.

The first three phases all have a strong influence on the results obtained. Care was taken that each phase represented, as closely as possible, conditions which will be encountered in the waste encapsulation process.

EXPERIMENTAL TEST PARAMETERS

The experimental parameters used in the compatibility tests were selected in accordance with the considerations set forth in the previous sections. The conditions chosen were aimed at providing sufficient data, within program funding and time limitations, to allow selection of suitable materials for safely containing the cesium and strontium wastes for the required storage periods.

Cesium Chloride Testing

The experimental conditions for the cesium chloride compatibility tests are shown in Table I. Only two containment materials were evaluated with cesium chloride, namely 316L stainless steel and Hastelloy C. Previous work at ORNL[3] had shown that 316L stainless steel was very resistant to attack by cesium chloride at relatively low temperatures. It was felt at the start of the compatibility program that the 316L stainless steel would provide satisfactory containment for the cesium chloride wastes under the anticipated storage conditions. Hastelloy C was tested as a backup material in case the 316L stainless steel did not prove satisfactory. There were two reasons for selecting Hastelloy C as the backup material. Hastelloy C was reported to have good resistance to attack by metal chlorides; and it was being evaluated with strontium fluoride and offered the possibility of standardizing on a single containment material.

Three waste compositions were evaluated. One consisted of CsCl with the normal process impurities (~2 wt% NaCl+KCl+RbCl). The other two

TABLE I Experimental Conditions for CsCl Compatibility Tests

NONRADIOACTIVE TESTS

Metals Tested	-- 316L stainless steel -- Hastelloy C
Waste Composition	-- 89 mole % CsCl - 11 mole % $BaCl_2$* -- 80 mole % CsCl - 20 mole % $BaCl_2$**
Test Temperatures	-- 400°C -- 600°C
Test Duration	-- 2,190 hours -- 4,380 hours -- 8,760 hours -- 17,520 hours -- 26,280 hours

RADIOACTIVE TESTS

Metals Tested	-- 316L stainless steel -- Hastelloy C
Initial Waste Composition	-- CsCl -- 80 mole % CsCl - 20 mole % $BaCl_2$**
Test Temperature	-- 400°C
Test Duration	-- 2,190 hours -- 4,380 hours -- 8,760 hours

* Corresponds to approximately 15 years decay assuming 40% ^{137}Cs in the cesium feed

** Corresponds to approximately 30 years decay (one half life) assuming 40% ^{137}Cs in the cesium feed

contained CsCl plus process impurities and barium (added as barium chloride) in amounts corresponding initially to approximately 15 and 30 years decay assuming the cesium initially contained 40% ^{137}Cs. The barium content of the radioactive waste increased during testing as the ^{137}Cs decayed. Since the radioactive tests lasted a maximum of one year, however, the increase in barium concentration during testing was slight.

In the 600°C tests the cesium chloride waste compositions consisted of a liquid and a solid phase. The exact amount of liquid phase present was not known because the phase diagram for the system was not available. The ternary system CsCl-KCl-NaCl has a eutectic which melts at about 478°C[6] and the CsCl-$BaCl_2$ system has a minimum melting point of 543°C.[7] A phase diagram for the quaternary system CsCl-NaCl-KCl-$BaCl_2$ has not been reported, but differential thermal analysis of the two nonradioactive waste compositions containing $BaCl_2$ indicated the presence of a liquid phase beginning at about 475°C.

In the tests with nonradioactive cesium chloride, duplicate capsules were tested for each set of conditions. The total number of capsules tested therefore was eighty. In the radioactive tests single samples were tested for each set of conditions; hence the total number of test specimens evaluated was twelve.

In addition to the tests outlined in Table I several other tests were carried out with CsCl to evaluate special factors. After the compatibility program was under way it was learned that Hastelloy C was to be replaced by a new alloy Hastelloy C-276. The new alloy was quite

similar to Hastelloy C in composition and properties (see Appendix), but possessed improved corrosion resistance after welding. Since it was possible that Hastelloy C might not be available for use in the WESF, a series of compatibility tests was run with the Hastelloy C-276 and nonradioactive CsCl wastes. The test conditions were similar to those given in Table I, but were limited to a maximum of twelve months duration. Current indications are that Hastelloy C will continue to be produced and both Hastelloy C and Hastelloy C-276 will be available for use.

It is possible that welding the various metals may affect their compatibility with the cesium chloride waste. Therefore, a series of six-month tests was carried out with nonradioactive CsCl and welded specimens of 316L stainless steel, Hastelloy C and Hastelloy C-276. Test conditions were similar to those given in Table I except for test duration. Both annealed and unannealed weld specimens were tested.

Strontium Fluoride Testing

The experimental conditions for the compatibility tests with strontium fluoride wastes are set forth in Tables II and III. Two groups of experiments were carried out with the strontium fluoride: a series of tests with four selected metals for periods up to three years (Table II), and a series of three-month tests with a variety of metals (Table III). Earlier work at the Martin Marietta Co.[3,4] had shown that Hastelloy C, Hastelloy X and Haynes 25 were the best materials for containing SrF_2 at elevated temperatures. These tests had been carried out for relatively short periods at temperatures up to 1000°C using relatively pure SrF_2. Based on these results Hastelloy C, Hastelloy X and Haynes 25 were

TABLE II Experimental Conditions for SrF_2 Compatibility Tests

NONRADIOACTIVE TESTS

Metals Tested	-- Hastelloy C -- Hastelloy X -- Haynes 25 -- 316L stainless steel
Waste Composition	-- SrF_2 -- 88 mole % SrF_2 - 6 mole % ZrF_4 - 6 mole % Zr* -- 74 mole % SrF_2 -13 mole % ZrF_4 -13 mole % Zr**
Test Temperature	-- 400°C -- 800°C
Test Duration	-- 2,190 hours -- 4,380 hours -- 8,760 hours -- 17,520 hours*** -- 26,280 hours

RADIOACTIVE TESTS

Metals Tested	-- Hastelloy C -- Hastelloy X -- Haynes 25 -- 316L stainless steel
Initial Waste Composition	-- SrF_2 -- 74 mole % SrF_2 - 13 mole % ZrF_4 - 13 mole % Zr
Test Temperature	-- 400°C
Test Duration	-- 2,190 hours -- 4,380 hours -- 8,760 hours

---

* Corresponds to approximately 11 years decay assuming 52% ^{90}Sr in the strontium feed

** Corresponds to approximately 28.8 years decay (one half life) assuming 52% ^{90}Sr in the strontium feed

*** Capsules containing SrF_2 alone were tested for a maximum of 12 months only

TABLE III Experimental Conditions for SrF_2* Scouting Studies

Metals Tested	-- Inconel 600 -- Haynes 25 -- Hastelloy C -- Hastelloy X -- Hastelloy F -- Udimet 700 -- Rene 41 -- Waspelloy -- Incoloy 804 -- Multimet -- TZM -- 304L stainless steel -- 316L stainless steel
Waste Composition	-- SrF_2 -- 88 mole % SrF_2 - 6 mole % ZrF_4 - 6 mole % Zr**
Test Temperature	-- 800°C
Test Duration	-- 2190 hours

* Nonradioactive SrF_2

** Corresponds to approximately 11 years decay assuming 52% ^{90}Sr in the strontium feed

selected for evaluation with the SrF_2 waste. In addition, 316L stainless steel was selected for testing with the SrF_2. The 316L was tested because of the desire to standardize, if possible, on a single containment material for both CsCl and SrF_2.

At the start of the compatibility program there was some doubt if any of four metals under consideration would be adequate to contain the SrF_2. Therefore, it was decided to carry out a series of scouting tests with various metals at 800°C. If all four primary candidates were found to be unsuitable for use, then the data obtained from the scouting studies would be used to select additional materials for extended testing.

Three SrF_2 waste compositions were tested. One consisted of SrF_2 plus process impurities (~4 wt% with NaF and CaF_2 being the principal impurities). The other two consisted of SrF_2, process impurities, plus zirconium tetrafluoride and zirconium metal. The two compositions corresponded to approximately eleven and twenty-nine years decay assuming the strontium initially contained 52% ^{90}Sr. The increase in the zirconium content of the radioactive waste during the test period (maximum one year) was negligible.

The nonradioactive SrF_2 tests with the four primary metals were run in duplicate. A total of 204 test capsules were tested. The radioactive tests were run with single samples and 24 test specimens were evaluated. The SrF_2 scouting tests were also run in duplicate and a total of 52 test specimens were used.

As was the case with CsCl, a number of additional compatibility tests were made with nonradioactive SrF_2 to evaluate special factors.

A series of tests, lasting up to one year, were run with Hastelloy C-276. Test conditions, except for time, were similar to those given in Table II. A second series of tests, lasting six months, was made with welded specimens of Hastelloy C, Hastelloy C-276, Hastelloy X and Haynes 25. Both annealed and unannealed weld specimens were tested. Test conditions were similar to those set forth in Table II except for time. WESF flowsheet calls for firing the SrF_2 at 1100°C prior to encapsulation. Several materials were tested as potential containers for the SrF_2 during the firing step. Metal and ceramic samples were individually packed in dried, but unfired, SrF_2 and fired for twenty-four hours at 1100°C in an argon atmosphere. The SrF_2 used was prepared by the WESF flowsheet, and contained normal process impurities. Materials evaluated included silica, alumina, magnesia, 316L stainless steel, 18-18-2, Haynes 25, Hastelloy C, tantalum, TZM, tungsten, Ta-10%W and platinum.

Cesium Diuranate Testing

The compatibility testing of cesium diuranate was limited to a series of short-term scouting studies with a variety of metals. The objective of the study was to develop sufficient information to be able to select the best materials for extended testing if the need for such tests should arise. (Extended testing would be required only if CsCl could not be used in the encapsulation process.) The experimental conditions for the cesium diuranate tests are summarized in Table IV. Duplicate samples were run for each set of conditions. No information on cesium diuranate compatibility has been reported in the literature. Selection of metals for testing was based on reported resistance to attack by other cesium and uranium compounds.

TABLE IV Experimental Conditions for Scouting Studies with Cesium Diuranate*

Metals Tested	-- Inconel 600 -- Haynes 25 -- Hastelloy C -- Hastelloy X -- Udimet 700 -- Zircaloy -- 304L stainless steel -- 316L stainless steel
Waste Composition	-- $Cs_2U_2O_7$ -- 89 mole % $Cs_2U_2O_7$ - 11 mole % BaU_2O_7**
Test Temperature	-- 400°C -- 1000°C
Test Duration	-- 2190 hours

* Nonradioactive $Cs_2U_2O_7$

** Corresponds to approximately 15 years decay assuming 40% ^{137}Cs in cesium feed

Strontium Pyrophosphate Testing

The experimental conditions for the strontium pyrophosphate compatibility tests are given in Table V. Duplicate samples were tested for each set of conditions. Since compatibility data were not available on strontium pyrophosphate, the metals tested were selected for their reported resistance to other strontium and phosphorus compounds. Test objectives were to develop sufficient information to allow selection of the best materials for extended testing if such testing should be required.

PREPARATION OF TEST CAPSULES

It is possible for the procedures used in preparing the test capsules to influence the compatibility results obtained. To minimize the influence of fabrication techniques, the procedures used in preparing the test capsules were standardized as much as possible, and were designed to duplicate, wherever possible, the procedures which were assumed would be used in the WESF.

Two types of test capsules were used in the compatibility testing program. For the tests with nonradioactive CsCl and SrF_2, individual test capsules were used. Each test capsule consisted of a metal can loaded with the appropriate compound and welded closed (see Figure 1-A). For the radioactive tests with CsCl and SrF_2 and the scouting tests with nonradioactive SrF_2, $Cs_2U_2O_7$ and $Sr_2P_2O_7$, composite test capsules were used (see Figure 1-B). The composite capsules consisted of stainless steel cans filled with alternate layers of the various test metals and the Cs or Sr compound. The use of composite capsules in a compatibility

TABLE V Experimental Conditions for Scouting Studies with Strontium Pyrophosphate*

Metals Tested	-- Inconel 600
	-- Haynes 25
	-- Hastelloy C
	-- Hastelloy X
	-- Udimet 700
	-- Waspelloy
	-- 304L stainless steel
	-- 316L stainless steel
Waste Composition	-- $Sr_2P_2O_7$
	-- 74 mole % $Sr_2P_2O_7$ - 13 mole % ZrP_2O_7 - 13 mole % Zr**
Test Temperature	-- 400°C
	-- 1000°C
Test Duration	-- 2190 hours

* Nonradioactive $Sr_2P_2O_7$

** Corresponds to approximately 28.8 years decay (one half life) assuming 52% ^{90}Sr in the strontium feed

test program may be criticized on the basis that interaction between the various metal materials in the capsule may occur. However, because of the great expense involved in using individual test capsules for the radioactive tests and scouting studies it was necessary to compromise and use composite capsules.

Layer-type capsule construction was also used with welded metal specimens. However, in every case the can and the welded metal were identical.

Compound Preparation

Compounds used in the compatibility tests were prepared using procedures similar to those proposed for the WESF (see Appendix). Unfortunately in some instances it was found, after the compounds had been prepared and testing had begun, that the plant flowsheets and stream compositions were different from those anticipated.

Nonradioactive cesium chloride was prepared from a simulated feed whose composition is given in Table VI. This composition was based on ARHCO estimates of the composition of the cesium solution entering the WESF. It was prepared by dissolving weighed amounts of reagent grade CsCl, KCl, NaCl and RbCl in distilled water. The feed solution was evaporated to dryness and the resulting solids were fired at 450°C. The solids were cooled to room temperature and ground to a fine powder (-100 mesh) in a ball mill using aluminum balls. The composition of the CsCl product is given in Table VI. Differential thermal analysis of the CsCl product showed endothermic reactions at about 390°C and 480°C. The small endotherm observed at 480°C is due to a low melting eutectic

TABLE VI Nonradioactive Cesium Feed and Product Compositions

Feed Composition

Component	Concentration, M
CsCl	0.58
NaCl	0.002
KCl	0.0058
RbCl	0.006
pH	5.8 - 5.9

CsCl Product

Element	Cation Composition, Wt%
Cs	98.9
Na	0.05
K	0.3
Rb	0.7

of CsCl-NaCl-KCl.[6] The endotherm at 390°C is due to the phase transition of the CsCl. Pure cesium chloride undergoes a phase transition, on heating, from a primitive cubic to a face-centered cubic structure starting at 475°C.[6] The presence of impurities in the CsCl prepared for the compatibility tests dropped the temperature at which the phase transition began to about 390°C. Thermogravimetric analysis of the CsCl indicated less than 0.01% water in the product.

Radioactive cesium chloride was prepared in a shielded cell using cesium solution obtained from ARHCO. Composition of the solution is given in Table VII. The solution was purified by ion exchange using a synthetic zeolite exchanger (Zeolon). The product from the ion exchange column was a cesium carbonate solution having the composition shown in Table VII. Ammonium hydroxide and ammonium carbonate were removed from the solution by boiling and the cesium carbonate was converted to cesium chloride by adding hydrochloric acid. The chloride solution was evaporated to dryness; the solid residue was fired at 450°C in air, cooled and ground using a mortar and pestle. Analytical data on a sample of the chloride product are shown in Table VII.

Nonradioactive strontium fluoride was prepared from a simulated feed whose composition is given in Table VIII. Again, the feed composition was based on ARHCO estimates of the composition of the Sr feed to the WESF. The flowsheet shown in the Appendix was used to prepare the fluoride. Feed solution was adjusted to pH 10 with sodium hydroxide and the resulting slurry was centrifuged to remove the solids. A 10 mole % excess of solid sodium fluoride was added to the supernate to precipitate

TABLE VII Radioactive Cesium Feed and Product Compositions

Feed Composition

Element	Concentration, M
^{137}Cs	441 Ci/ℓ
Cs	0.1
Na	0.67
K	0.33
Rb	0.001
NH_4^+	0.0008
pH	10.7

Ion Exchange Column Product

Element	Concentration, M
Cs	0.053
Na	0.0006
K	0.0023
Rb	0.0001

CsCl Product

Element	Cation Composition, Wt%
K	2.0
Na	0.1
Rb	0.05
Si	0.02
Ba	0.02
Cu	0.02
Mg	0.01
Al	<0.001
Cs (by difference)	97.78

TABLE VIII Nonradioactive Strontium Feed and Product Compositions

Feed Composition

Component	Concentration, M
$Sr(NO_3)_2$	0.4
$NaNO_3$	0.4
$Fe(NO_3)_3$	0.008
$Mg(NO_3)_2$	0.12
$Al(NO_3)_3$	0.008
$Ca(NO_3)_2$	0.04
HNO_3	0.5

SrF_2 Product

Element	Cation Composition, Wt%
Sr	96.6
Na	2.0
Ca	1.0
Mg	0.3
Al	0.02
Fe	0.01

strontium fluoride and the slurry was digested for one hour at 60°C. After cooling, the fluoride was filtered, washed, and dried at 100°C. The dried fluoride was calcined at 1000°C, cooled, and ground to a -100 mesh powder in a ball mill. A typical analysis of the fluoride product is shown in Table VIII.

Differential thermal analysis of the product showed a small endotherm at about 820°C due to a low melting eutectic resulting from the impurities present. As the fluoride was heated above 820°C, melting continued until approximately 1360°C when all the material was molten. Thermogravimetric analysis indicated that firing at 1000°C removed most of the water from the fluoride. The residual water was less than 0.01%.

Radioactive strontium fluoride was prepared in a shielded cell using the procedure described above. Radioactive feed solution, whose composition is shown in Table IX, was obtained from ARHCO. Composition of the solution was substantially different from the simulated feed used in preparing the nonradioactive SrF_2. However, the composition of the radioactive SrF_2, as shown in Table IX, was quite similar to that of the nonradioactive SrF_2. This shows the pH 10 purification step is quite effective in removing most impurities from the strontium feed solution.

Cesium diuranate was prepared by reacting cesium carbonate solution with uranyl nitrate solution (containing a minimum of free acid). The resulting precipitate was filtered, washed with water, fired at 1100°C, cooled, and ground in a ball mill to -100 mesh. Analysis of the material showed a cesium content of 30.7% and a uranium content of 55.9%.

TABLE IX Radioactive Strontium Feed and Product Compositions

Feed Composition

Component	Concentration, M
^{90}Sr	0.13
$Sr(NO_3)_2$	0.25
$Ca(NO_3)_2$	0.011
$Fe(NO_3)_3$	0.0053
$Mg(NO_3)_2$	0.037
$Pb(NO_3)_2$	0.0027
$Ba(NO_3)_2$	0.0027

SrF_2 Product

Element	Cation Composition, Wt%
Sr (By difference)	∿96.3%
Na	3.0
Ca	0.6
Mg	0.05
Al	0.015
Cu	0.01
Fe	0.01
Pb	0.01
K	0.01
Mn	0.002
Ba	<0.001

Barium diuranate was prepared by reacting barium hydroxide with an aqueous solution of uranyl nitrate. The precipitate was filtered, washed with water, fired at 1100°C, cooled, and ground to -100 mesh in a ball mill.

Strontium pyrophosphate was prepared using the simulated strontium feed solution. After adjusting the solution to pH 10 with NaOH and centrifuging, the supernate was treated with sodium hydrogen phosphate (Na_2HPO_4) to precipitate the strontium. The slurry was digested for one hour at 70°C and then filtered. After water washing, the cake was fired at 1100°C to form the pyrophosphate. The product was ground to -100 mesh in a ball mill.

Zirconium pyrophosphate was prepared in similar fashion by reacting sodium hydrogen phosphate with zirconium nitrate solution. The precipitate was filtered, washed, fired at 1100°C, and ground in a ball mill.

All of the compounds prepared were stored in sealed glass jars, until ready for use, to prevent moisture pickup.

Other chemicals used in preparing the test capsules were obtained from commercial sources. The CsCl was obtained from Varlacoid Chemical Co. and had a reported purity of 99.9+%. Chemical analysis confirmed this purity. Zirconium fluoride was obtained from A. D. Mackay, Inc., as an anhydrous powder of 99% purity. The zirconium metal (-200 mesh) was also obtained from A. D. Mackay, Inc., as a 99% pure powder. It was stored under water (because of its incendiary character) and was vacuum-dried prior to use.

To simulate the effect of radioactive decay, mixtures of $CsCl-BaCl_2$ and SrF_2-ZrF_4-Zr were prepared by blending weighed amounts of the various components. For the nonradioactive tests, weighed amounts of CsCl and $BaCl_2$ were mixed in a ball mill for at least two hours using Alundum balls and a porcelain jar. The nonradioactive SrF_2, ZrF_4, and zirconium powder were also blended in a ball mill. The jar was purged thoroughly with argon prior to milling to prevent oxidation of the zirconium metal. The radioactive mixtures were prepared in the shielded cell.

Can Fabrication

The metal cans used in preparing the nonradioactive test capsules were machined from bar stock. Can dimensions are shown in Figure 2-A. All internal surfaces of the cans were machined to a No. 32 finish. All cans of a given material, used in the test program, were prepared from a single heat of bar stock. Manufacturers' data on the various metals used are presented in the Appendix.

The cans used in preparing the radioactive test capsules were machined from a single piece of 316L stainless steel bar stock. Can dimensions are shown in Figure 2-B. Two different can lengths were used (for reasons which will be discussed later) with the CsCl cans being one inch longer than the SrF_2 cans. Metal specimens used in the radioactive tests were machined from the same bar stock used to prepare the individual test cans. Each sample was 0.5 in. diameter by 0.125 in. thick.

Weld specimens were prepared using 0.50-in.- square by 0.125-in.- thick metal specimens cut from bar stock. A TIG weld was placed across

the face of each specimen. Some specimens were annealed at 700°C prior to testing. Metal cans used to contain the weld specimens were machined from the same bar stock as the weld specimen. Can dimensions were as shown in Figure 2-A.

The metal cans used in the scouting studies with SrF_2, $Sr_2P_2O_7$ and $Cs_2U_2O_7$ were fabricated from one-inch schedule 80 304L stainless steel pipe and 1/4-inch 304L stainless steel plate (see Figure 2-C). The metal specimens used in the tests were cut from plate or sheet. Each piece was nominally 0.5 in. square by 0.125 in. thick.

After machining, all the metal cans and test specimens were cleaned with trichloroethylene in an ultrasonic cleaner, washed with acetone, and dried.

Can Loading

Two different procedures were used to load the cesium and strontium compounds into the metal cans. Step pressing in an inert atmosphere was used in preparing the nonradioactive test capsules. First a metal can was pressed into a hardened steel die block. The die block and can were then placed in a small argon atmosphere gloved box which surrounded the ram of a hydraulic press. A small amount of the compound to be tested was placed in the metal can. A close-fitting plunger was inserted in the can and a pressure applied (see Figure 3-A). The pressure was held for one minute and released. The plunger was removed from the can, additional compound was placed in the can, and the pressing operation was repeated. This step-wise loading operation was repeated as many

times as necessary to fill the can to the desired level. The can lid was then pressed into place, and the can was ejected from the die block.

The procedure was modified slightly for the capsules used in the scouting studies and with those used in testing welded specimens. After a layer of compound had been pressed into the can, a metal test specimen was placed on top of the compound layer and spaced away from the can wall. Additional compound was placed on top of the metal specimen and the pressing operation repeated. A second metal was added followed by additional compound. The layer type construction was continued until the can was filled. With the capsules containing weld specimens, only one metal was tested in each capsule.

Cesium chloride was pressed to about 50-60% of theoretical density. Each can containing CsCl was filled approximately half full. Strontium fluoride was pressed to 80-90% of theoretical density and each can was completely filled. Cesium diuranate and strontium pyrophospate were compacted to about 60% of theoretical density and each can was completely filled.

Step pressing was used also to load the capsules containing the radioactive compounds. The procedure varied slightly from that just described. Pressing was done in a shielded cell in an air atmosphere. A modified hydraulic jack (see Figure 3-B) was used for the pressing operation; and compound densities obtained were limited to 30-40% of theoretical. First a layer of compound was pressed into the can. Then a metal specimen was inserted, followed by additional compound, and the pressing was repeated. The entire operation was repeated until all the

metal specimens were in place. Each cesium chloride capsule contained two metal samples (Hastelloy C and 316L stainless steel) and each strontium fluoride capsule contained three metal samples (Hastelloy C, Hastelloy X and Haynes 25). Cesium chloride capsules were approximately 40% filled with the compound while strontium fluoride capsules were 60% filled with compound. After each can was loaded the metal lid was pressed in place.

Can Welding

All the metal cans were sealed by welding the lids in place. Electron beam (EB) welding was used with the nonradioactive capsules. Excellent weld penetration was obtained with all the can metals used. Over 300 capsules were sealed without any indication of leaking welds. For welding the compatibility test containers, electron beam welding has two advantages over conventional welding techniques. The high vacuum of the weld chamber serves to out-gas the capsule and hence remove most of the oxidizing gases and moisture that might be present in the can. The total heat input to the can is less with electron beam welding than with conventional welding methods. This reduces the possibility of vaporization of the compound from the can during welding. Even so, with the CsCl-bearing cans it was necessary to limit the material in the can, and maintain a substantial distance from the top of the CsCl layer to the weld area.

Figure 4 shows a typical nonradioactive cesium chloride capsule in various stages of construction. Figure 5 shows a typical capsule used in the scouting studies.

It was necessary to weld the radioisotope-containing capsules in a remote facility. An electron beam welder was not available, and it was necessary to use a tungsten inert gas (TIG) welder to seal the capsule lids in place. Figure 6 shows the welder in operation sealing a $^{90}SrF_2$ capsule. Welded SrF_2 and CsCl capsules are shown in the foreground along with several capsules used in radiolysis tests (see later section). Leak checks were performed on all the welded capsules.

Significantly more heat is generated during TIG welding than during EB welding, and there is a distinct possibility of volatilizing the CsCl during TIG welding. For this reason the CsCl capsules were substantially longer than the SrF_2 capsules and the capsules were only partially filled. This allowed a relatively large distance (>1.5 inch) to be maintained between the top of the cesium chloride layer and the weld area. With this design, CsCl volatilization during welding was not a problem. Even with SrF_2, which has a much higher melting point than CsCl, a distance of at least 0.5 inches was maintained between the SrF_2 and the weld area.

The compatibility capsules were tested at various temperatures in air atmosphere muffle furnaces. To prevent external oxidation of the capsules at high temperatures many of the capsules were sealed in protective jackets under vacuum. Capsules tested at 1000°C were sealed in Inconel 600 jackets. Capsules tested at 600°C and 800°C were sealed in Vycor jackets and the nonradioactive capsules tested at 400°C were sealed in glass jackets. Radioactive capsules, which were tested at 400°C, were run without protective jackets.

Capsule Testing

All testing of the capsules was carried out in resistance-heated muffle furnaces. Control of furnace temperatures was by proportioning controllers; in every case the temperatures were maintained within ± 10°C of the control temperature. In most cases the temperature variation was less than ± 2°C. The temperature profile of each furnace chamber was measured prior to testing, and the maximum variation observed was ± 15°C at a control temperature of 1000°C.

Furnace reliability was excellent. Three furnace failures were encountered during the nonradioactive tests. All three were due to failure of furnace control systems; two resulted from thermocouple failures, and one from a relay failure. In each case the furnace power was shut off and no overheating of the test capsule occurred. One furnace failure occurred during the radioactive tests and was the result of a burned out heating element.

CAPSULE ANALYSIS AND EVALUATION

When each test was concluded the capsule was removed from the furnace and cooled to room temperature. The protective jacket, if any, was removed. The capsule was then sectioned with an abrasive saw using a water-cooled rubber-bonded silicon carbide blade. Individual nonradioactive capsules were sectioned as shown in Figure 7. Capsules used in the scouting studies were sectioned lengthwise so that each metal specimen in the capsule was divided into two approximately equal sections. Capsules containing the welded specimens were sectioned in identical fashion.

Radioactive capsules were opened in a shielded cell using a water-cooled abrasive saw. Each capsule was cut as shown in Figure 8. The portion of the lid remaining in the capsule, after cutting, was removed with a modified bolt puller. The metal test specimens were removed from the capsule and sectioned with an abrasive saw as shown in Figure 8.

The extent of interaction between the test metals and compounds in the nonradioactive capsules was determined by metallographic techniques and electron microprobe analysis. After sectioning, a portion of the capsule or test specimen was mounted in a holder and the cut surface was polished and etched. The etched surface was examined under a microscope and photomicrographs were taken of the areas showing maximum interaction. The sample was then subjected to electron microprobe analysis in the same area. Attempts were made with some capsules to identify the interaction products by x-ray diffraction analysis. Hardness measurements were performed on a selected number of test specimens.

Only metallographic techniques were used to determine the interaction between the metal test specimens and the radioactive compounds. (At the time the tests were carried out an electron microprobe capable of handling highly radioactive samples was not available.) After sectioning, the metal sample was mounted in a holder and the cut surface was polished and etched. The surface was examined by microscope and low magnification (20x) photographs were taken of the entire surface. Photomicrographs (100 and 500x) were obtained of the areas showing maximum metal attack.

RADIOLYSIS EXPERIMENTS

Due to the high radiation field inside the strontium and cesium containers, the possibility exists for radiolytic decomposition of the chemical compounds present. This could possibly lead to pressurization of the capsules if the decomposition reaction(s) produces gaseous compounds. Radiolytic decomposition of trace amounts of water, for example, could present a serious threat to container integrity. To determine if radiolysis does present a problem a series of experiments was carried out in which the internal pressure of capsules containing $^{137}CsCl$ or $^{90}SrF_2$ was monitored as a function of time.

The cans used in the radiolysis tests were machined from 316L stainless steel bar stock (see Figure 6). A dual-range pressure gage was welded to each can via a section of 1/4-inch schedule 40 316L stainless steel pipe. The radioactive compound to be tested was step-pressed into the can using the hydraulic jack used to load the radioactive compatibility capsules. The capsules were then closed by TIG welding the lids in place. Capsule temperature was substantially above ambient during welding. As a result, when the capsule cooled the pressure gage indicated a slight vacuum. Capsules were stored in a shielded cell and allowed to come to equilibrium temperature. The internal pressure of each capsule was then followed as a function of time.

EXPERIMENTAL RESULTS AND INTERPRETATION

A combination of metallographic examination and electron microprobe analysis was used to determine the extent of waste-container

interaction in the nonradioactive test capsules. Evaluation of the radioactive samples was based only on metallographic examination. In general there was good agreement between the metallographic and microprobe evaluations of waste-metal interactions. Because of this agreement only a portion of the nonradioactive samples were subjected to electron microprobe analysis. Hardness measurements were made on some metal samples from the nonradioactive tests. However, no meaningful data were obtained and hardness was dropped as a means of measuring metal attack. The use of x-ray diffraction to identify reaction products was unsuccessful and was discontinued after several attempts.

In many instances it was difficult to obtain an exact quantitative measure of the extent of waste-metal interaction from either the microprobe or photomicrographs. Data presented in the following tables are qualitative estimates of the depth of metal affected by the waste for each test period. In each case the value reported represents the maximum attack observed. Zero interaction was assumed when the metal surface in contact with the waste was essentially unchanged from reference metal specimens (photomicrographs of the reference metal samples are shown in Figure 9). Where very slight attack was found an arbitrary value of <1 mil was assigned to the affected metal. More extensive metal attack is reported in one mil increments.

Several types of metal attack were observed in the various test capsules. They included the following:

- A general layer-type attack of the metal surface with formation of a distinct reaction layer.

- Intergranular attack with diffusion occurring along grain boundaries.
- Dissolution of the metal surface without a distinct reaction layer.
- Pitting.
- Subsurface void formation in the metal phase due to selective leaching of metal components.
- Changes in the microstructure of the metal phase.

Most of the metal samples exhibited two or more types of attack. In some cases interpretation of the photomicrographs is difficult without additional information; and the conclusions reached as regards metal microstructure may be subject to question. For this reason photomicrographs of most of the test specimens are included in the report and the reader can make his own interpretation of the metal structure.

CESIUM CHLORIDE COMPATIBILITY

The experimental data obtained in the cesium chloride compatibility tests are summarized in Table X. The results of the work support the original assumption that 316L stainless steel is a satisfactory material for containing cesium chloride wastes at 400°C. In almost every instance the Hastelloy C samples showed more attack than their corresponding 316L samples. It appears likely, however, that Hastelloy C (or Hastelloy C-276) could be used to contain the cesium chloride at 400°C, at least for relatively short periods of time.

TABLE X Cesium Chloride Compatibility Data

RADIOACTIVE CESIUM CHLORIDE

Metal	Waste Composition	Temperature °C	Depth of Metal Affected, mils		
			2,190 hrs	4,380 hrs	8,760 hrs
316L SS	A*	400	<1	<1	1
316L SS	C***	400	<1	<1	1
Hastelloy C	A	400	<1	<1	2
Hastelloy C	C	400	<1	<1	2

NONRADIOACTIVE CESIUM CHLORIDE

Metal	Waste Composition	Temperature °C	Depth of Metal Affected, mils				
			2,190 hrs	4,380 hrs	8,760 hrs	17,520 hrs	26,250 hrs
316L SS	B**	400	0	0	0	<1	1
316L SS	B	600	0	0	0	1	2
316L SS	C	400	0	0	<1	<1	<1
316L SS	C	600	<1	0	<1	1	2
Hastelloy C	B	400	0	0	<1	<1	1
Hastelloy C	B	600	0	<1	<1	2	3
Hastelloy C	C	400	0	0	<1	2	3
Hastelloy C	C	600	0	<1	2	4	5
Hastelloy C-276	B	400	0	0	<1	---	---
Hastelloy C-276	C	400	0	<1	<1	---	---

* A CsCl
** B 89 mole % CsCl - 11 mole % $BaCl_2$
*** C 80 mole % CsCl - 20 mole % $BaCl_2$

The extent of waste-metal interaction in the radioactive cesium chloride capsules was determined from photomicrographs. In general the metal specimens tested with the radioactive cesium chloride showed slightly more attack than samples tested with nonradioactive cesium chloride. The increased rate of attack observed with the radioactive waste does not appear to be sufficient to raise doubt as to the successful containment of cesium chloride at 400°C.

Photomicrographs of 316L stainless steel samples tested with the radioactive cesium chloride wastes are presented in Figures 10 and 11. The maximum attack observed after twelve months at 400°C was about one mil. There was little visual evidence of intergranular penetration. Some pitting and subsurface void formation was present. Carbide precipitation (or possibly sigma phase) was evident in the region near the sample surface and along grain boundaries. The extent of carbide precipitation increased with time at temperature.

The 316L stainless steel capsules used to contain the radioactive cesium chloride waste and metal specimens were also sectioned and examined. The capsule samples showed less attack than the corresponding 316L stainless steel test specimens (see Figure 12). Reasons for the reduced attack of the capsule surface are not known. It could be due to differences in metal surface characteristics, or to differences in the degree of metal-waste contact.

The addition of barium chloride to the radioactive cesium chloride waste appeared to have little effect on the observed attack of the 316L stainless steel.

The 316L stainless steel capsules tested at 400°C with nonradioactive cesium chloride wastes showed very little attack (see Figures 13 and 14). Both the photomicrographs and electron microprobe analysis indicated very little intergranular corrosion. Some carbide precipitation was evident along grain boundaries and slip planes. The capsules tested at 600°C showed significantly more attack. There is definite evidence of intergranular penetration as well as a general layer type attack of the metal surface (see Figure 15). Carbide precipitation along grain boundaries and slip planes is much heavier than in corresponding capsules tested at 400°C.

The Hastelloy C specimens tested with radioactive cesium chloride showed slightly more attack than the corresponding 316L samples. Photomicrographs of the Hastelloy C samples are shown in Figures 16 and 17. All Hastelloy C samples showed evidence of some intergranular corrosion. In addition there was some dissolution of the metal surface and pitting. The Hastelloy C samples tested with nonradioactive cesium chloride showed substantially more attack than equivalent 316L samples, especially at the longer time periods and at 600°C (see Figures 18-20). At 400°C there was substantial surface dissolution and some intergranular penetration. At 600°C surface dissolution and pitting was significantly increased, but there was little apparent increase in intergranular corrosion. In the tests with nonradioactive wastes, the waste containing the most barium chloride appeared to be the most corrosive to the Hastelloy C. This effect was not observed in the radioactive tests or the tests with 316L stainless steel.

Tests with Hastelloy C-276 and nonradioactive cesium chloride gave results comparable with those obtained from Hastelloy C. Photomicrographs of Hastelloy C-276 samples are shown in Figure 21. Electron microprobe analysis indicated some intergranular corrosion, but the penetration was no worse than with Hastelloy C.

Welding appeared to have little effect on the compatibility of 316L stainless steel and Hastelloy C with nonradioactive cesium chloride (see Table XI). Both unannealed and annealed weld samples showed very little attack as the photomicrographs in Figures 22 and 23 show.

The possibility exists for crevice corrosion to occur in the cap area of the test capsules. The appropriate sections of a number of nonradioactive capsules were analyzed. Both the 316L stainless steel and Hastelloy C capsules showed some indications of crevice corrosion (see Figure 24). The extent of corrosion did not appear to increase significantly with time. Capsules tested for three months showed approximately the same amount of corrosion as those tested for thirty-six months.

STRONTIUM FLUORIDE COMPATIBILITY

Results of the strontium fluoride compatibility studies (except the scouting studies) are summarized in Tables XII and XIII. The data indicate that Haynes 25 is the preferred material for containing the strontium fluoride waste. Hastelloy X shows the least resistance to attack while Hastelloy C shows more resistance than Hastelloy X but less than Haynes 25. It appears that either Haynes 25 or Hastelloy C could be used to contain strontium fluoride waste at 400°C for relatively long periods of time.

TABLE XI Compatibility of Welded Metals with Cesium Chloride

Metal	Waste Composition	Temperature °C	Depth of Metal Affected, mils 2,920 hrs	4,380 hrs
316L	A*	400	0	<1
316L (annealed)	A	400	0	<1
316L	B**	400	0	<1
316L (annealed)	B	400	0	<1
Hastelloy C	A	400	0	<1
Hastelloy C (annealed)	A	400	0	<1
Hastelloy C	B	400	0	<1
Hastelloy C (annealed)	B	400	0	<1

* 89 mole % CsCl + 11 mole % $BaCl_2$
** 80 mole % CsCl + 20 mole % $BaCl_2$

TABLE XII Radioactive Strontium Fluoride Compatibility Data

Metal	Waste Composition	Temperature °C	Depth of Metal Affected, mils		
			2,190 hrs	4,380 hrs	8,760 hrs
Haynes 25	A*	400	< 1	2	2
Haynes 25	B**	400	< 1	1	3
Hastelloy C	A	400	< 1	3	3
Hastelloy C	B	400	< 1	2	3
Hastelloy X	A	400	< 1	4	4
Hastelloy X	B	400	< 1	2	5
316L SS	A	400	< 1	< 1	2
316L SS	B	400	< 1	< 1	2

* A SrF_2
** B 74 mole % SrF_2 - 13 mole % ZrF_4 - 13 mole % Zr

TABLE XIII Nonradioactive Strontium Fluoride Compatibility Data

Metal	Waste Composition	Temperature °C	Depth of Metal Affected, mils				
			2,190 hrs	4,380 hrs	8,760 hrs	17,520 hrs	26,280 hrs
Haynes 25	A*	400	0	<1	<1	---	---
Haynes 25	A	800	<1	<1	<1	---	---
Haynes 25	B**	400	0	1	<1	<1	1
Haynes 25	B	800	<1	<1	<1	1	1
Haynes 25	C***	400	0	<1	<1	<1	<1
Haynes 25	C	800	<1	<1	<1	1	2
Hastelloy C	A	400	0	<1	<1	---	---
Hastelloy C	A	800	<1	<1	1	---	---
Hastelloy C	B	400	0	<1	<1	<1	2
Hastelloy C	B	800	<1	2	<1	2	3
Hastelloy C	C	400	0	<1	<1	1	<1
Hastelloy C	C	800	<1	1	2	3	3
Hastelloy X	A	400	0	<1	<1	---	---
Hastelloy X	A	800	0	<1	<1	---	---
Hastelloy X	B	400	0	<1	<1	2	1
Hastelloy X	B	800	1	<1	<1	3	2
Hastelloy X	C	400	0	<1	1	1	2
Hastelloy X	C	800	1	<1	1	3	3
316L SS	A	400	0	0	<1	<1	---
316L SS	A	800	5	3	2	3	---
316L SS	B	400	0	<1	1	<1	---
316L SS	B	800	1	2	2	2	---
316L SS	C	400	0	<1	1	<1	---
316L SS	C	800	2	2	2	1	---

* A SrF_2
** B 88 mole % SrF_2 - 6 mole % ZrF_4 - 6 mole % Zr
*** C 74 mole % SrF_2 - 13 mole % ZrF_4 - 13 mole % Zr

The 316L stainless steel might also be satisfactory for containment at 400°C.

Based on the photomicrographs obtained, waste-metal interaction was substantially greater with the radioactive wastes than with the nonradioactive wastes. This applied to all four metals tested. It is difficult to place a quantitative value on the increased attack observed with the radioactive wastes. With every metal, however, the corrosion rate was more than doubled.

Photomicrographs of Haynes 25 samples tested with the radioactive strontium fluoride wastes are shown in Figures 25 and 26. All of the samples show the effects of surface dissolution and pitting. Specimens tested for twelve months show some degree of intergranular attack. Addition of zirconium tetrafluoride and zirconium metal to the strontium fluoride waste did not appear to influence the waste-metal interaction.

Nonradioactive strontium fluoride wastes were much less corrosive to Haynes 25 at 400°C than the radioactive wastes. Haynes 25 capsules tested for three years with nonradioactive wastes exhibited less attack than samples tested for one year with the radioactive wastes (see Figures 27-29). Again some surface dissolution was apparent on most samples. There was little evidence of intergranular attack. At 800°C attack of the Haynes 25 by the nonradioactive SrF_2 was significantly greater than at 400°C (see Figures 30 and 31). Surface dissolution was greater and pitting was apparent in some specimens (especially those capsules in which zirconium had not been added to the waste). However, neither the photomicrographs nor the electron microprobe analysis

indicated that intergranular attack was a problem. The samples tested at 800°C all showed evidence of intragranular and grain boundary precipitate formation. The precipitate was not identified. In both the 400 and 800°C with nonradioactive SrF_2 the presence of zirconium in the waste appeared to reduce the metal attack slightly.

Hastelloy C exhibited less resistance to attack by the strontium fluoride wastes than the Haynes 25. Photomicrographs of Hastelloy C samples tested with the radioactive wastes indicated a layer-type attack of all samples (Figures 32 and 33). Pitting and subsurface void formation was evident, as well, in some samples. There was little visual indication of intergranular attack. Addition of zirconium tetrafluoride and zirconium metal to the waste had little apparent effect on the corrosion of the Hastelloy C.

Nonradioactive tests with Hastelloy C showed substantially more attack than the corresponding Haynes 25 tests. The attack observed was significantly less, however, than with the radioactive waste. Samples tested at 400°C for three years with the nonradioactive wastes showed much less attack than samples tested one year with the radioactive waste. Samples tested for 36 months at 800°C with the nonradioactive waste showed about the same level of attack as those tested for one year with the radioactive waste. The Hastelloy C samples tested at 400°C showed layer-type attack with some pitting (see Figures 34-36). Electron microprobe analysis indicated that intergranular attack was not significant. The presence of ZrF_4 and Zr metal in the waste appeared to increase the rate of attack slightly.

At 800°C the attack of the Hastelloy C was greatly increased, especially in those capsules in which zirconium had been added to the waste (see Figures 37-39). Samples in contact with the zirconium-containing waste showed a layer-type attack with selective leaching of alloy components. Electron microprobe analysis showed the reaction layer was largely depleted of nickel; and that there was a buildup of zirconium and nickel in the SrF_2 adjacent to the reaction layer. Intergranular attack did not appear to be significant.

The tests run with Hastelloy C-276 and nonradioactive strontium fluoride indicate little difference between Hastelloy C and Hastelloy C-276 in their resistance to attack by the waste. The data obtained with the Hastelloy C-276 are summarized in Table XIV. The type of attack observed with the C-276 was identical to that found in the Hastelloy C capsules.

The Hastelloy X showed less resistance to attack by the strontium fluoride than the other three metals tested. Photomicrographs of Hastelloy X specimens evaluated with radioactive strontium fluoride wastes are presented in Figures 40 and 41. The types of attack found varied somewhat between samples. Those samples tested for three months showed dissolution of the metal surface with some pitting and intergranular penetration. Samples tested for six and twelve months exhibited a layer-type attack with what appears to be some selective leaching. Intergranular attack was not as apparent as in the three-month samples. The presence of ZrF_4 and zirconium in the waste did not appear to affect the rate of metal attack.

The Hastelloy X samples tested with nonradioactive wastes showed

TABLE XIV SrF_2 - Hastelloy C-276 Compatibility Data

Waste Composition	Temperature °C	Depth of Metal Affected, mils		
		2,190 hrs	4,380 hrs	8,760 hrs
A*	400	0	<1	1
B**	400	0	<1	<1
C***	400	0	<1	<1

* A SrF_2

** B 88 mole % SrF_2 - 6 mole % ZrF_4 - 6 mole % Zr

*** C 74 mole % SrF_2 - 13 mole % ZrF_4 - 13 mole % Zr

less attack than the corresponding radioactive samples; capsules tested for three years at 400°C showed far less attack than radioactive samples tested for one year. Even samples tested for three years at 800°C showed no more attack than the radioactive samples tested for one year. The Hastelloy X samples tested at 400°C showed a slight indication of layer-type attack. However, electron microprobe analysis indicated substantial intergranular penetration which was not obvious from the photomicrographs (see Figures 42-44). At 800°C the capsules tested with SrF_2 showed only slight attack (Figure 45). However, the Hastelloy X tested with the zirconium-containing waste showed extensive attack (Figures 46 and 47). The photomicrographs showed a layered attack with selective leaching. As was the case with Hastelloy C, electron microprobe analysis showed a depletion of nickel in the reaction zone and a buildup of nickel and zirconium in the SrF_2 adjacent to the reaction layer. However, the microprobe indicated less intergranular penetration than in the capsules tested at 400°C.

At 400°C the 316L stainless steel appeared to be about as resistant to attack by the strontium fluoride waste as Haynes 25. However, at 800°C the 316L stainless steel was attacked at a much faster rate than the Haynes 25. In the tests with radioactive strontium fluoride the 316L capsules served as the test specimens. This differed from the other radioactive metal tests in which metal discs were packed in the fluoride. Photomicrographs of the 316L capsules are shown in Figures 48 and 49. The capsules were sectioned such that the exposed face represented a segment of the capsule circumference. This accounts for the curved surface

which is apparent in some of the photomicrographs. The 316L stainless steel capsules tested for three and six months showed only slight evidence of attack. Much greater attack was evident in the capsules tested for twelve months. Layer-type attack predominated with what appears to be selective dissolution. There is little evidence of intergranular attack.

The 316L stainless steel samples tested with nonradioactive strontium fluoride at 400°C showed very little attack (Figures 50-52). The samples tested at 800°C showed much greater attack. In addition, the attack observed did not appear to be time dependent. Metal specimens tested for three and six months were as badly attacked as samples tested for twenty-four months (Figures 53-55). The addition of zirconium metal and zirconium tetrafluoride to the waste had a definite effect on the attack of the 316L stainless steel. When zirconium was not present in the waste there was a layer-type attack of the metal, and microprobe analysis gave no indication of intergranular attack. When zirconium was present the layer-type attack was greatly reduced. However, microprobe analysis indicated some intergranular corrosion which is not obvious in the photomicrographs.

Welding appeared to have little effect on the compatibility of the various metals with the strontium fluoride wastes at 400°C. Results of the tests with welded samples are summarized in Table XV. Both annealed and unannealed weld samples were evaluated and little attack was observed with any of the metals.

The cap areas of several of the nonradioactive test capsules were examined for possible crevice corrosion. All four of the metals tested did show indications of crevice corrosion, but the attack did not appear

TABLE XV Compatibility of Welded Metals with Strontium Fluoride at 400°C

Metal	Waste Composition	Depth of Metal Affected, mils 2,190 hrs	4,380 hrs
Haynes 25	A*	0	0
Haynes 25 (annealed)	A	< 1	< 1
Haynes 25	B**	< 1	< 1
Haynes 25 (annealed)	B	< 1	< 1
Hastelloy C	A	0	< 1
Hastelloy C (annealed)	A	0	< 1
Hastelloy C	B	< 1	< 1
Hastelloy C (annealed)	B	0	1
Hastelloy X	A	< 1	< 1
Hastelloy X (annealed)	A	0	< 1
Hastelloy X	B	0	< 1
Hastelloy X (annealed)	B	< 1	< 1

* A SrF_2
** B 84 mole % SrF_2 - 13 mole % ZrF_4 - 13 mole % Zr

to increase with time. Capsules tested for thirty-six months showed no more attack than those tested for three and six months.

The scouting tests with strontium fluoride were made as a safety precaution in case all four metals evaluated in the detailed tests were found to be unsatisfactory. The tests lasted for three months at 800°C and thirteen metals were tested including the four metals studied in detail. Results of the tests are summarized in Table XVI. The data confirm that Haynes 25, Hastelloy C and Hastelloy X are more resistant to attack by strontium fluoride at 800°C than most metals. Only Inconel 600 and TZM, of the other metals tested, appeared to be as resistant to attack. In fact, the TZM appeared to be completely unaffected by contact with the strontium fluoride (see Figures 56 and 57).

Several materials were tested as potential container materials for firing strontium fluoride. The tests were carried out at 1100°C and lasted for twenty-four hours. Results are summarized in Table XVII. Tungsten was the best of the materials tested. Additional tungsten samples were tested for longer time periods (up to seven days) and none showed any evidence of attack by the fluoride.

CESIUM DIURANATE COMPATIBILITY

Cesium diuranate wastes were tested with various metal specimens at 400 and 1000°C. The tests lasted for 2,190 hours. At 1000°C all of the metals showed extensive attack by the waste. Some of the test specimens (0.125 inches thick) were completely consumed. Because of the excessive attack of the samples it was impossible to obtain a quantitative measure

TABLE XVI Compatibility Data from SrF_2 Scouting Studies

Metal	Waste Composition	Temperature °C	Depth of Metal Affected, mils 2,190 hours
Hastelloy C	A*	800	1
Hastelloy C	B**	800	< 1
Hastelloy X	A	800	< 1
Hastelloy X	B	800	0
Hastelloy F	A	800	1
Hastelloy F	B	800	2
Inconel 600	A	800	< 1
Inconel 600	B	800	< 1
Haynes 25	A	800	< 1
Haynes 25	B	800	< 1
Udimet 700	A	800	2
Udimet 700	B	800	3
Rene 41	A	800	2
Rene 41	B	800	1
Waspelloy	A	800	2
Waspelloy	B	800	< 1
Incaloy 804	A	800	2
Incaloy 804	B	800	2
Multimet	A	800	2
Multimet	B	800	1
TZM	A	800	0
TZM	B	800	0
304L SS	A	800	2
304L SS	B	800	1
316L SS	A	800	2
316L SS	B	800	2

* A SrF_2

** B 88 mole % SrF_2 - 6 mole % ZrF_4 - 6 mole % Zr

TABLE XVII Metal Attack by SrF_2 After 24 Hours at 1100°C

Material Tested	Depth of Material Affected (mils)
316L SS	5
Hastelloy C	4
Haynes 25	2
18-18-2 Alloy	2
Platinum	2
TZM	1
Tantalum	1
Tungsten	0
Ta - 10% W	3
Impervious Alumina	~5
Impervious Magnesia	~10
Quartz	>10

of the corrosion rate. Hastelloy X showed the least attack of the metals and it was more than half consumed. Examination of the residual Hastelloy X samples showed extensive subsurface void formation, probably due to selective dissolution of one or more components of the alloy. Little difference in waste-metal interaction was observed between the capsules containing cesium diuranate and those containing cesium diuranate plus barium diuranate.

Metal specimens tested at 400°C showed far less attack. Results of the tests are given in Table XVIII. Photomicrographs of metal test specimens are presented in Figures 58 and 59. Haynes 25 and Hastelloy X samples showed essentially no attack. The other samples, except for the zircaloy, show only slight attack. The zircaloy was badly corroded, especially by the waste containing barium diuranate. Except for the zircaloy, the presence of barium diuranate in the waste had little visual effect on the metal corrosion observed. These results indicate that a variety of metals can probably be used to safely contain cesium diuranate at 400°C for long periods of time.

STRONTIUM PYROPHOSPHATE COMPATIBILITY

Strontium pyrophosphate wastes were tested with various metals for 2,190 hours at 400 and 1000°C. At 1000°C all of the metal specimens showed substantial attack and some were completely consumed. Figure 60 shows two of the sectioned capsules. Attack of the test pieces is readily apparent. Photomicrographs of some of the metal specimens are shown in Figures 61 and 62.

TABLE XVIII Cesium Diuranate Compatibility Data

Metal	Waste Composition	Temperature °C	Depth of Metal Affected, mils 2,190 hours
Haynes 25	A*	400	0
Haynes 25	B**	400	0
Hastelloy C	A	400	<1
Hastelloy C	B	400	<1
Hastelloy X	A	400	0
Hastelloy X	B	400	0
Inconel 600	A	400	1
Inconel 600	B	400	<1
Udimet 700	A	400	<1
Udimet 700	B	400	<1
Zircaloy	A	400	5
Zircaloy	B	400	10
304L SS	A	400	<1
304L SS	B	400	<1
316L SS	A	400	<1
316L SS	B	400	<1

* A $Cs_2U_2O_7$

** B 89 mole % $Cs_2U_2O_7$ - 11 mole % BaU_2O_7

Samples tested at 400°C showed little or no evidence of attack (see Table XIX). Only the 304L stainless steel was corroded to a measurable extent. Photomicrographs of various test specimens are shown in Figures 63 and 64. The presence of zirconium metal in the waste had no apparent effect on waste-metal interaction. Based on the short-term test results it appears that a variety of metals could probably be used to contain a strontium pyrophosphate waste for long periods of time at 400°C.

RADIOLYSIS OF PACKAGED WASTES

The radiolysis experiments carried out with radioactive cesium chloride and strontium fluoride test capsules gave no indication of potential pressurization problems. Capsule pressures were monitored as a function of time and no unusual pressure excursions were observed in any of the capsules.

When the capsules were sealed by welding each capsule had an internal pressure of approximately one atmosphere. As the sealed capsule cooled, after welding, a vacuum developed inside the capsule. The sealed capsules were stored on a metal bench in the shielded cell, and each reached an equilibrium temperature with the surroundings. The equilibrium temperature was initially about 150°C, and decreased slightly as the heat output of the capsules decreased with time. The initial vacuum of the various capsules ranged from 8 to 15 inches of mercury. Pressures inside the capsules have fluctuated somewhat with time, but at no time has the pressure of any of the capsules reached one atmosphere absolute. The tests have been under way about three years and will continue indefinitely.

TABLE XIX Strontium Pyrophosphate Compatibility Data

Metal	Waste Composition	Temperature °C	Depth of Metal Affected, mils 2,190 hours
Haynes 25	A*	400	0
Haynes 25	B**	400	0
Hastelloy C	A	400	0
Hastelloy C	B	400	0
Hastelloy X	A	400	0
Hastelloy X	B	400	0
Inconel 600	A	400	0
Inconel 600	B	400	0
Udimet 700	A	400	0
Udimet 700	B	400	0
Waspelloy	A	400	0
Waspelloy	B	400	0
304L SS	A	400	<1
304L SS	B	400	1
316L SS	A	400	0
316L SS	B	400	0

* A $Sr_2P_2O_7$

** B 74 mole % $Sr_2P_2O_7$ - 13 mole % SrP_2O_7 - 13 mole % Zr

The results indicate that capsule pressurization due to radiolysis of the waste should not be a problem. However, the data do not rule out the possibility of radiolysis occurring, with gas formation, and the gaseous products subsequently reacting with the container material.

ESTIMATES OF LONG-TERM ATTACK

The Waste Encapsulation concept calls for the storage of cesium and strontium wastes for 600 years. Safe storage requires insured container integrity throughout the storage period. It is necessary, therefore, to be able to accurately assess the effects of long-term waste-container interaction on container integrity. This can only be done by extrapolating the short-term compatibility data which can be obtained in reasonable time periods.

To extrapolate the short-term compatibility data to long time periods it is necessary to know, or be able to approximate, the form of the rate equation(s) for metal attack. The problem is further complicated by the fact that the reaction temperature is continually decreasing as the heat output of the container decreases with time. However, it is reasonable to ignore the changing temperature and extrapolate compatibility data obtained at the maximum anticipated waste-container interface temperature of 400°C (all experimental data show that metal attack by the wastes decreases as the interface temperature decreases). A considerable safety factor is introduced by extrapolating data obtained at 400°C because the actual interface temperature will be far below that temperature for most of the storage period.

The compatibility data, reported in the previous section, show that the radioactive wastes are more corrosive to the test metals than the corresponding nonradioactive wastes. Therefore, estimates of long-term metal attack will be based principally on data obtained from the radioactive tests. It is difficult to determine the form(s) of the rate equation which should be used from the limited radioactive data available. Even using the data obtained in the nonradioactive tests there is considerable doubt as to which rate equation should be used.

The metal attack can be estimated using a linear rate equation. The linear rate equation will predict a maximum metal attack; but it is extremely doubtful that it is applicable to the problem under consideration. Considering the type of attack observed in most of the metal samples (subsurface void formation, layer-type corrosion, intergranular penetration, etc.), and the fact that solid-solid reactions are probably involved, it is much more likely that parabolic or logarithmic rate equations should be used to extrapolate the compatibility data. Close examination of the limited data available indicates that in most cases a parabolic rate equation will probably provide the most accurate estimate of long-term metal attack.

The metal attack data reported in the earlier tables were stated in one mil increments (i.e., 1.5 mil attack was reported as 2 mils, 0.5 mils as <1 mil). In predicting the long-term metal attack, using the parabolic rate equation, the data as reported could not be used. Instead it was necessary to determine as closely as possible from the photomicrographs (and microprobe data) the extent of metal attack and use this data in predicting long-term attack.

The results of the compatibility tests show cesium chloride waste, prepared by the WESF flowsheet, can be safely contained in 316L stainless steel at 400°C for short periods of time. The rate of attack of the 316L stainless steel at 400°C is extremely slow, and one can predict safe storage at 400°C for very long periods of time. The depth of metal affected by the cesium chloride waste as a function of storage time was estimated using the radioactive compatibility data and a parabolic rate equation of the form

$$D^2 = k_1 t + k_2$$

where

D = depth of metal affected

t = storage time at 400°C

k_1 = constant

k_2 = constant

The estimated metal attack obtained by the extrapolation of the short-term data is shown in Figure 65. The estimate indicates that the waste can be safely contained in 316L stainless steel at 400°C for the required storage period. Similar extrapolations (also shown in Figure 65) were made using the data obtained with the nonradioactive cesium chloride wastes. The predicted attack of the 316L stainless steel, even at 600°C, is much less than the predicted attack by the radioactive waste.

There are several possible explanations for the increased attack found with the radioactive cesium chloride compared with the nonradioactive material. It is possible the radioactive wastes contained

impurities not present in the nonradioactive waste. These impurities, even at trace levels, might affect the rate of metal attack. The radioactive test capsules were loaded and TIG welded in an air atmosphere shielded cell. The nonradioactive capsules were loaded in an argon atmosphere gloved box and electron beam welded in a vacuum chamber. It is possible that the radioactive cesium chloride may have picked up traces of water, from the atmosphere, which were trapped in the capsule when it was sealed (cesium chloride is slightly hygroscopic). Similar moisture pickup by the nonradioactive capsules was extremely unlikely. If moisture was present in the radioactive capsules it could have a pronounced effect on the attack of the stainless steel, possibly through the formation of hydrogen chloride. It is also possible that the high radiation field present in the radioactive capsule might affect the rate of metal attack. Possible radiolysis of the cesium chloride or impurities might also affect the rate of attack.

Current WESF design calls for only one major change from the CsCl flowsheet shown in the Appendix. Melt casting will be used instead of step-pressing to load the CsCl into the container. As a result the CsCl will be present in the container as a slug of approximately theoretical density. However, due to shrinkage on cooling the bulk density of the CsCl in the container will be substantially less than the theoretical density (about 70-80%). As a result the degree of contact between the container wall and the CsCl slug will be much less than if the cesium chloride had been step-pressed into the capsule. This reduced contact should serve to reduce the degree of attack of most of the metal surface.

Hastelloy C shows substantially more attack by both the radioactive and nonradioactive CsCl than the 316L. Figure 66 shows the estimated attack of the Hastelloy C during long-term storage. The estimates indicate that Hastelloy C could be used to safely contain the radioactive CsCl waste at 400°C for the required storage period; however, 316L stainless steel is the preferred material. Hastelloy C-276 appears to be about equal to Hastelloy C in its resistance to attack by the chloride waste.

The addition of $BaCl_2$ to the radioactive CsCl waste appeared to have little effect on the metal attack observed. In the tests with inert CsCl, the addition of $BaCl_2$ appeared to increase the attack of the Hastelloy C to a slight degree.

The effects of long-term storage on strontium fluoride-metal compatibility were also estimated using the short-term compatibility data and a parabolic rate equation. The estimates indicate, on an overall basis, that of the four metals tested, Haynes 25 has the greatest resistance to attack by the strontium fluoride. Estimated long-term attack of the Haynes 25 is shown in Figure 67. The estimates indicate that the fluoride waste can be safely contained in Haynes 25 at 400°C for the required storage period. They also show that the nonradioactive fluoride could be safely contained in Haynes 25 at 800°C for similar time periods.

The radioactive strontium fluoride wastes are much more corrosive to Haynes 25 (and other metals tested) than the nonradioactive wastes. Possible explanations for the increased attack found with the radioactive wastes are the same as those discussed in regard to radioactive cesium chloride. Analysis indicated the radioactive strontium fluoride, prepared

by the WESF flowsheet, contained some impurities (including Ba, Cu, K, Mn and Pb) not present in the nonradioactive waste. These impurities, although present in the radioactive waste at low levels, may have accounted for the increased attack. If water was present in the radioactive test capsules, it might also be quite deleterious.

The substantial difference in attack of the Haynes 25 between the radioactive and nonradioactive wastes indicates that additional purification of the strontium fluoride waste prior to encapsulation is probably desirable. Additional compatibility testing to determine the effects of impurities on strontium fluoride compatibility appears warranted.

The 316L stainless steel shows approximately the same resistance to attack at 400°C by both radioactive and nonradioactive strontium fluoride as does the Haynes 25. However, at 800°C the 316L stainless steel is attacked at a much greater rate than the Haynes 25. Estimates for the long-term attack of the 316L stainless steel are shown in Figure 68. While the 316L stainless steel appears to be on a par with Haynes 25 at 400°C, the Haynes 25 is the preferred material because of its better resistance to attack at high temperature. In addition, the 316L stainless steel radioactive data was obtained from 316L capsule samples while the Haynes 25 data was obtained from metal discs contained in the capsules. In similar tests with cesium chloride, 316L capsule samples showed less attack than 316L discs contained in the capsules. Using similar reasoning one might expect 316L discs in contact with the radioactive strontium fluoride to show more attack than the 316L capsule samples.

The Hastelloy C exhibited somewhat less resistance to attack at

400°C than either the Haynes 25 or 316L stainless steel. However, at 800°C the Hastelloy C was much more resistant to attack than the 316L but less resistant than the Haynes 25. Estimates of long-term attack of the Hastelloy C are given in Figure 69. The data available indicate that the Hastelloy C-276 should be about equivalent to the Hastelloy C in its resistance to attack by the fluoride waste. Based on the long-term estimates it appears that the strontium fluoride waste can be adequately contained at 400°C in either Hastelloy C or Hastelloy C-276 for the required storage period.

Hastelloy X shows less resistance to attack by the strontium fluoride waste at 400°C than the other metals tested. The radioactive waste appeared to be especially corrosive to the Hastelloy X. At 800°C the Hastelloy X has greater resistance to attack than the 316L stainless steel. Estimates of the effects of long-term storage on attack of the Hastelloy X are given in Figure 70. Even though the Hastelloy X is attacked more rapidly at 400°C than the other three metals, it appears that it too could be used to contain the strontium fluoride waste for the required storage period.

The estimates of long-term attack indicate that any of the four metals tested could probably be used to contain strontium fluoride at 400°C. Table XX gives a comparison of the attack predicted for each metal by the radioactive strontium fluoride waste. Haynes 25 shows the least attack and is the preferred material on a compatibility basis.

The addition of ZrF_4 and Zr metal to the radioactive SrF_2 waste appeared to have little or no influence on the metal attack observed. In the tests with inert SrF_2, however, the addition of zirconium did

TABLE XX Estimated Attack of Metals at 400°C by Radioactive Strontium Fluoride

Storage Time (Years)	Depth of Metal Affected, mils			
	Haynes 25	316L SS	Hastelloy C	Hastelloy X
10	9	10	14	18
50	21	22	30	40
100	30	32	43	55
300	52	54	74	99
600	73	76	105	134

have a definite effect. In the tests with Haynes 25 the presence of zirconium in the waste reduced the metal attack slightly. With the Hastelloy C and Hastelloy X the addition of zirconium to the waste increased the attack significantly, especially at 800°C.

Container pressurization resulting from gas formation due to radiolysis does not appear to be a problem with either the CsCl or SrF_2 wastes. No pressure buildup was detected in any of the radiolysis test capsules.

Based on the results of the scouting tests, the containment of strontium pyrophosphate and cesium diuranate at 400°C should not be a problem. A variety of metals can probably be used to contain the two compounds for long periods of time at 400°C.

CONCLUSIONS

As a result of the information developed in the current study, the following recommendations can be made regarding the containment of the cesium chloride and strontium fluoride wastes produced in the WESF.

1. The preferred material for containing the cesium chloride waste is 316L stainless steel. Estimates of the effects of long-term storage on attack of the 316L show the cesium chloride can be adequately contained at 400°C for the required storage period using the current container design (total container wall thickness = 0.204 in.). Estimates show that Hastelloy C or Hastelloy C-276 would also provide adequate containment, but 316L is the preferred material.

2. Haynes 25 is the preferred material for containing the strontium fluoride waste, and based on estimates of long-term attack will

provide safe containment of the waste for the required storage period using a double container having a total wall thickness of 0.240 inches. The 316L stainless steel can also be used to contain the waste at 400°C, but it is not recommended for use because of its much poorer high temperature resistance.

3. Hastelloy C will also adequately contain the strontium fluoride waste at 400°C, but will be less resistant to attack than the Haynes 25. Reasons other than compatibility, such as ease of welding compared to Haynes 25, may make Hastelloy C (or C-276) the preferred material for use in the WESF.

ACKNOWLEDGEMENTS

Most of the experimental work covered in this report was performed by C. L. Nelson and R. J. Elovich. Metallographic examination of radioactive samples was performed by the Radiometallurgy section of the Westinghouse Hanford Company. Microprobe analysis and metallography of nonradioactive samples were provided by W. I. Clark of Westinghouse Hanford Company and R. H. Beauchamp of BNW. G. L. Borsheim and E. L. Moore of ARHCO provided information and technical guidance during the course of the study.

REFERENCES

1. F. K. McTaggart and A. G. Turnbull, Aust. J. Chem., 17, pp. 727-30, 1964.

2. T. S. Soine and H. T. Fullam, Unpublished Data, Pacific Northwest Laboratory, 1968.

3. S. J. Rimshaw and E. E. Ketchen, Compatibility Data Sheets for Ce-144, Cs-137, Curium and Sr-90, ORNL-4189, Union Carbide Corporation, ORNL, Oak Ridge, Tennessee, November 1967 (Confidential).

4. W. A. Vogele, Strontium-90 Fuel Program Monthly Progress Report, MND-2848-47, Martin Marietta Corporation, Baltimore, Maryland, May 1966 (Confidential).

5. F. J. Maraglia, Compatibility of Strontium Space Fuel Forms, MND-3062-27, Martin Marietta Corporation, Baltimore, Maryland, June 1966 (Confidential).

6. H. T. Fullam, Mat. Res. Bull., 7, pp. 289-300, 1972.

7. Z. A. Mateiko, E. S. Yaqub'yan and G. A. Bukhalova, Russian Journal of Inorganic Chemistry (English Trans.), p. 1291, 1966.

APPENDIX

A. FIGURES

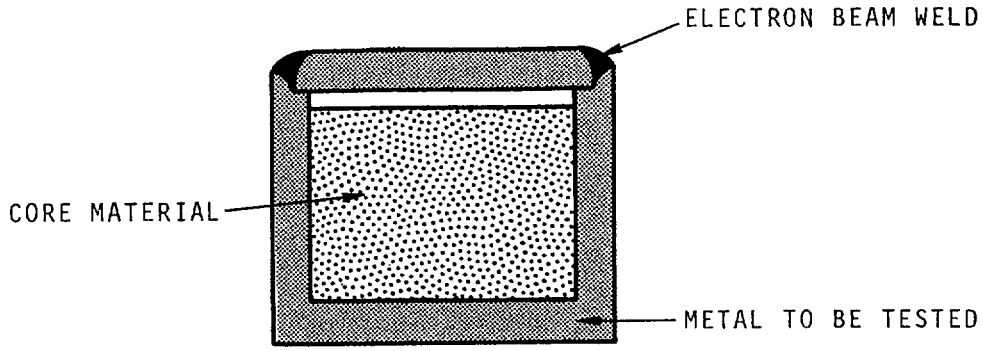

A. INDIVIDUAL TEST COUPLES

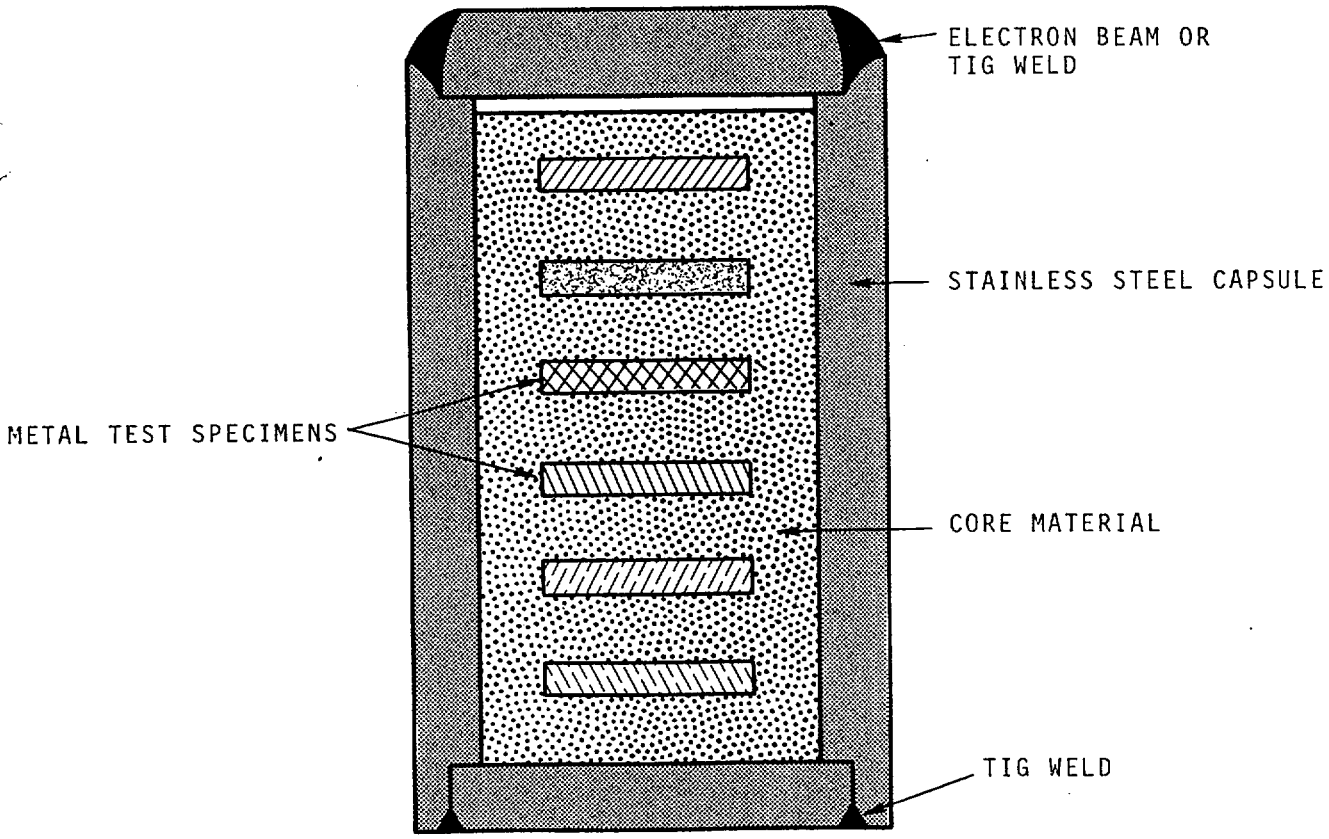

B. COMPOSITE TEST COUPLES

FIGURE 1. Compatibility Test Capsules

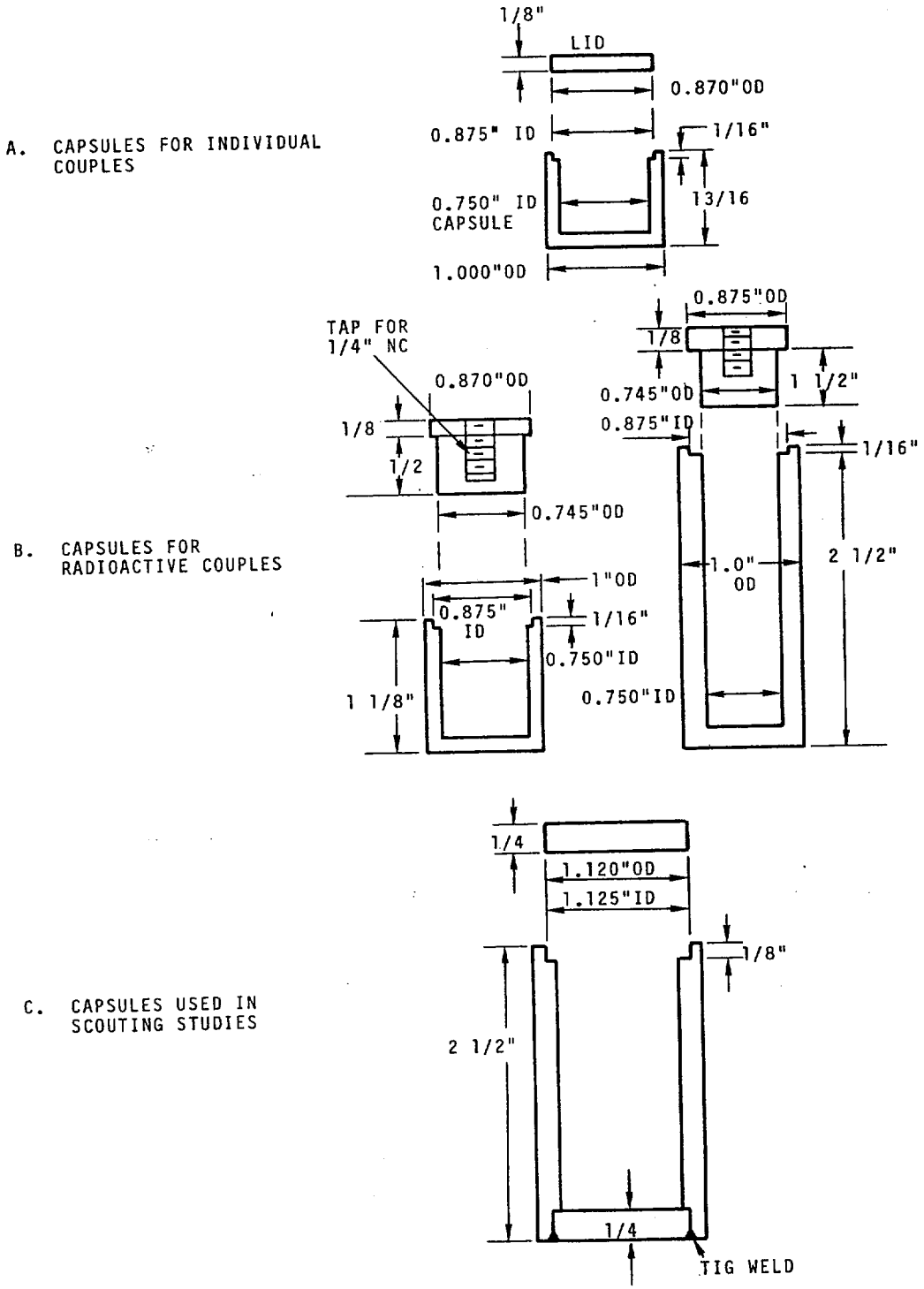

FIGURE 2. Metal Cans Used in Fabricating Test Capsules

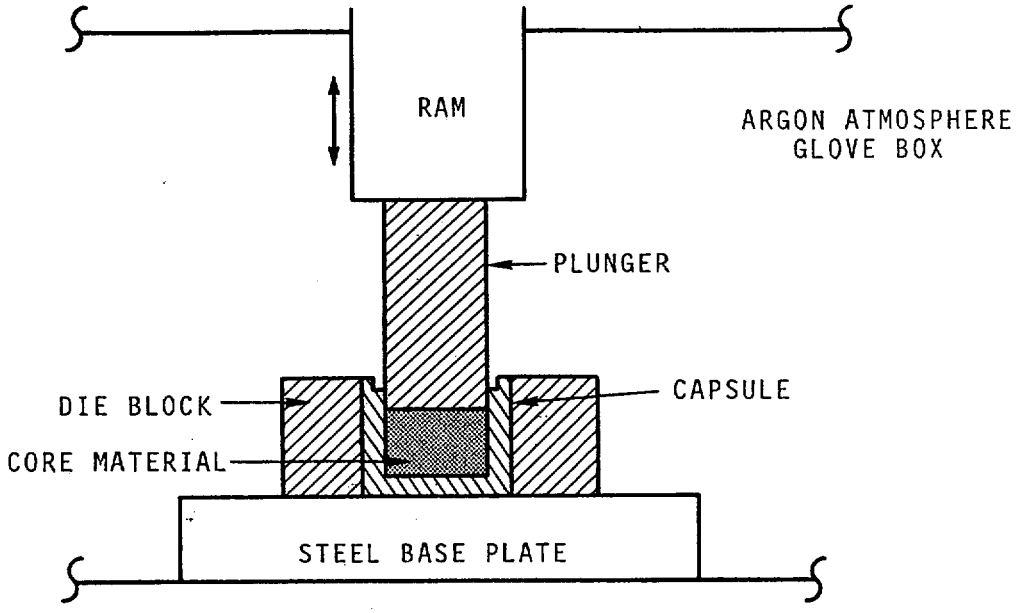

A. APPARATUS FOR LOADING NON-RADIOACTIVE COUPLES

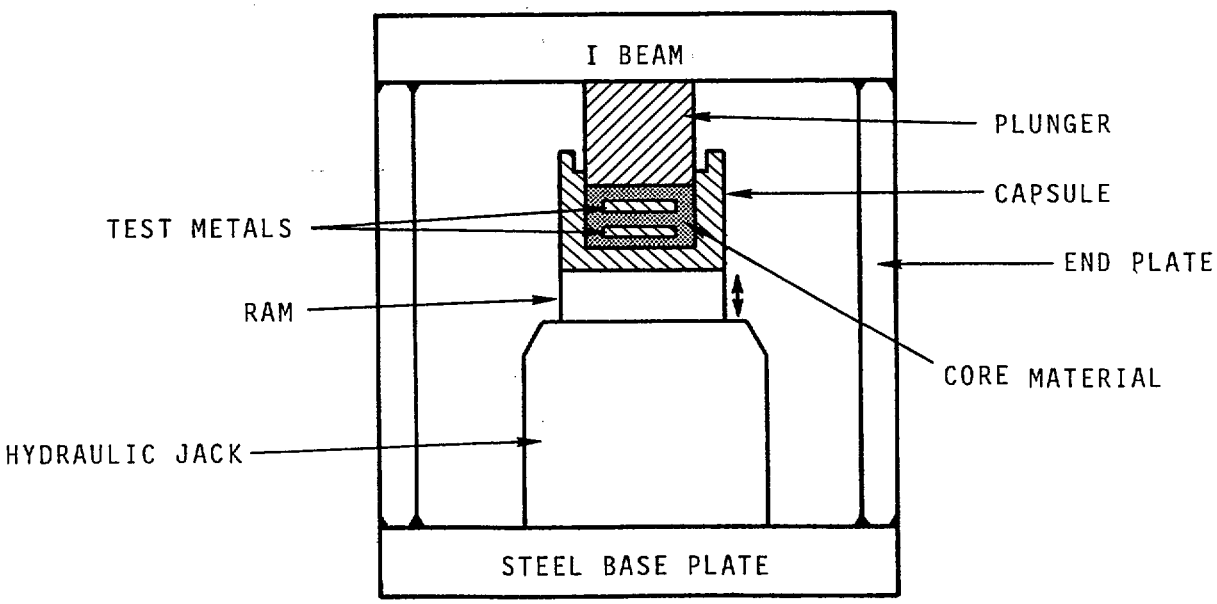

B. APPARATUS FOR LOADING RADIOACTIVE CAPSULES

FIGURE 3. Equipment for Loading Test Capsules

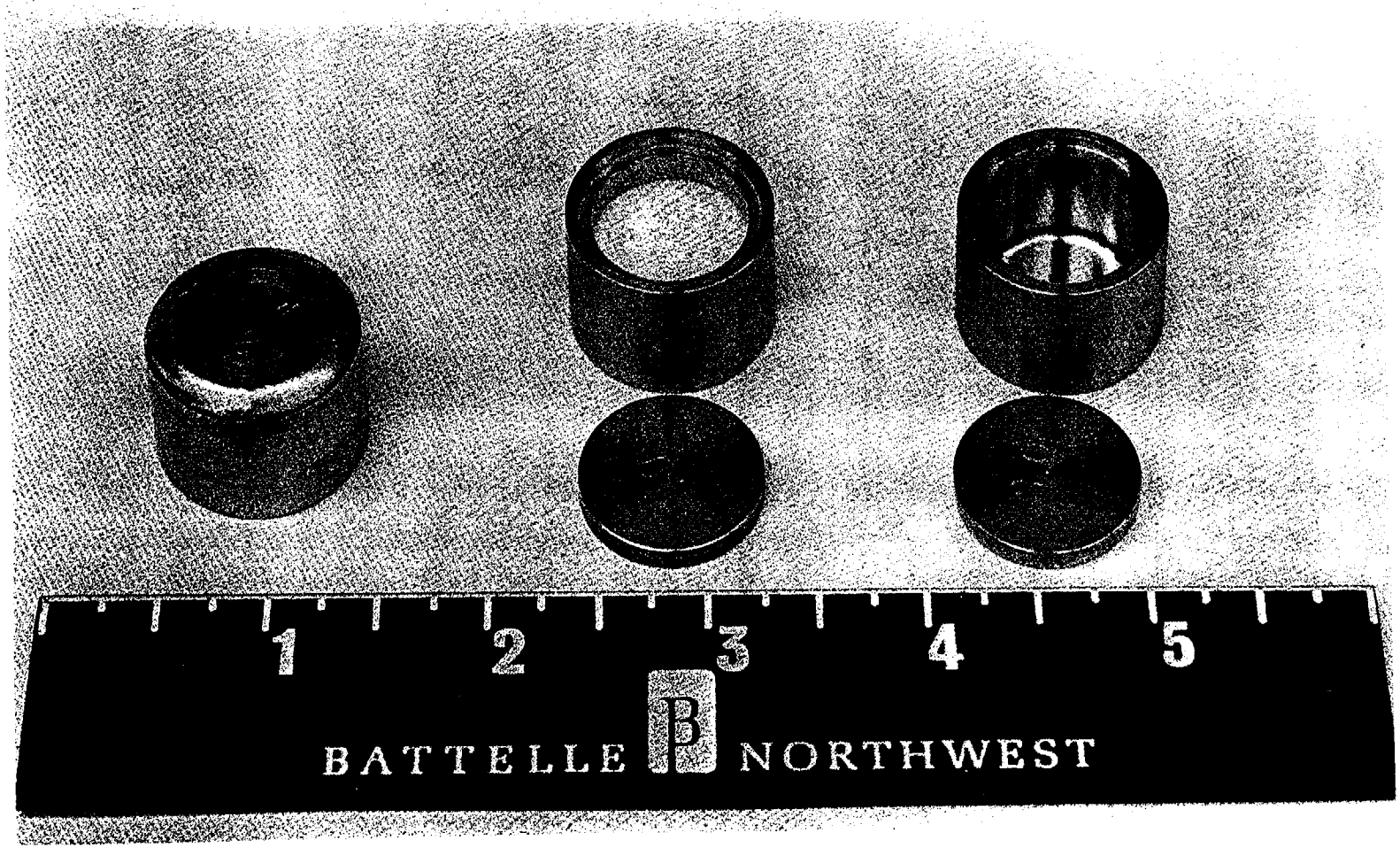

FIGURE 4. Cesium Chloride Capsule in Various Stages of Fabrication

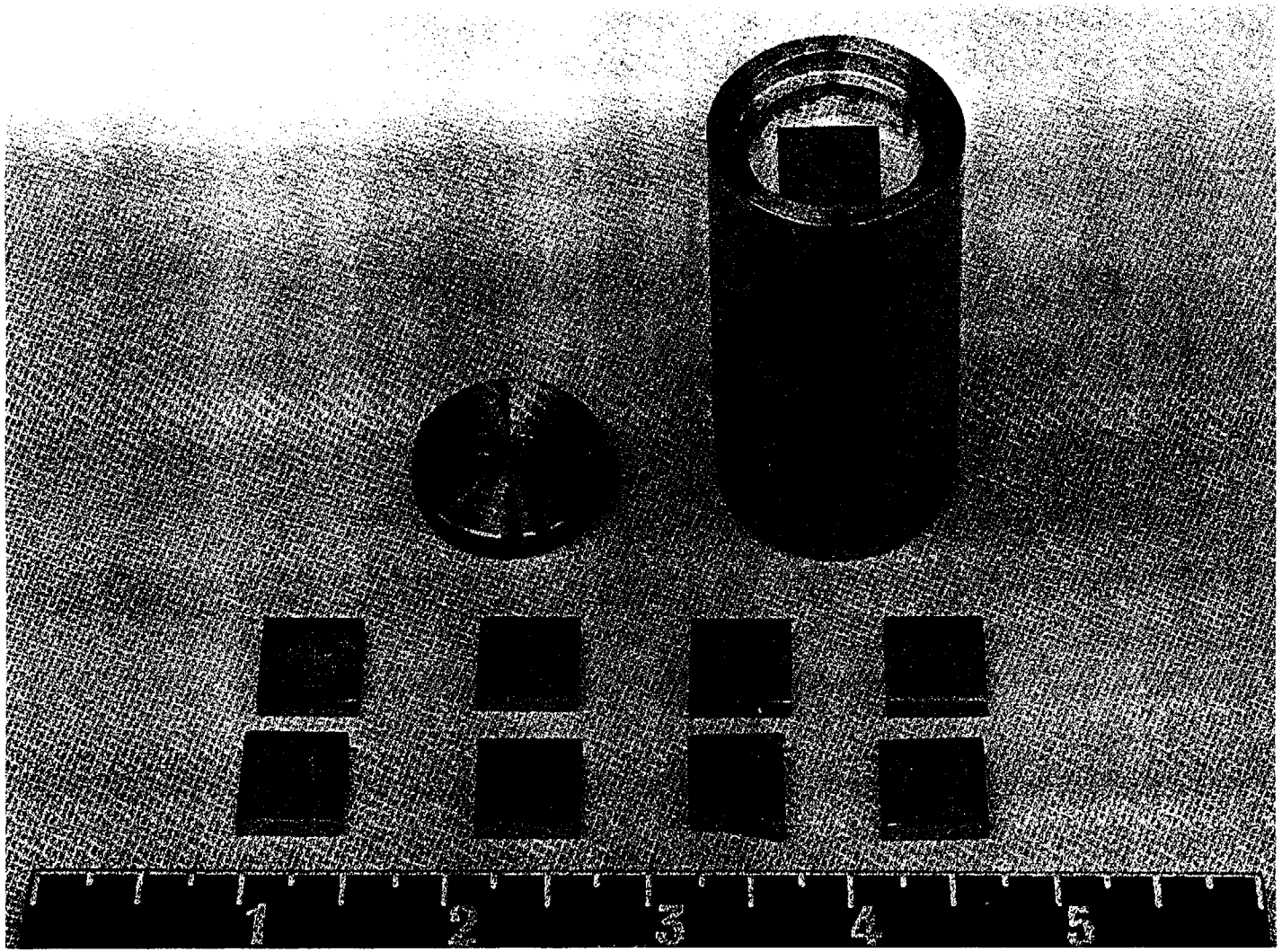

FIGURE 5. Capsule Used in Scouting Studies

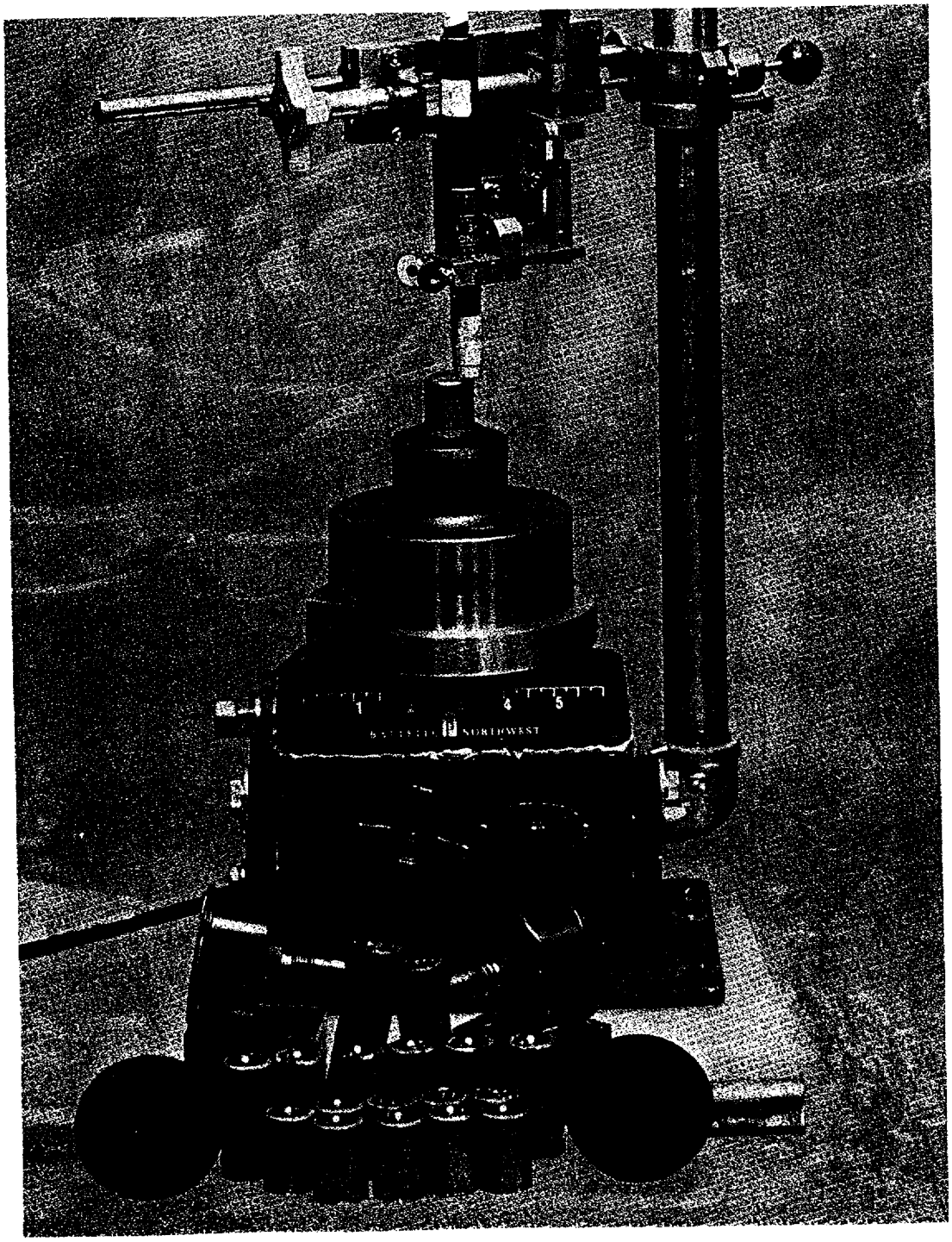

FIGURE 6. Welding Radioactive Capsules in Shielded Cell

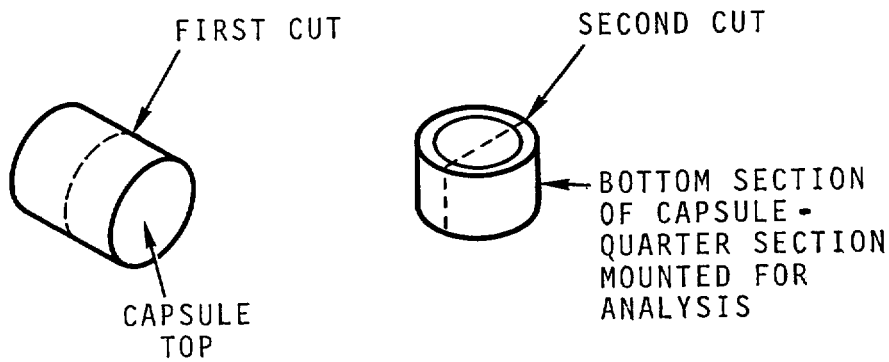

FIGURE 7. Sectioning of Individual Test Capsules

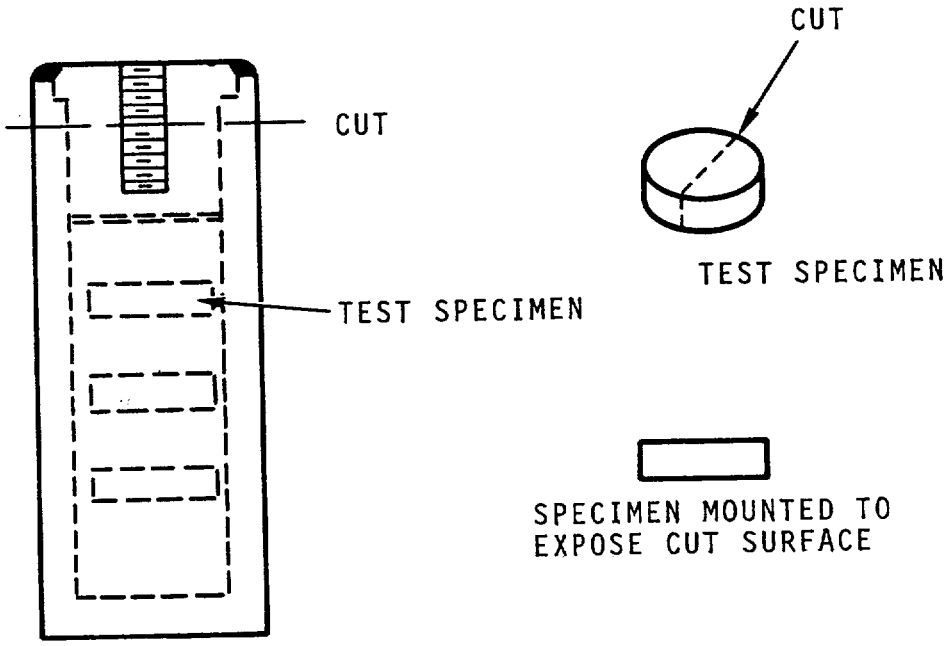

FIGURE 8. Sectioning of Radioactive Test Capsules

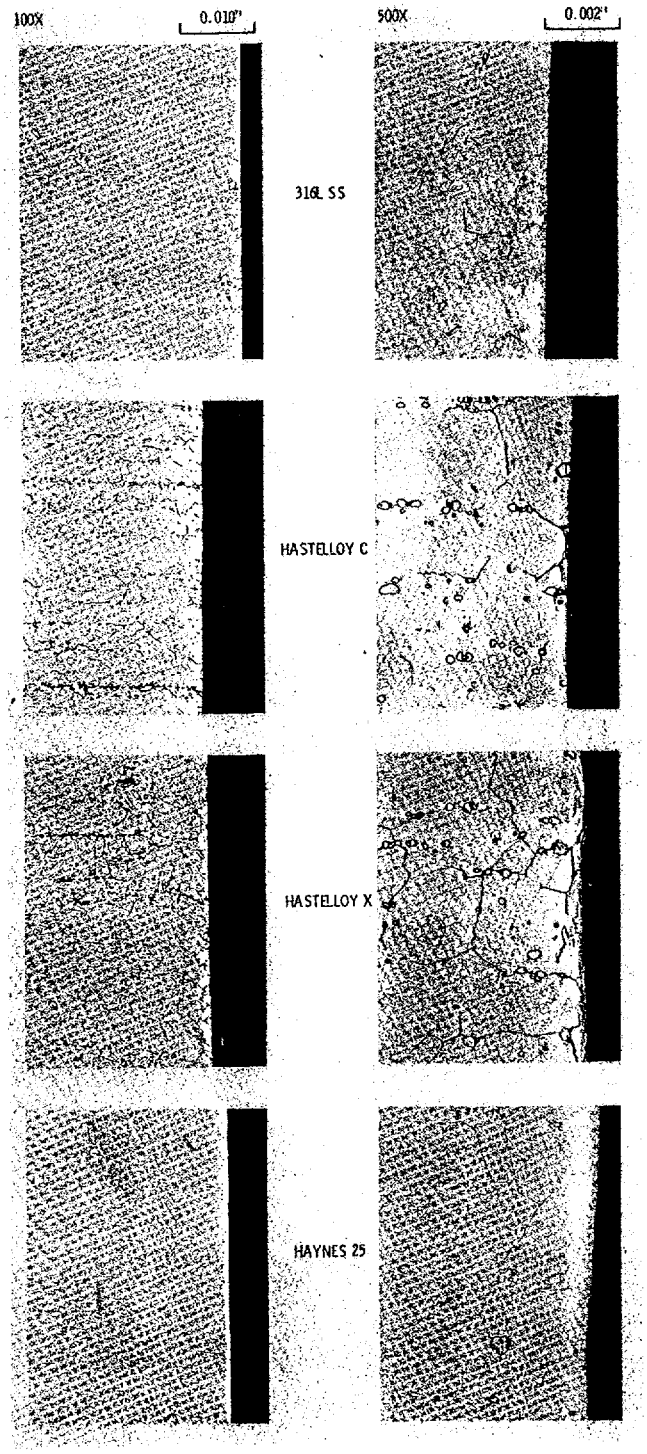

FIGURE 9. Reference Metal Samples

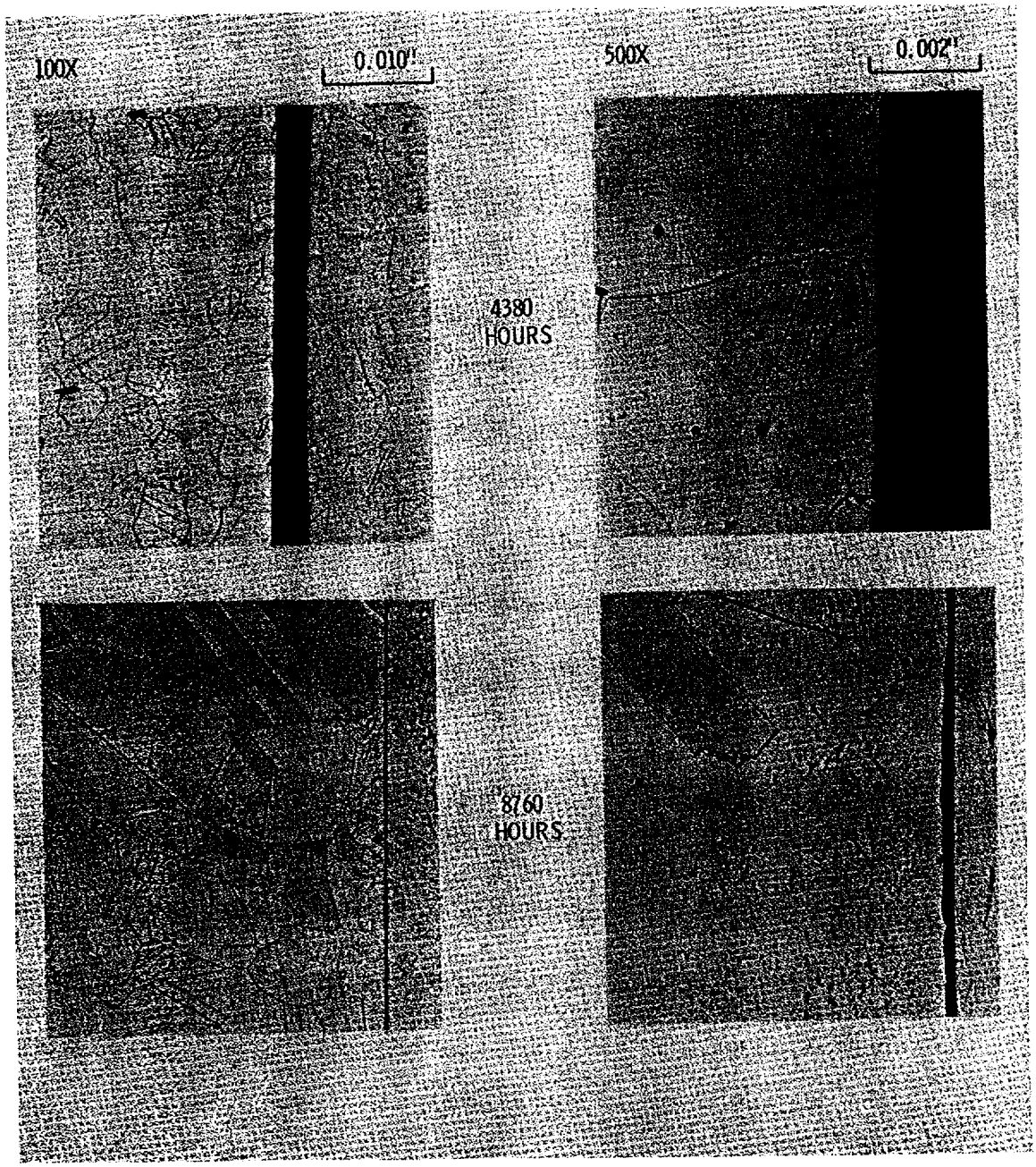

FIGURE 10. Samples of 316L Stainless Steel Tested with Radioactive CsCl at 400°C

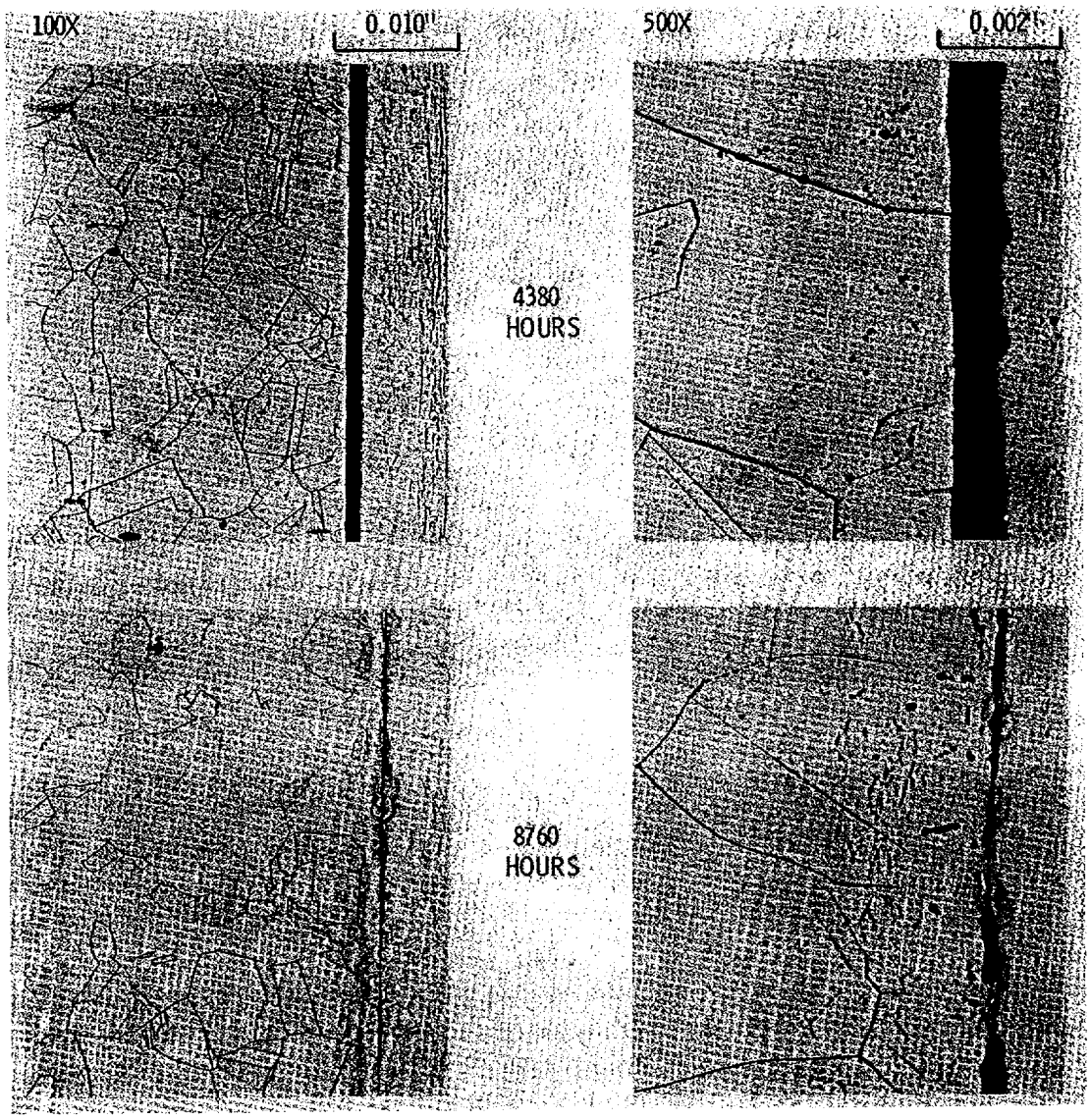

FIGURE 11. Samples of 316L SS Tested with Radioactive CsCl - 20 mole % $BaCl_2$ at 400°C

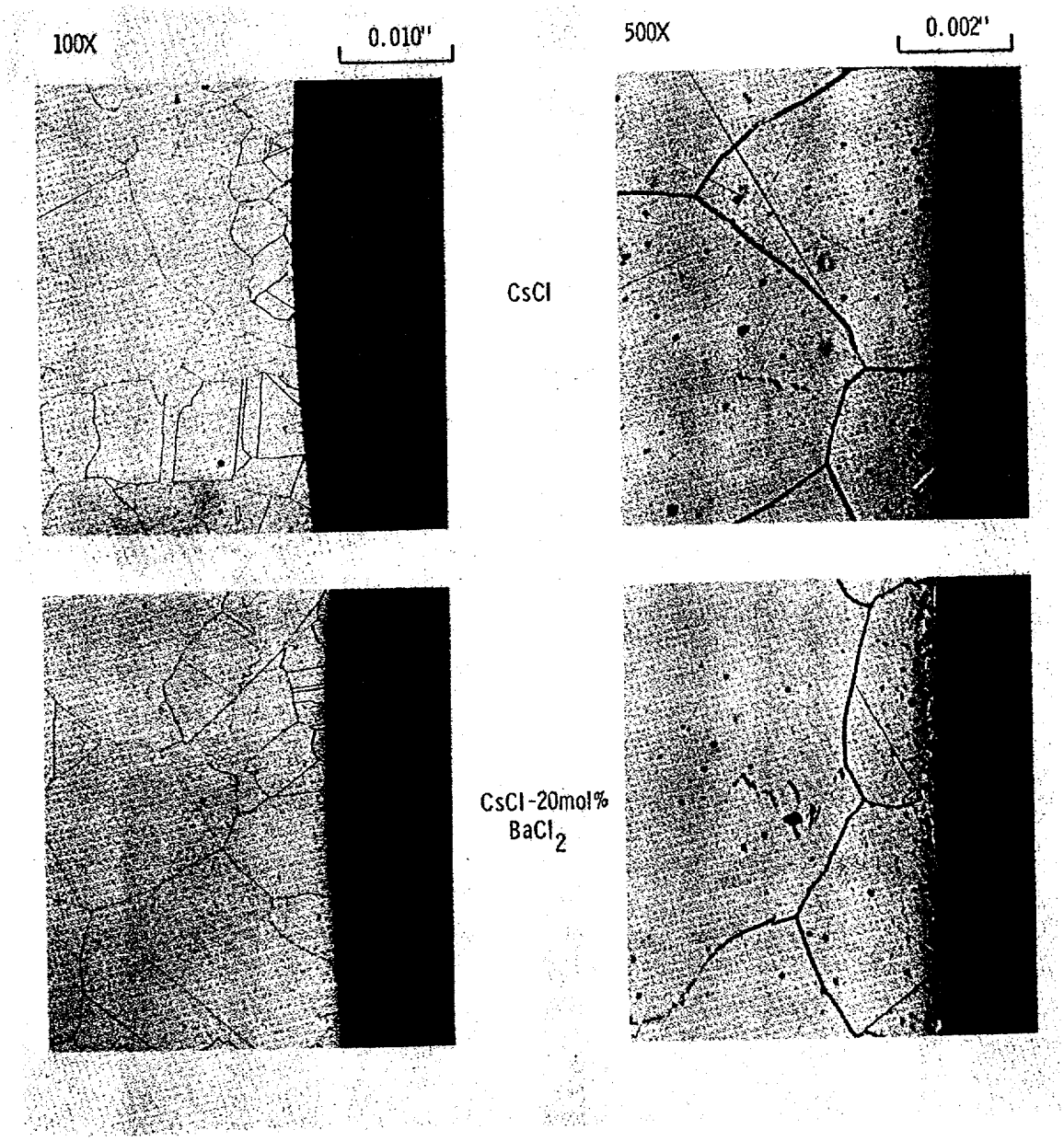

FIGURE 12. Sections of 316L SS Capsules after Contact with Radioactive CsCl at 400°C

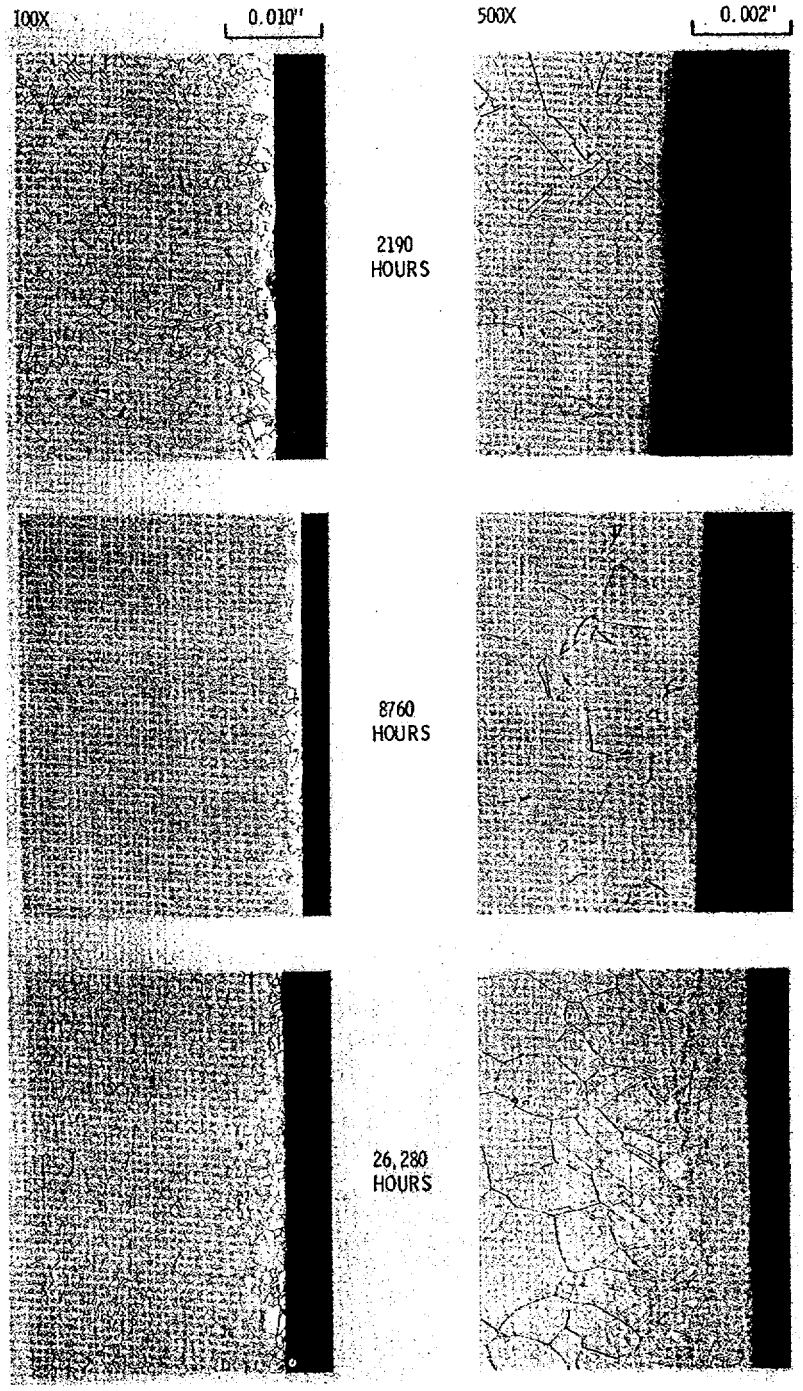

FIGURE 13. Test Specimens - 316L SS/Nonradioactive CsCl - 11 mole % $BaCl_2$ at 400°C

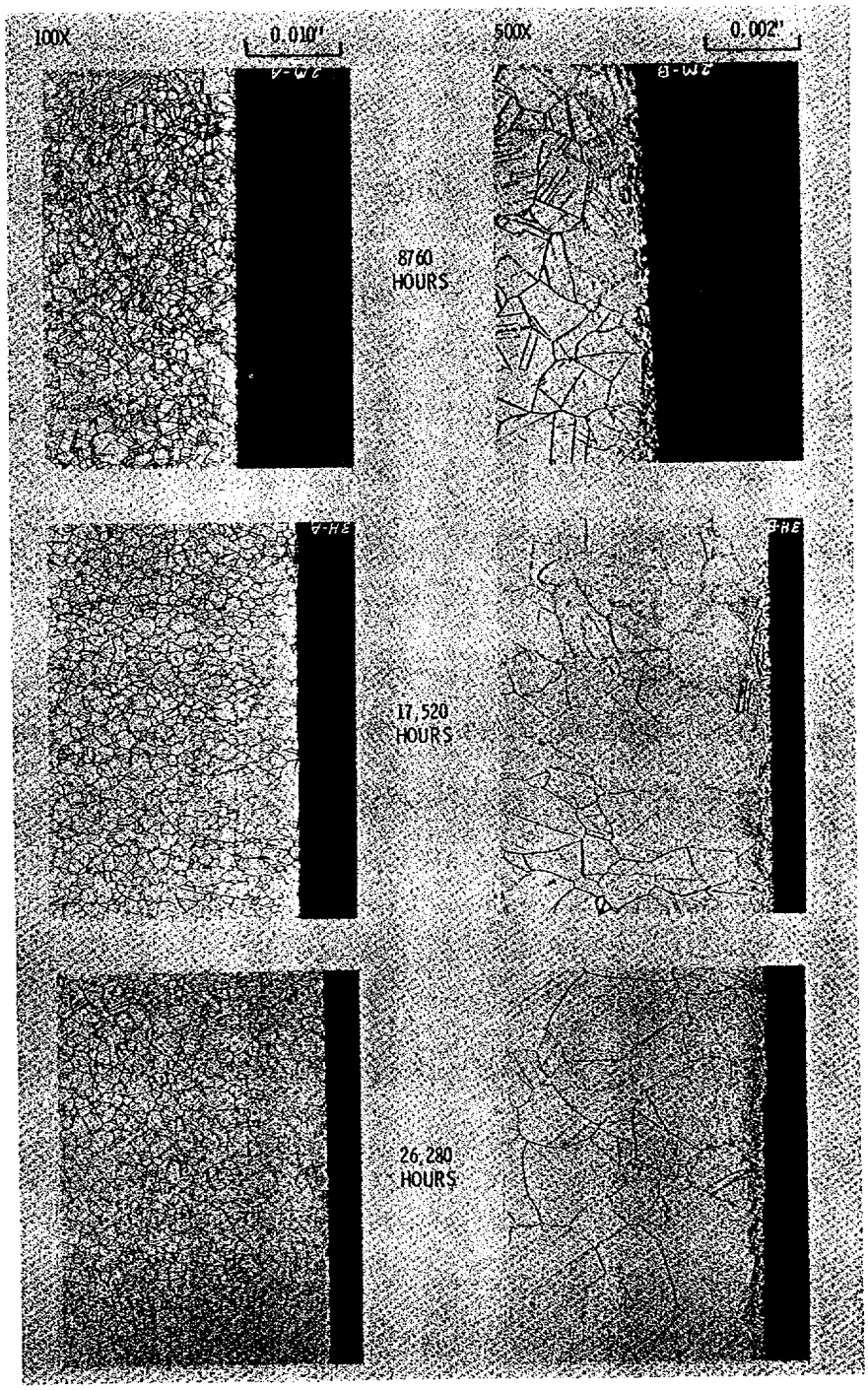

FIGURE 14. Test Specimens - 316L SS/Nonradioactive CsCl - 20 mole % $BaCl_2$ at 400°C

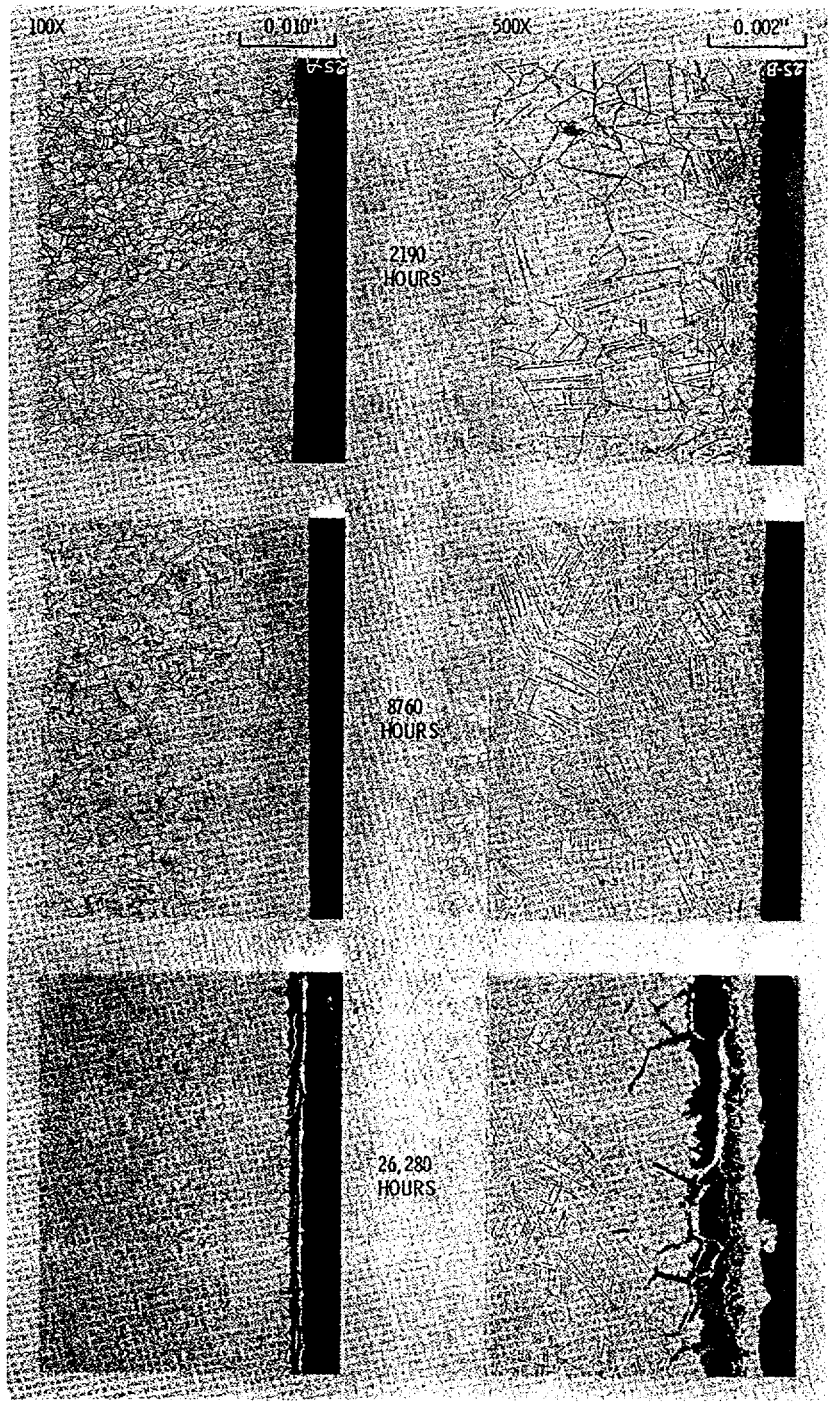

FIGURE 15. Test Specimens - 316L SS/Nonradioactive CsCl - 20 mole % $BaCl_2$ at 600°C

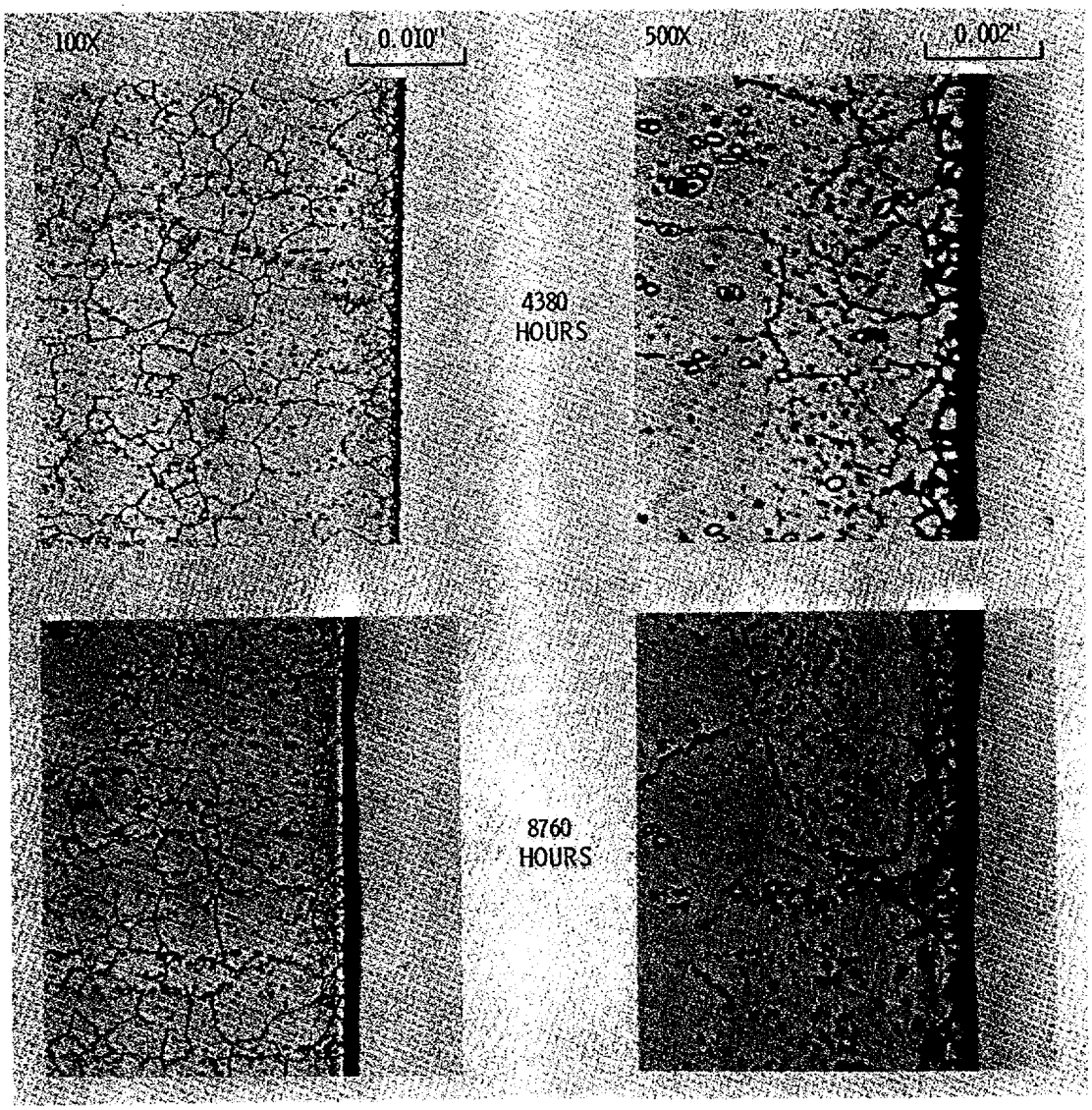

FIGURE 16. Samples of Hastelloy C Tested with Radioactive CsCl at 400°C

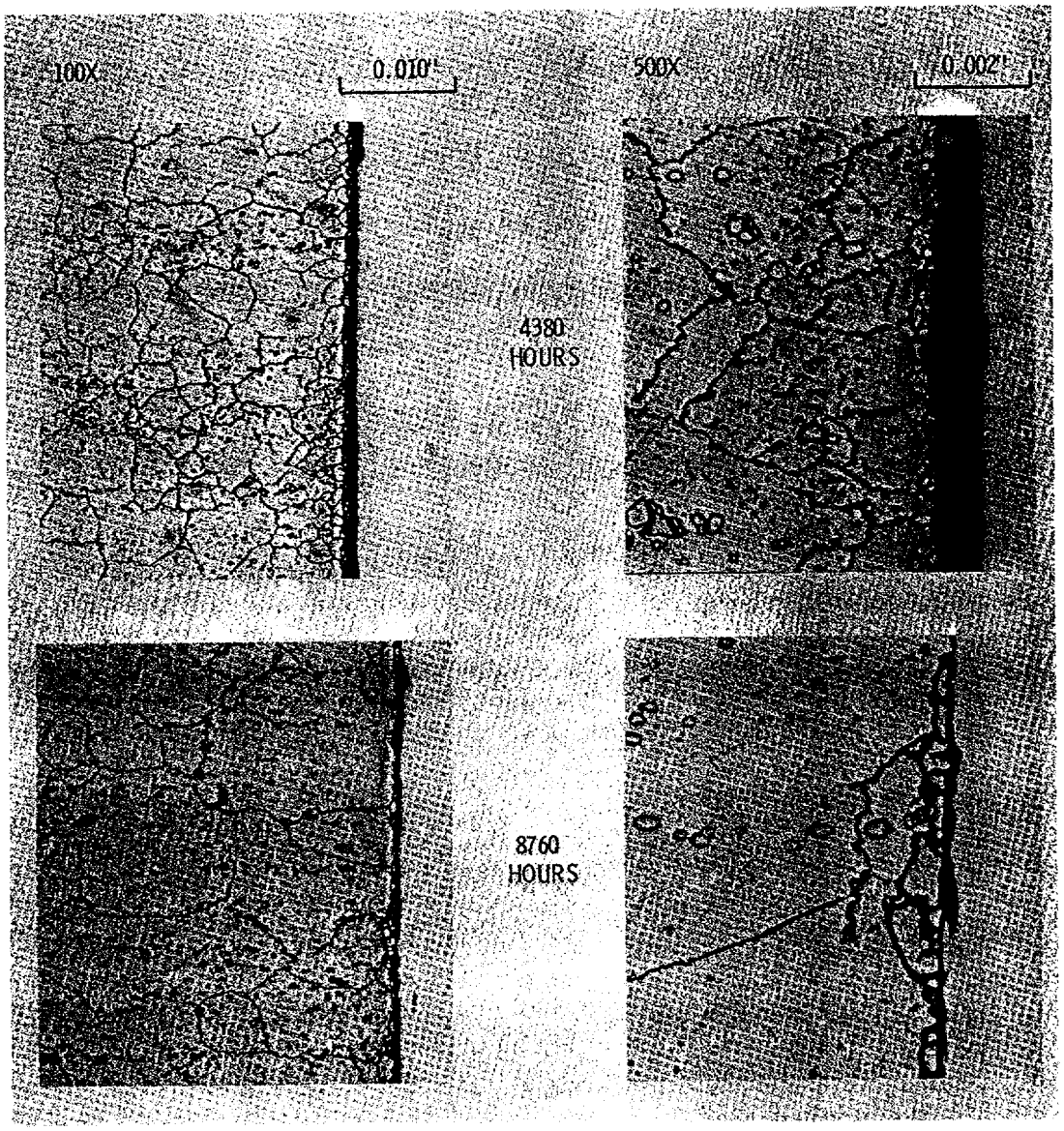

FIGURE 17. Samples of Hastelloy C Tested with Radioactive CsCl - 20 mole % $BaCl_2$ at 400°C

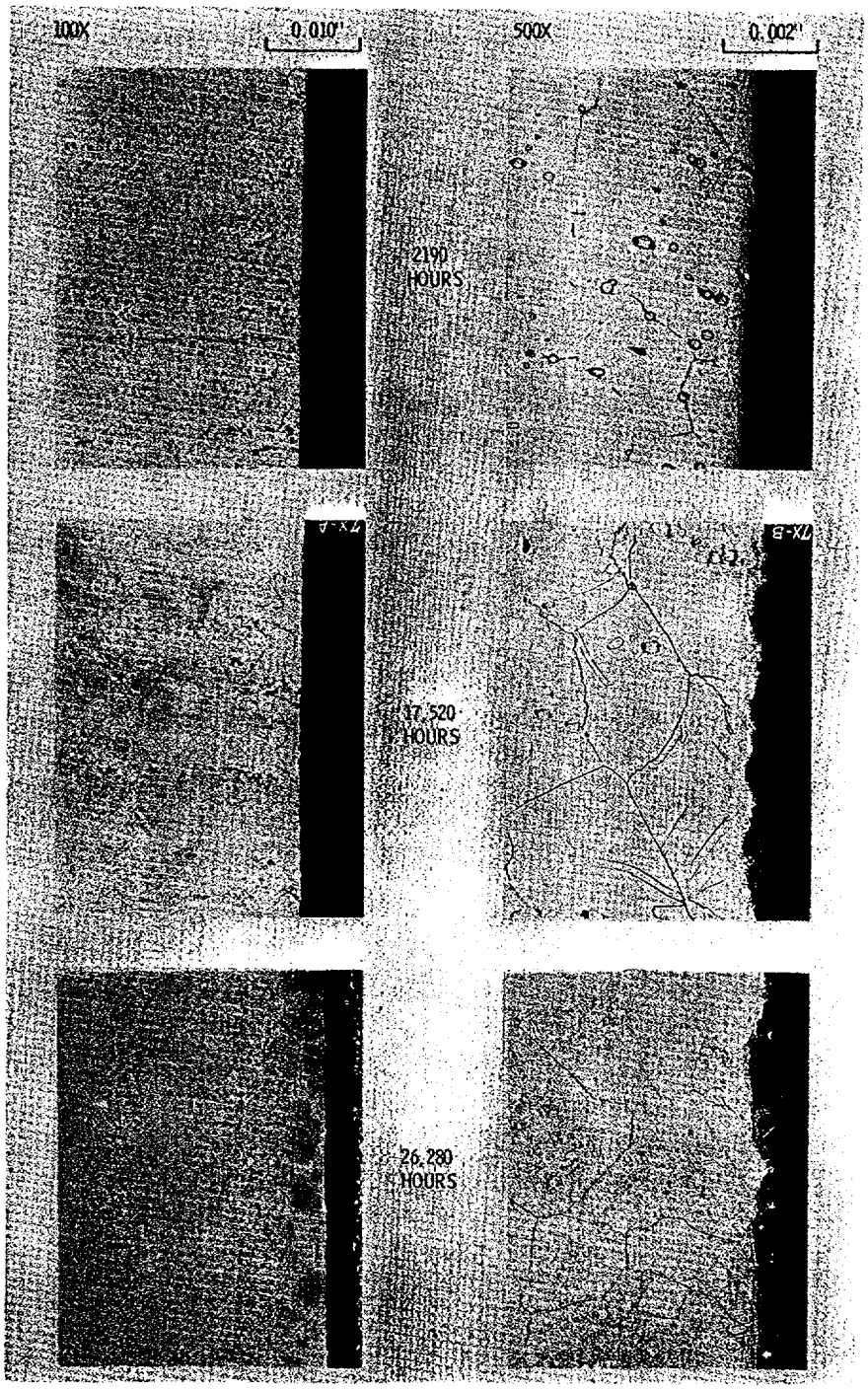

FIGURE 18. Test Specimens - Hastelloy C/Nonradioactive CsCl - 11 mole % $BaCl_2$ at 400°C

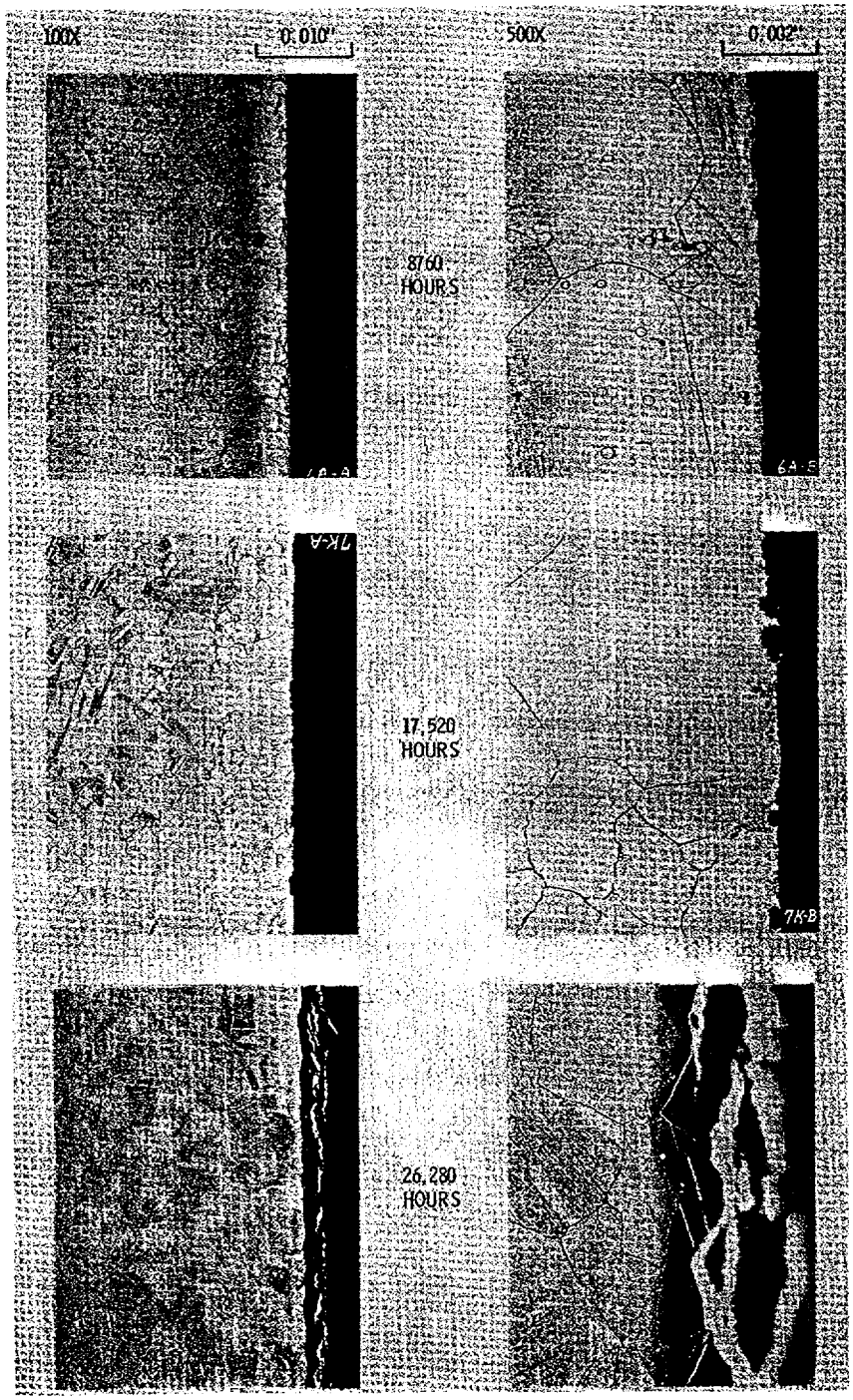

FIGURE 19. Test Specimens - Hastelloy C/Nonradioactive CsCl - 20 mole % $BaCl_2$ at 400°C

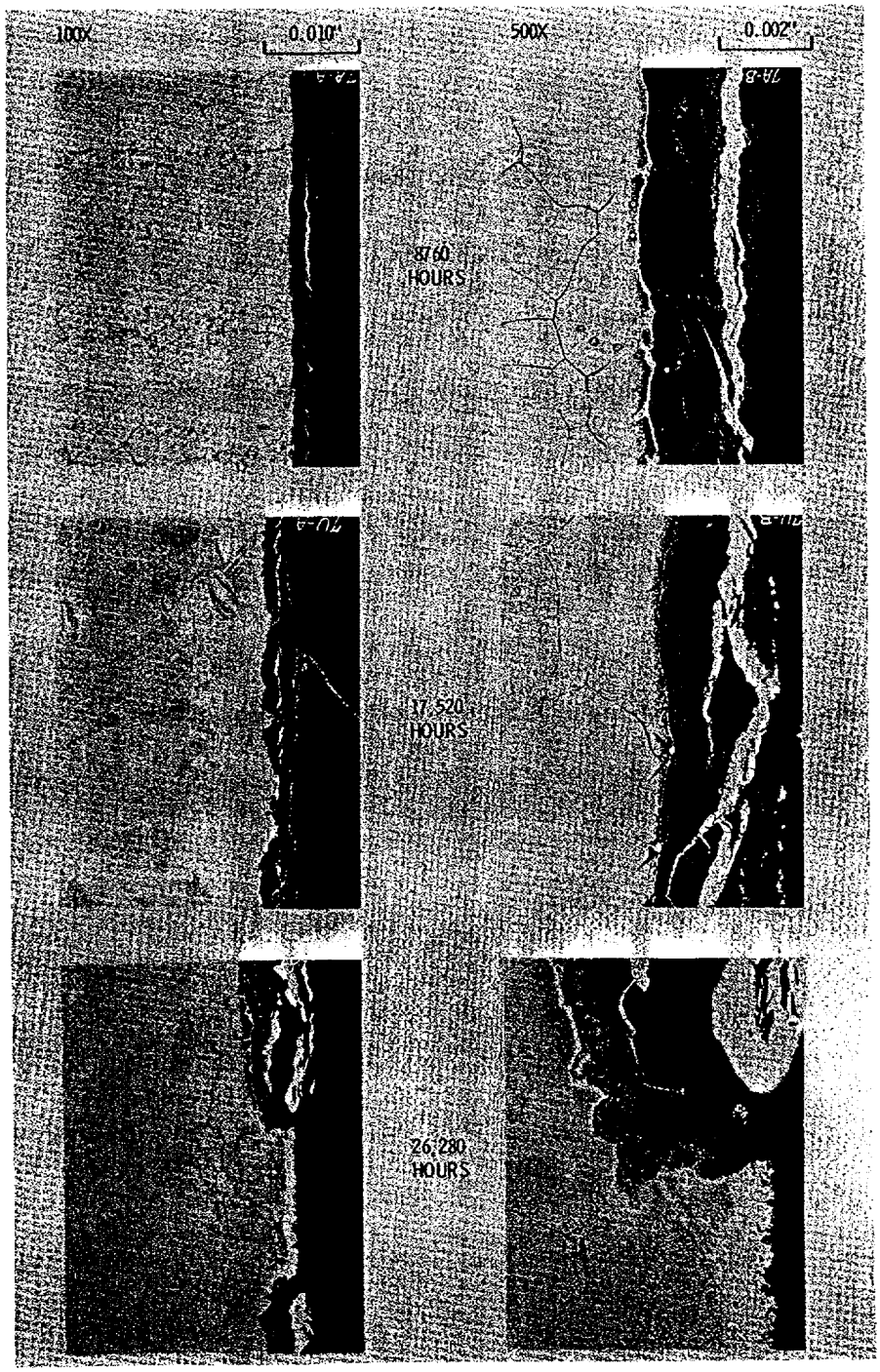

FIGURE 20. Test Specimens - Hastelloy C/Nonradioactive CsCl - 20 mole % $BaCl_2$ at 600°C

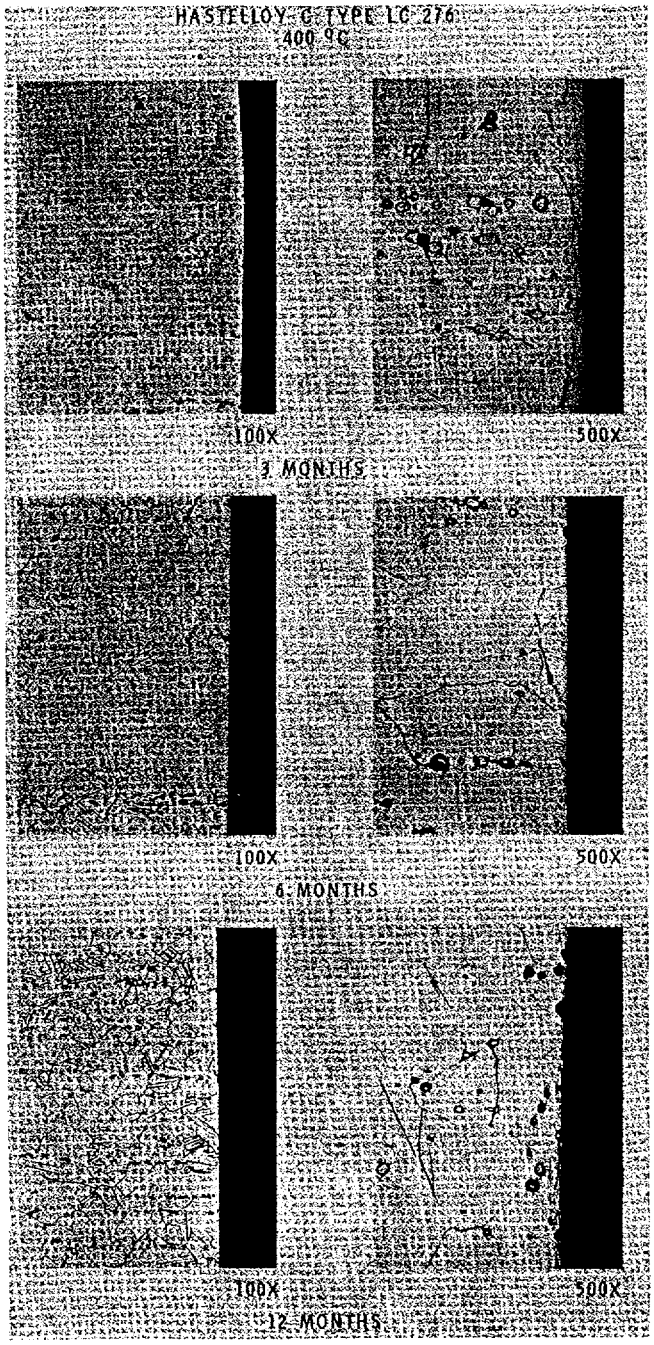

FIGURE 21. Test Specimens - Hastelloy C-276/Nonradioactive CsCl - 11 mole % $BaCl_2$ at 400°C

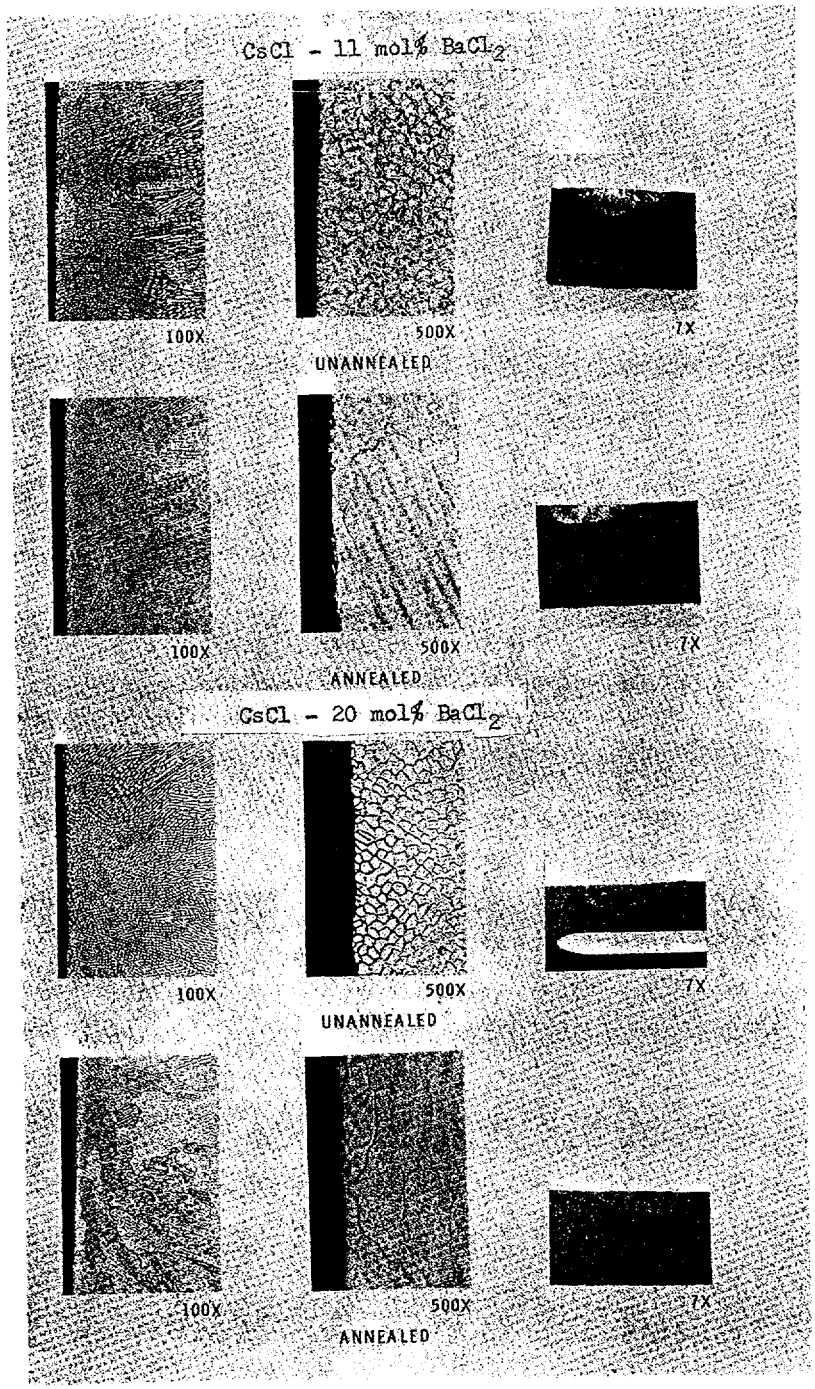

FIGURE 22. Welded 316L SS Samples Tested with Non-radioactive CsCl at 400°C for 4380 Hours

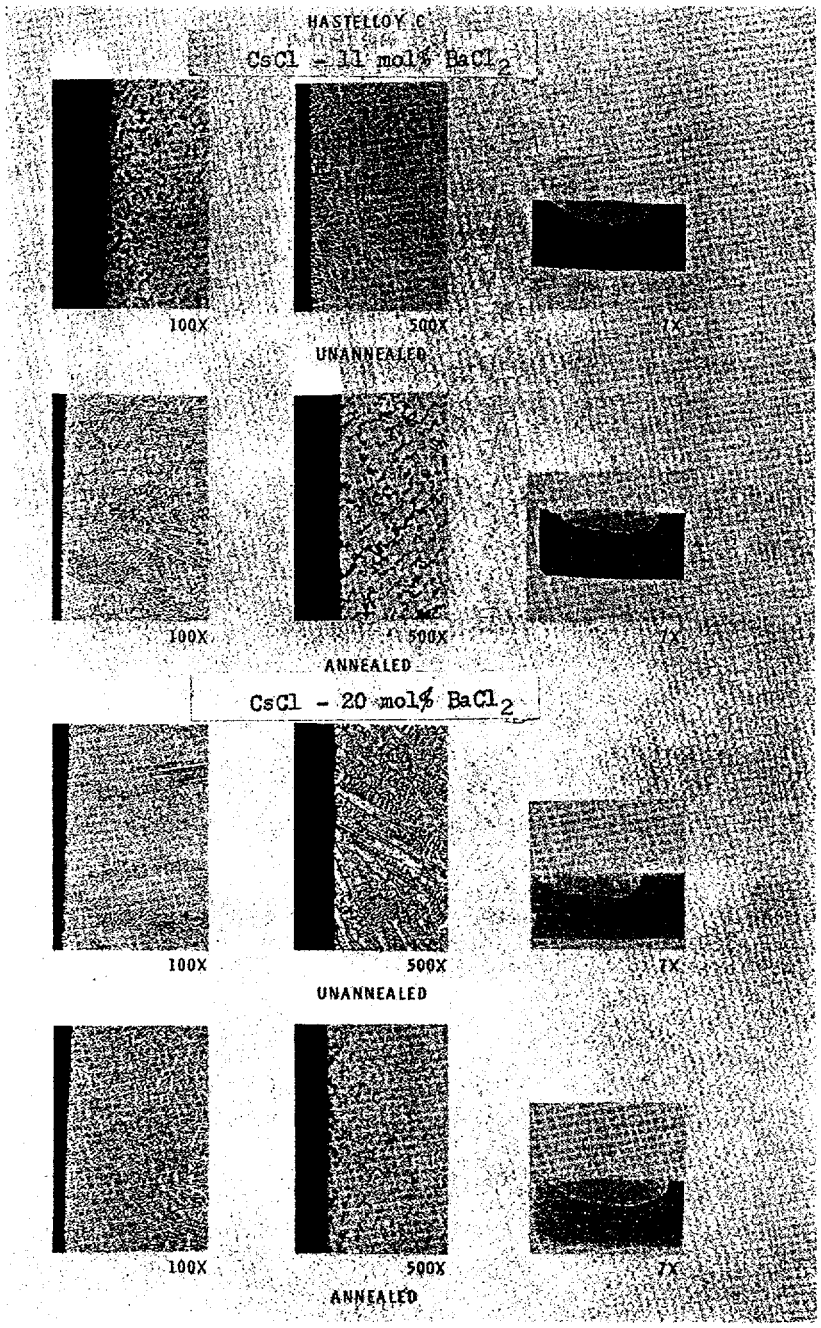

FIGURE 23. Welded Hastelloy C Samples Tested with Non-radioactive CsCl at 400°C for 4380 Hours

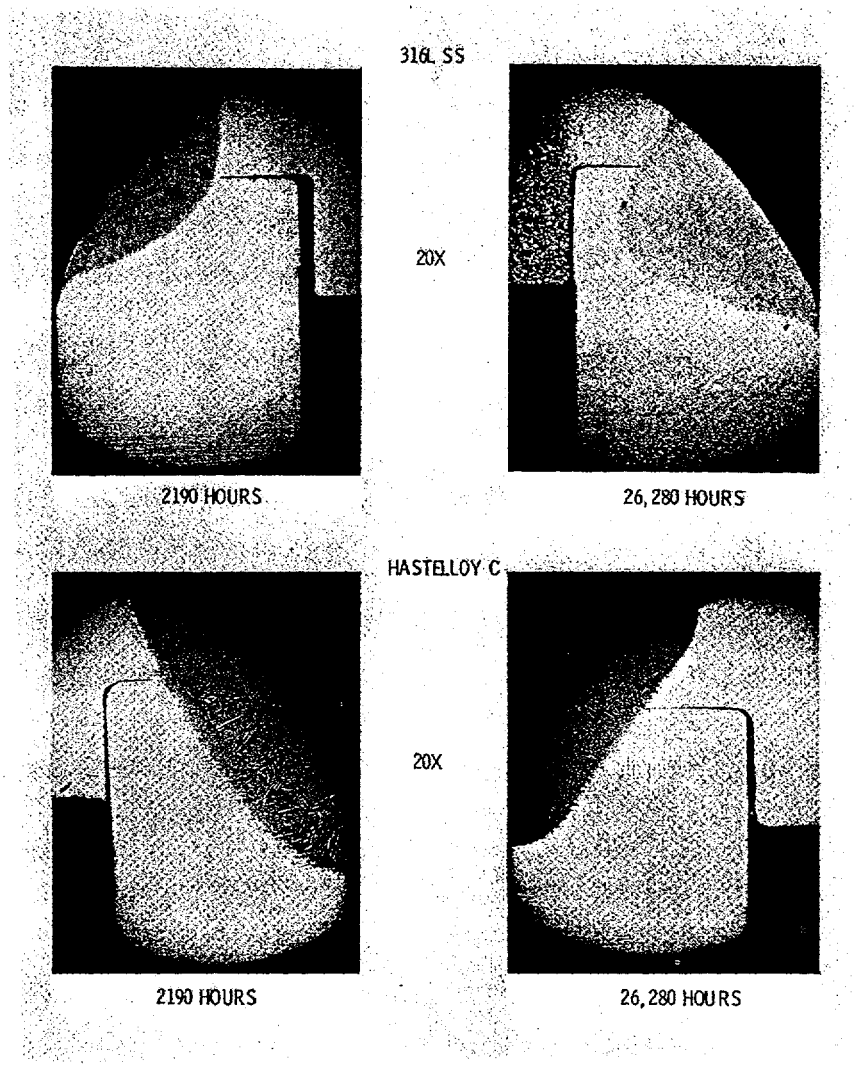

FIGURE 24. Crevice Corrosion in Nonradioactive CsCl Capsules

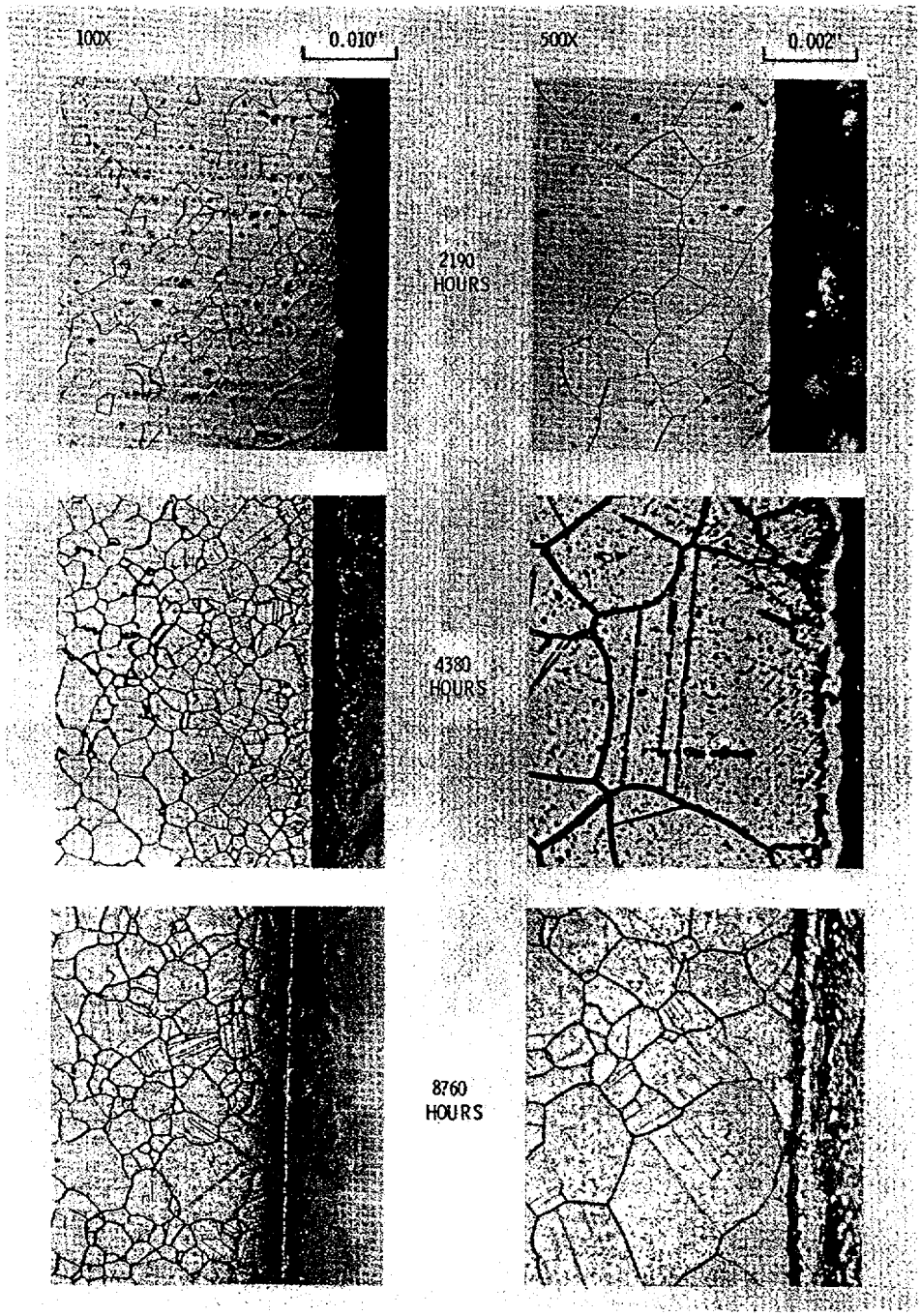

FIGURE 25. Samples of Haynes 25 Tested with Radioactive SrF_2 at 400°C

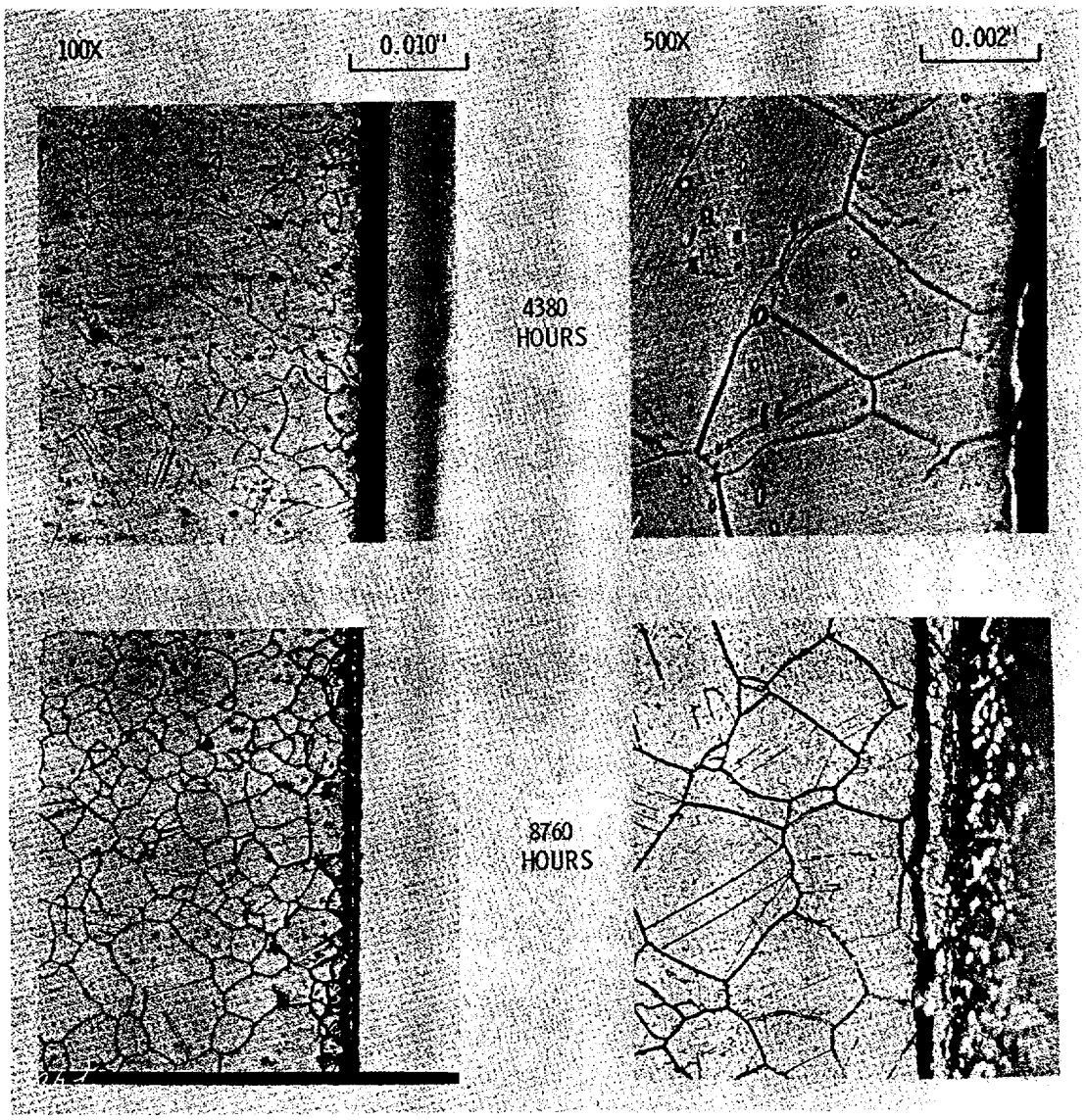

FIGURE 26. Samples of Haynes 25 Tested with Radioactive SrF_2 - 13 mole % ZrF_4 - 13 mole % at 400°C

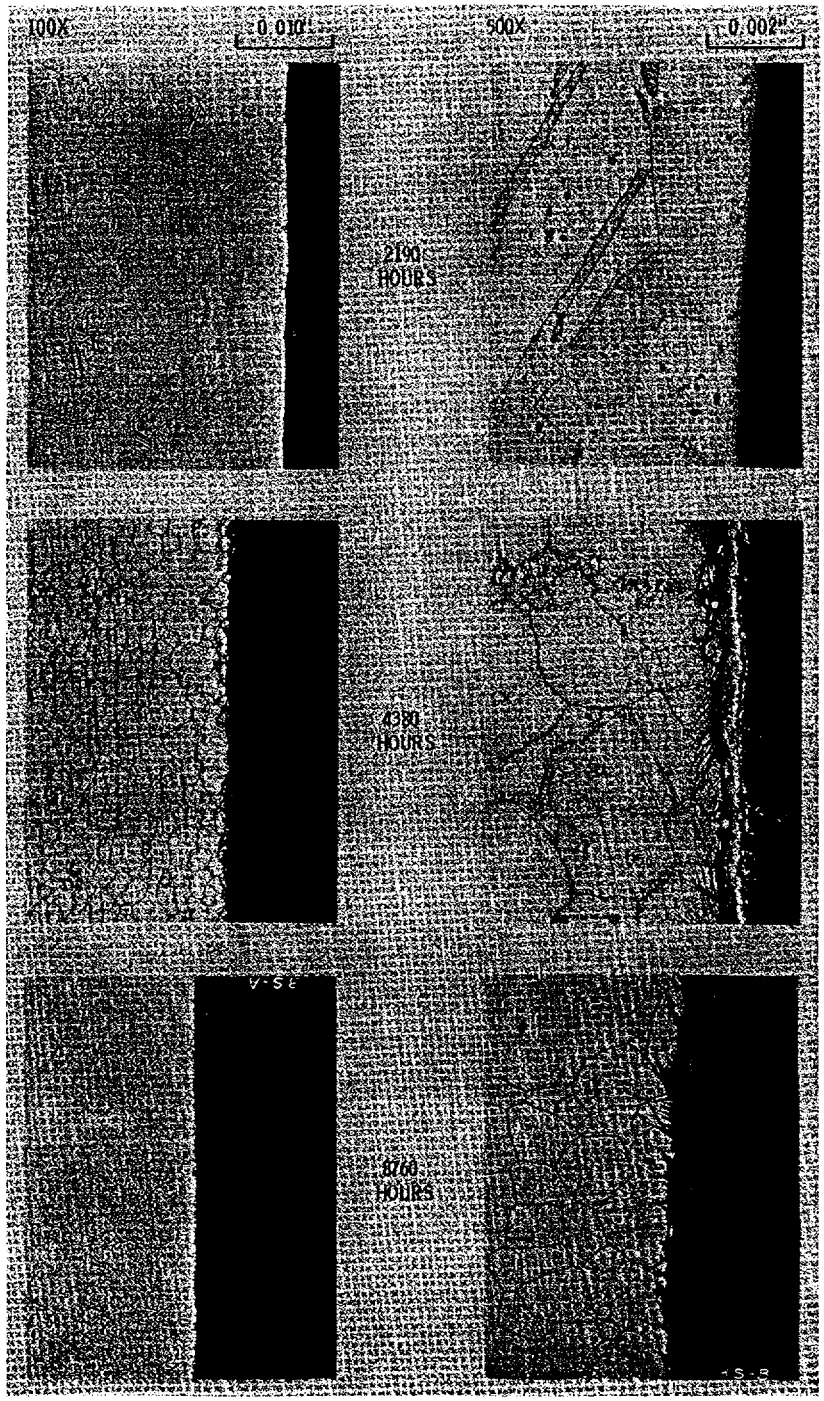

FIGURE 27. Test Specimens - Haynes 25/Nonradioactive SrF_2 at 400°C

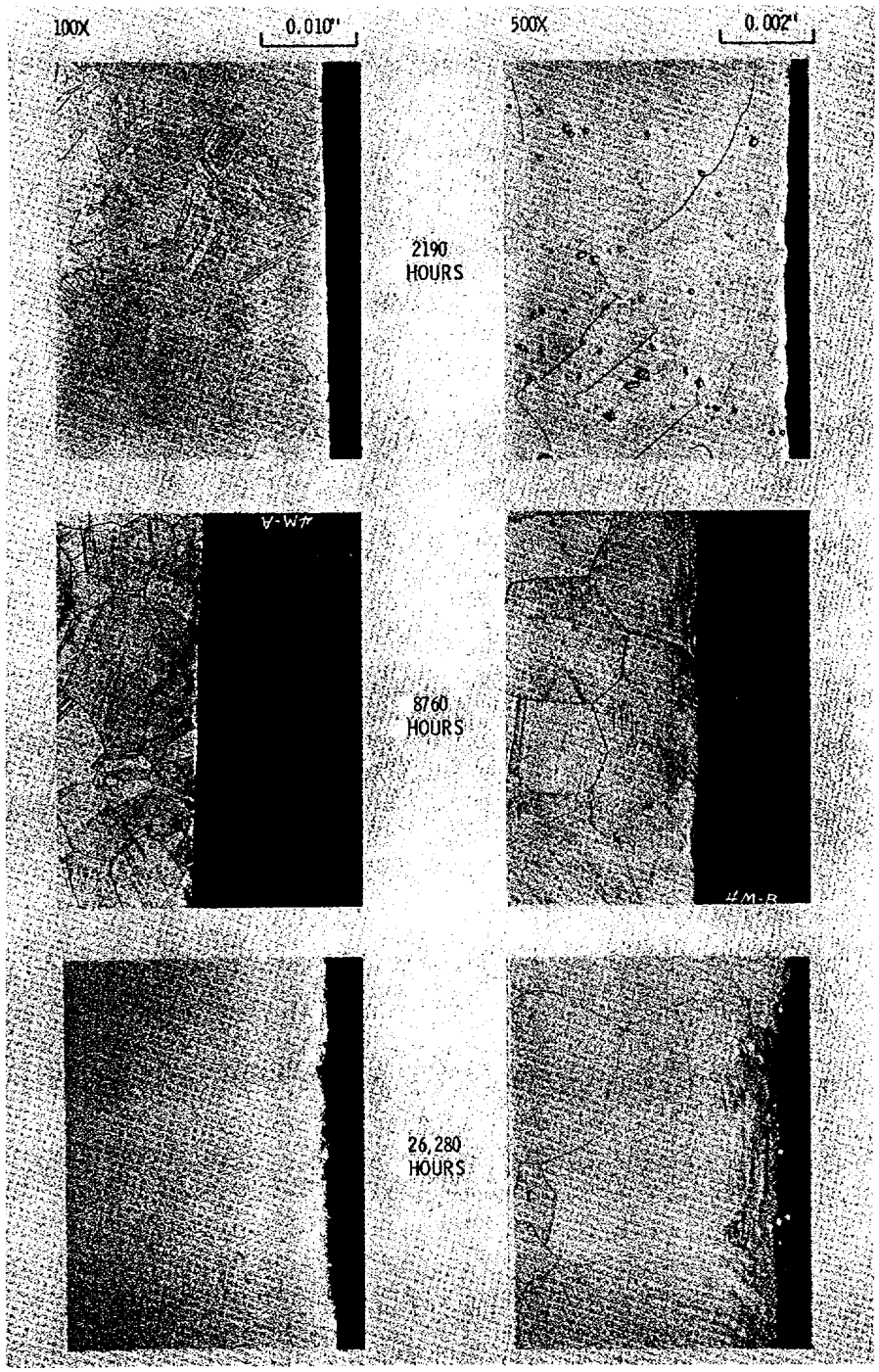

FIGURE 28. Test Specimens - Haynes 25/Nonradioactive SrF_2 - 6 mole % ZrF_4 - 6 mole % Zr at 400°C

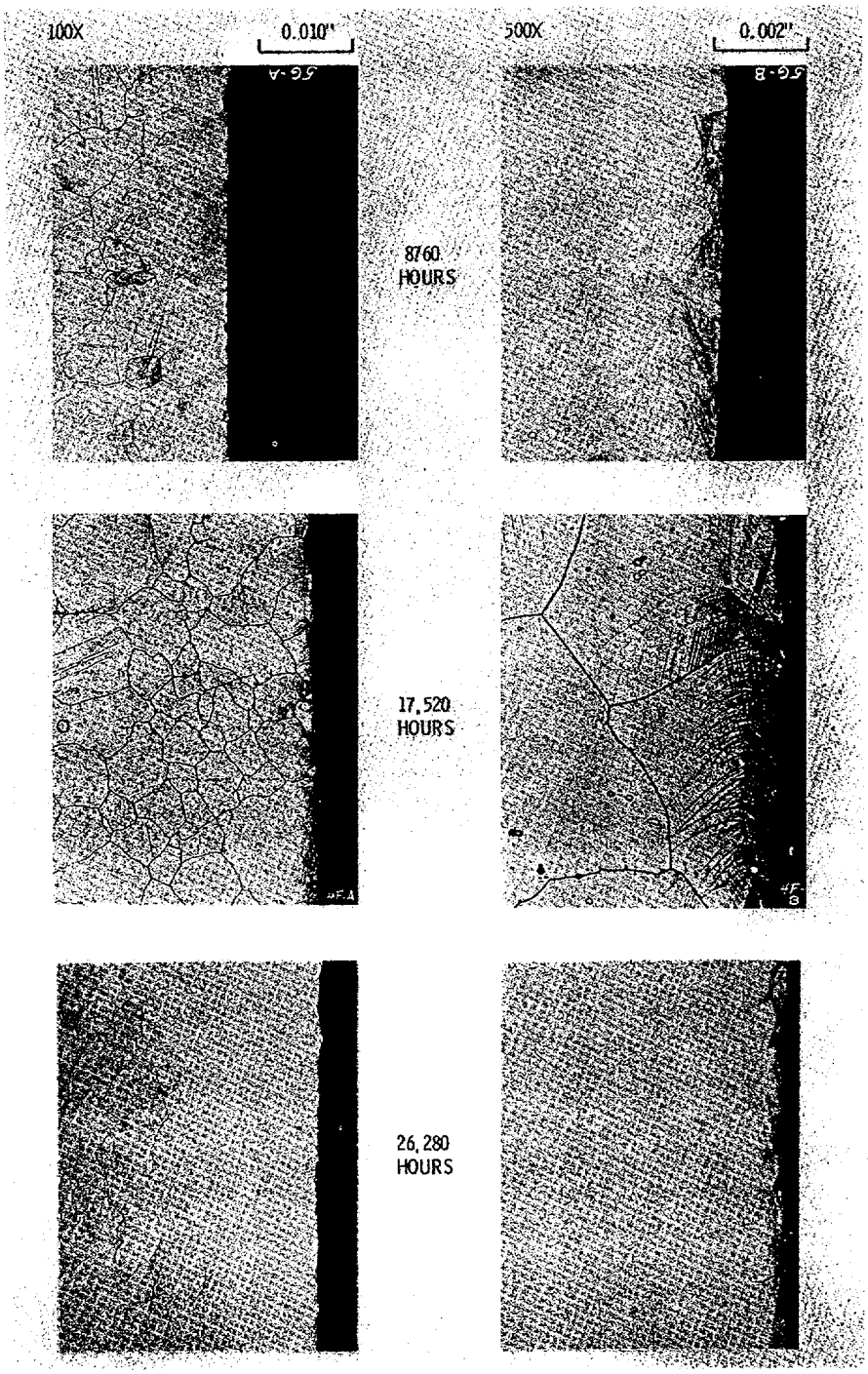

FIGURE 29. Test Specimens - Haynes 25/Nonradioactive SrF_2 - 13 mole % ZrF_4 - 13 mole % Zr at 400°C

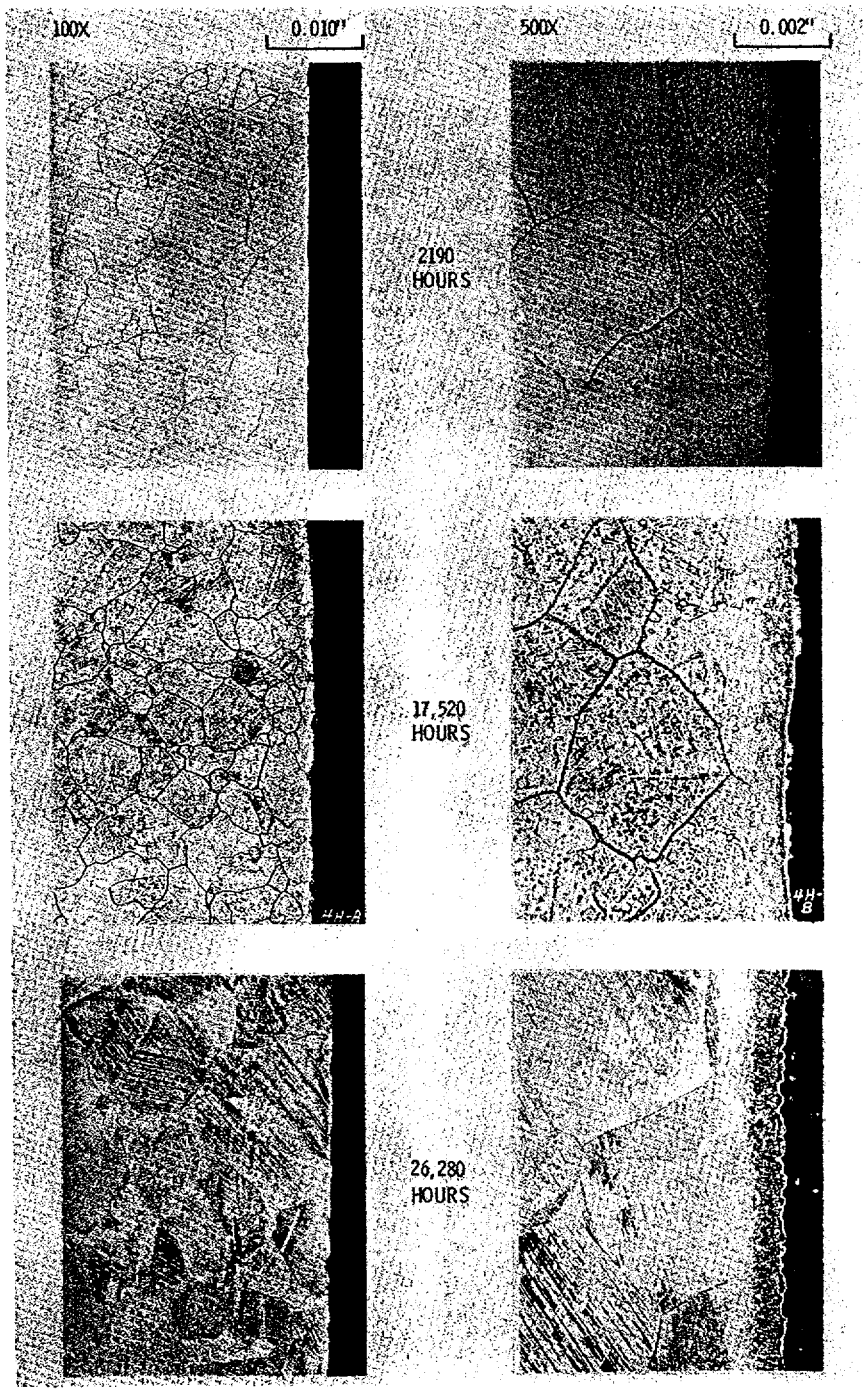

FIGURE 30. Test Specimens - Haynes 25/Nonradioactive SrF_2 - 6 mole % ZrF_4 - 6 mole % Zr at 800°C

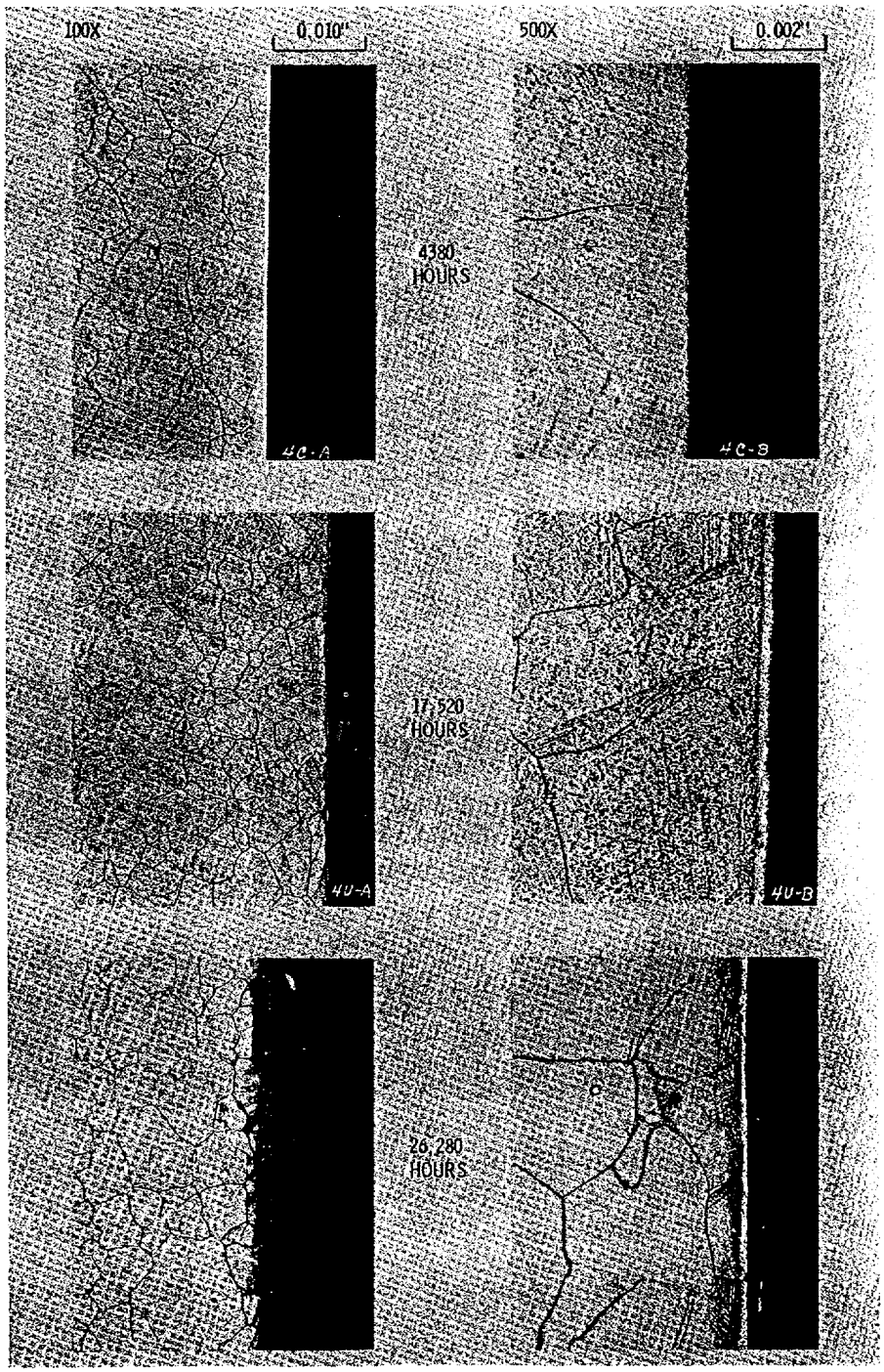

FIGURE 31. Test Specimens - Haynes 25/Nonradioactive SrF_2 - 13 mole % ZrF_4 - 13 mole % Zr at 800°C

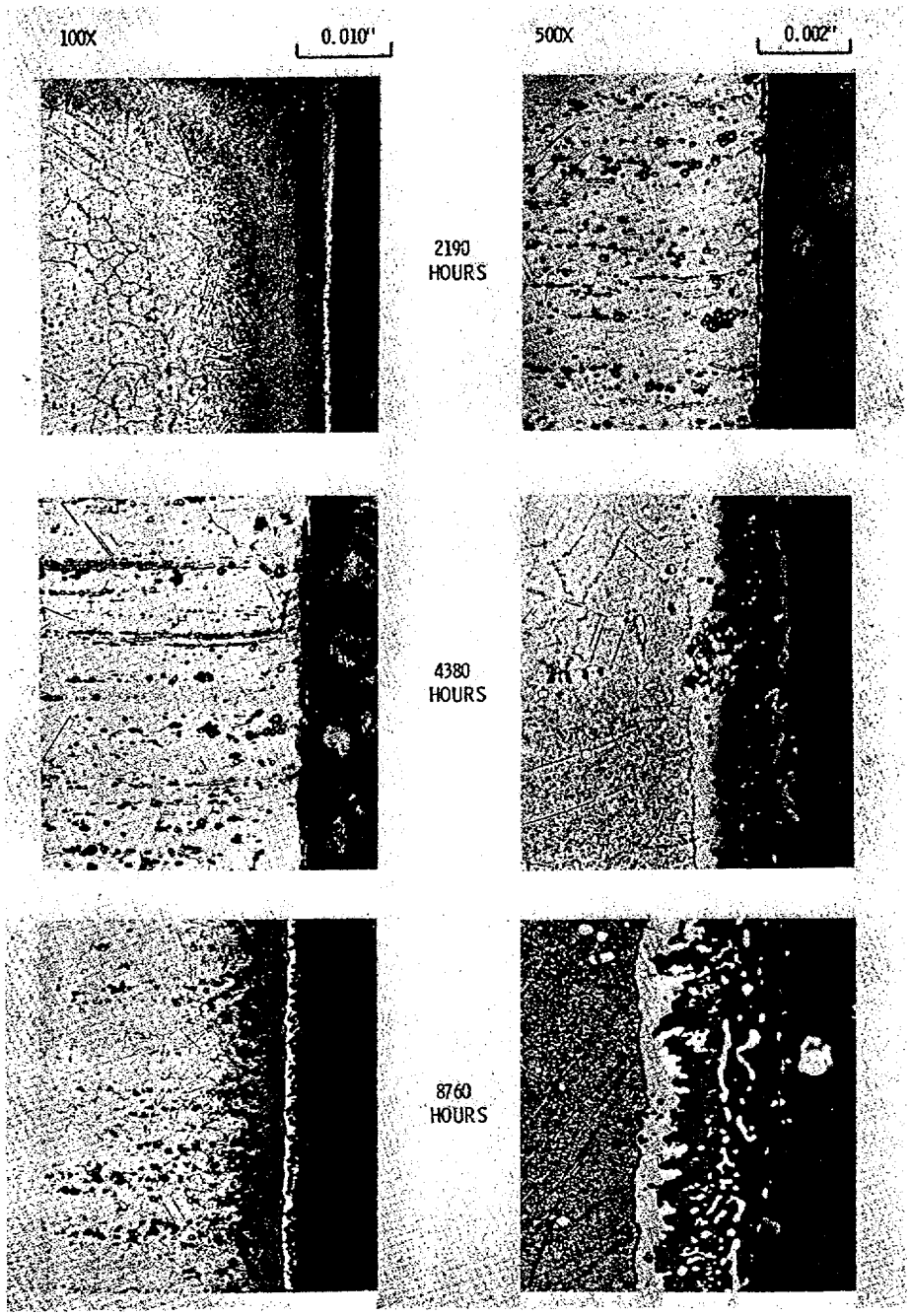

FIGURE 32. Samples of Hastelloy C Tested with Radioactive SrF_2 at 400°C

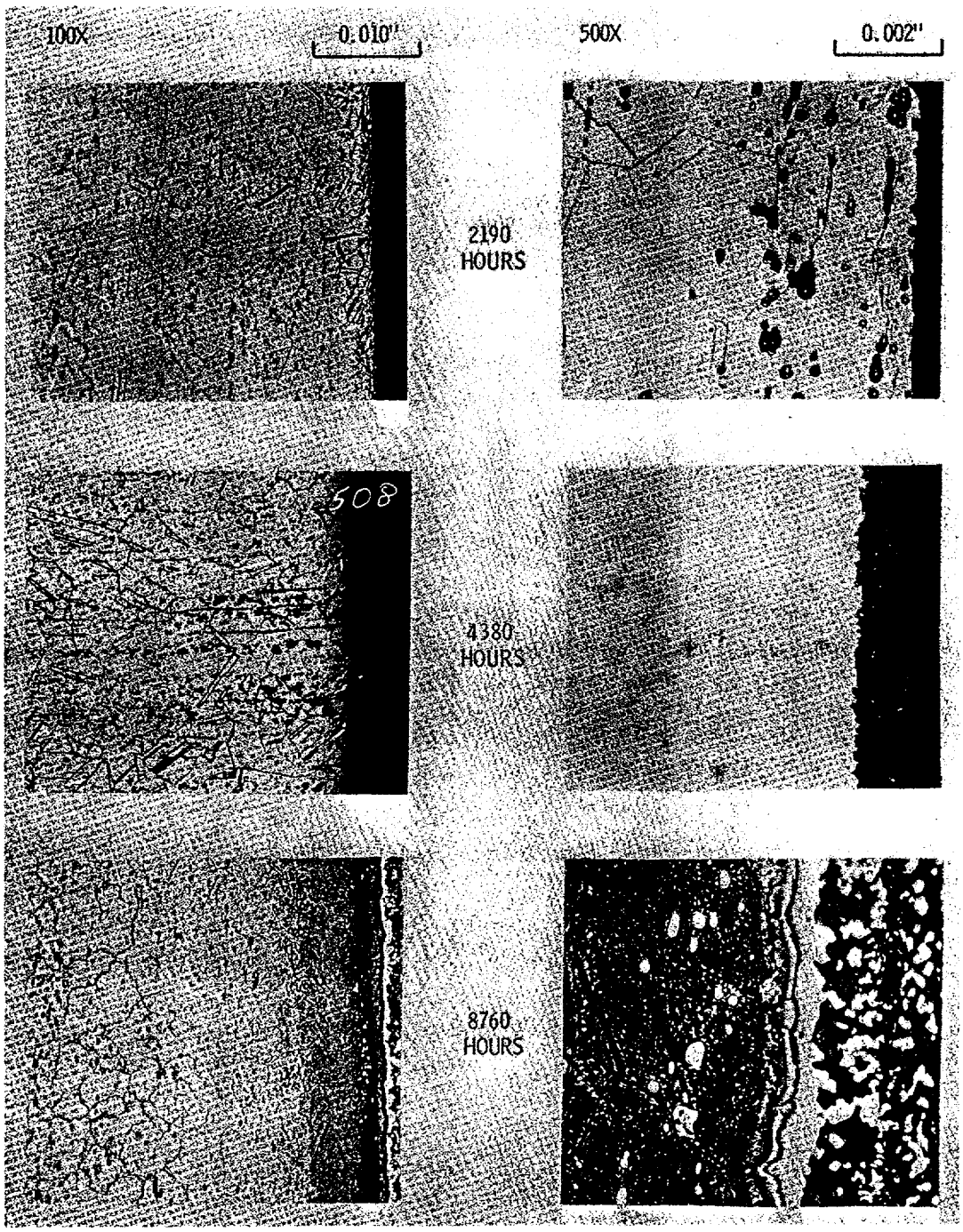

FIGURE 33. Samples of Hastelloy C Tested with Radioactive SrF_2 - 13 mole % ZrF_4 - 13 mole % Zr at 400°C

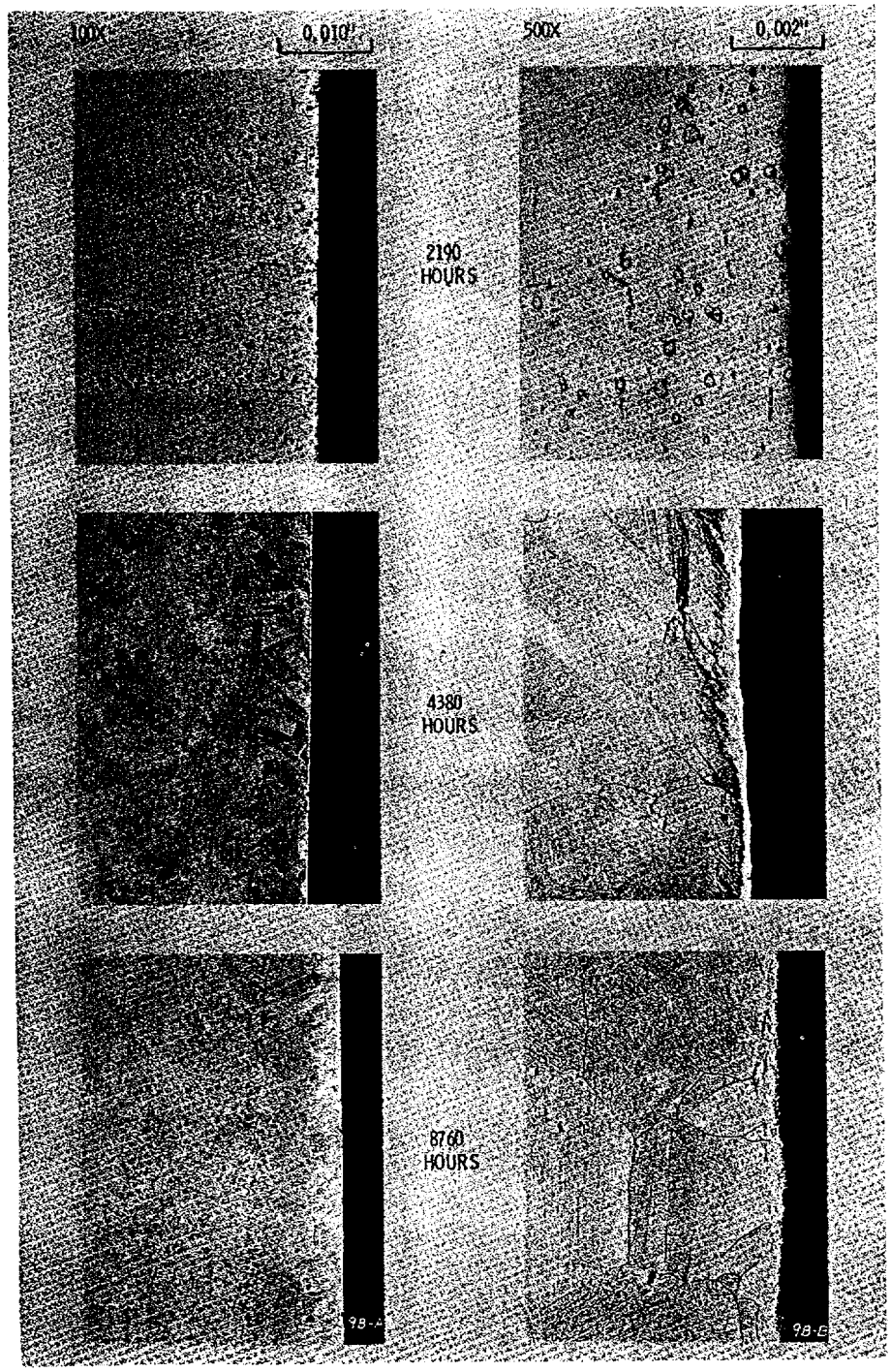

FIGURE 34. Test Specimens - Hastelloy C/Nonradioactive SrF_2 at 400°C

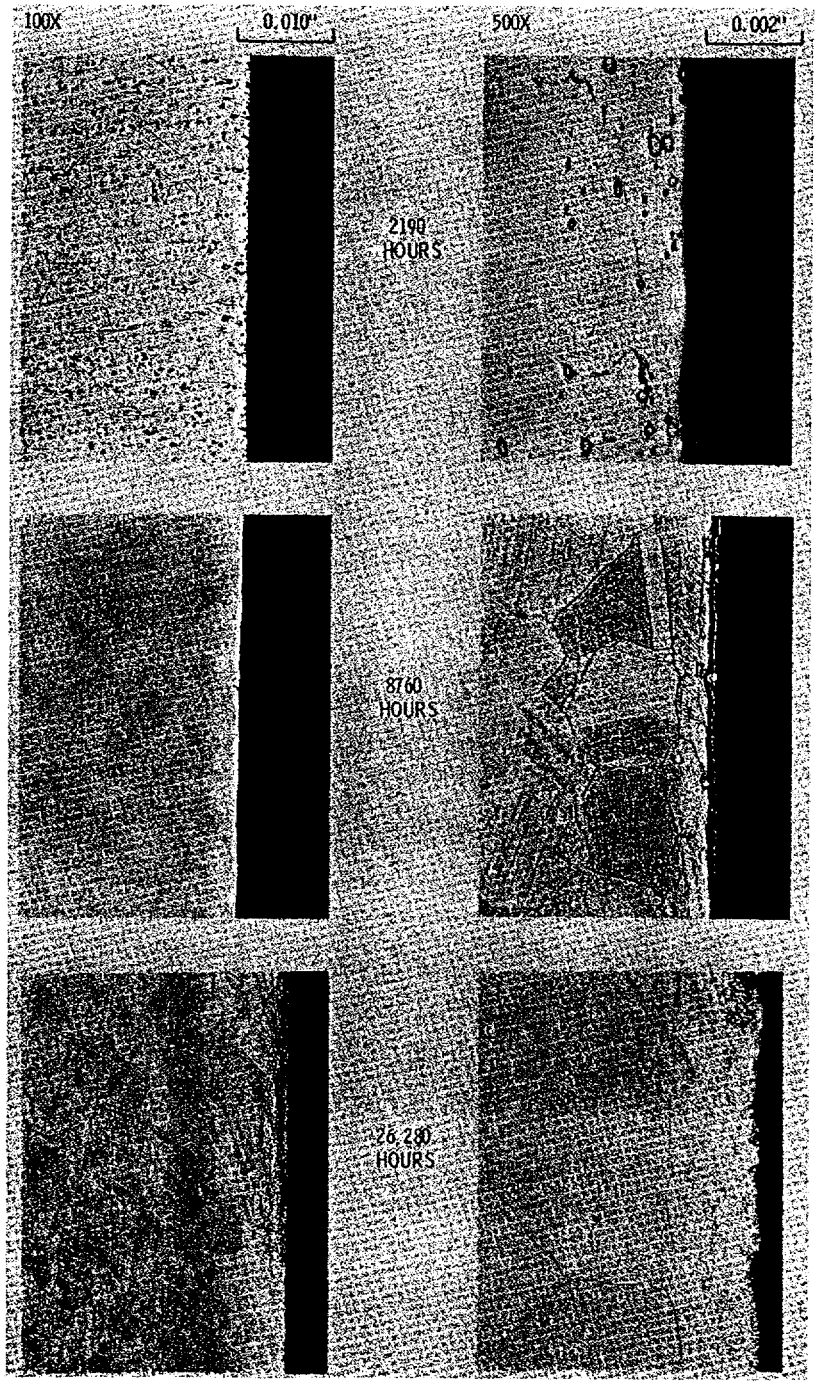

FIGURE 35. Test Specimens - Hastelloy C/Nonradioactive SrF_2 - 6 mole % ZrF_4 - 6 mole % Zr at 400°C

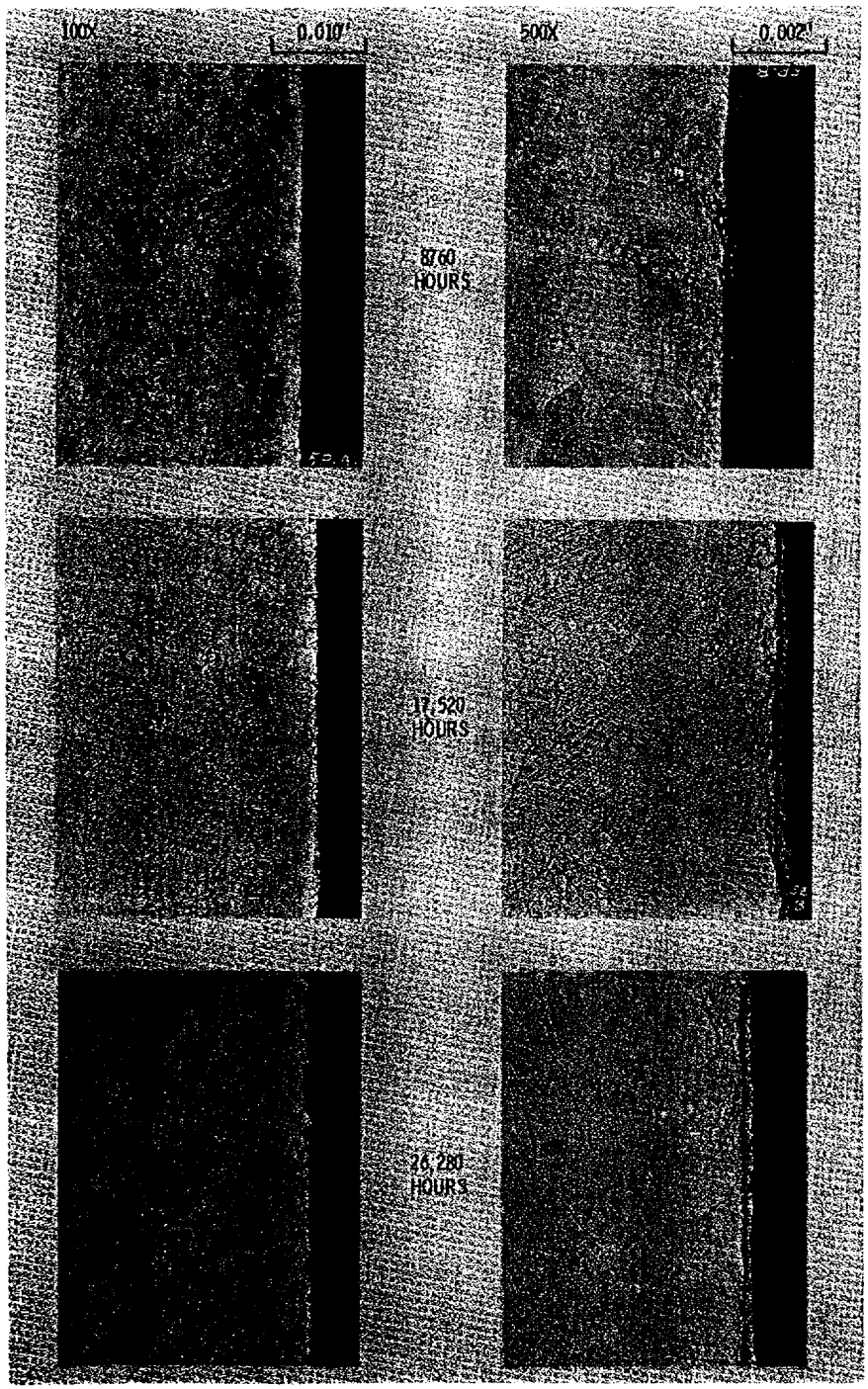

FIGURE 36. Test Specimens - Hastelloy C/Nonradioactive SrF_2 - 13 mole % ZrF_4 - 13 mole % Zr at 400°C

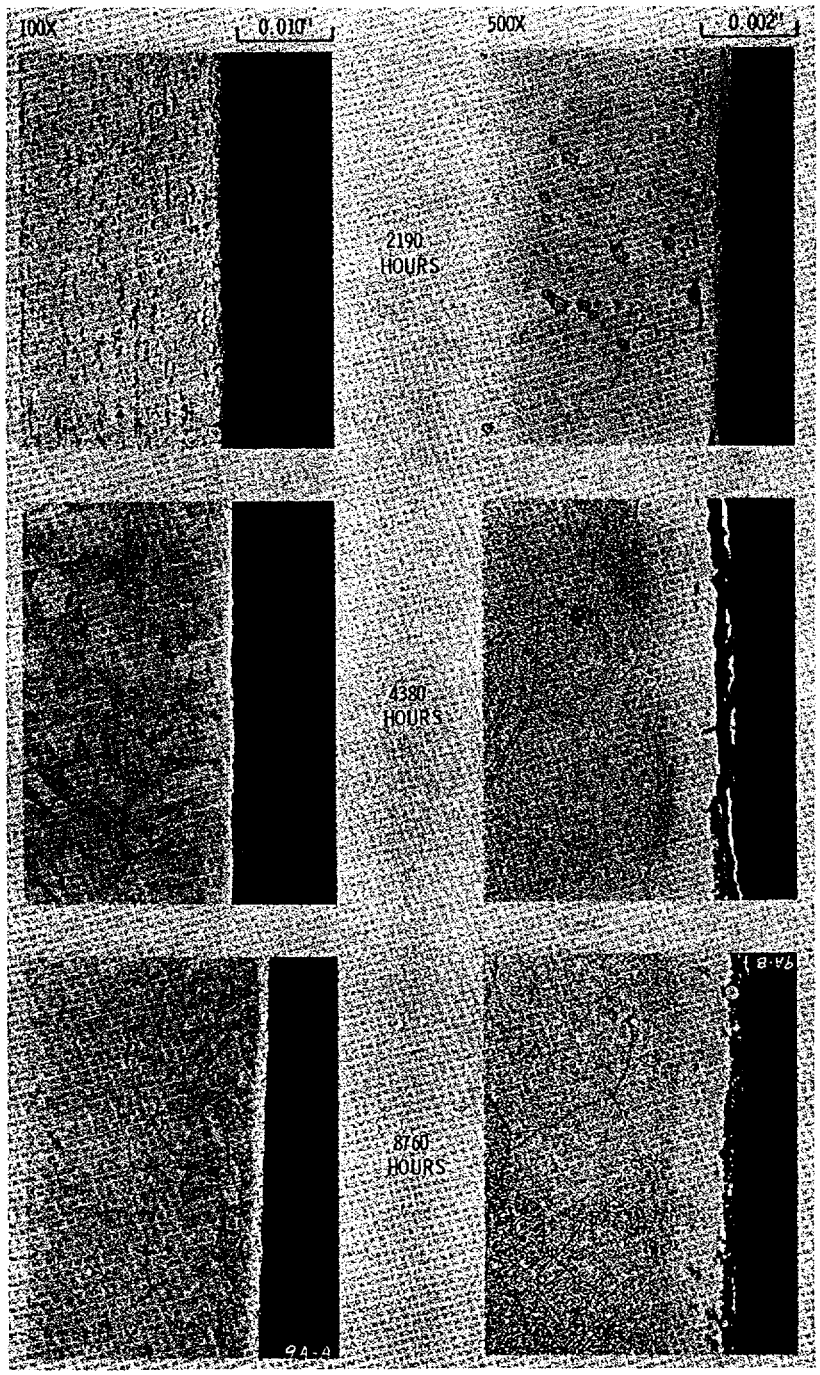

FIGURE 37. Test Specimens - Hastelloy C/Nonradioactive SrF_2 at 800°C

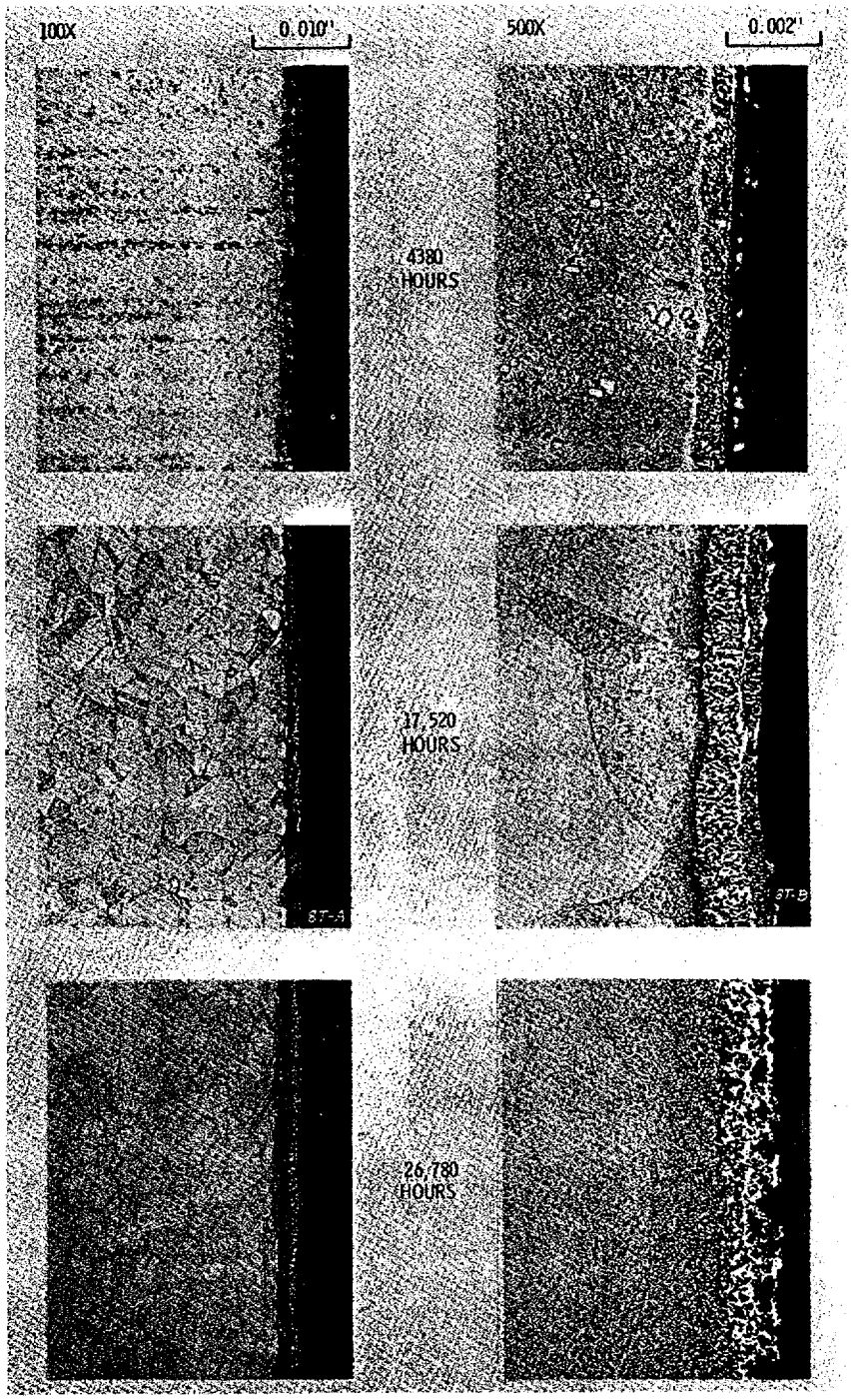

FIGURE 38. Test Specimens - Hastelloy C/Nonradioactive SrF_2 - 6 mole % ZrF_4 - 6 mole % Zr at 800°C

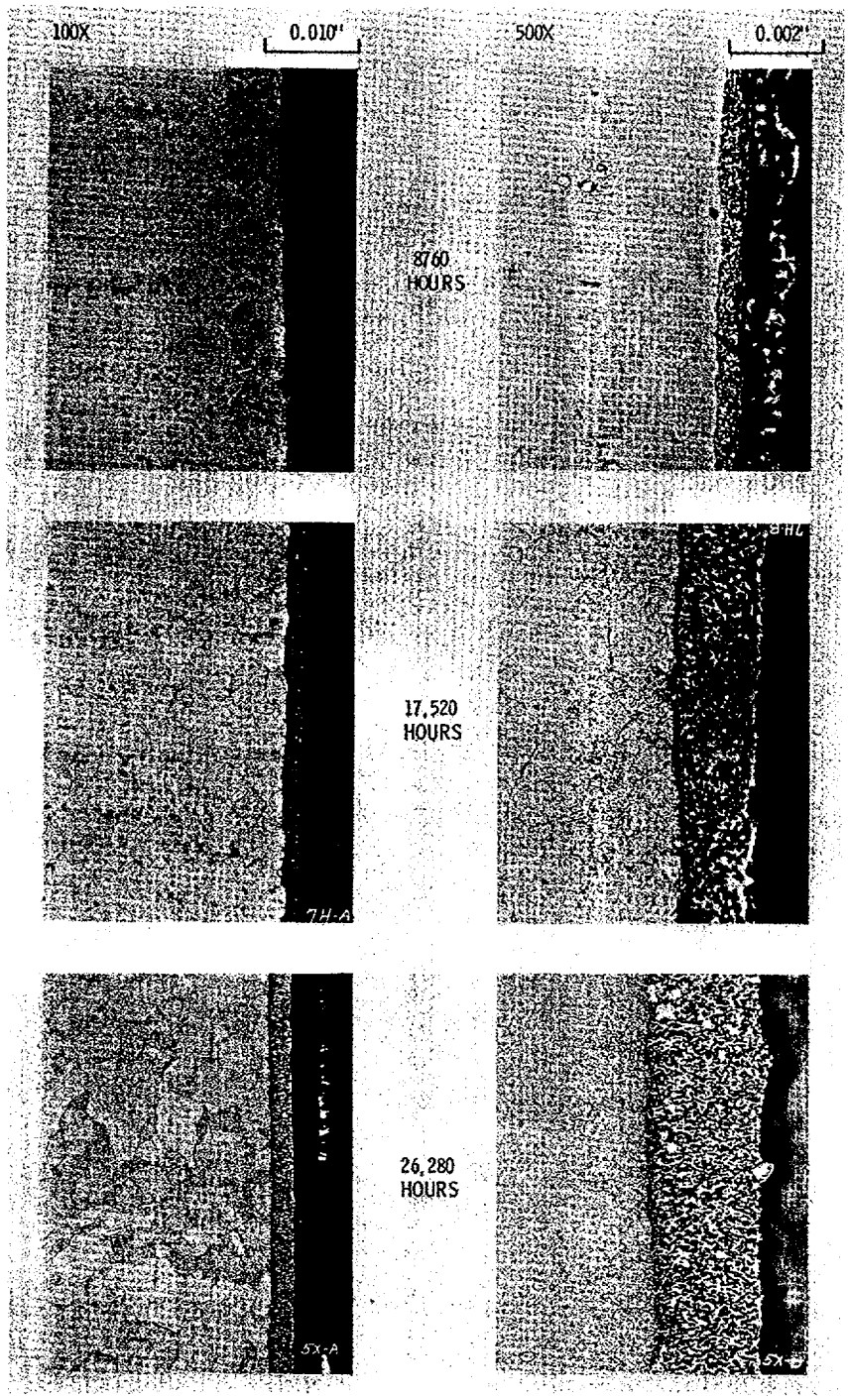

FIGURE 39. Test Specimens - Hastelloy C/Nonradioactive SrF_2 - 13 mole % ZrF_4 - 13 mole % Zr at 800°C

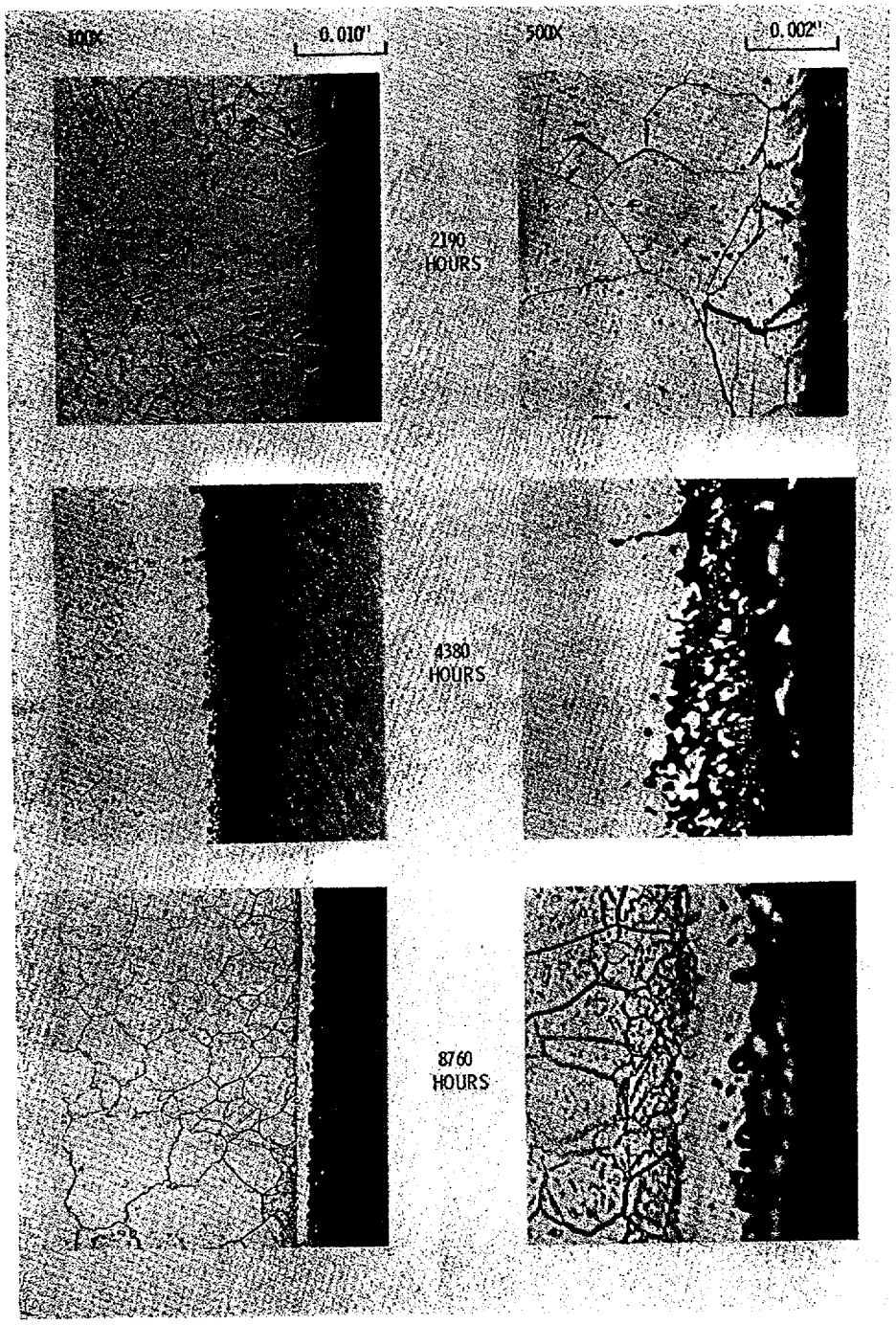

FIGURE 40. Samples of Hastelloy X Tested with Radioactive SrF_2 at 400°C

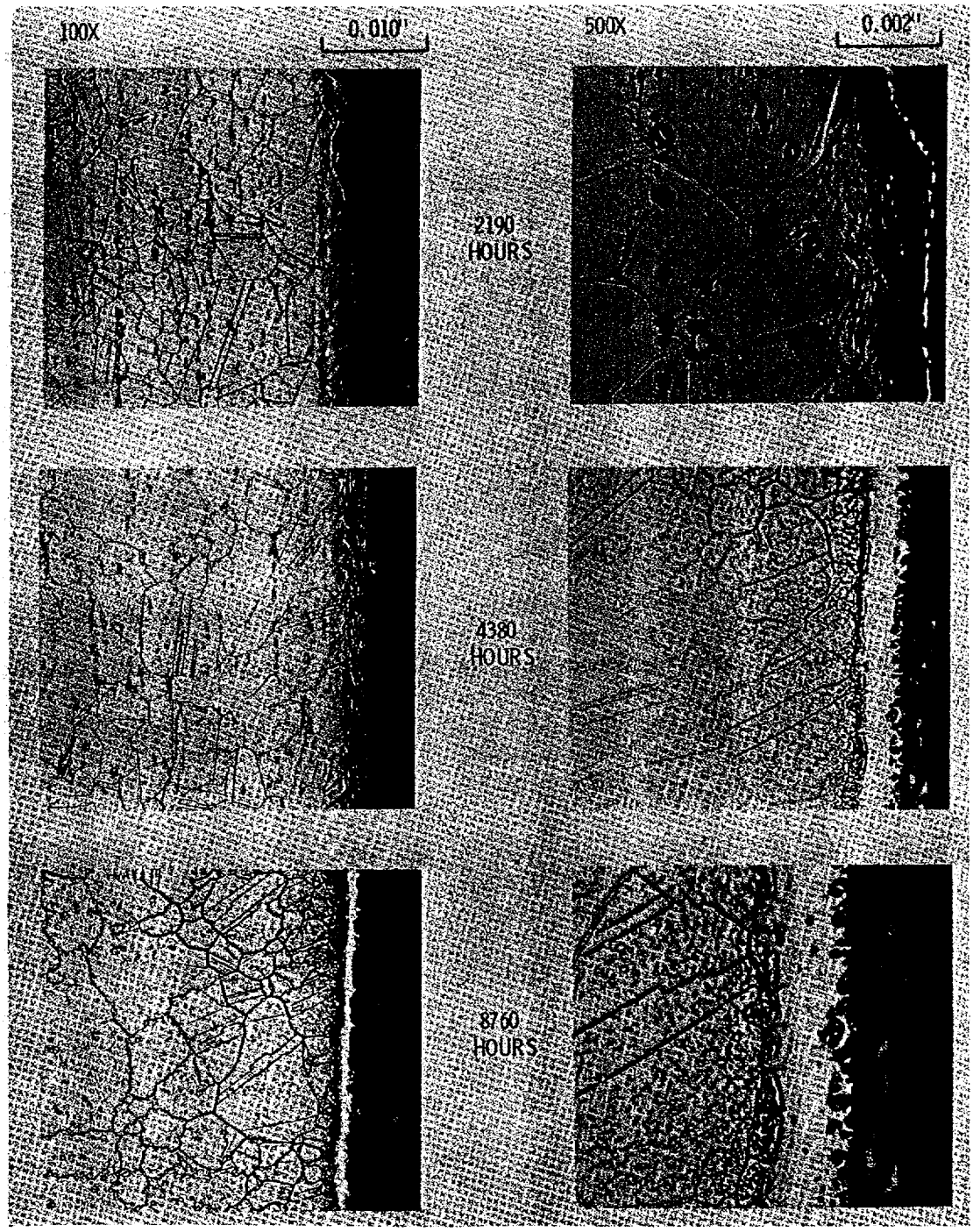

FIGURE 41. Samples of Hastelloy X Tested with Radioactive SrF_2 - 13 mole % ZrF_4 - 13 mole % Zr at 400°C

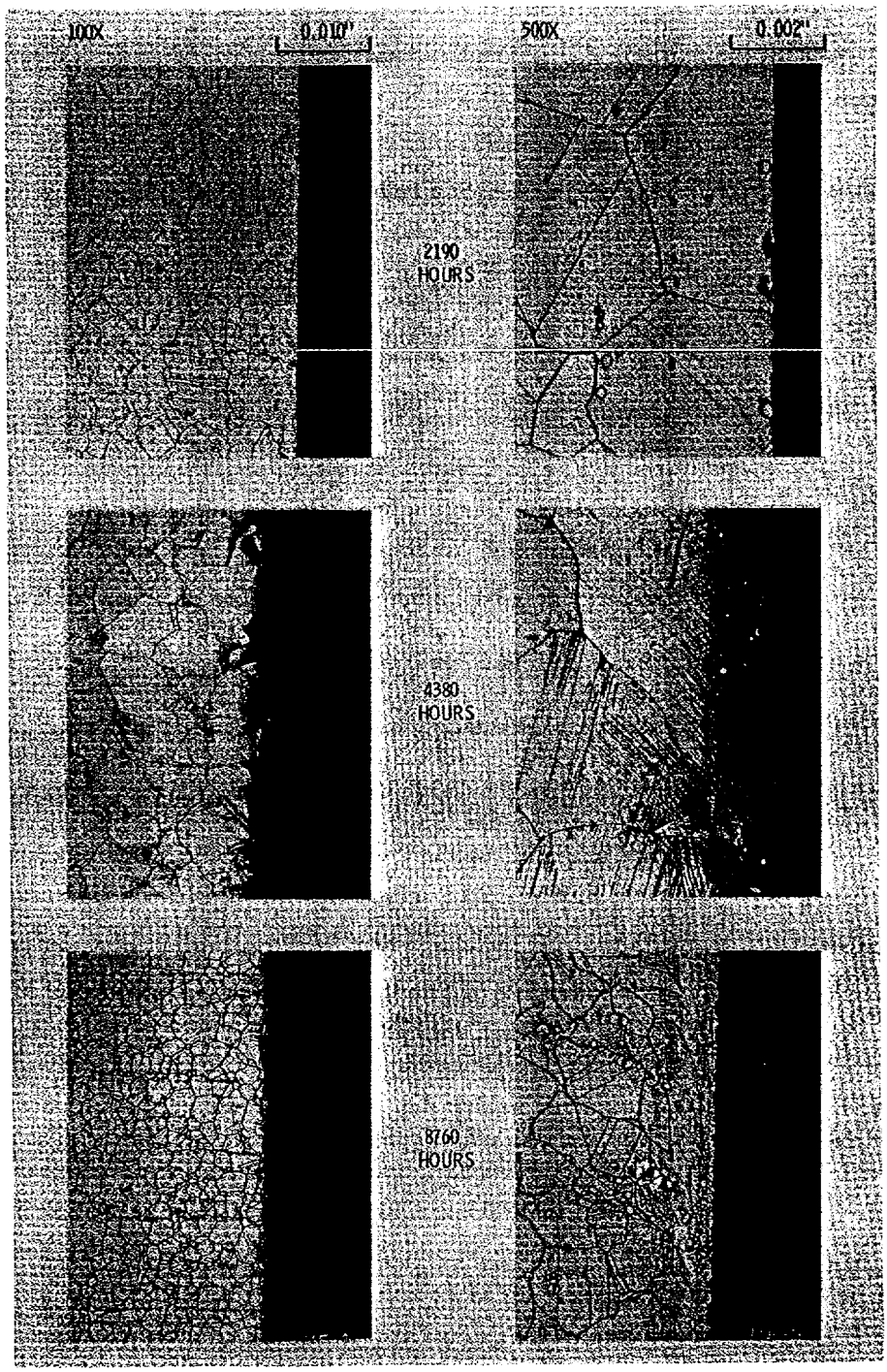

FIGURE 42. Test Specimens - Hastelloy X/Nonradioactive SrF_2 at 400°C

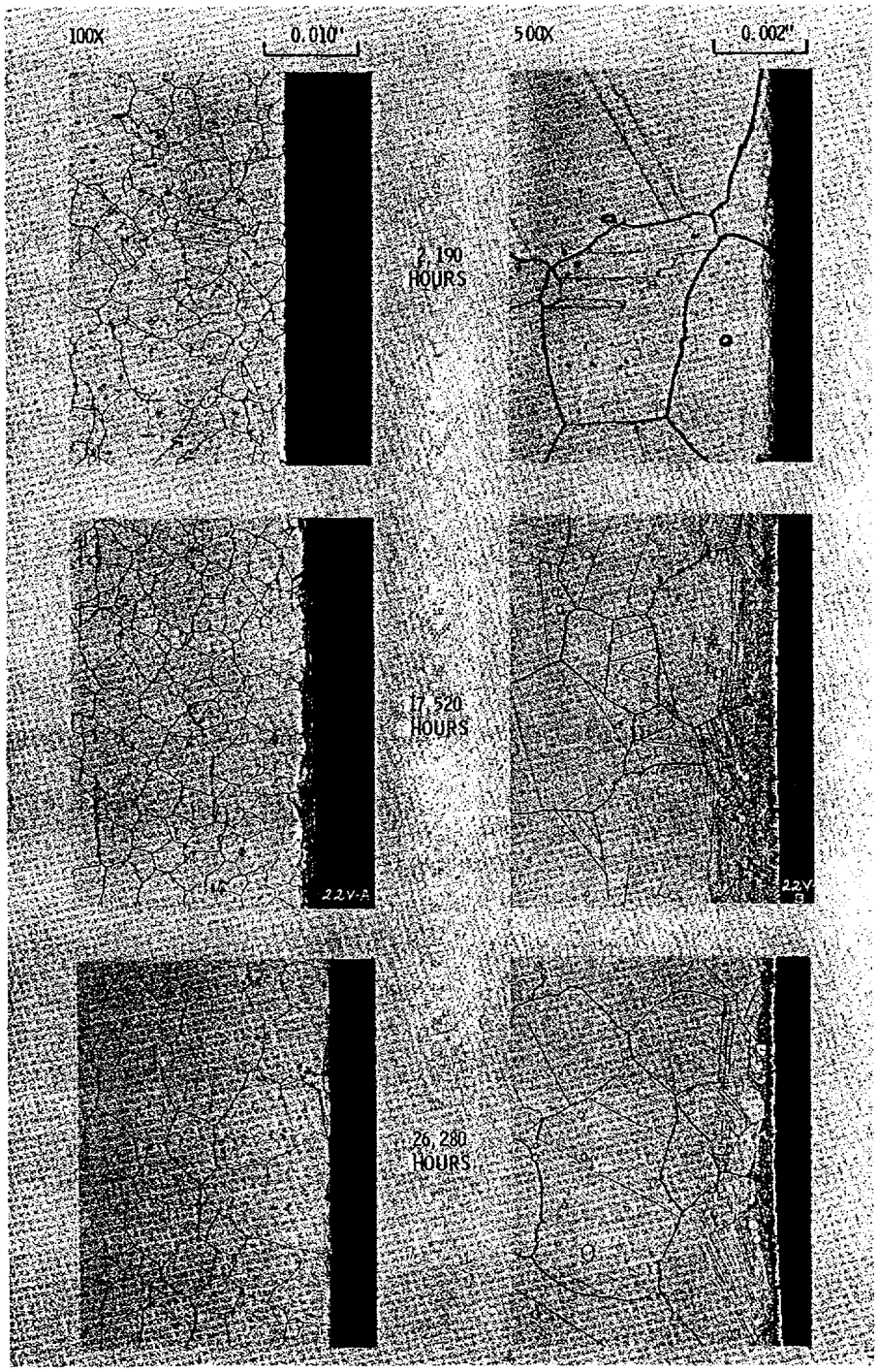

FIGURE 43. Test Specimens - Hastelloy X/Nonradioactive SrF_2 - 6 mole % ZrF_4 - 6 mole % Zr at 400°C

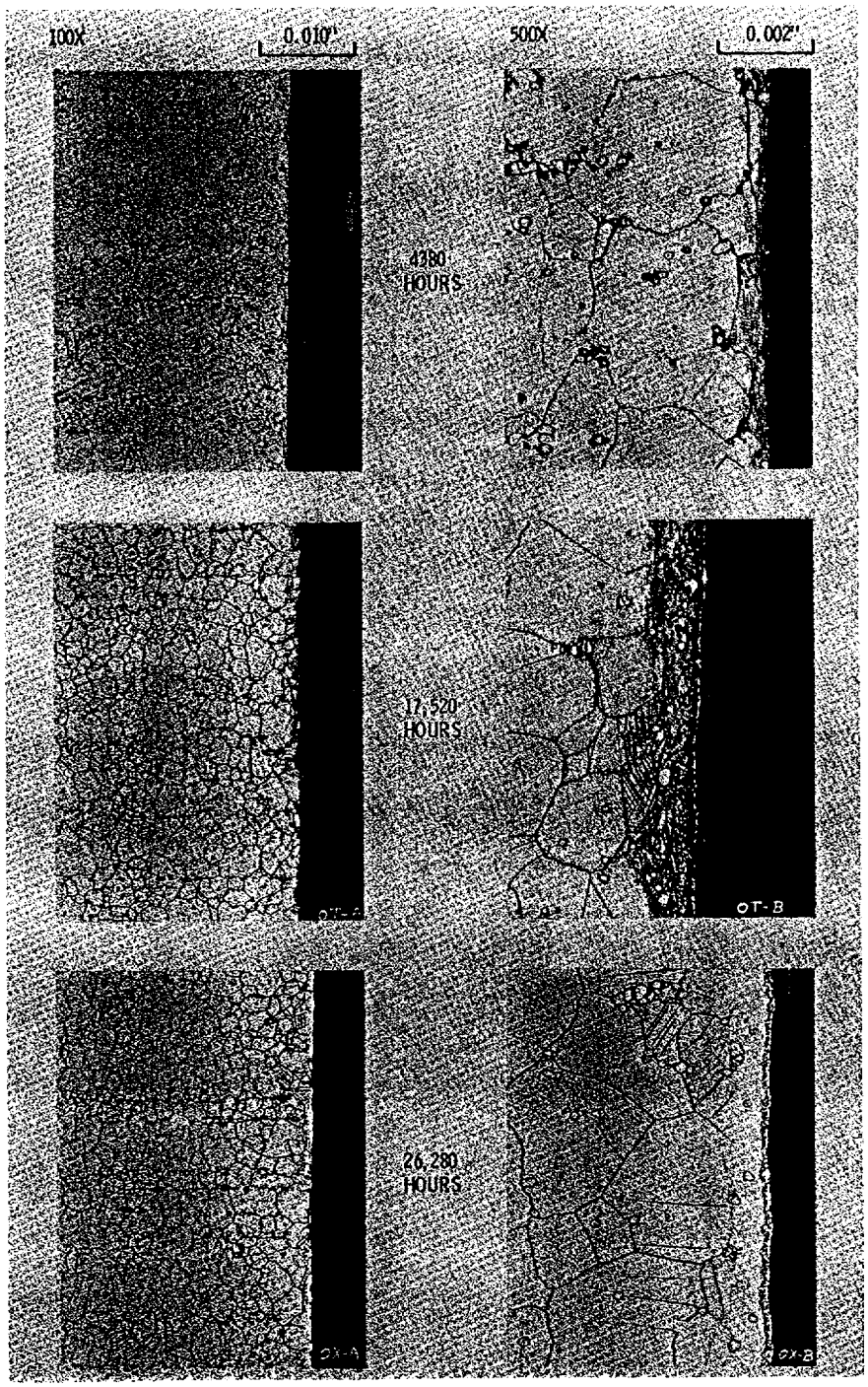

FIGURE 44. Test Specimens - Hastelloy X/Nonradioactive SrF_2 - 13 mole % ZrF_4 - 13 mole % Zr at 400°C

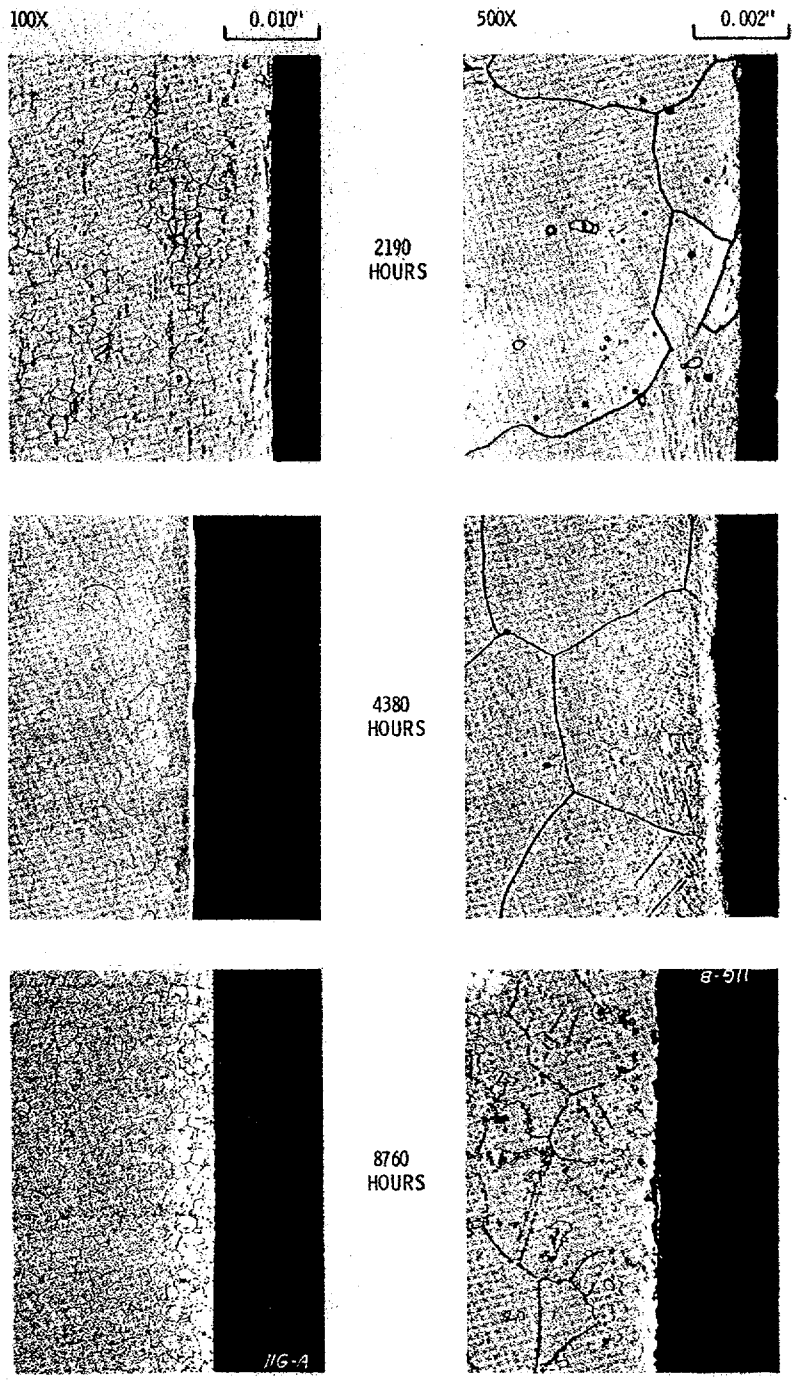

FIGURE 45. Test Specimens - Hastelloy X/Nonradioactive SrF_2 at 800°C

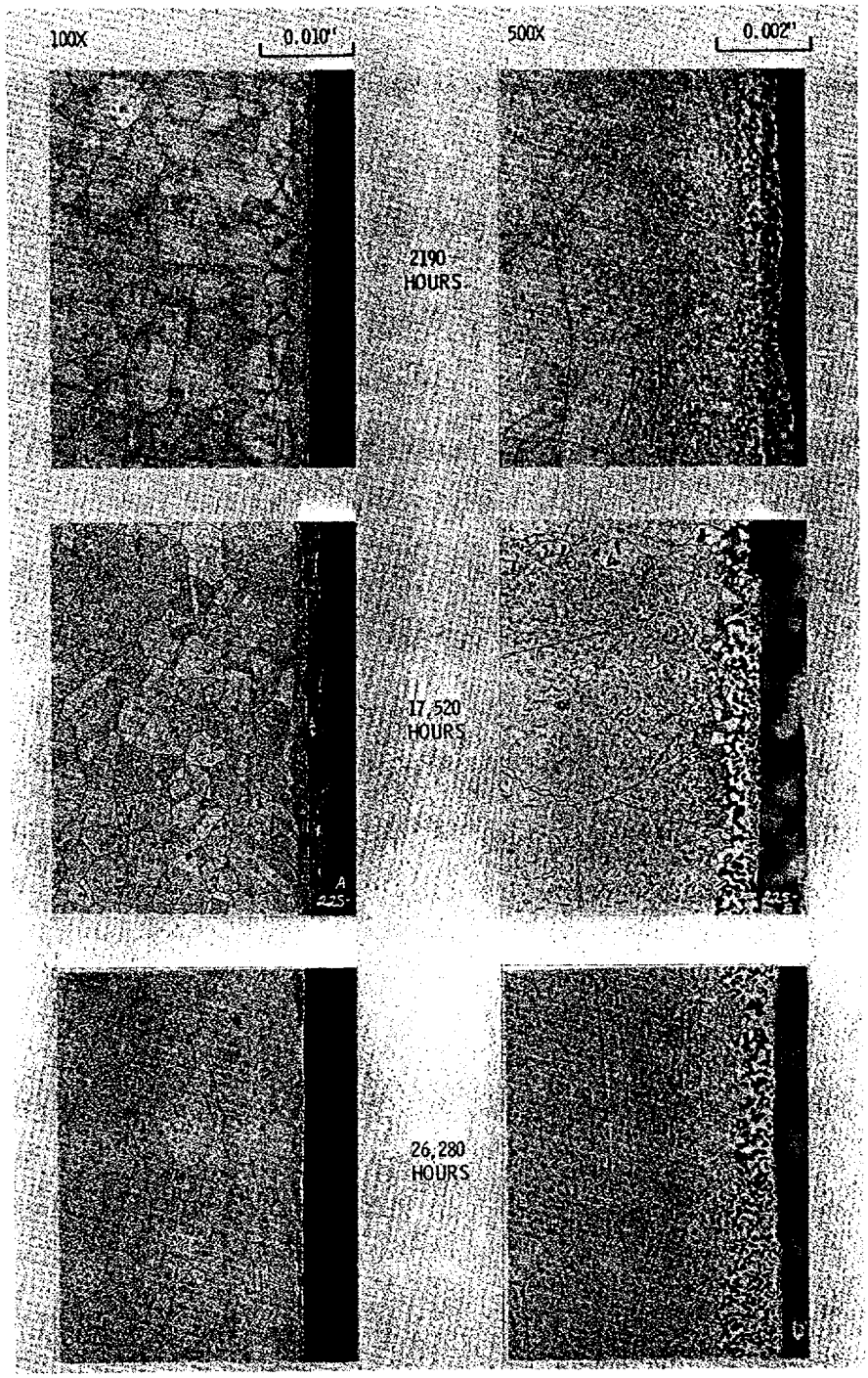

FIGURE 46. Test Specimens - Hastelloy X/Nonradioactive SrF_2 - 6 mole % ZrF_4 - 6 mole % Zr at 800°C

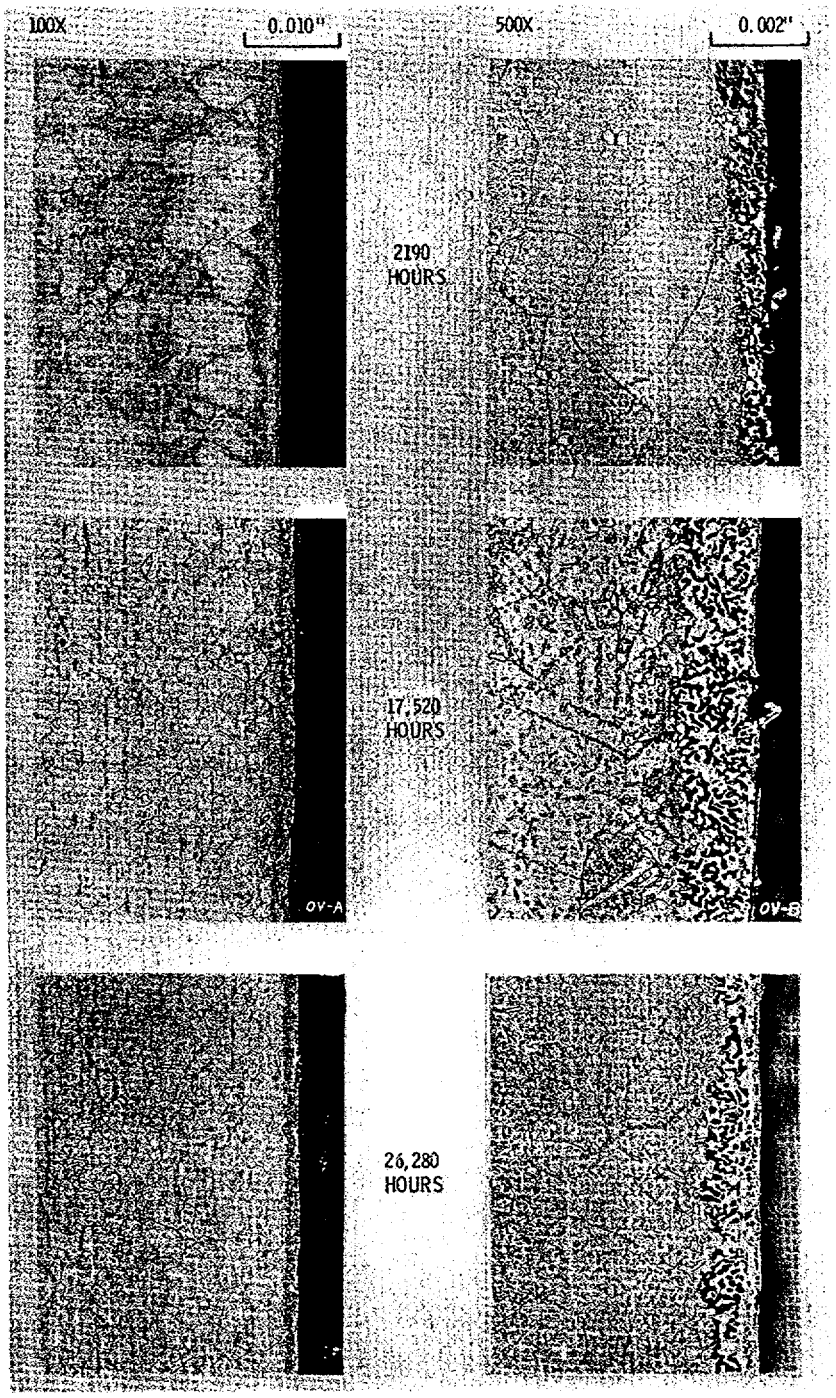

FIGURE 47. Test Specimens - Hastelloy X/Nonradioactive SrF_2 - 13 mole % ZrF_4 - 13 mole % Zr at 800°C

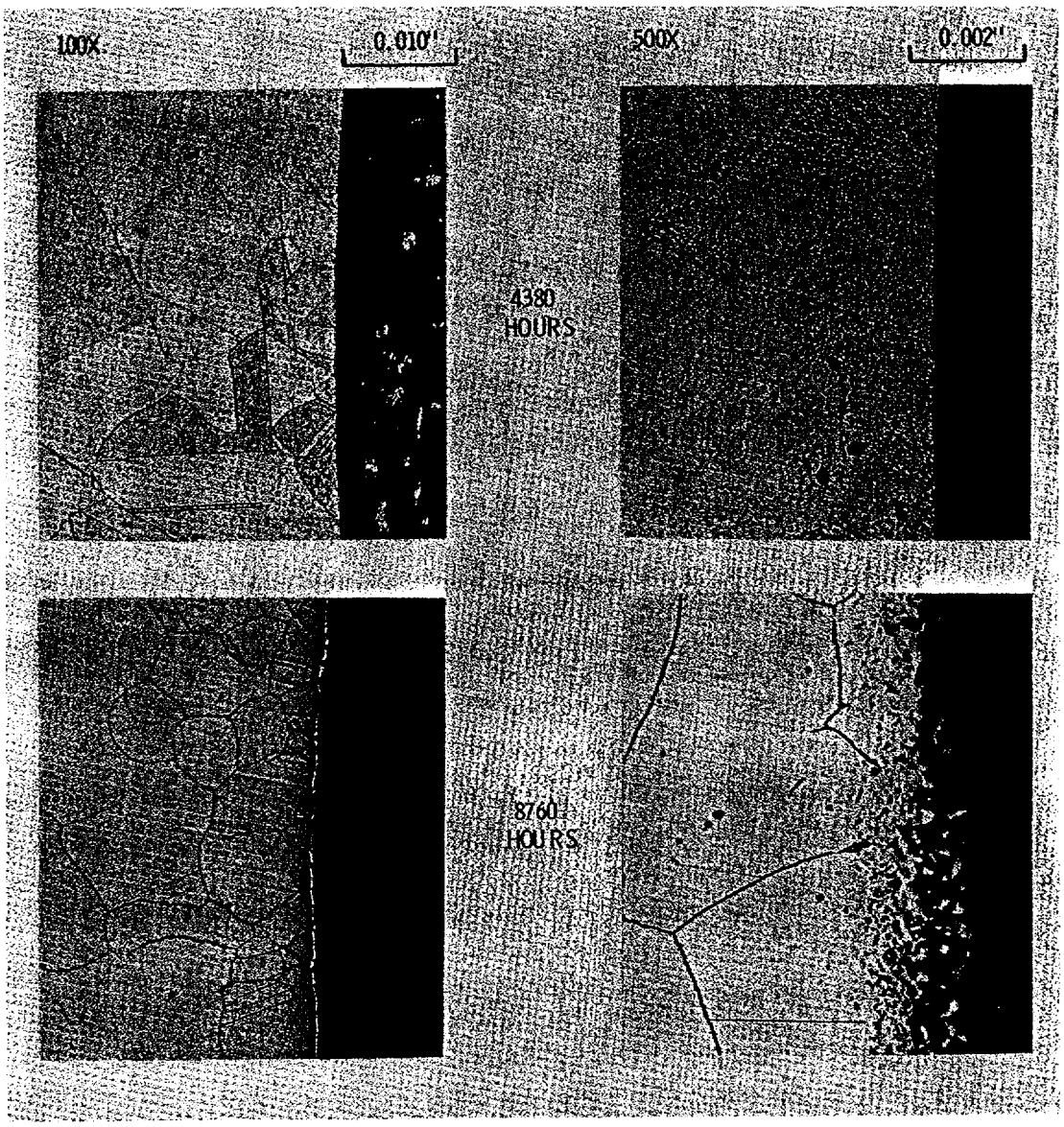

FIGURE 48. Samples of 316L SS Tested with Radioactive SrF_2 at 400°C

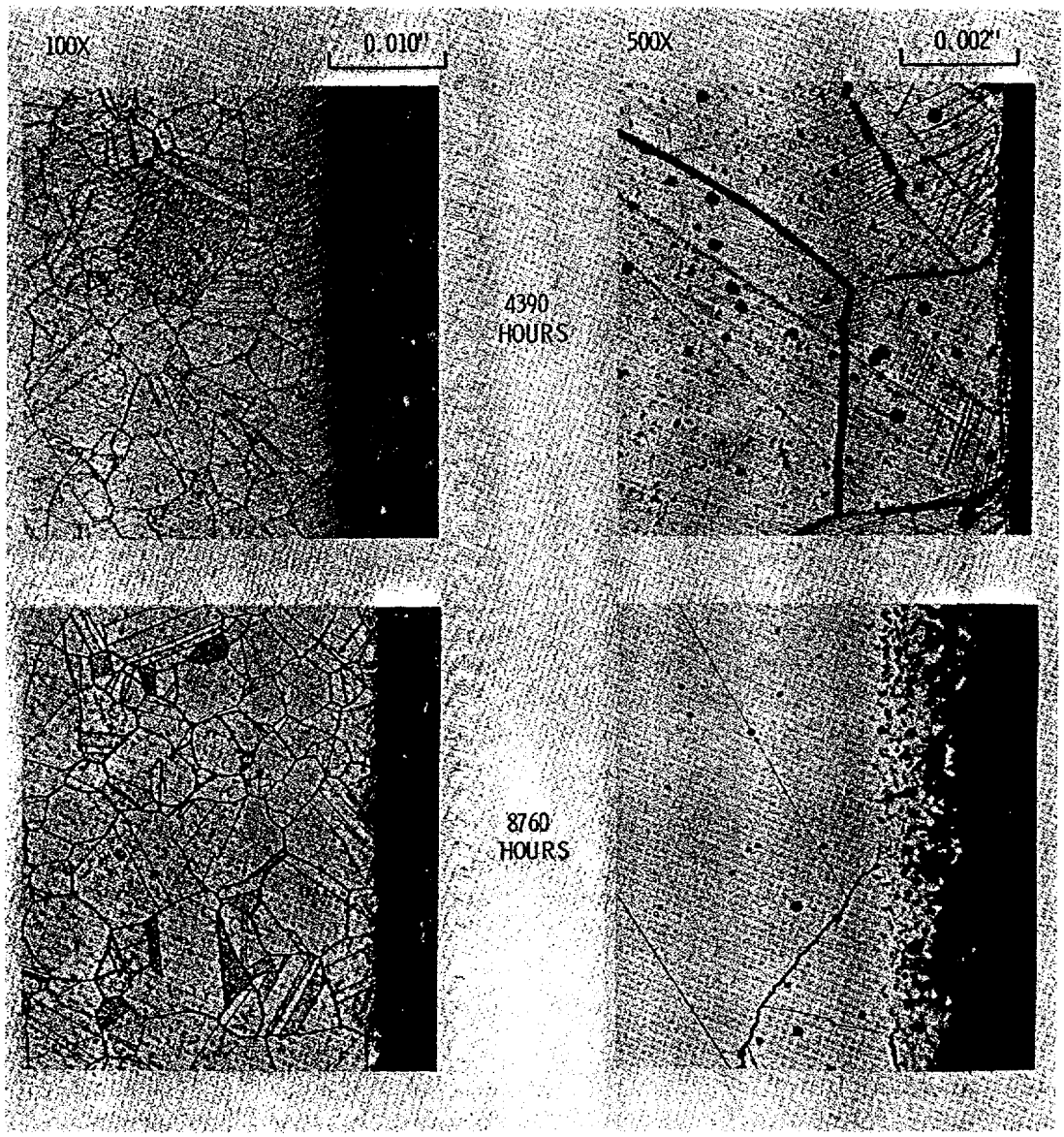

FIGURE 49. Samples of 316L SS Tested with Radioactive SrF_2 - 13 mole % ZrF_4 - 13 mole % Zr at 400°C

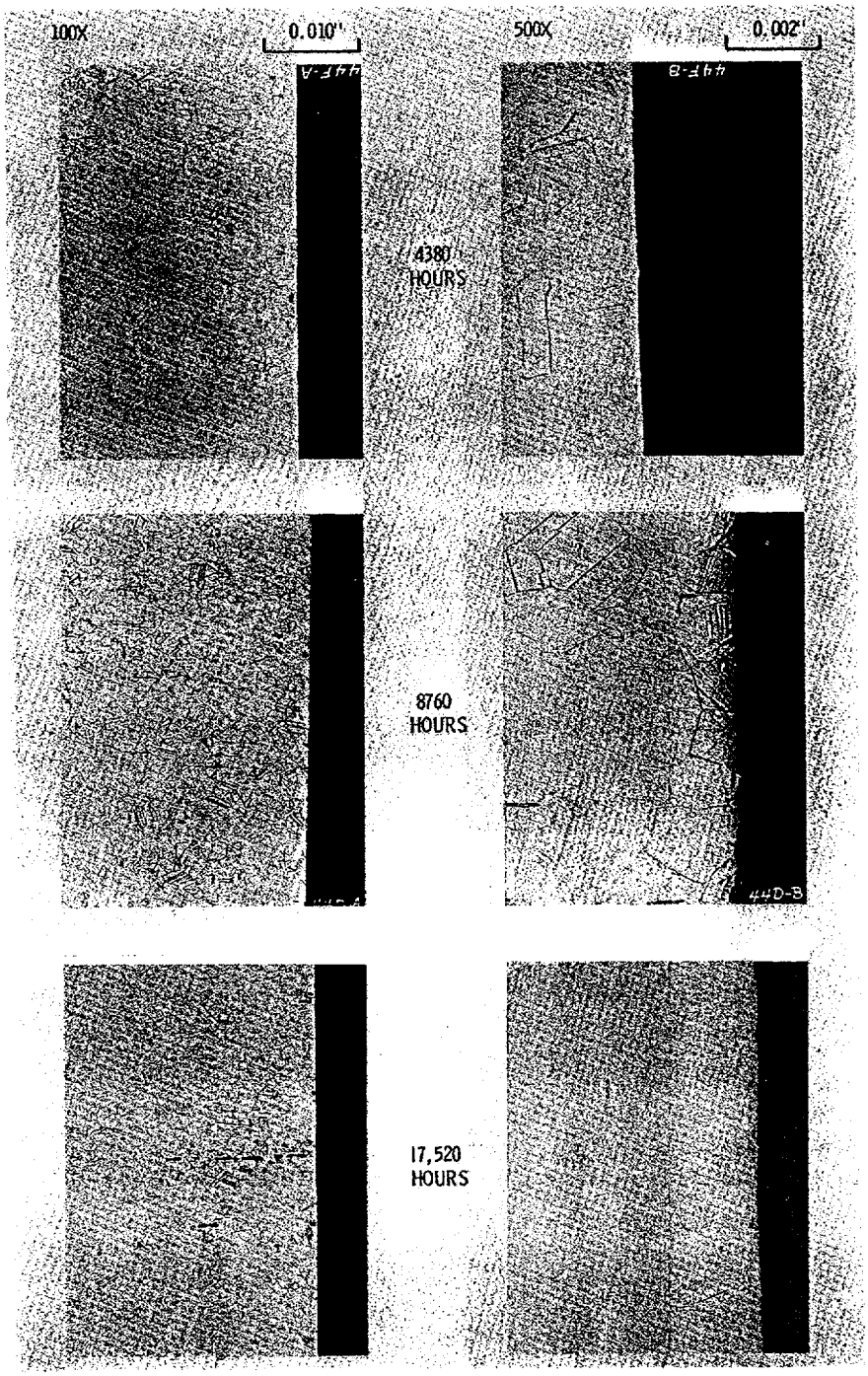

FIGURE 50. Test Specimens - 316L SS/Nonradioactive SrF_2 at 400°C

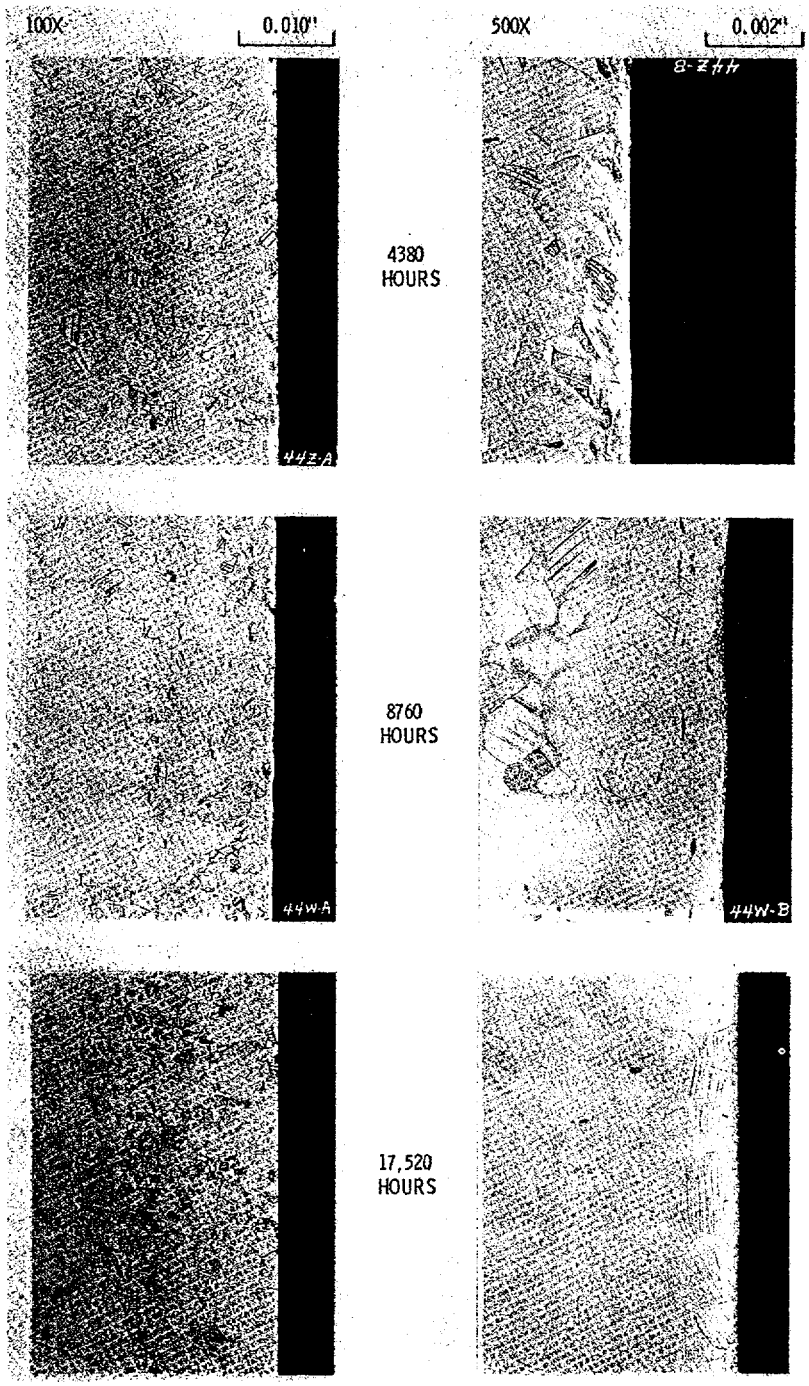

FIGURE 51. Test Specimens - 316L SS/Nonradioactive SrF_2 - 6 mole % ZrF_4 - 6 mole % Zr at 400°C

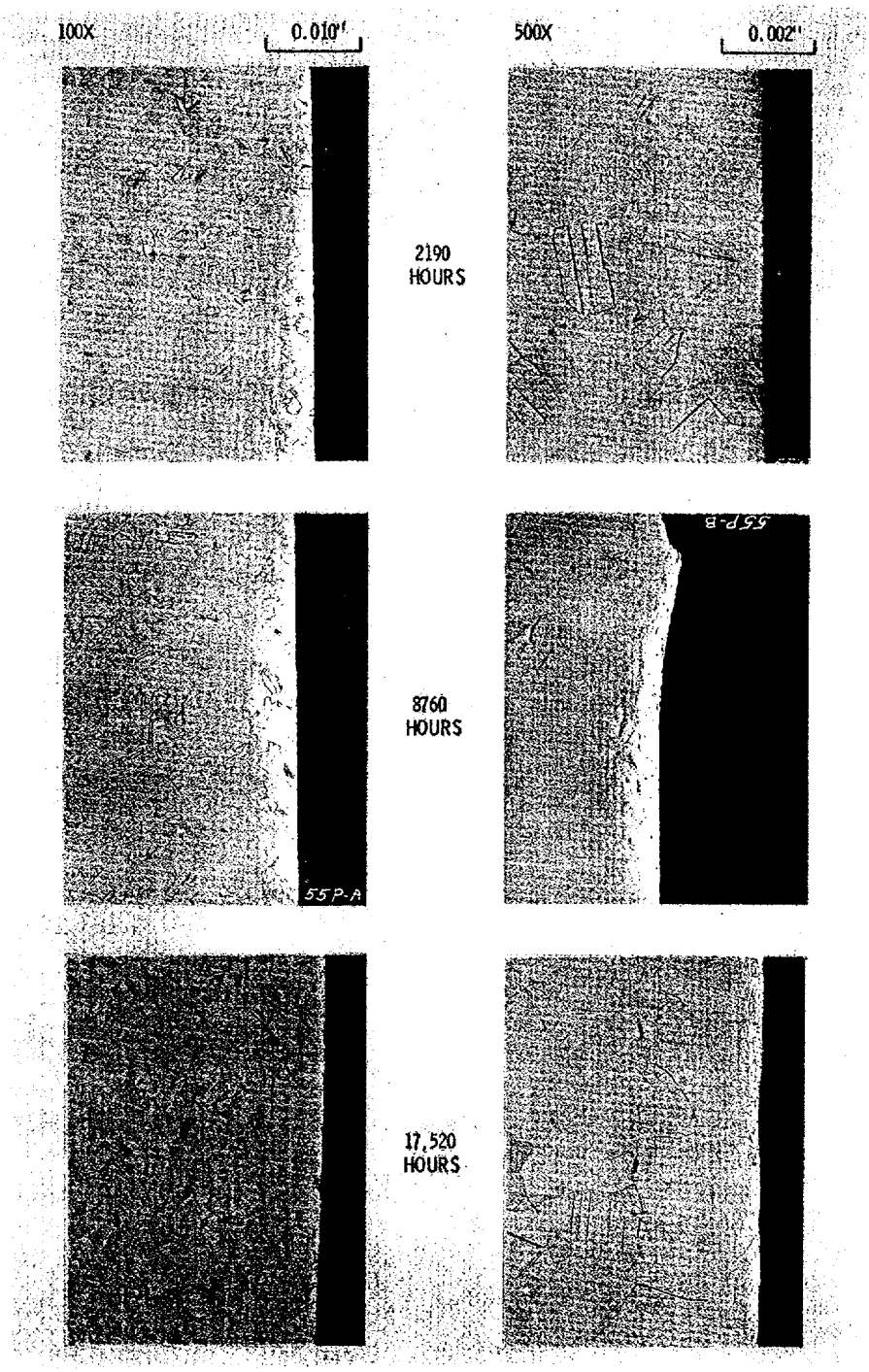

FIGURE 52. Test Specimens - 316L SS/Nonradioactive SrF_2 - 13 mole % ZrF_4 - 13 mole % Zr at 400°C

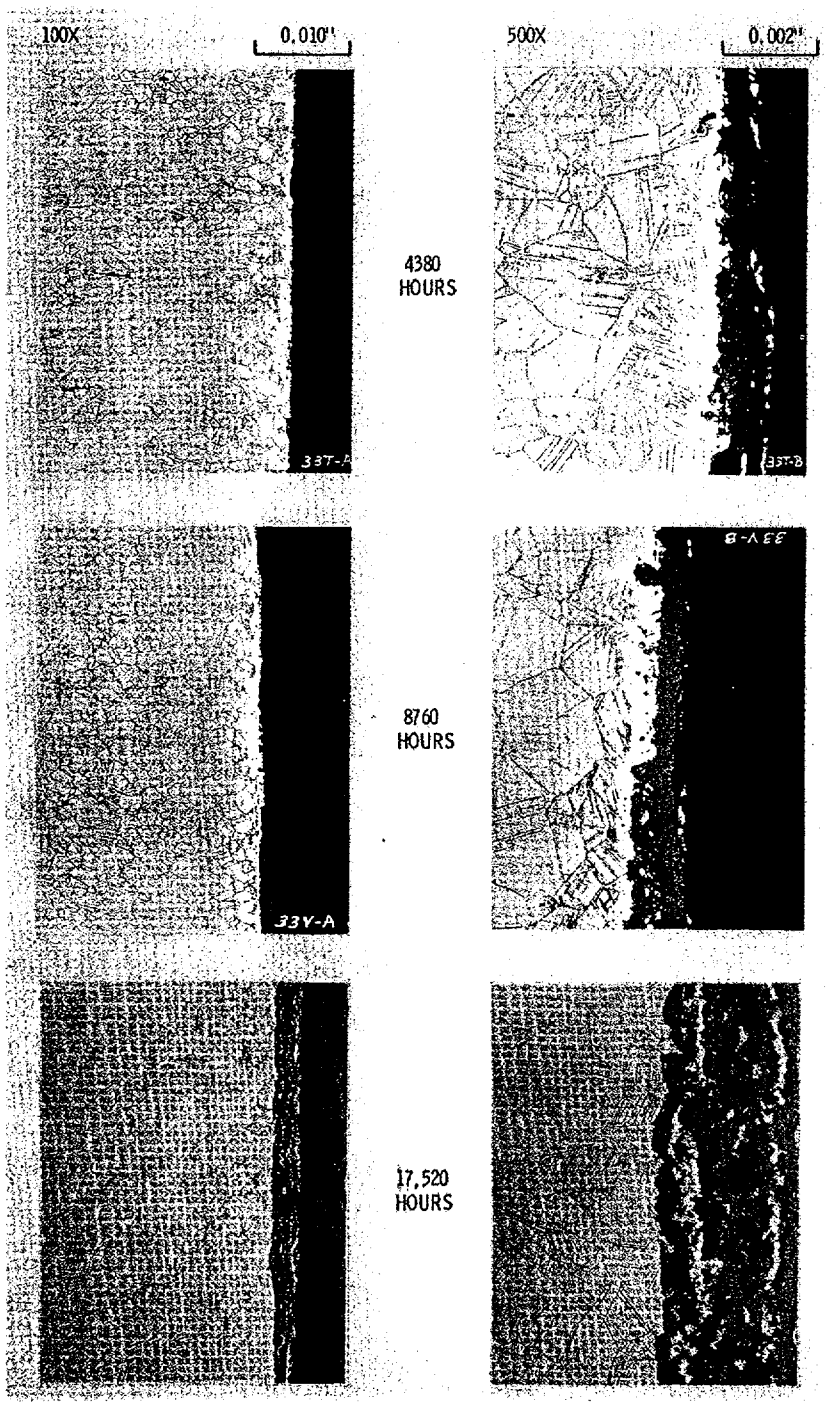

FIGURE 53. Test Specimens - 316L SS/Nonradioactive SrF_2 at 800°C

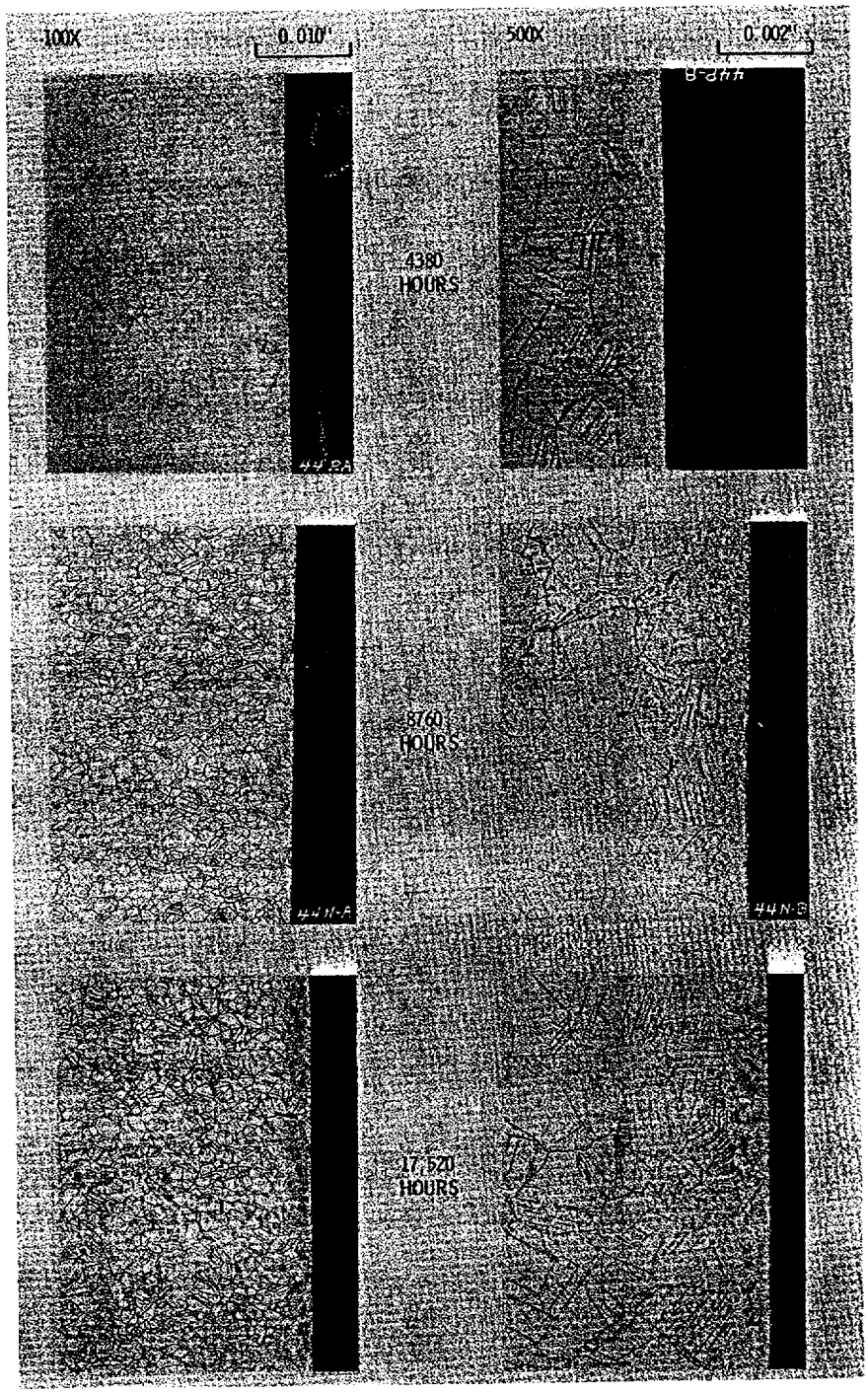

FIGURE 54. Test Specimens - 316L SS/Nonradioactive SrF_2 - 6 mole % ZrF_4 - 6 mole % Zr at 800°C

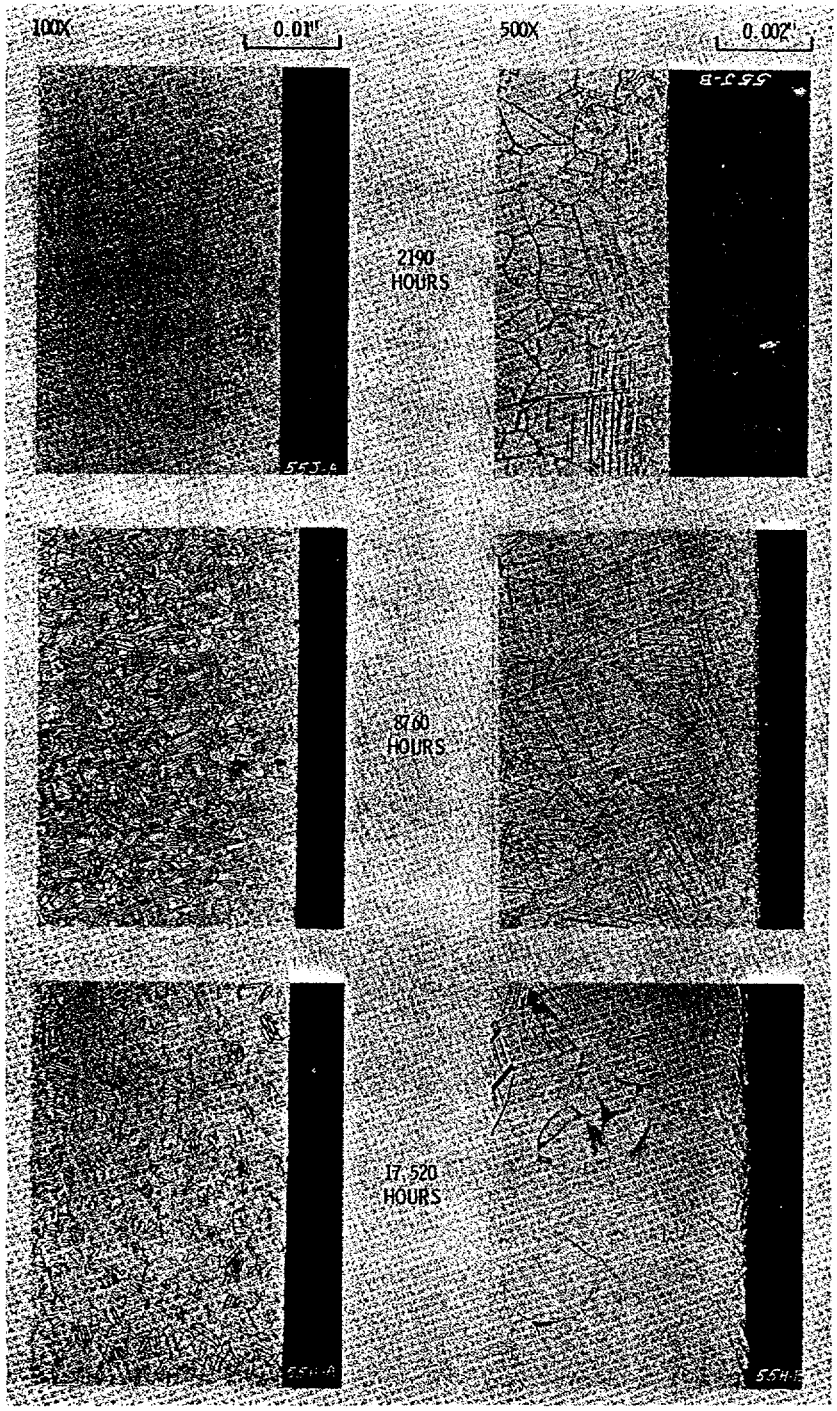

FIGURE 55. Test Specimens - 316L SS/Nonradioactive SrF_2 - 13 mole % ZrF_4 - 13 mole % Zr at 800°C

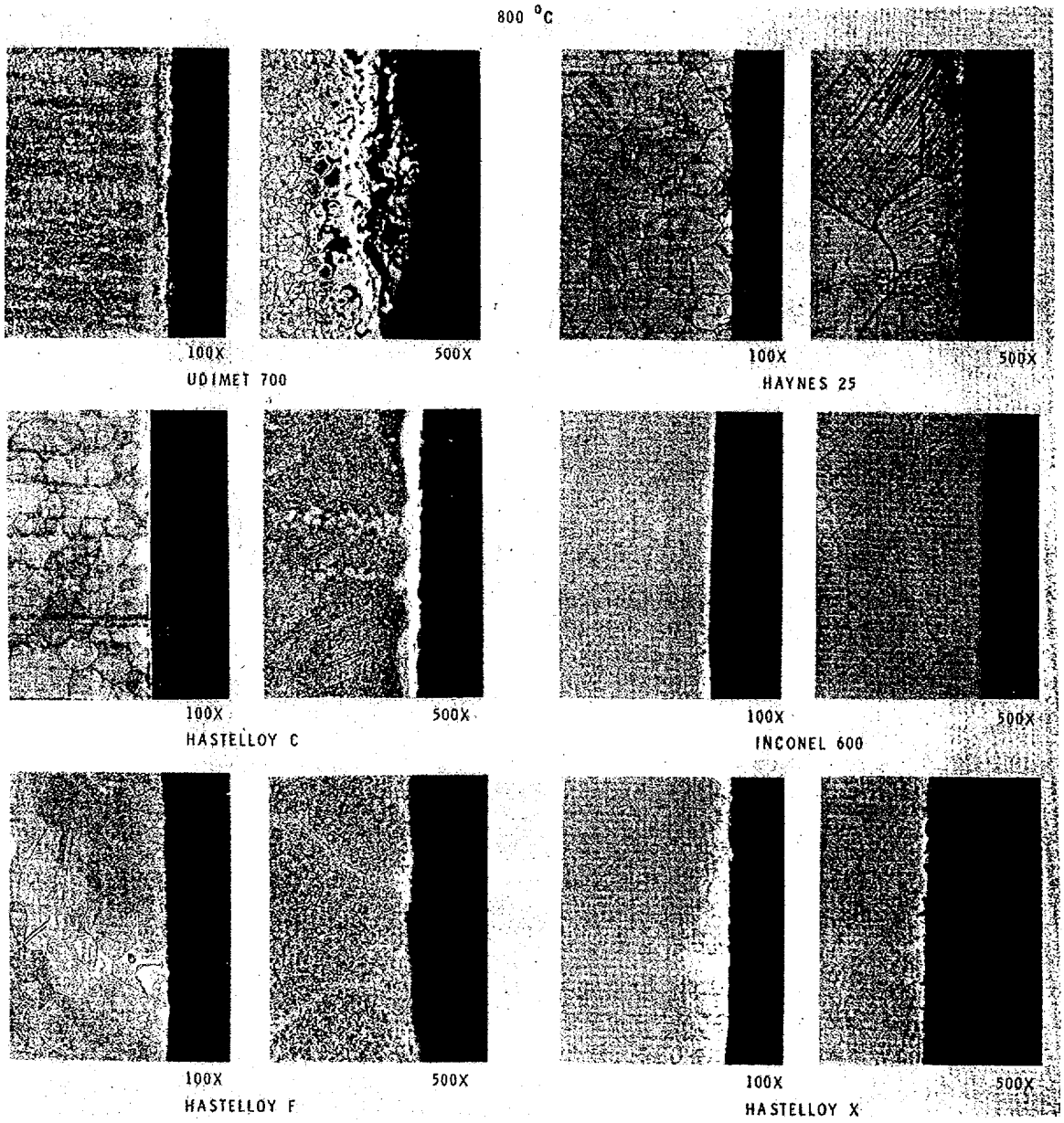

FIGURE 56. Test Specimens from Scouting Tests with Nonradioactive SrF_2 at 800°C

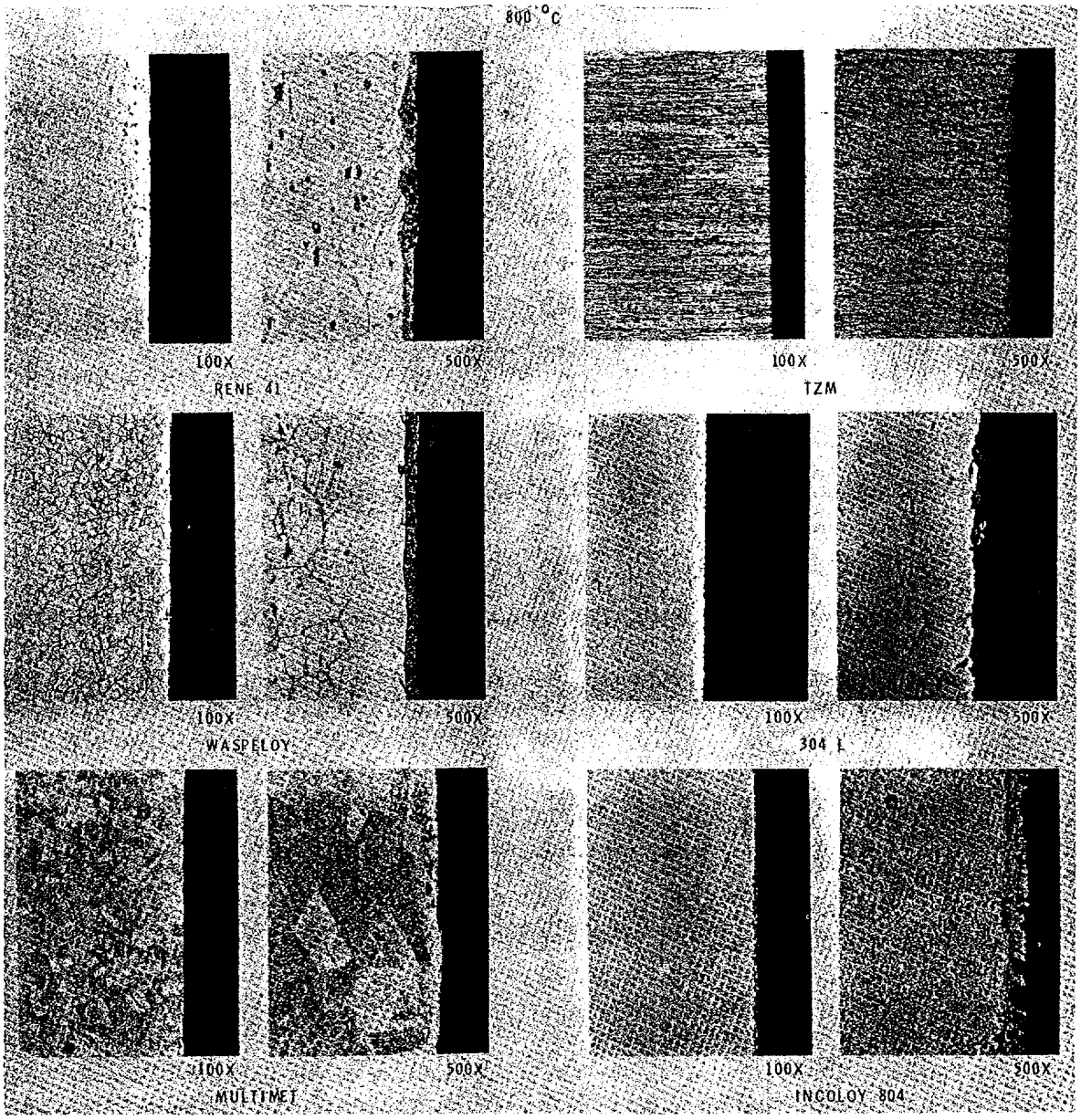

FIGURE 57. Test Specimens from Scouting Tests with SrF_2 - 6 mole % ZrF_4 - 6 mole % Zr at 800°C

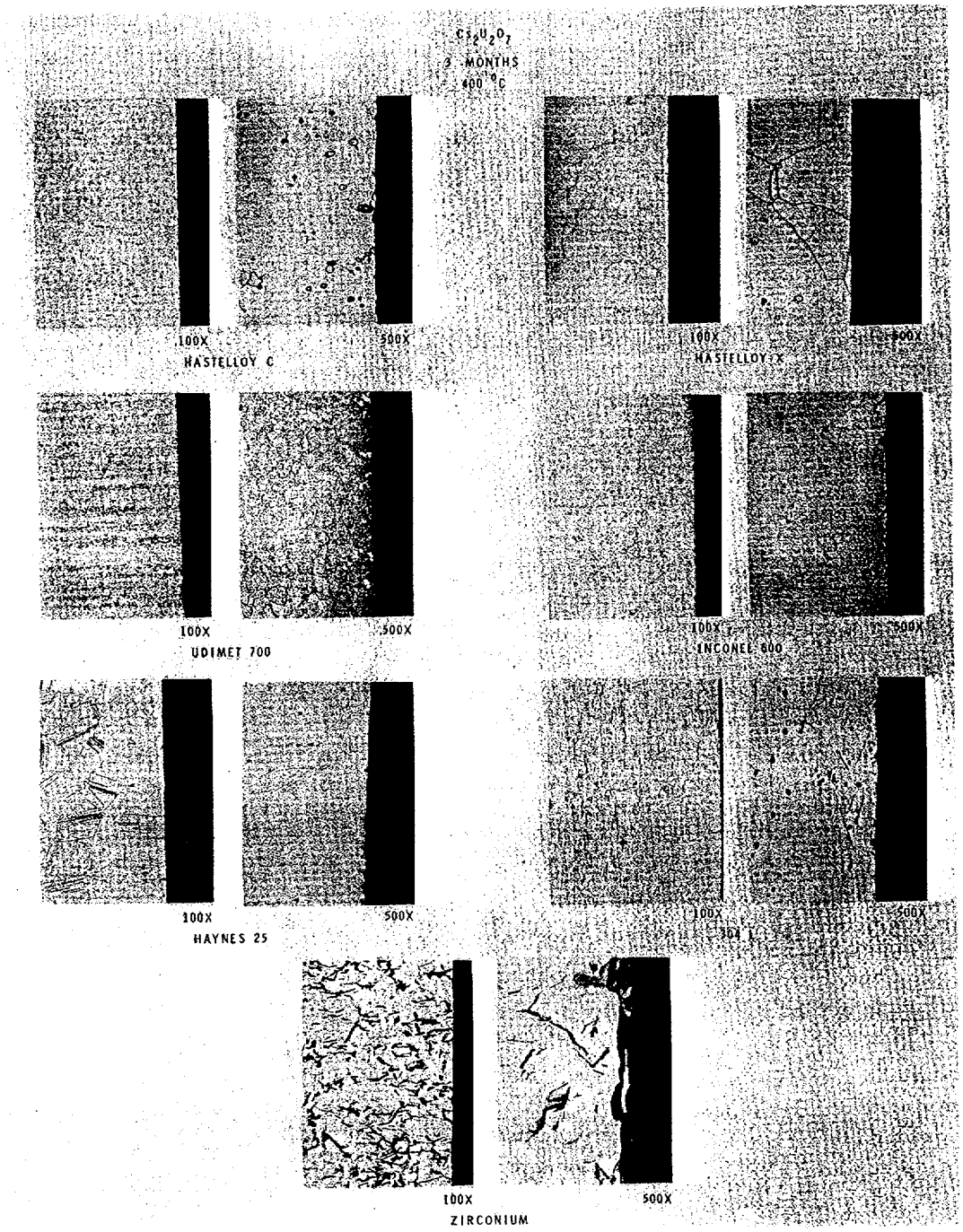

FIGURE 58. Metal Specimens from 400°C Tests with $Cs_2U_2O_7$

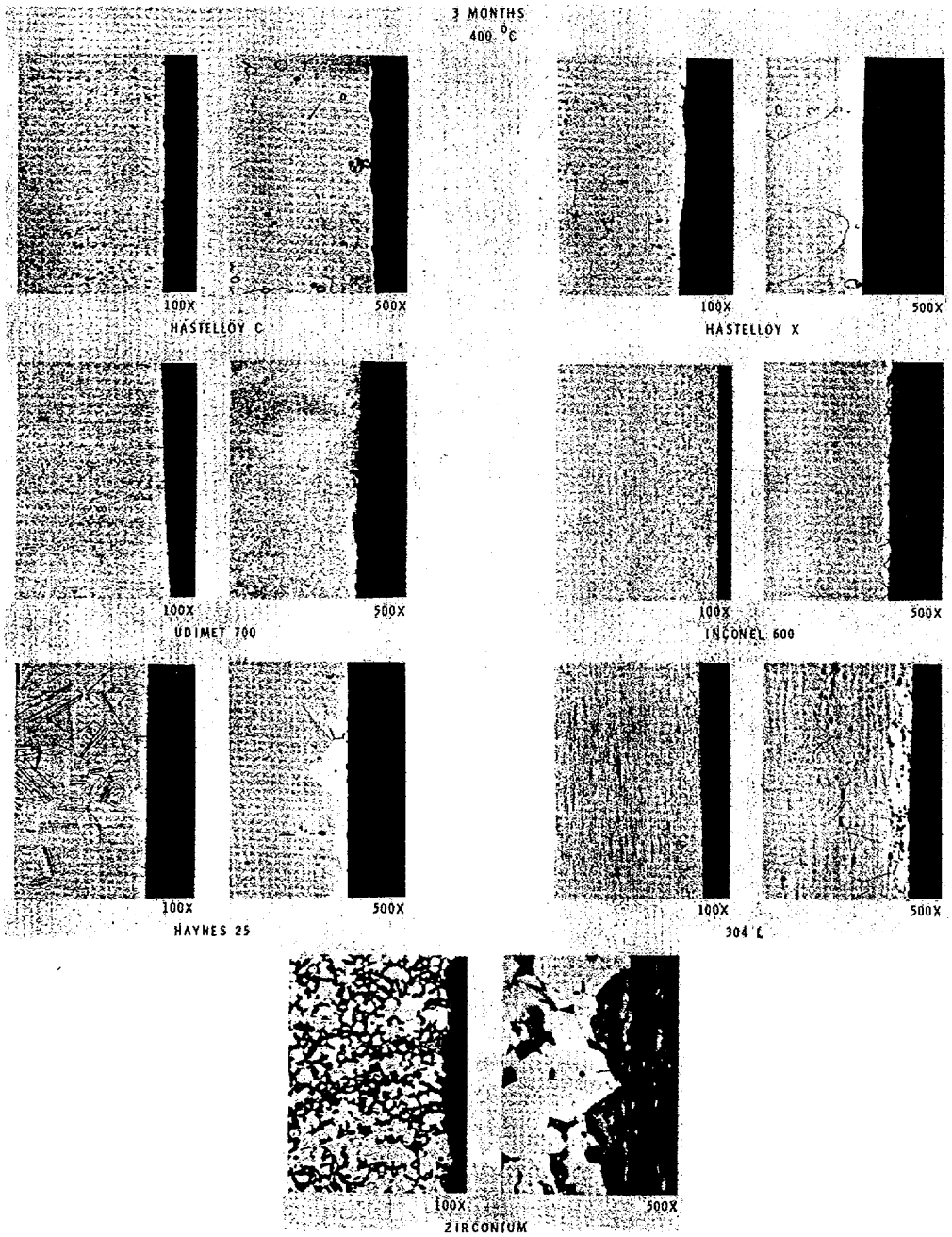

FIGURE 59. Metal Specimens from 400°C Tests with $Cs_2U_2O_7$ - 11 mole % BaU_2O_7

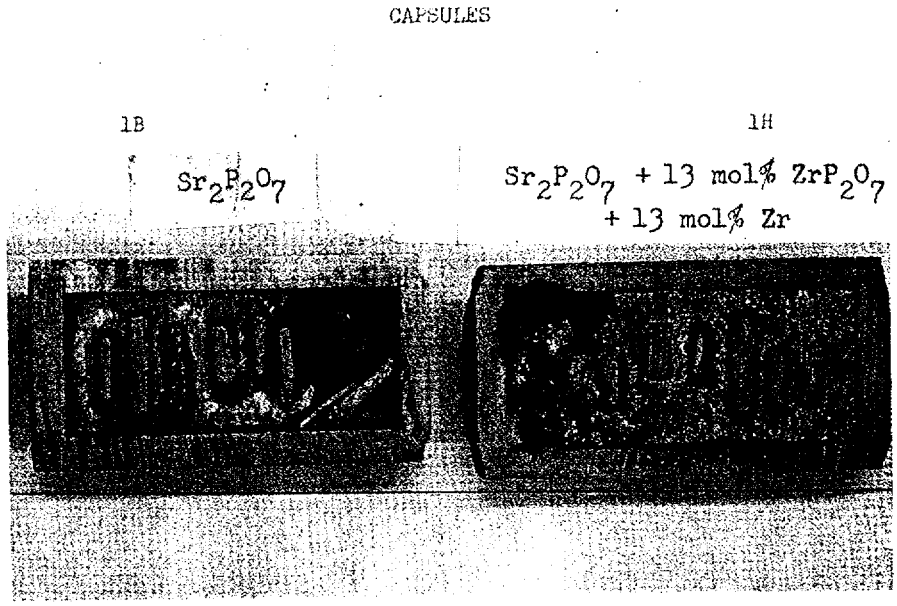

FIGURE 60. Sectioned $Sr_2P_2O_7$ Capsules - Tested at 1000°C for 3 Months

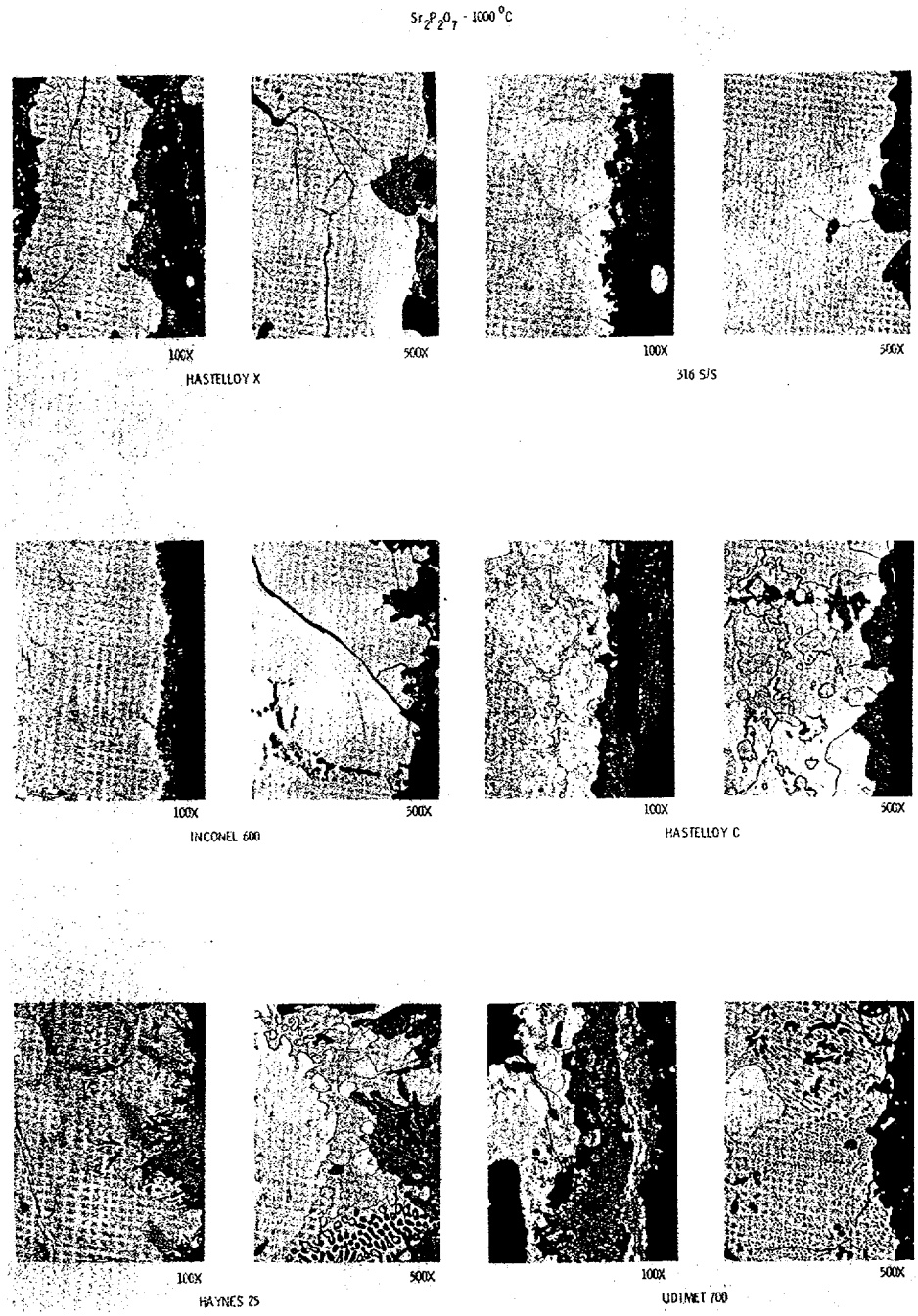

FIGURE 61. Metal Samples from 3-Month - 1000°C Tests with $Sr_2P_2O_7$

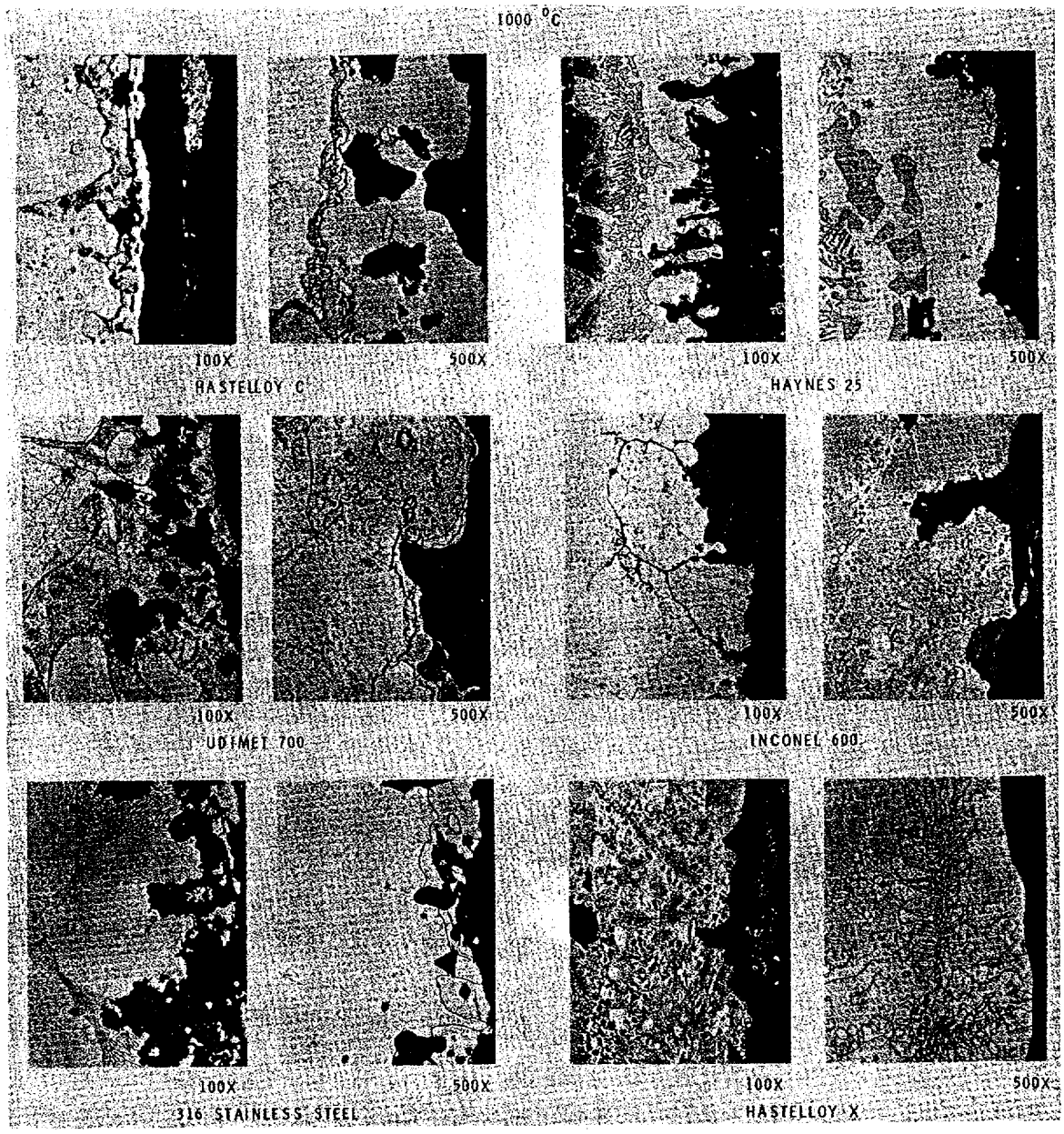

FIGURE 62. Metal Specimens from 3-Month - 1000°C Tests with $Sr_2P_2O_7$ - 13 mole % ZrP_2O_7 - 13 mole % Zr

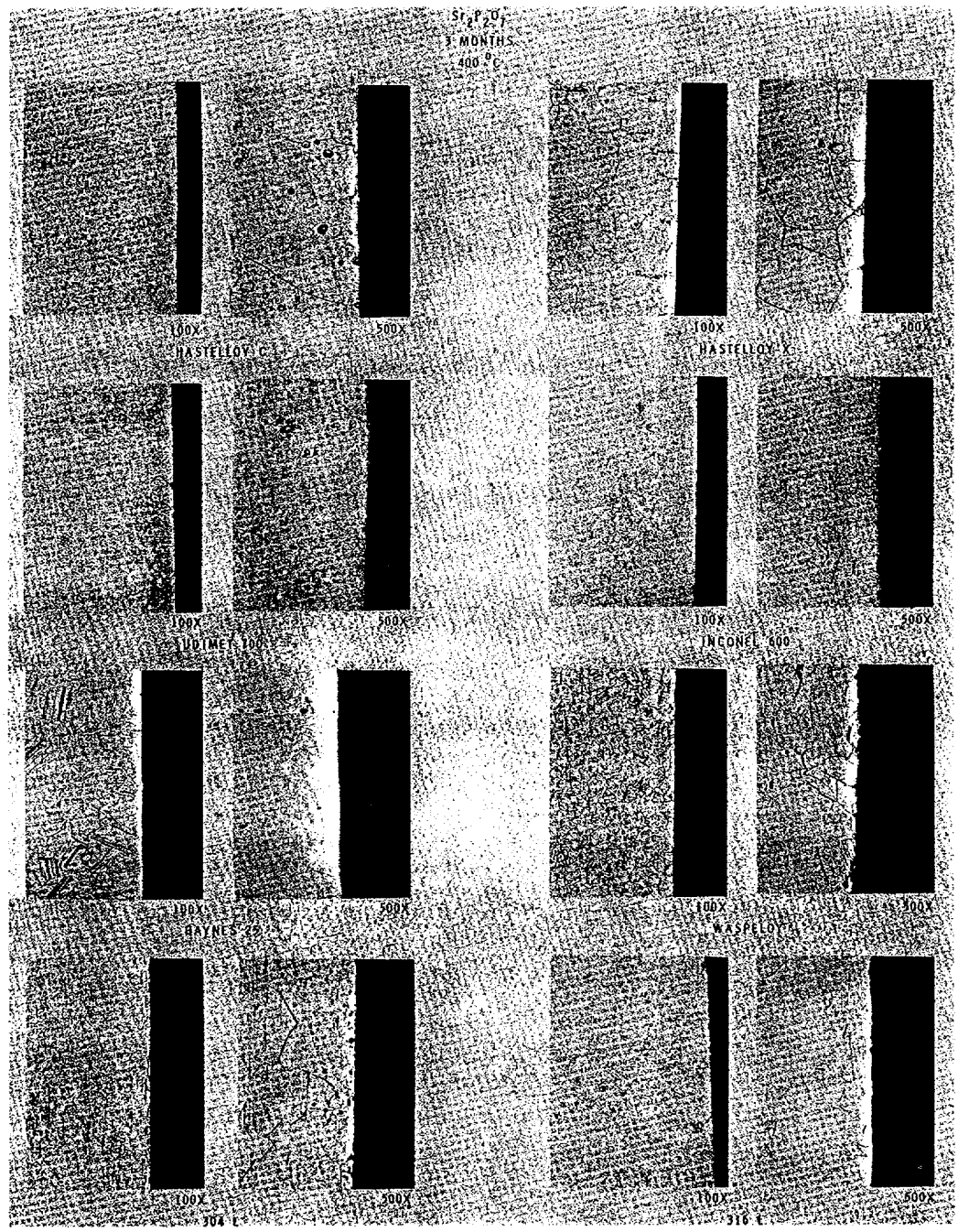

FIGURE 63. Metal Specimens from 3-Month - 400°C Tests with $Sr_2P_2O_7$

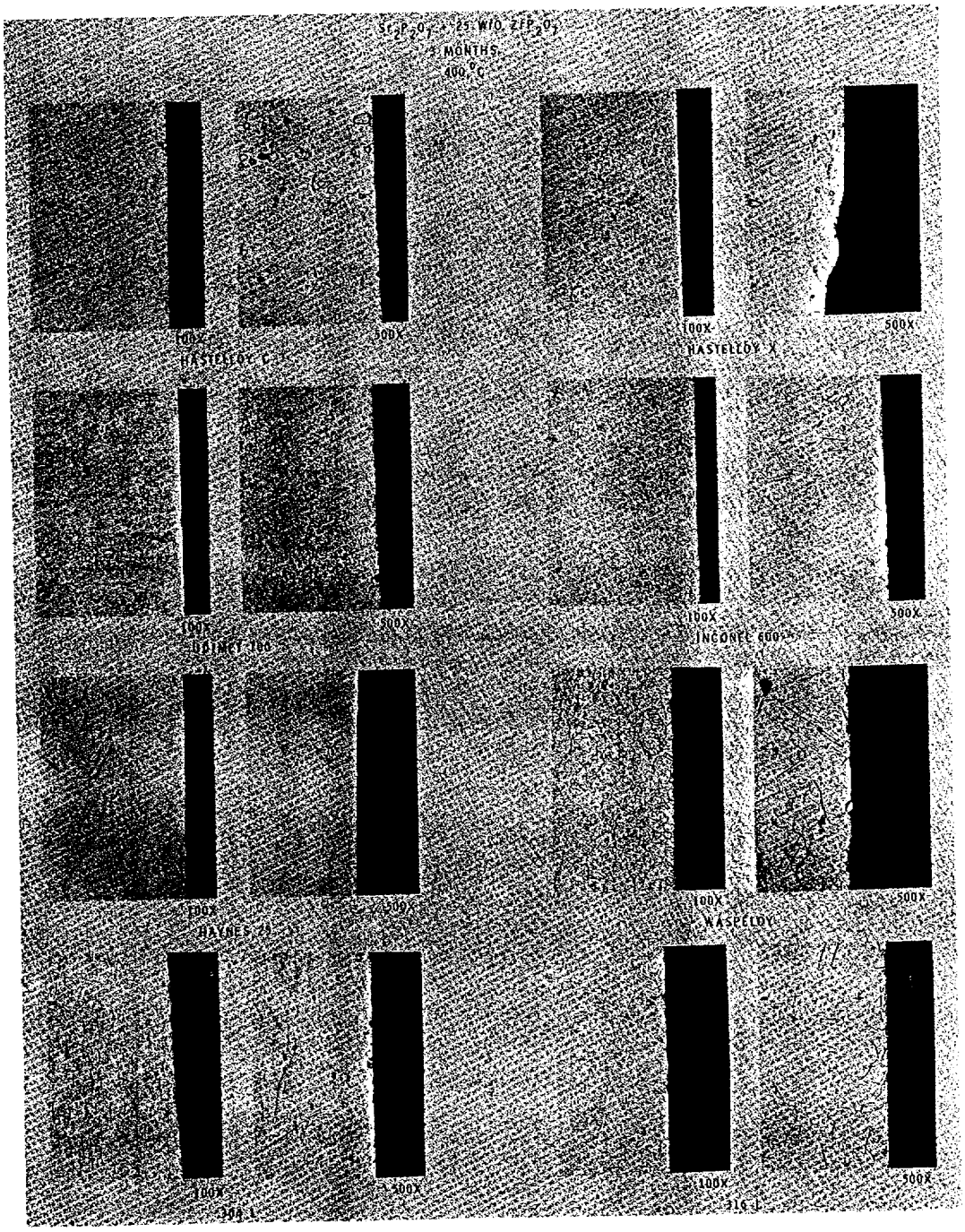

FIGURE 64. Metal Specimens from 3-Month - 400°C Tests with $Sr_2P_2O_7$ - 13 mole % ZrP_2O_7 - 13 mole % Zr

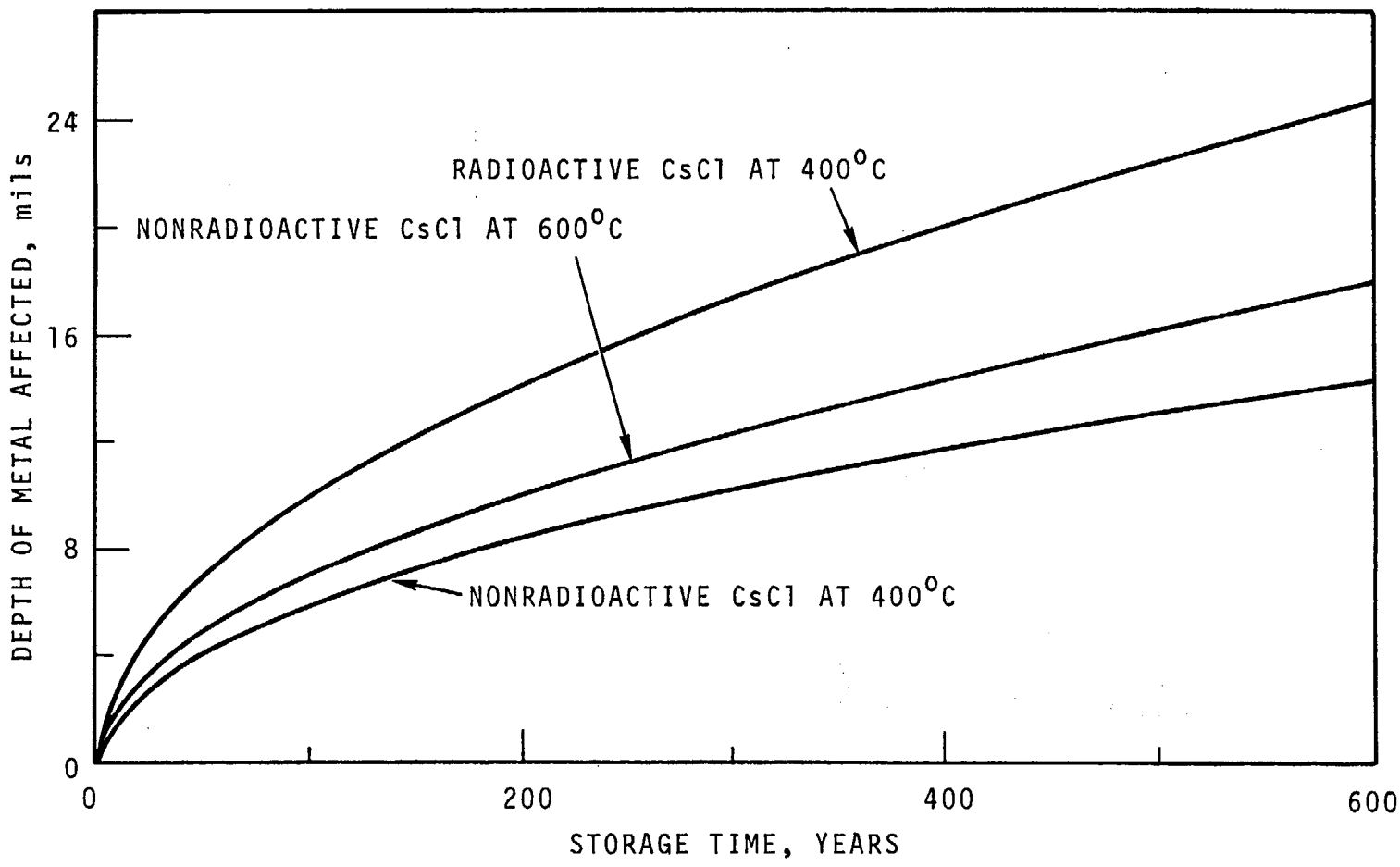

FIGURE 65. Estimated Long-Term Attack of 316L Stainless Steel by CsCl

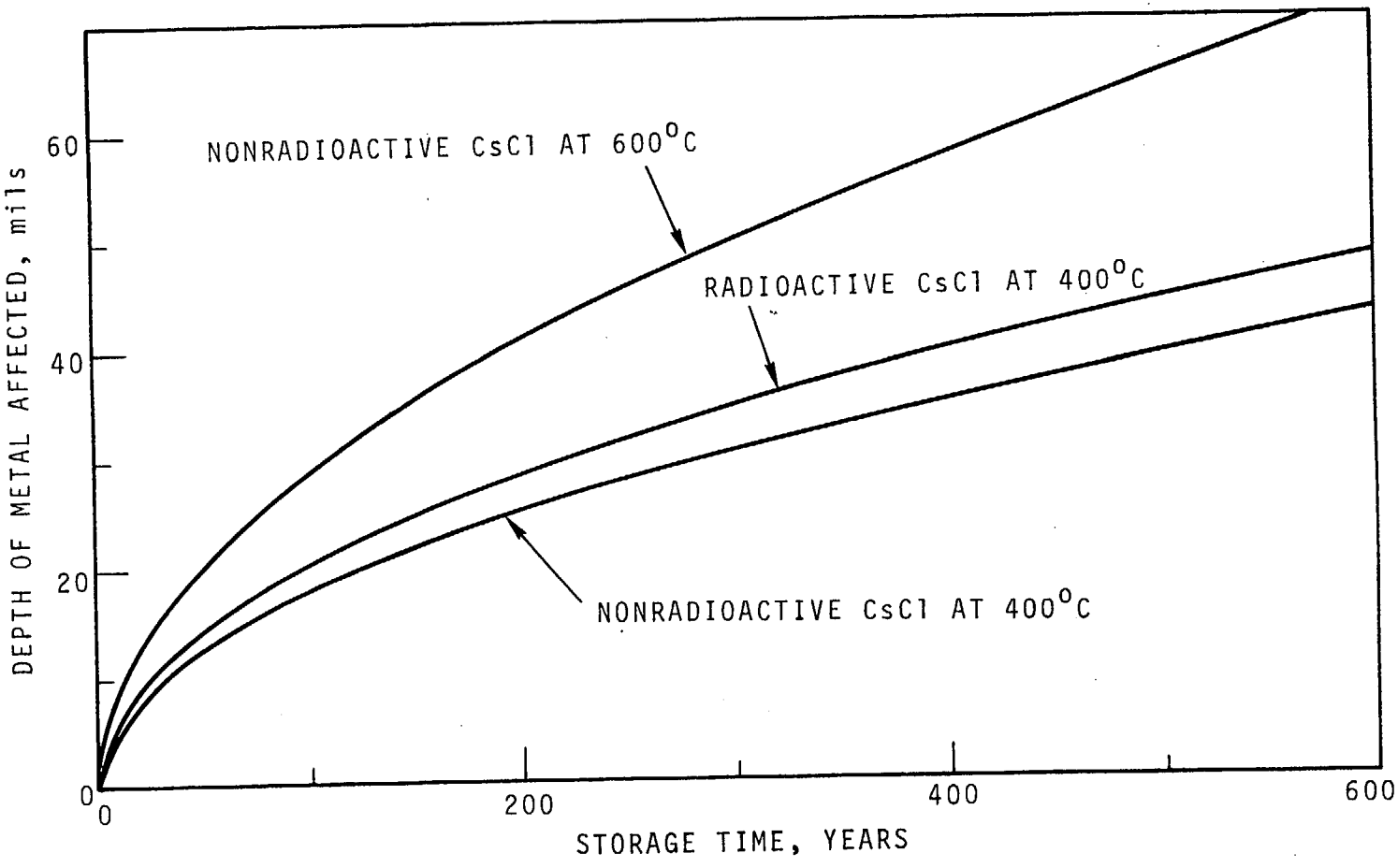

FIGURE 66. Estimated Long-Term Attack of Hastelloy C by CsCl

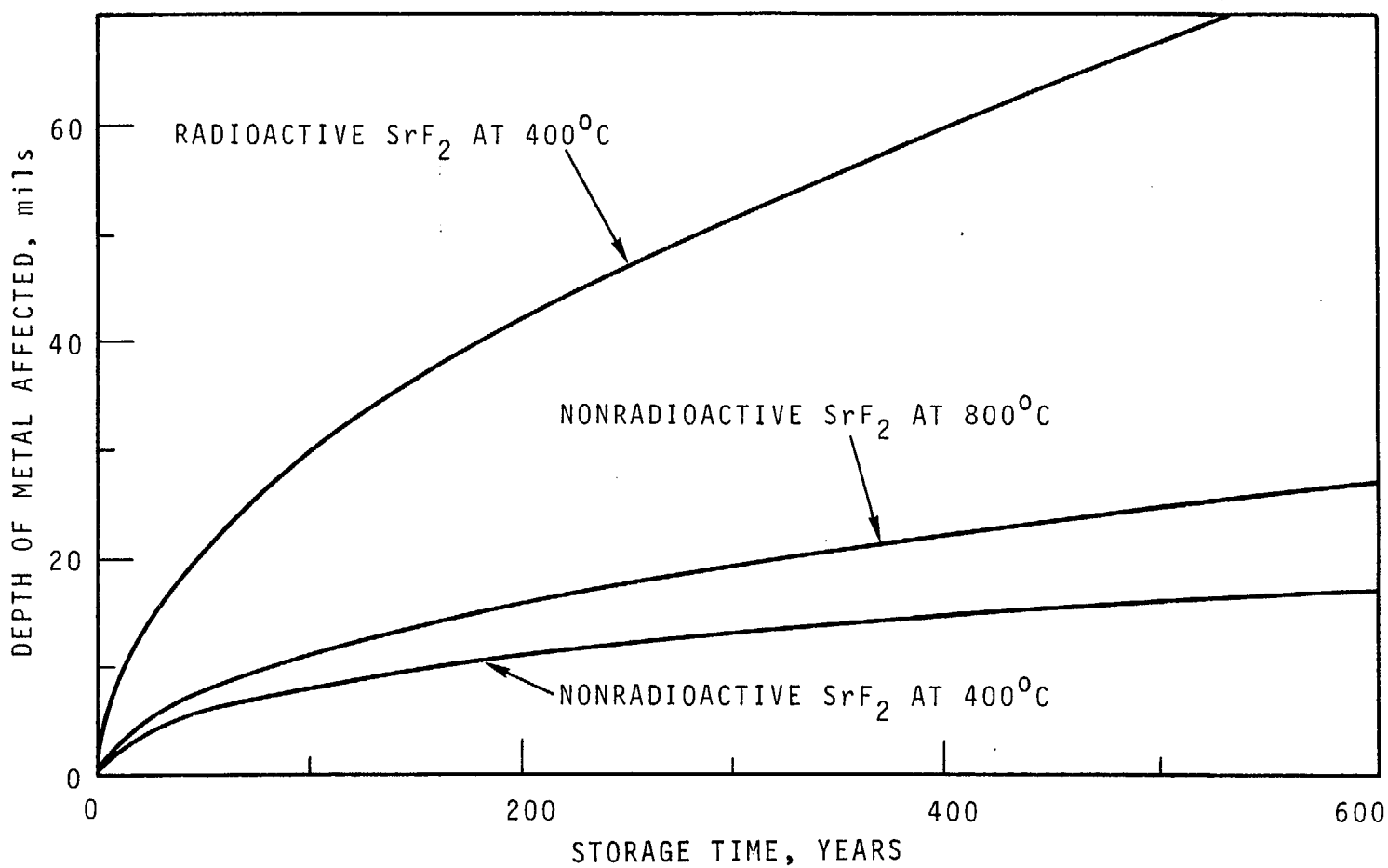

FIGURE 67. Estimated Long-Term Attack of Haynes 25 by SrF_2

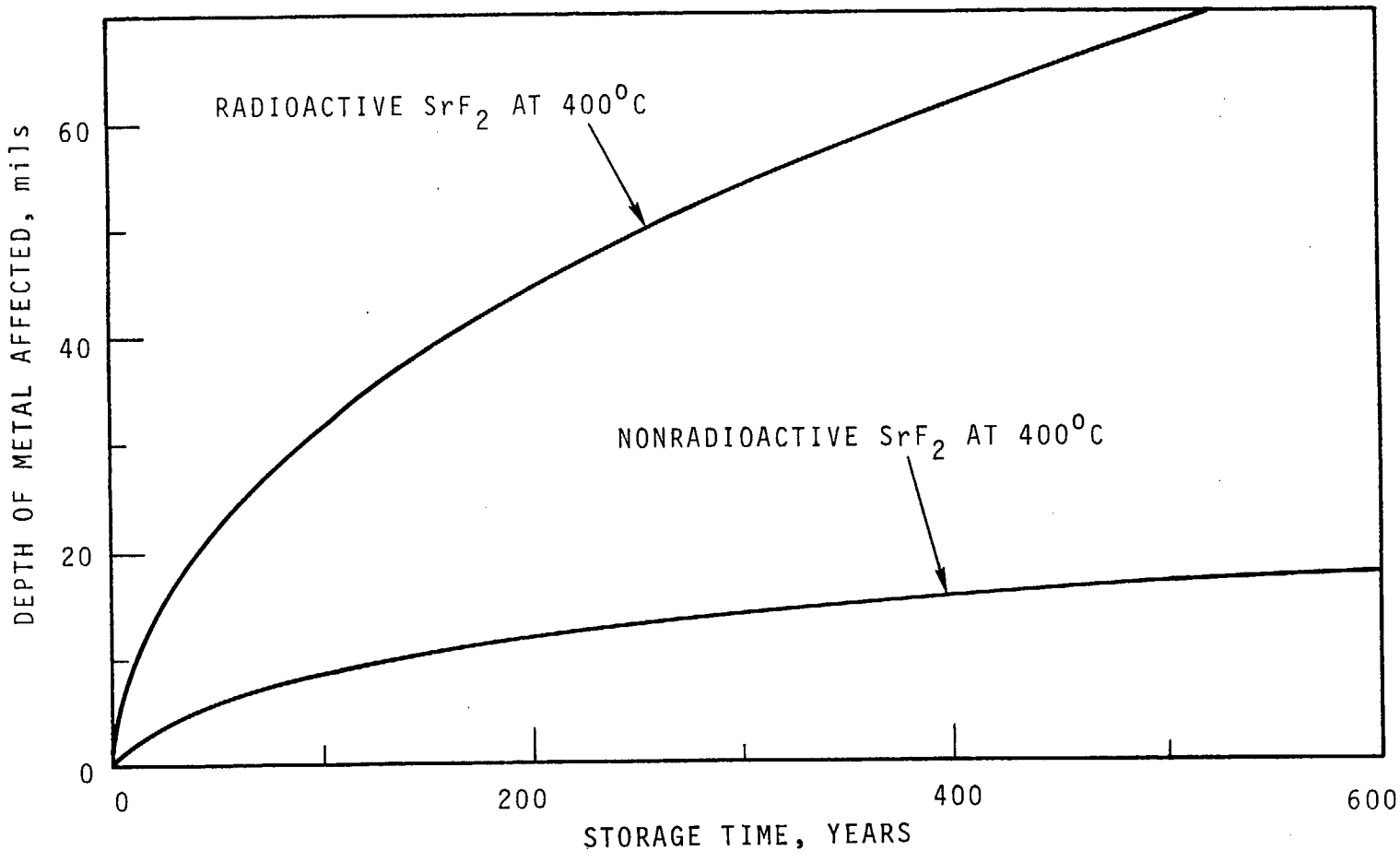

FIGURE 68. Estimated Long-Term Attack of 316L Stainless Steel by SrF_2

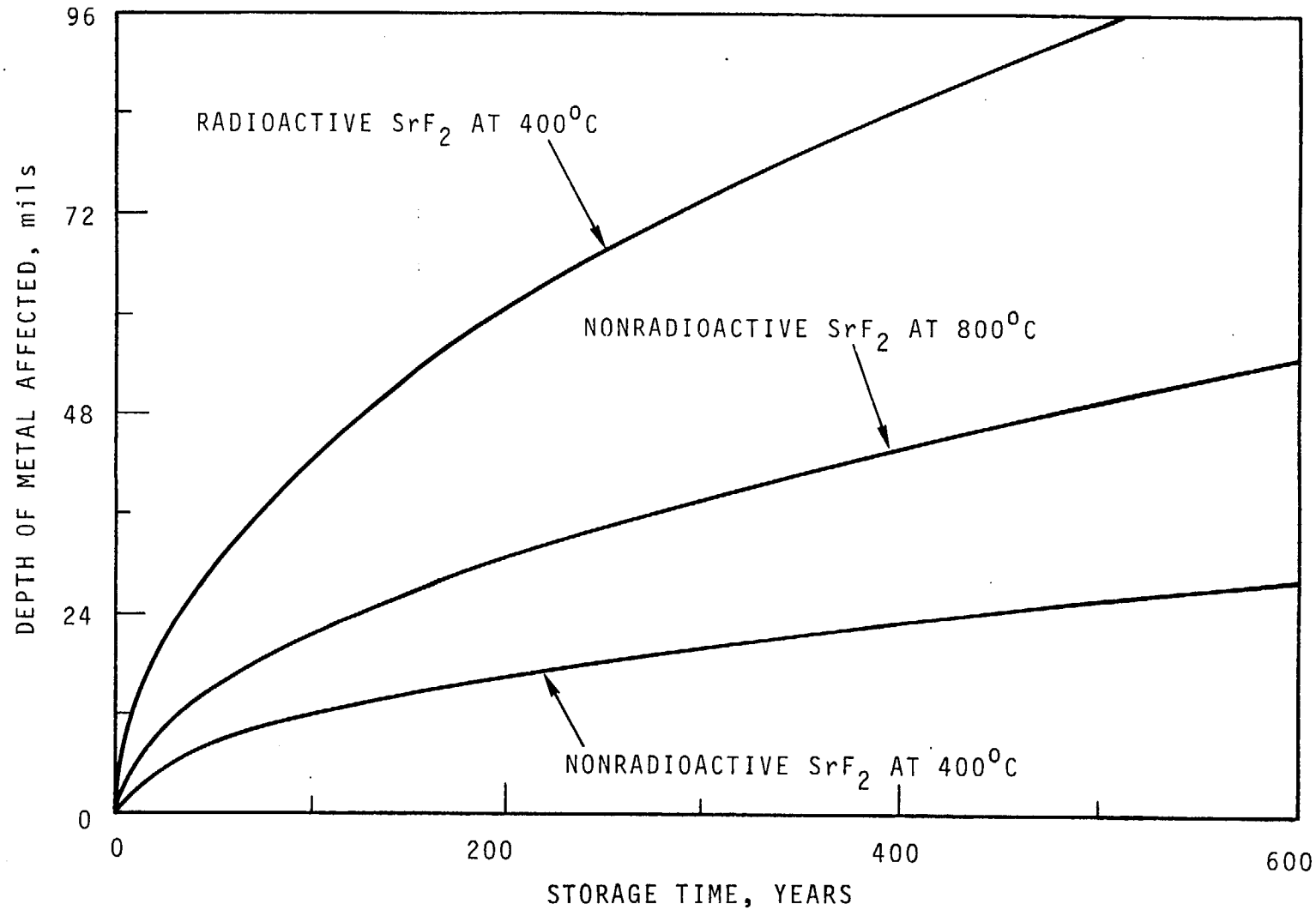

FIGURE 69. Estimated Long-Term Attack of Hastelloy C by SrF_2

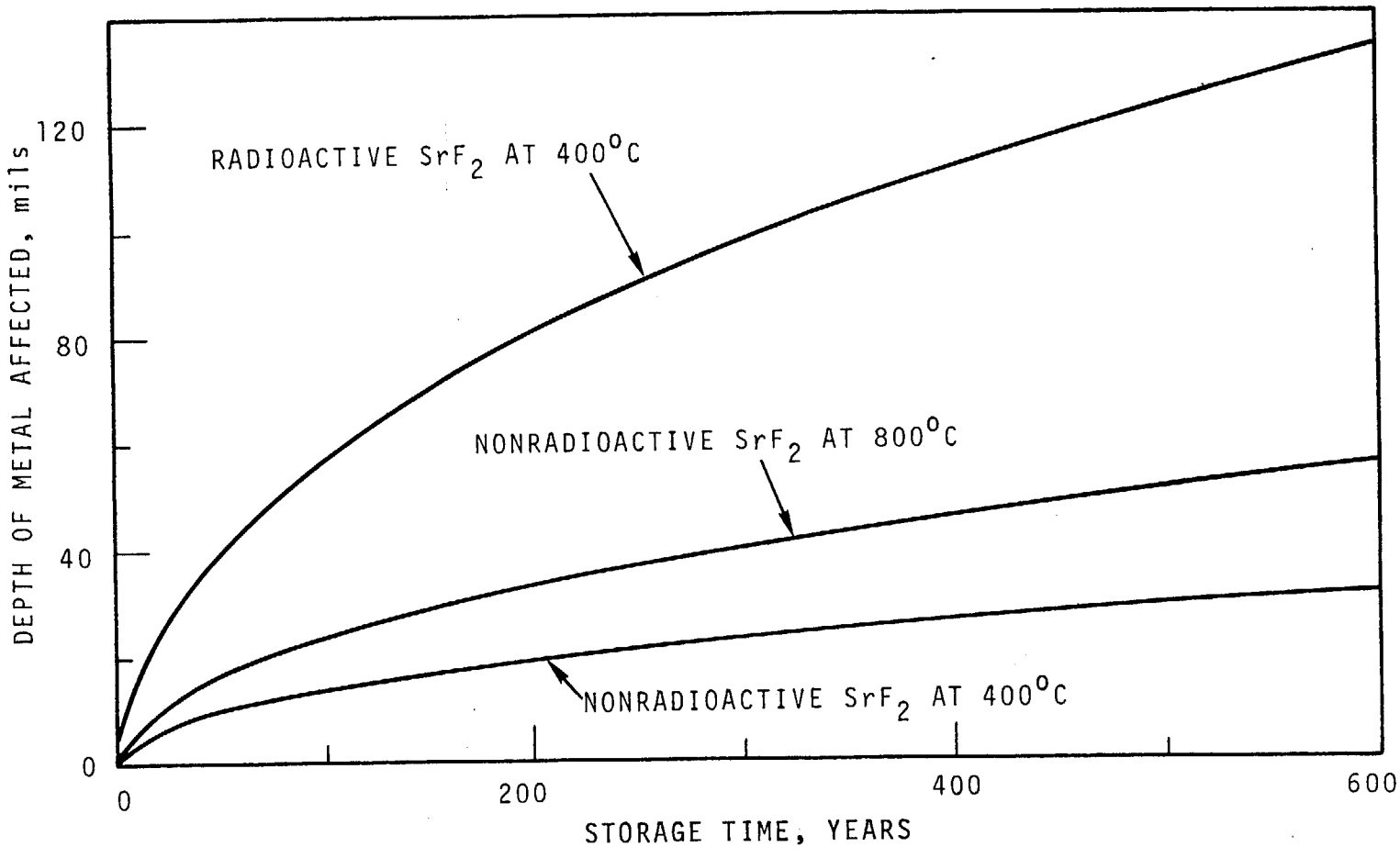

FIGURE 70. Estimated Long-Term Attack of Hastelloy X by SrF_2

B. WESF FLOWSHEETS

When this compatibility study was initiated the flowsheets which will be used in the WESF were not completely defined. To prepare the CsCl and SrF_2 used in the compatibility studies it was necessary to anticipate what operations would be used in the WESF flowsheets. The flowsheets used for preparing the CsCl and SrF_2 used in these studies are presented in the following figures. Subsequent developments have shown that the actual WESF flowsheets will be similar to those shown with the following minor modifications:

1. The cesium concentration from the thermosyphon concentrator will be ∿1.25M instead of 0.5M.
2. In the SrF_2 flowsheet a sulfate precipitation step, to provide additional purification, will be used between the solvent extraction and hydroxide precipitation steps.
3. No milling of the SrF_2 product, after firing at 1100°C, is planned.

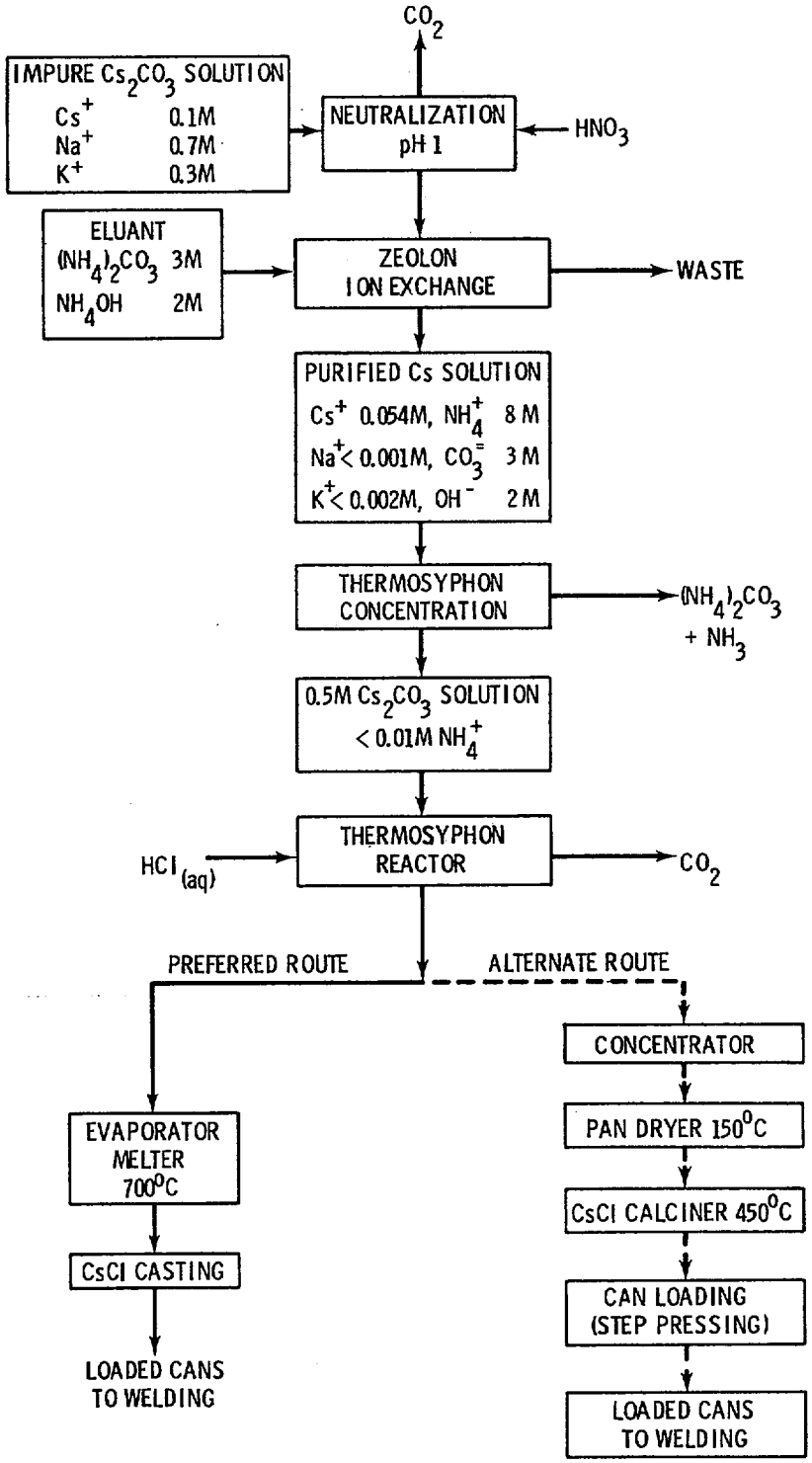

Flowsheet for Encapsulation of Cesium Chloride

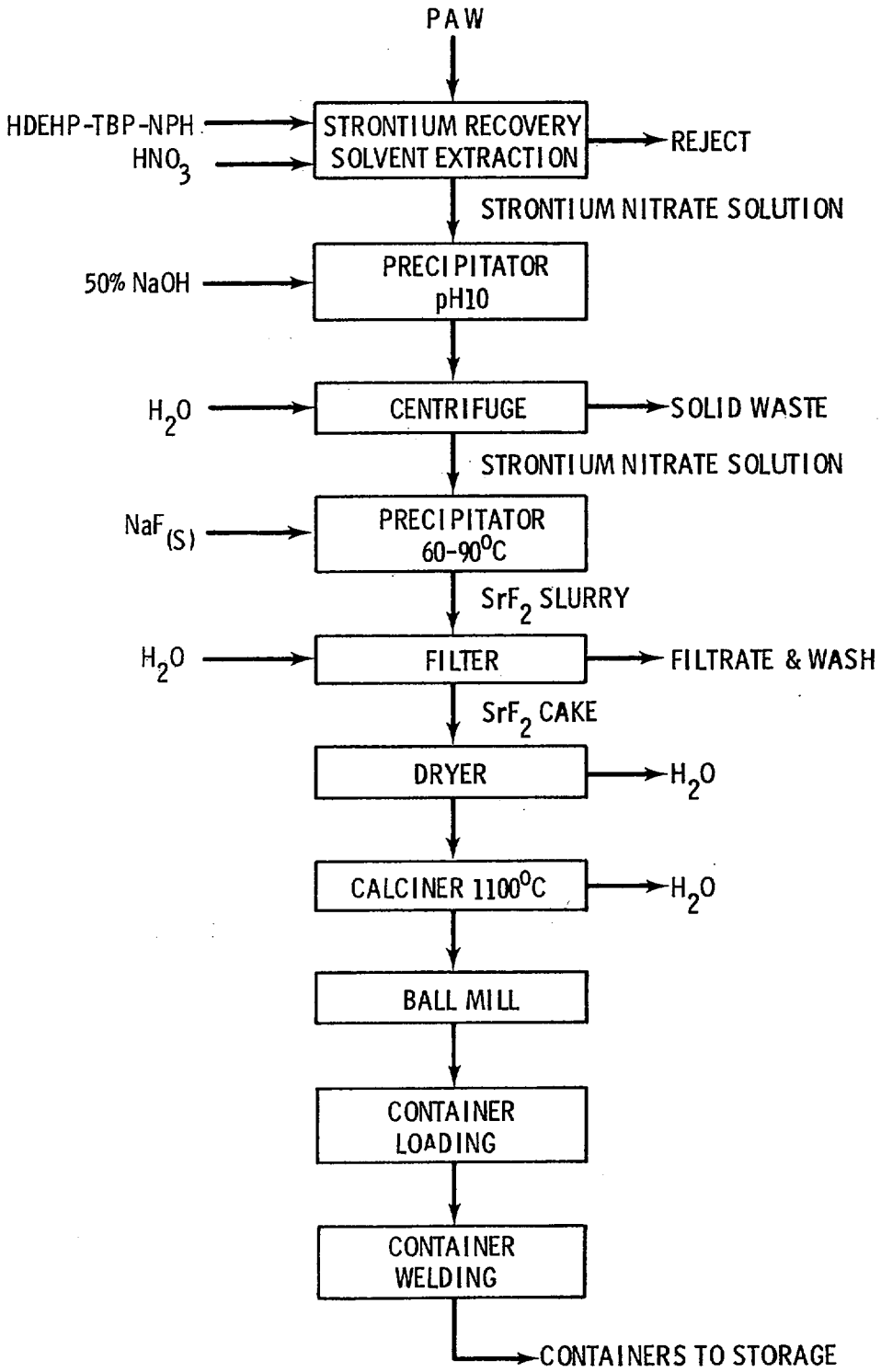

Flowsheet for Encapsulation of Strontium Fluoride

C. CHEMICAL ANALYSIS AND MECHANICAL TESTS OF TEST METALS

316L STAINLESS STEEL

One Inch Diam. Round
Annealed - Cond. A

Physical Properties:

Yield	- 69,000 psi
Tensile	- 91,500 psi
Elongation	- 40.5%
Red. of Area	- 71%
Brinell	- 178

Chemical Analysis:

C	0.026%	Cr	17.34%
Mn	1.78%	Ni	13.38
P	0.021	Mo	2.15
S	0.012	Cu	0.18
Si	0.012	Fe	Balance

Intergranular Corrosion Tests: OK

HASTELLOY C

One Inch Diam. Cold Rolled Bar

Tensile Test at Room Temperature:

Ultimate	- 115,250 psi
0.2% Yield	- 50,700 psi
Elong. in 4D inches	- 56.0%

Chemical Analysis:

Cr	15.55%	Ni	Balance
W	3.77	Mn	0.47%
Fe	5.51	V	0.29
C	0.04	Mo	15.78
Si	0.63	P	0.016
Co	1.10	S	0.004

HASTELLOY C-276

One Inch Diam. Hot Rolled Bar
Min C HRG - 5000

Tensile Test at Room Temperature:

Ultimate	-	115,200 psi
0.2% Yield	-	52,350
Elong. in 4D inches	-	62.0%

Chemical Analysis:

Cr	16.10%	Ni	Balance
W	3.61	Mn	0.45%
Fe	5.24	V	0.21
C	0.003	Mo	15.86
Si	0.01	P	0.018
Co	1.30	S	0.004

HASTELLOY X

One Inch Diam. Hot Rolled Bar - CEVM

Tensile Test at Room Temperature:

Ultimate	-	120,100 psi
0.2% Yield	-	56,950 psi
Elong. in 4D inches	-	64.0%

Chemical Analysis:

Cr	21.46%	Ni	Balance
W	0.52	Mn	0.73%
Fe	18.00	Mo	9.04
C	0.10	P	0.018
Si	0.19	S	0.003
Co	1.27		

HAYNES 25

One Inch Diam. Hot Rolled Bar - CEVM

Tensile Test at Room Temperature:

Ultimate	-	138,500 psi
0.2% Yield	-	63,250 psi
Elong. in 4D inches	-	64.0%

HAYNES 25 (continued)

Chemical Analysis:

Cr	20.45%	Co	Balance
W	15.10	Ni	9.93%
Fe	1.95	Mn	1.03
C	0.07	P	0.016
Si	0.07	S	0.011

DISTRIBUTION

No. of Copies	
OFFSITE	
1	AEC Chicago Patent Group G. H. Lee
5	AEC Division of Applied Technology F. D. Haines J. E. Machurek J. N. Maddox L. A. Miller W. E. Mott
1	AEC Division of Production & Materials Management W. L. Lennemann
1	AEC Division of Waste Management & Transportation R. W. Ramsey
179	AEC Technical Information Center
3	Union Carbide Corporation (ORNL) J. H. Gillette E. Lamb (2)
2	Westinghouse Astronuclear Laboratory Frank Arcella
ONSITE-HANFORD	
1	AEC Chicago Patent Group R. W. Poteat
3	AEC Richland Operations Office O. J. Elgert H. A. House E. B. Jackson

DISTRIBUTION (CONT.)

No. of Copies	
22	Atlantic Richfield Hanford Company
	G. E. Benedict
	G. L. Borsheim
	D. A. Bruce/D. N. Berger
	R. P. Corlew
	J. B. Fecht
	R. C. Forsman
	J. C. Hall
	W. M. Harty
	R. E. Isaacson
	J. R. LaRiviere
	C. W. Malody
	E. L. Moore
	J. D. Moore
	G. A. Nicholson
	G. G. Renfro
	L. M. Richards
	R. C. Roal
	H. P. Shaw
	A. E. Smith
	P. W. Smith
	D. D. Wodrich
	H. A. Zweifel
32	Battelle Northwest
	J. M. Batch
	R. E. Burns
	H. T. Fullam (20)
	J. H. Jarrett
	L. K. Mudge
	R. E. Nightingale
	R. S. Paul
	L. D. Perrigo
	H. H. Van Tuyl
	Technical Information Files (3)
	Technical Publications